NOAA OAR Special Report

doi:10.7289/V5125QK9

PMEL Tsunami Forecast Series: Vol. 5
A Tsunami Forecast Model for Newport, Oregon

Marie Eblé
NCTR Staff

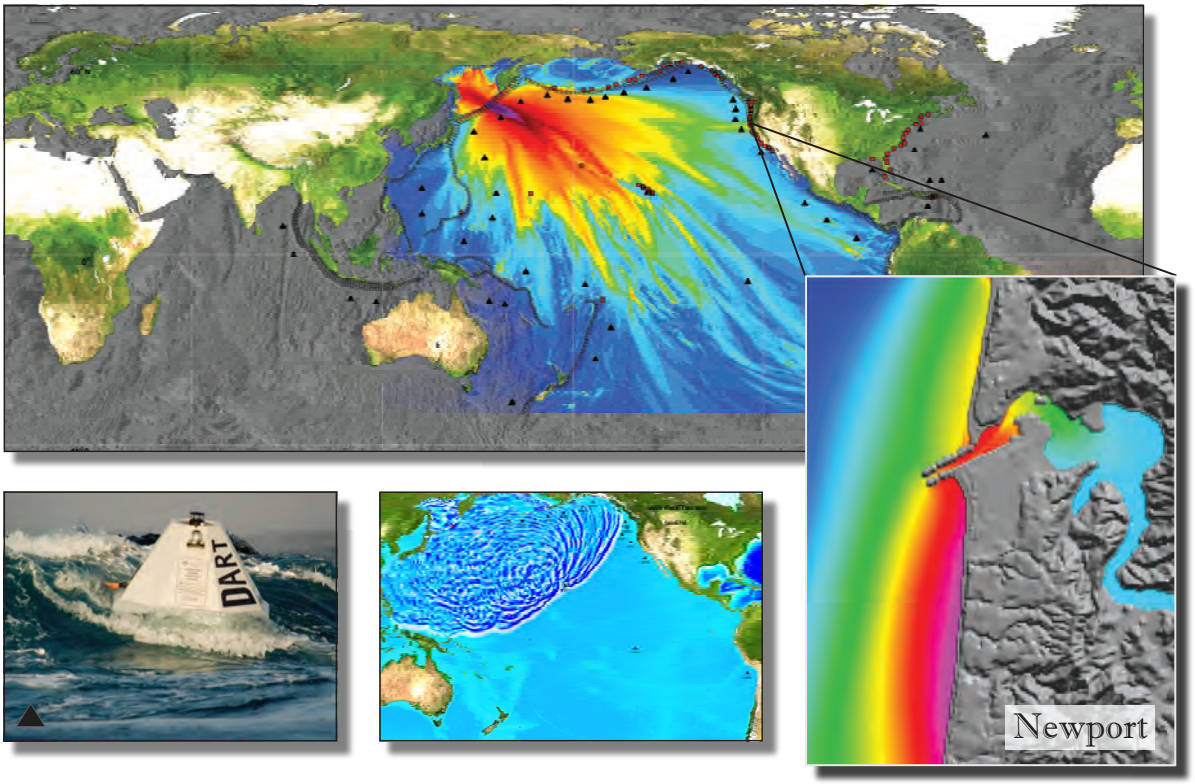

NOAA Center for Tsunami Research (NCTR)
Pacific Marine Environmental Laboratory

Front cover image: Overview of NOAA tsunami forecast system. Top frame illustrates components of the tsunami forecast using the 15 November 2006 Kuril Islands tsunami as an example: DART systems (black triangles), pre-computed tsunami source function database (unfilled black rectangles) and high-resolution forecast models in the Pacific, Atlantic, and Indian oceans (red squares). Colors show computed maximum tsunami amplitudes of the off-shore forecast. Black contour lines indicate tsunami travel times in hours. Lower panels show the forecast process sequence left to right: tsunami detection with the DART system (third generation DART ETD is shown); model propagation forecast based on DART observations; coastal forecast with high-resolution tsunami inundation model.

PDF versions of the PMEL Tsunami Forecast Series reports are available at
`http://nctr.pmel.noaa.gov/forecast_reports`

NOAA OAR Special Report

PMEL Tsunami Forecast Series: Vol. 5
A Tsunami Forecast Model for Newport, Oregon

M. Eble[1] and NCTR Staff[1,2]

1 NOAA/Pacific Marine Environmental Laboratory (PMEL), Seattle, WA
2 Joint Institute for the Study of the Atmosphere and Ocean (JISAO), University of Washington, Seattle, WA

Second Edition, November 2014

doi:10.7289/V5125QK9

UNITED STATES DEPARTMENT OF COMMERCE

Penny Pritzker
Secretary

NATIONAL OCEANIC AND ATMOSPHERIC ADMINISTRATION

Kathryn Sullivan
Under Secretary for Oceans and Atmosphere/Administrator

Office of Oceanic and Atmospheric Research

Craig McLean
Acting
Assistant Administrator

NOTICE from NOAA

Mention of a commercial company or product does not constitute an endorsement by NOAA/OAR. Use of information from this publication concerning proprietary products or the tests of such products for publicity or advertising purposes is not authorized. Any opinions, findings, and conclusions or recommendations expressed in this material are those of the authors and do not necessarily reflect the views of the National Oceanic and Atmospheric Administration.

First Edition: published March 2010

Second Edition: published November 2014

Contribution No. 3449 from NOAA/Pacific Marine Environmental Laboratory

Contribution No. 1771 from Joint Institute for the Study of the Atmosphere and Ocean (JISAO)

Also available from the National Technical Information Service (NTIS)

(http://www.ntis.gov)

Contents

List of Figures v

List of Tables xi

Foreword xiii

Abstract 1

1. Background and Objectives 1

2. Forecast Methodology 3

3. Model Development 5

3.1 Forecast area 5

3.2 Historical events and coastal water level observations 6

3.3 Bathymetry and topography 8

3.4 Model setup 10

4. Results and Discussion 11

4.1 Model validation 11

4.2 Model robustness and stability 14

5. Summary and Conclusion 17

6. Acknowledgments 18

7. References 19

FIGURES 21

Appendix A. 65

A1. Reference model *.in file for Newport, Oregon 65

A2. Forecast model *.in file for Newport, Oregon 65

Appendix B. Pacific Ocean Unit Sources 67

Appendix C. Synthetic Testing Report: Newport, Oregon 115

C1. Purpose 115

C2. Testing procedure 115

C3. Results 116

Glossary 125

List of Figures

1 Aerial view of Yaquina Bay showing the South Beach area in the foreground and historic Nye Beach along the opposite shore; detailed view of the NOAA Marine Operations Center – Pacific. 23

2 Aerial view of Newport, Oregon. The arrow shows the approximate location of the South Beach tide gauge used for comparison with model results (from NCTR/Oregon Graduate Institute CCALMR archives). 24

3 Evacuation map for Newport, Oregon, developed in the mid-1990s by the Oregon Department of Geology and Mineral Industries in consultation with local officials. 25

4 Map of the Pacific Ocean basin showing the location of the 11 historical events used to test and validate the Newport model. Relative earthquake magnitude is shown by the varying sizes and colors of the filled circles. 26

5 Digital elevation model constructed in 2004 by the NOAA Center for Tsunami Research for Newport, Oregon. 27

6 Bathymetry and topography for the reference inundation model grids A, B, and C. The topography of the C grid is shown using contours with 40 m intervals. 28

7 Bathymetry and topography for the tsunami forecast model grids A, B, and C. The topography of the C grid is shown using contours with 40 m intervals. 29

8 Difference plot showing the result of subtracting the digital elevation model constructed by the National Geophysical Data Center in 2008 from the digital elevation model constructed by the NOAA Center for Tsunami Research in 2004. The primary differences are evident along the coast from inclusion of LIDAR data in the 2008 model. 30

9 Model results for the 1946 Unimak Mw 8.5 event. The upper two panels show the forecast and reference model maximum wave height predictions. The lower panel shows the forecast and reference model wave amplitudes at the Newport tide gauge. 31

10 Model results for the 1960 Chile Mw 9.5 event. The upper two panels show the forecast and reference model maximum wave height predictions. The lower panel shows the forecast and reference model wave amplitudes at the Newport tide gauge. 32

11 Model results for the 1964 Alaska Mw 9.2 event. The upper two panels show the forecast and reference model maximum wave height predictions. The lower panel shows the forecast and reference model wave amplitudes at the Newport tide gauge. 33

12 Model results for the 1996 Andreanof Mw 7.9 event. The upper two panels show the forecast and reference model maximum wave height predictions. The lower panel shows the forecast model and reference model wave amplitudes at the Newport tide gauge. 34

13 Model results for the 2006 Tonga Mw 8.0 event. The upper two panels show the forecast and reference model maximum wave height predictions. The lower panel shows the forecast model and reference model wave amplitudes at the Newport tide gauge. 35

14 Model results for the 1994 Kuril Mw 8.3 event. The upper two panels show the forecast and reference model maximum wave height predictions. The lower panel shows the forecast model and reference model wave amplitudes at the Newport tide gauge. 36

15 Model results for the 2006 Kuril Mw 8.3 event. The upper two panels show the forecast and reference model maximum wave height predictions. The lower panel shows the forecast model and reference model wave amplitudes at the Newport tide gauge. 37

16 Model results for the 2007 Kuril Mw 8.1 event. The upper two panels show the forecast and reference model maximum wave height predictions. The lower panel shows the forecast model and reference model wave amplitudes at the Newport tide gauge. 38

17 Model results for the 2009 Samoa Mw 8.1 event. The upper two panels show the forecast and reference model maximum wave height predictions. The lower panel shows the forecast model and reference model wave amplitudes at the Newport tide gauge. 39

18 Model results for the 2010 Chile Mw 8.8 event. The upper two panels show the forecast and reference model maximum wave height predictions. The lower panel shows the forecast and reference model, and observed wave amplitudes at the Newport tide gauge. 40

19 Model results for the 2007 Solomon Mw 8.1 event. The upper two panels show the forecast and reference model maximum wave height predictions. The lower panel shows the forecast and reference model, and observed wave amplitudes at the Newport tide gauge. 41

20 Map of the Pacific Ocean Basin showing the locations of the 19 simulated Mw 9.3 events, the Mw 7.5 medium event, and the micro-tsunami event used to test and validate the Newport model. 42

21 Results from the forecast model for the KISZ 1–10 synthetic event. The upper panel shows the map of predicted maximum wave height in the Newport C grid and the lower panel shows the time series of wave amplitude at the tide gauge location. 43

22 Results from the forecast model for the KISZ 22–31 synthetic event. The upper panel shows the map of predicted maximum wave height in the Newport C grid and the lower panel shows the time series of wave amplitude at the tide gauge location. 44

23 Results from the forecast model for the KISZ 32–41 synthetic event. The upper panel shows the map of predicted maximum wave height in the Newport C grid and the lower panel shows the time series of wave amplitude at the tide gauge location. 45

24 Results from the forecast model for the KISZ 56–65 synthetic event. The upper panel shows the map of predicted maximum wave height in the Newport C grid and the lower panel shows the time series of wave amplitude at the tide gauge location. 46

25 Results from the forecast model for the ACSZ 6–15 synthetic event. The upper panel shows the map of predicted maximum wave height in the Newport C grid and the lower panel shows the time series of wave amplitude at the tide gauge location. 47

26 Results from the forecast model for the ACSZ 16–25 synthetic event. The upper panel shows the map of predicted maximum wave height in the Newport C grid and the lower panel shows the time series of wave amplitude at the tide gauge location. 48

27 Results from the forecast model for the ACSZ 22–31 synthetic event. The upper panel shows the map of predicted maximum wave height in the Newport C grid and the lower panel shows the time series of wave amplitude at the tide gauge location. 49

28 Results from the forecast model for the ACSZ 50–59 synthetic event. The upper panel shows the map of predicted maximum wave height in the Newport C grid and the lower panel shows the time series of wave amplitude at the tide gauge location. 50

29 Results from the forecast model for the ACSZ 56–65 synthetic event. The upper panel shows the map of predicted maximum wave height in the Newport C grid and the lower panel shows the time series of wave amplitude at the tide gauge location. 51

30 Results from the forecast model for the CSSZ 1–10 synthetic event. The upper panel shows the map of predicted maximum wave height in the Newport C grid and the lower panel shows the time series of wave amplitude at the tide gauge location. 52

31 Results from the forecast model for the CSSZ 37–46 synthetic event. The upper panel shows the map of predicted maximum wave height in the Newport C grid and the lower panel shows the time series of wave amplitude at the tide gauge location. 53

32 Results from the forecast model for the CSSZ 89–98 synthetic event. The upper panel shows the map of predicted maximum wave height in the Newport C grid and the lower panel shows the time series of wave amplitude at the tide gauge location. 54

33 Results from the forecast model for the CSSZ 102–111 synthetic event. The upper panel shows the map of predicted maximum wave height in the Newport C grid and the lower panel shows the time series of wave amplitude at the tide gauge location. 55

34 Results from the forecast model for the NTSZ 30–39 synthetic event. The upper panel shows the map of predicted maximum wave height in the Newport C grid and the lower panel shows the time series of wave amplitude at the tide gauge location. 56

35 Results from the forecast model for the NVSZ 28–37 synthetic event. The upper panel shows the map of predicted maximum wave height in the Newport C grid and the lower panel shows the time series of wave amplitude at the tide gauge location. 57

36 Results from the forecast model for the MOSZ 1–10 synthetic event. The upper panel shows the map of predicted maximum wave height in the Newport C grid and the lower panel shows the time series of wave amplitude at the tide gauge location. 58

37 Results from the forecast model for the NGSZ 3–12 synthetic event. The upper panel shows the map of predicted maximum wave height in the Newport C grid and the lower panel shows the time series of wave amplitude at the tide gauge location. 59

38 Results from the forecast model for the EPSZ 6–15 synthetic event. The upper panel shows the map of predicted maximum wave height in the Newport C grid and the lower panel shows the time series of wave amplitude at the tide gauge location. 60

39 Results from the forecast model for the RNSZ 12–21 synthetic event. The upper panel shows the map of predicted maximum wave height in the Newport C grid and the lower panel shows the time series of wave amplitude at the tide gauge location. 61

40 Results from the forecast model for the MEDI7.5 synthetic event forced by a small rupture of NTSZ B36. The upper panel shows the predicted maximum wave height in the Newport C grid; the lower panel shows the time series of wave amplitude at the tide gauge location. 62

41 Results from the forecast model for the MICRO3 synthetic event forced by a Mw 7.5 rupture of ACSZ B6. The upper panel shows the predicted maximum wave height in the Newport C grid; the lower panel shows the time series of wave amplitude at the tide gauge location. 63

B1 Aleutian–Alaska–Cascadia Subduction Zone unit sources. 69

B2 Central and South America Subduction Zone unit sources. 75

B3 Eastern Philippines Subduction Zone unit sources. 87

B4 Kamchatka–Bering Subduction Zone unit sources. 89

B5 Kamchatka–Kuril–Japan–Izu–Mariana–Yap Subduction Zone unit sources. 91

B6 Manus–Oceanic Convergent Boundary Subduction Zone unit sources. 99

B7 New Guinea Subduction Zone unit sources. 101

B8 New Zealand–Kermadec–Tonga Subduction Zone unit sources. 103

B9 New Britain–Solomons–Vanuatu Subduction Zone unit sources. 107

B10 New Zealand–Puysegur Subduction Zone unit sources. 111

B11 Ryukyu–Kyushu–Nankai Subduction Zone unit sources. 113

C1 Response of the Newport forecast model to synthetic scenario KISZ 22–31 (α=25). Maximum sea surface elevation for A, B, and C grids. Sea surface elevation time series at the C-grid warning point. 118

C2 Response of the Newport forecast model to synthetic scenario ACSZ 56–65 (α=25). Maximum sea surface elevation for A, B, and C grids. Sea surface elevation time series at the C-grid warning point. 119

C3 Response of the Newport forecast model to synthetic scenario CSSZ 89–98 (α=25). Maximum sea surface elevation for A, B, and C grids. Sea surface elevation time series at the C-grid warning point. 120

C4 Response of the Newport forecast model to synthetic scenario NTSZ 30–39 (α=25). Maximum sea surface elevation for A, B, and C grids. Sea surface elevation time series at the C-grid warning point. 121

C5 Response of the Newport forecast model to the 2006 Tonga tsunami. Maximum sea surface elevation for A, B, and C grids. Sea surface elevation time series at the C-grid warning point. 122

C6 Response of the Newport forecast model to the 2006 Kuril tsunami. Maximum sea surface elevation for A, B, and C grids. Sea surface elevation time series at the C-grid warning point. 123

List of Tables

1 Historical events used for validation of the Newport, Oregon, tsunami forecast model. 7

2 MOST setup of the reference and forecast models for Newport, Oregon. 10

3 Synthetic tsunami events used in the forecast model testing for Newport, Oregon. 15

B1 Earthquake parameters for Aleutian–Alaska–Cascadia Subduction Zone unit sources. 70

B2 Earthquake parameters for Central and South America Subduction Zone unit sources. 76

B3 Earthquake parameters for Eastern Philippines Subduction Zone unit sources. 88

B4 Earthquake parameters for Kamchatka–Bering Subduction Zone unit sources. 90

B5 Earthquake parameters for Kamchatka–Kuril–Japan–Izu–Mariana –Yap Subduction Zone unit sources. 92

B6 Earthquake parameters for Manus–Oceanic Convergent Boundary Subduction Zone unit sources. 100

B7 Earthquake parameters for New Guinea Subduction Zone unit sources. 102

B8 Earthquake parameters for New Zealand–Kermadec–Tonga Subduction Zone unit sources. 104

B9 Earthquake parameters for New Britain–Solomons–Vanuatu Subduction Zone unit sources. 108

B10 Earthquake parameters for New Zealand–Puysegur Subduction Zone unit sources. 112

B11 Earthquake parameters for Ryukyu–Kyushu–Nankai Subduction Zone unit sources. 114

C1 Maximum and minimum amplitudes at the Newport, Oregon, warning point for synthetic and historical events tested using SIFT 3.2 and obtained during development. 117

Foreword

SEVERAL PACIFIC OCEAN BASIN tsunamis have been recognized as a potential hazard to United States coastal communities since the mid-twentieth century, when multiple destructive tsunamis caused damage to the states of Hawaii, Alaska, California, Oregon, and Washington. In response to these events, the United States, under the auspices of the National Oceanic and Atmospheric Administration (NOAA), established the Pacific and Alaska Tsunami Warning Centers, dedicated to protecting United States interests from the threat posed by tsunamis. NOAA also created a tsunami research program at the Pacific Marine Environmental Laboratory (PMEL) to develop improved warning products.

The scale of destruction and unprecedented loss of life following the December 2004 Sumatra tsunami served as the catalyst to refocus efforts in the United States on reducing tsunami vulnerability of coastal communities, and on 20 December 2006, the United States Congress passed the "Tsunami Warning and Education Act" under which education and warning activities were thereafter specified and mandated. A "tsunami forecasting capability based on models and measurements, including tsunami inundation models and maps" is a central component for the protection of United States coastlines from the threat posed by tsunamis. The forecasting capability for each community described in the PMEL Tsunami Forecast Series is the result of collaboration between the National Oceanic and Atmospheric Administration office of Oceanic and Atmospheric Research, National Weather Service, National Ocean Service, National Environmental Satellite, Data, and Information Service, the University of Washington's Joint Institute for the Study of the Atmosphere and Ocean, National Science Foundation, and United States Geological Survey.

NOAA Center for Tsunami Research

PMEL Tsunami Forecast Series: Vol. 5
A Tsunami Forecast Model for Newport, Oregon

M. Eble[1] and NCTR Staff[1,2]

Abstract. The National Oceanic and Atmospheric Administration has developed a tsunami forecast model for Newport, Oregon, as part of an effort to provide tsunami forecasts for United States coastal communities. The forecast model is a set of nested grids constructed by incrementally subsampling and smoothing a reference high-resolution digital elevation model. During this process, forecast model results were monitored for deviations from those computed with the more accurate, higher-resolution model. Validation and stability testing of the tsunami forecast model developed for this economically important and populous coastal community was conducted to ensure model performance and robustness across a suite of scenarios. A total of 11 historical tsunami events and 19 synthetically generated mega-tsunami (Mw 9.3) events around the Pacific basin were used for validation and stability testing of the Newport forecast model. Validation results show that model output track observed data within an expected accuracy tolerance, thus providing a quantitative estimate of the tsunami time series, inundation, and runup at Newport for tested events. In addition to robustness, reproducibility of results was verified by comparing 2009 development results with those attained during end-to-end operational system testing performed in 2013. The differences noted in this report are attributed to the Method of Splitting Tsunami numerical code updates made after the Newport model was developed (2004) and updated (2009). Of greatest significance, 2013 test results more accurately compare with observations during the 2011 Tohoku tsunami than the earlier development results. Overall, validation results combined with benchmarking show that the forecast model developed for Newport consistently generates 4 hr of tsunami simulation in significantly less than 10 min of CPU time without compromising forecast results for all scenarios tested.

1. Background and Objectives

The National Oceanic and Atmospheric Administration (NOAA) Center for Tsunami Research (NCTR) at the NOAA Pacific Marine Environmental Laboratory (PMEL) has developed a tsunami forecasting capability for operational use by NOAA's two Tsunami Warning Centers located in Hawaii and Alaska (Titov *et al.*, 2005). The capability is contained within an application suite designed to quickly and efficiently provide accurate basin-wide warnings of approaching tsunami waves. Termed Short-term Inundation Forecast of Tsunamis (SIFT), the application combines a graphical user interface with data ingestion and numerical models to produce estimates of tsunami wave arrival times, amplitudes, and inundation or flooding at each of the coastal communities prioritized by the National Weather Service Tsunami Warning Centers in partnership with state emergency managers.

1 NOAA/Pacific Marine Environmental Laboratory (PMEL), Seattle, WA
2 Joint Institute for the Study of the Atmosphere and Ocean (JISAO), University of Washington, Seattle, WA

The SIFT system integrates several key components: deep-ocean observations of tsunamis in real time, a basin-wide precomputed propagation database of water level and flow velocities based on potential seismic unit sources, an inversion or fitting algorithm to refine the tsunami source based on the observations during an event, and tsunami forecast models, alternatively known as Standby Inundation Models (SIMs).

The tsunami forecast model for Newport, Oregon, is one of 75 developed to forecast tsunami impact at populous and/or economically or logistically important communities located along the Pacific and Atlantic ocean coasts and along coasts of the Caribbean Sea. Situated on the north central coast of Oregon, Newport is approximately 210 km south of the Oregon border with Washington State and approximately 215 km southwest of the city of Portland. Yaquina Bay and Estuary form a natural divide between Newport proper and the marina district. Most of Newport's residential population of approximately 10,000 (Census, 2010) live in Newport proper, north of Yaquina Bay, in close proximity to city services and infrastructure. Seasonally, the population of Newport increases significantly due to its popularity as a seaside tourist destination. Tourism and a vibrant fishing industry dominate the Newport area economy. At the mouth of Yaquina Bay sits Yaquina Head, on which a 28 m tall lighthouse has stood since 1873. Yaquina Head draws hikers and tide pool enthusiasts. The bay front area along the north shore of Yaquina Bay, including historic Nye Beach, is both a major tourist destination and home to the largest commercial fishing fleet in Oregon. Catches of Dungeness crab, Albacore tuna, Pacific whiting, shrimp, halibut, and great varieties of rockfish routinely pass through the Port of Newport. In addition, the port area serves as a recreational center for fishing, boating, and other waterfront activities. South of the Yaquina Bay Bridge is the South Beach area, where the Oregon Coast Aquarium is co-located with NOAA's Hatfield Marine Science Center and Marine Operations Center – Pacific. The renowned Oregon Coast Aquarium draws visitors from around the world. Recently constructed and occupied, the NOAA Marine Operations Center – Pacific is homeport to four NOAA research vessels and supports additional vessels homeported in Hawaii and Alaska. The historic bridge across Yaquina Bay is itself revered as an artwork and recognized as a critical link in the Oregon coastal transportation system. Oregon Highway 101, the main roadway along the Oregon Coast, crosses the historic Yaquina Bay Bridge, and the junction with Oregon Highway 20, one of the main connections between the coast and the Willamette Valley, is just north of the bridge. Aerial views of Yaquina Bay in **Figure 1** show the potential vulnerability to tsunami impact of the low-lying South Beach area (in the foreground of **Figure 1a**) and the historic Nye Beach district along the opposite shore of the Yaquina River. The Yaquina Bay Bridge spans the river mouth and serves as the single connecting point between the city of Newport and South Beach.

Newport supports a large population, relies heavily on tourism, and supports commercial fishing and timber industries, all vital to both regional and state economies. The objective of this report is to detail development of the Newport tsunami forecast model. This model is used in near-real time to protect the community from the potential impact posed by a tsunami if generated.

2. Forecast Methodology

The general methodology for modeling tsunami impact along coastal areas, including Newport, Oregon, is to computationally propagate tsunami waves across a set of three nested grids (A, B, and C), each of which is successively finer in resolution, moving from offshore to onshore. Within the finest resolution grid C, the nearshore details are resolved to the point that model output can be directly compared with tide gauge observations. The C grid, then, serves as the operational basis for the National Weather Service to provide an estimate of wave arrival time, wave amplitude, and simulation of wave inundation onto dry land before tsunami waves reach a coastline.

Development of the operational tsunami forecast grid set starts with construction, by either NOAA National Geophysical Data Center (NGDC) or NCTR, of a relatively high-resolution (typically 1/3-arc-sec, ~7 m) digital elevation model using all bathymetry and topography data available at the time of construction. Data from federal and state government, university, and private sources are incorporated into a large spatial extent area in order to reproduce wave dynamics along the coastline for which inundation is to be computed. A high-resolution baseline set of grids with typical resolution on the order of 2/3 arc sec (~14 m) is then developed from the digital elevation model. Since accurate forecasting of tsunami impact along a coastline relies not only on grid resolution but also on numerical computation, the high-resolution grid set is not used operationally. This is because a resolution of 2/3 arc sec, although coarser than the 1/3-arc-sec digital elevation model, still requires a significant amount of run time in which to complete tsunami wave simulation. Rather, once developed, the high-resolution grid set, or model, is used as reference for development of the more computationally efficient tsunami forecast grid set, or model. Hereafter referred to as the "reference model," the high-resolution model is iteratively reduced in size, and resolution is further coarsened by subsampling and smoothing to maximize tsunami forecast model grid resolution while decreasing numerical run time. The trade-off between high resolution and computation time presents a significant challenge during tsunami forecast model development but is necessary in order to produce a set of grids that will meet operational requirements to provide 4 hr of tsunami simulation within 10 min of wall-clock time. For this reason, tsunami forecast models are often referred to as "optimized" models. The overarching goal is to maximize the amount of time that an at-risk community has to react to a tsunami threat by providing accurate information quickly. The process of model optimization is described by Tang *et al.* (2009).

Each of the 75 community-specific tsunami forecast grid sets, or models, developed and reported in this technical report series collectively represent one element of the NOAA operational forecast capability. The complete forecast methodology incorporates additional elements in order to operationally propagate tsunami waves across tsunami forecast grids and provide both rapid and accurate estimates of wave arrival time, wave height, and inundation immediately after a tsunami has been generated. Combined, these elements form the SIFT application

developed jointly by NCTR and National Weather Service. Specifically, a precomputed tsunami propagation database, deep-ocean observations, a numerical model for computation, and a graphical user interface are the remaining elements that round out the forecast methodology.

The propagation database element consists of water elevations and flow velocities precomputed for a continuous series of 50 × 100 (km) unit sources along all known subduction zones within each ocean basin. Gica *et al.* (2008) provide details of database generation. Complimentary to the database, the observation element serves to constrain numerical computation to the actual tsunami rather than to the earthquake mechanism. As tsunami waves propagate across the ocean, observations at Deep-ocean Assessment and Recording of Tsunamis (DART®) and equivalent international tsunameter platforms are ingested into the SIFT application in near-real time. High-quality, deep ocean observations from other technologies may at some time provide additional constraints. The actual tsunami, as observed in the deep ocean where it is free of nonlinear processes, is compared with sea surface elevation computed solely from original earthquake source parameters through an inversion, or fitting, algorithm. The result is an observation-constrained estimate of the tsunami source; in other words, identification of propagation database unit sources that best reproduce the observed tsunami waves. These database unit sources are then linearly combined to produce synthetic boundary conditions of water elevation and flow velocities, to initiate the tsunami forecast computations.

The Method of Splitting Tsunami (MOST) numerical model is used in the SIFT application as the numerical computation element. MOST is a suite of numerical simulation codes capable of simulating three processes of tsunami evolution: generation, transoceanic propagation, and inundation of dry land. Tsunami wavelengths are significantly larger than the water depth through which they propagate so the underlying physics are governed by the shallow water equations.

The MOST model has been verified for applicability to tsunami modeling with extensive testing against a number of laboratory experiments and benchmarks (Synolakis *et al.*, 2008; National Tsunami Hazard Mitigation Program, 2012). In addition, tsunami forecast models developed for use with MOST have been successfully used for simulations of many historical tsunami events. In particular, events impacting the Pacific Ocean Basin after individual tsunami forecast models have been developed have been used to show individual and collective model accuracy and efficiency (Titov and González,1997; Titov *et al.*, 2005; Titov, 2009; Tang *et al.*, 2009; Wei *et al.*, 2008). Comparison of model forecasts with observations at deep-ocean and coastal tide gauge locations, with inundation survey results after each successive tsunami event, continue to show the robustness of individual methodology elements as well as that of the collective application. Of specific interest, these results continue to validate the Newport tsunami forecast model for use in both real-time forecasting and scientific research applications.

3. Model Development

A 1/3-arc-sec (~7 m resolution) digital elevation model for Newport, Oregon, was constructed and completed on 28 September 2004 by the NCTR. The "best available" bathymetric, topographic, and coastal shoreline data at the time of development were used to construct this model. Data were compiled from a variety of sources, including the NGDC, the NOAA National Ocean Service (NOS), the U.S. Geological Survey (USGS), the U.S. Army Corps of Engineers (USACE), the Oregon Bureau of Land Management, the NOAA Coastal Services Center, and the Oregon Geospatial Data Clearinghouse. A more detailed discussion of the bathymetric and topographic data used to construct the digital elevation model, and how these data were processed, is provided in Section 3.3.

Following digital elevation model construction, three high-resolution reference grids were developed. Due to the limited extent of the 1/3-arc-sec digital elevation model, only the highest-resolution C grid was developed from this grid. The larger but coarser A and B grids were developed independently using data further discussed in Section 3.3. Once developed, the reference grids were duplicated and then iteratively subsampled. At each coarsening iteration, results were compared with those from the reference model and with observations to ensure that forecast model results remained consistent with the reference model, and that both retained accuracy sufficient for operational use. The resultant set of subsampled grids, the Newport tsunami forecast model, was tested for stability and performance on both the developer server and through the operational SIFT forecast system. Upon testing completion, the Newport tsunami forecast model was transitioned to the National Weather Service for incorporation into NOAA's two Tsunami Warning Centers in Hawaii and Alaska. Specifics of the Newport tsunami forecast model development and testing results are discussed in Section 4 of this report.

3.1 Forecast area

Newport is a city located on the west coast of the continental U.S. along the north central coast of Oregon. The population center of the city lies to the north of the Yaquina Estuary formed at the mouth of the Yaquina River, where the river flows into the Pacific Ocean. The region that includes Newport is dominated by the river and its network of tributaries. Newport and the city of Toledo, ~24 km upriver, are the sole incorporated cities within the watershed (`http://oregonexplorer.info/northcoast/NorthCoastWatersheds/YaquinaWatershed`). Due to a large marsh, the estuary is an important breeding ground and habitat for a large variety of waterfowl and migratory birds (Oregon Coast Aquarium, 2010). As shown in **Figure 2**, this geomorphology poses a challenge for ensuring the well being of the populace and protecting the infrastructure so vitally important to the local and state economies. An evacuation map developed from hazard assessment modeling for the southern portion of Newport by the Oregon Department of Geology and Mineral Industries, shown in **Figure 3**, graphically shows this challenge.

The Yaquina Estuary is closely coupled with the Pacific Ocean offshore of Newport. The estuarine area is approximately 4329 acres, with the contributing watershed calculated to be 655 square km (Audubon Society of Portland, 2014). Geographically, a narrow channel connects the main inland portion of the estuary with the Pacific Ocean. Multiple embayments and channels distinguish the estuary from the upstream Yaquina River. The tidal influence is large and typically extends to river mile 26. The Oregon Coastal Management program has classified the estuary as a deep draft estuary, with jetties and a main channel that are both maintained. A channel depth of approximately 7 m is maintained by the USACE to ensure commercial and recreational watercraft navigation. The large extent of waterways and estuarine environments provides numerous pathways for tsunami impact along the Newport and South Beach coast, so care was taken to represent these within the limits of resolution during development of the Newport tsunami forecast model.

3.2 Historical events and coastal water level observations

The city of Newport does not contain within its boundaries a dedicated water level sensor. Instead, NOS established a tide gauge station at South Beach on the Yaquina River in 1967. Maintenance and usage considerations over the years resulted in relocation, and, in December 1990, the currently occupied tide gauge location of 124.04167°W longitude, 44.6250°N latitude was established. Along with physical location, hardware and software have been updated over the years. Changes in sampling interval have resulted in dissemination of increasingly higher-resolution data for use by operational staff and researchers. The once commonly reported 6 min sampling interval was decreased to 1 min. A secondary unit additionally provides 15 sec data upon manual interrogation of tide gauges at most Pacific Basin locations and those at specific Atlantic and Caribbean locations. Reporting of a tide gauge or other water level sensor has also undergone revision over the years. Historically, the electronics housing location alone was recorded and served as the published location for the tide gauge sensor. At some locations, however, the tide gauge and electronics housing are separated by as much as 100 m or more, so NOS now accurately records the position of both the tide gauge and the electronics housing obtained separately from GPS fixes. The South Beach water level sensor and electronics are in close proximity of one another, and so occupy the same tsunami forecast model grid unit. At this tide gauge location, mean water level is recorded to be 2.8 m and mean high water recorded at 3.8 m. The average tidal excursion is recorded as 1.9 m.

Tsunami water level data were available for validation of the Newport tsunami forecast model during 6 of 11 historical events chosen for testing. All 11 events are listed in **Table 1**. Events were chosen to maximize representation of basin-wide seismic sources and to balance earthquake magnitude range with observation availability. Event epicenters, therefore, are distributed around the Pacific Basin, as shown graphically in **Figure 4**. Before validation of the tsunami forecast model predicted water level time series, the observed time series was quality controlled. Outliers exceeding six standard deviations from a running mean were first eliminated from the entire tsunami event portion of the time series. The tidal signal that dominates each record was then removed by filtering. A 3 hr (180 min) low-pass

Table 1: Historical events used for Newport, Oregon, to validate the tsunami forecast model.

Earthquake / Seismic				Model		
Event	**USGS Date Time (UTC) Epicenter**	**CMT Date Time (UTC) Centroid**	**Magnitude Mw**	**Tsunami Magnitude[1]**	**Subduction Zone**	**Tsunami Source**
1946 Unimak	01 Apr 12:28:56 52.75°N 163.50°W		[2]8.5	8.5	Aleutian-Alaska-Cascadia (ACSZ)	7.5 × b23 + 19.7 × b24 + 3.7 × b25
1960 Chile	22 May 19:11:14 [3]38.29°S 74.50°W		[4]9.5		Central-South America (CSSZ)	Kanamori and Cipar (1974)
1964 Alaska	28 Mar 03:36:00 [3]61.02°N 147.65°W		[3]9.2	9.0	Aleutian-Alaska-Cascadia (ACSZ)	a34 × 15.4 + a35 × 19.4 + z34 × 48.3 + b34 × 18.3 + b35 × 15.1
1994 East Kuril	04 Oct 13:22:58 43.73°N 147.321°E	04 Oct 13:23:28.5 43.60°N 147.63°E	[5]8.3	8.1	Kamchatka-Kuril-Japan-Izu-Mariana-Yap (KISZ)	9.0 × a20
1996 Andreanof	10 Jun 04:03:35 51.56°N 175.39°W	10 Jun 04:04:03.4 51.10°N 177.410°W	[5]7.9	7.8	Aleutian-Alaska-Cascadia (ACSZ)	2.40 × a15 + 0.80 × b16
2006 Tonga	03 May 15:26:39 20.13°S 174.161°W	03 May 15:27:03.7 20.39°S 173.47°W	[5]8.0	8.0	New Zealand-Kermadec-Tonga (NTSZ)	6.6 × b29
2006 Kuril	15 Nov 11:14:16 46.607°N 153.230°E	15 Nov 11:15:08 46.71°N 154.33°E	[5]8.3	8.1	Kamchatka-Kuril-Japan-Izu-Mariana-Yap (KISZ)	[6]4 × a12 + 0.5 × b12 + 2 × a13 + 1.5 × b13
2007 Kuril	13 Jan 04:23:20 46.272°N 154.455°E	13 Jan 04:23:48.1 46.17°N 154.80°E	[5]8.1	7.9	Kamchatka-Kuril-Japan-Izu-Mariana-Yap (KISZ)	-3.64 × b13
2007 Solomon	01 Apr 20:39:56 8.481°S 156.978°E	01 Apr 20:40:38.9 7.76°S 156.34°E	[3]8.1	8.2	New Britain-Solomons-Vanuatu (NVSZ)	12.0 × b10
2009 Samoa	29 Sep 17:48:10 15.509°S 172.034°W	29 Sep 17:48:26.8 15.13°S 171.97°W	[5]8.1	8.1	New Zealand-Kermadec-Tonga (NTSZ)	[6]3.96 × a34 + 3.96 × b34
2010 Chile	27 Feb 06:34:14 35.909°S 72.733°W	27 Feb 06:35:15.4 35.95°S 73.15°W	[5]8.8	8.8	Central-South America (CSSZ)	[6]a88 × 17.24 + a90 × 8.82 + b88 × 11.86 + b89 × 18.39 + b90 × 16.75 + z88 × 20.78 + z90 × 7.06

[1] Preliminary source – derived from source and deep-ocean observations
[2] López and Okal (2006)
[3] United States Geological Survey (USGS)
[4] Kanamori and Cipar (1974)
[5] Centroid Moment Tensor
[6] Tsunami source was obtained in real time and applied to the forecast

filter was applied to eliminate non-tidal frequencies. An 8 min low-pass filter was applied to eliminate background noise, the source of which is due to a combination of ambient environmental and instrumental characteristics. During some events, 15 sec data were available due to hardware upgrade so were uploaded directly from the South Beach tide gauge secondary unit by manually interrogating the unit via modem technology. These 15 sec data were decimated, or subsampled, after filtering to 1 min ΔT for direct comparison with predictions, provided at a 1 min interval consistently for all of the events.

3.3 Bathymetry and topography

Accurate bathymetry and topography are crucial for development of the reference and forecast models, especially for predicting inundation of the nearshore environment. Ideally, the digital elevation model serves as the basis for each of the three nested grids, A, B, and C. In some regions, however, the digital elevation model does not encompass all three of the desired grid extents, so A and possibly B grids need to be constructed separately. The extent of the 1/3-arc-sec merged bathymetric and topographic digital elevation model constructed for Newport included only the C grid. Specific to digital elevation model and C-grid development, data sources include 5 m Aircraft Laser/GPS Mapping Light Detection and Ranging (LIDAR) data from the USGS National Elevation Dataset and Digital Orthophoto Quads from NOS hydrographic surveys. Hydrographic surveys conducted in 1927, 1928, and 1953 from the NOAA NGDC Geophysical Data Management System (GEODAS) and USACE datasets consisting of surveys in 2002, 2003, and 2004 were used for development. More accurate data collected later superseded older dataset segments in overlapping areas. The primary limiting factors during construction were scale, age, and resolution of the surveys. Each dataset went through a stringent quality-control procedure by respective originators prior to dissemination. Topographic datasets were analyzed individually and in relation to one another. Vegetation and man-made structures were removed from LIDAR data by visual analysis with orthophotos. The bathymetric and topographic grids were merged into a single grid referenced in the vertical to the U.S. base elevation standard, the North American Vertical Datum of 1988 (NAVD88), and to the North American Datum 1983 in the horizontal. The vertical datum was subsequently adjusted to mean high water by using an average based on tide gauge observations within the grid extent. The resultant digital elevation model, shown in **Figure 5**, has an extent of latitude 44.7000–44.5400°N, longitude 124.0000–124.1500°W. Latitudinally, the grid has an even spacing of 61.8 m, or 2.0 arc sec. The longitudinal spacing is also even, but the delta is ~58.7 m, or 2.7 arc sec. The central grid position is latitude 44.6170°N; longitude 124.0670°W. The grid in Environmental Systems Research Institute ArcGIS raster format is available for download from either the NGDC or from the Oregon Department of Geology web sites. For the A and B grids, the best data available in 2004 were gathered for Newport and vicinity in order to increase the extents necessary to encompass the larger B grid and the regional A grid. A 6-arc-sec Oregon coast grid and a 36-arc-sec Pacific Northwest grid were combined, resampled, and error-checked to extend the domain for the desired grid extents.

The reference model was designed to encompass a large region. Extending from south of Vancouver Island and the Strait of Juan de Fuca to the southern geographical boundary of Oregon, the A grid covers a sizable geographic region. The offshore extent reaches a maximum depth of 4000 m. The reference B grid extends from southwest Washington in the north to Waldport, Oregon, in the south. Offshore, the B grid extends to a maximum depth of 500 m. The reference C grid extends from Seaside, Oregon, in the north, to just north of Ona Beach State Park, Oregon. The maximum offshore depth within the reference C grid is 60 m. In order to expedite tsunami forecasts for operational use, the latitudinal extents of each grid were reduced. The A grid northern boundary was moved from Vancouver Island to southwest Washington, and the B grid was clipped along the its northern boundary. The northern extent of southwest Washington was relocated south to Seaside, Oregon. For both A and B grids, resolution and maximum offshore depth remained the same as that of the corresponding reference grid. In order to compute inundation within required time limits, the forecast model C grid was geographically reduced and the resolution was decreased from 1/3 arc sec to 2.7 arc sec in the x direction (longitude) and 2.0 arc sec in y (latitude). The final extents of the Newport tsunami forecast model grids are as follows. The A grid extends from latitude 43.99–45.99°N and longitude 123.00–127.00°W. In latitude, the grid is an evenly spaced 1113.2 m, equating to 36.0 arc sec. In longitude, the grid is again evenly spaced with an interval of ~790 m, equating to 36.0 arc sec. The extent of the B grid is 44.45–44.80°N latitude, 123.95–124.30°W longitude. The spacing of this grid in latitude is an even 185.6 m, or 6 arc sec. In longitude, the grid is again evenly spaced with an interval of ~132 m, or 6 arc sec. The grid extents for both the Newport reference and tsunami forecast models are summarized in **Table 2**. In addition, all extents are shown graphically in **Figures 6** and **7**.

In 2008, the NGDC completed construction of a central Oregon digital elevation model that included Newport. For the most part, bathymetric, topographic, and shoreline data incorporated into this 2008 digital elevation model overlap with data listed above and used in construction of the 2004 digital elevation model by the NCTR. The 2008 model, however, included LIDAR data acquired along the Newport shoreline after 2004. The LIDAR survey extensively covered the coastline along the full extent of the grid so represented a significant source of new data. The vertical datum, or base elevation reference point, for each digital elevation model is the same NAVD88. Carignan *et al.* (2009) provide details of the Central Oregon digital elevation model constructed by the NGDC.

The differences between the digital elevation model constructed by the NCTR in 2004 and that constructed by the NGDC in 2008 were examined to determine if redevelopment of the tsunami forecast model was warranted. The differences, shown graphically in **Figure 8**, are confined to the shoreline where LIDAR data were added in 2008. Specifically, the 2008 digital elevation model shows laser pulse light particle scatter returns that reflect coastal vegetation. The 2008 grid, therefore, was not corrected to bare earth, so the 2004 digital elevation model remains an appropriate basis for tsunami forecast model development. Therefore, redevelopment of the tsunami forecast model using the 2008 digital elevation model is not warranted at the time of this Newport tsunami forecast model report publication.

Table 2: MOST setup of the reference and forecast models for Newport, Oregon.

		Reference Model				Forecast Model			
Grid	**Region**	**Coverage Lat [°N] Lon [°W]**	**Cell Size ["]**	**nx × ny**	**Time Step [sec]**	**Coverage Lat [°N] Lon [°W]**	**Cell Size ["]**	**nx × ny**	**Time Step [sec]**
A	San Juan de Fuca	48.99–43.0 128–123.01	36×36	500×600	3.6	45.99–43.99 127–123	36×36	401×201	2.7
B	Central Oregon	45.889–44.360 124.5–123.5	6×6	600×918	1.8	44.797–44.448 124.3–123.952	6×6	210×210	2.7
C	Newport	44.700–44.540 124.150–124.0	1.35×1.33	405×432	0.6	44.660–44.5402 124.12–124.001	2.7×2	162×216	2.7
Minimum offshore depth [m]			5				5		
Water depth for dry land [m]			0.1				0.1		
Friction coefficient (n^2)			0.0009				0.0009		
CPU time for a 4 hr simulation			87 min				87 min		

Computations were performed on a single Intel Xeon processor at 3.6 GHz, Dell PowerEdge 1850.

3.4 Model setup

The MOST suite of numerical codes is used in forecast model development and operationally to provide an estimate of tsunami amplitude, first wave arrival time, and inundation of normally dry land (Titov and González, 1997; Synolakis *et al.*, 2007; Tang *et al.*, 2009). MOST is a finite difference method that takes input from a precomputed propagation-run database and, subsequently, via a series of nested grids, resolves the nearshore bathymetry and topography to provide forecasts at coastal locations. Adjustable parameters, including time step interval and number, nearshore wet/dry boundary depth, coarse wet/dry boundary depth, friction (Manning roughness coefficient), output time, grid size, grid resolution, and grid position, provide location-specific flexibility throughout forecast model development. Once tested, these parameters remain fixed from run to run, under the assumption that the parameters and features are likely location-dependent. Specifically, each location possesses unique bathymetric and topographic characteristics that must be adequately accounted for. The set of model parameters used for the Newport reference and forecast models are provided in **Table 2** along with grid extents, previously described. The actual run files for each are given in Appendix A.

4. Results and Discussion

4.1 Model validation

To test the performance of the reference and forecast models developed for operational use for Newport, Oregon, 11 historical tsunami events were modeled. Source details for each of these events are provided in **Table 1**. Observations at the South Beach tide gauge recorded during the 1994 Kuril, 1996 Andreanof Islands, 2006 Kuril, 2007 Kuril, 2009 Samoa, and 2010 Chile events were used to validate model predictions. Tsunami forecast model predictions were compared with those of the reference model for the 11 historical events, and also with tide gauge observations during each of the six events identified above. Maximum expected tsunami wave height within the C grid and the time series predicted at the tide gauge by the reference and forecast models for the 11 historical events are plotted in **Figures 9–19**; event-specific tide gauge observations are plotted as a third time series in the six corresponding event figures.

Maximum tsunami wave height maps for the 11 historical events show that the reference model consistently predicts slightly higher tsunami wave amplitudes than predicted by the forecast model. This suggests a loss of wave energy as the tsunami propagates across the lower-resolution forecast model grids. The highest amplitudes occur along the coast, most typically south of the Newport breakwater, and not inside Yaquina Bay. For all events, the reference and forecast model results are visually well correlated in prediction of first wave arrival time and magnitude. Later waves are less correlated, possibly due to the effect of differing bathymetries and grid resolutions on waves as they reflect and refract within the C-grid domain. There is, however, generally good agreement in the amplitude of later waves predicted by the reference and forecast models.

The 1946 Unimak earthquake, at a magnitude of Mw 8.5, generated the earliest of the 11 historical tsunamis modeled. Of these events, Unimak is the fourth largest in terms of earthquake magnitude and third largest in terms of predicted response at the South Beach tide gauge. Results, presented in **Figure 9**, show generally good agreement between reference and forecast model predictions. Ocean maxima, however, are noted as being higher from the reference model than the forecast model. Amplitudes predicted by both models inside the breakwater are similar in magnitude. Wave amplitudes predicted by the reference and forecast models at the South Beach tide gauge (**Figure 9**, lower panel) are well correlated, with maximum wave amplitudes predicted to be approximately 0.25 m.

The 1960 Chile (**Figure 10**) and 1964 Alaska (**Figure 11**) events are the largest in terms of both magnitude and impact of the 11 historical events modeled and presented here. (Note that the maximum wave color map used for both of these figures has been "pushed" so that details within the bay are visually identifiable.) As **Figure 10** shows, the largest waves predicted by the reference and forecast models along the open ocean coastline for the 1960 Chile tsunami show consistency. As was the case for the 1946 Unimak event, the reference model predicts

slightly higher maxima than predicted by the forecast model, at approximately 1.5 and 1.2 m, respectively. Upstream the river mouth and inside Yaquina Bay, the maximum wave amplitudes are roughly half of those predicted in the open ocean: specifically, 0.7 and 0.6 m, respectively, so the difference between reference and forecast model predictions is less. At the tide gauge location, the two predicted time series agree well in timing and magnitude, with the main difference being the lower drawdown in the reference model prediction. The observed maximum amplitude of 0.61 m (NGDC, 2009) is reproduced by both the reference and forecast models. For the 1964 Alaska tsunami, the reference and forecast models predict maximum offshore wave amplitudes in excess of 2 m. Maxima inside Yaquina Bay are predicted to be 1.4 m by the reference model and 1.7 m by the forecast model. For this event, the forecast model produces slightly higher amplitudes inside the bay than those predicted by the reference model. At the Newport tide gauge location, the amplitude of 0.3 m is reported by NGDC (2009) during the 1964 event. At first glance, this appears to represent a significant discrepancy from the ~1 m maximum amplitude predicted by both reference and forecast models. However, the location of the tide gauge was moved in 1967, three years after the 1964 Alaska event, so the grid cell from which predictions are extracted is not representative of the 1964 observation. In addition, the NGDC wave amplitude is approximated as ½ wave height (peak to adjacent wave trough). This value is approximately 0.6 m for the first wave of the forecast model. Absence of the observed tide gauge record and unknown location of the measurements make the direct comparison of the model results with observations difficult and uncertain in this case.

The 1996 Andreanof Islands and 2006 Tonga historical events are the smallest of the 11 modeled in both magnitude and impact at Newport. Model predictions and tide gauge observations for the 1996 Andreanof Islands event, plotted in **Figure 12**, show agreement between reference and forecast model predictions for signals in which identification of the tsunami is difficult. For this event and some others, local background energy, or "noise," results in a signal-to-noise ratio that is too low to clearly determine when the "initial" wave arrives. Results of modeling the 2006 Tonga event are shown in **Figure 13**. Predicted maximum waves along the open beaches are on order 0.17 m and less than 0.10 m within Yaquina Bay. Reference and forecast model-predicted time series, shown in the lower panel, are well matched for the initial three waves.

The three historical Kuril events of 1994, 2006, and 2007 were each generated by earthquakes of moderate magnitude. As shown in **Figure 4**, the 1994 and 2006 tsunamis were generated by magnitude Mw 8.3 earthquakes but were located along different sections of the Kuril subduction zone. The 2007 tsunami was generated by a magnitude Mw 8.1 earthquake but the source was co-located with that of the 2006 event. Results for the more eastern 1994 Kuril event, presented in **Figure 14**, show consistency between reference and forecast model predictions. Inside Yaquina Bay, both models predict maxima less than 0.15 m. A comparison of model-predicted time series with tide gauge observations shows agreement in maximum amplitude but a lag in the timing of model results. The difference in travel time may be due, in part, to the actual tsunami source being in a different location than that defined within the 50 × 100 km unit source block(s) selected. Additional reasons for the travel time discrepancy may include cumulative bathymetry

error for the Pacific propagation model grid and model approximation error. For the 2006 event, results, presented in **Figure 15**, show predictions approaching 0.20 m along the open coast within the reference model C grid. Predictions from the forecast model are generally lower along the open coast. Observations at the tide gauge appear to show under-prediction by both the reference and forecast models, but all records, predicted and observed alike, are quite noisy. When results are compared with time series observations during the 1994 event, reference and forecast models more closely predict the maximum amplitude observed during the 1994 event than they predict for the larger maximum amplitude observed during the 2006 event. However, forecast model predictions mirror those of the reference model for the first waves and throughout the time series for both events. For the 2007 Kuril event, results predicted by both the reference and forecast models are 0.10–0.15 m along the open coast and negligible inside Yaquina Bay, as shown in **Figure 16**. Observations at the tide gauge appear to show larger amplitude waves, but this may be misleading as predicted and observed records are both noisy. The smaller amplitudes predicted for the 2007 are consistent with this event being smaller in magnitude than the 1994 and 2006 events. Overall, model predictions for all three events are consistent in showing higher waves along the open coast within the C grid and lower waves inside Yaquina Bay. Reference and forecast model predictions for the same magnitude 1994 and 2006 events are well correlated and are also consistent in prediction of impact that both events have on Newport, This may be an indication that magnitude overrides exact location for determining impact at Newport along the Kuril subduction zone.

The 2009 Samoa and 2010 Chile historical events are significantly different in terms of magnitude but similar in terms of impact at Newport. The impact range, as observed in the time series plots in **Figures 17** and **18**, is between +/– 0.1 m. The **Figure 17** upper panel maps show that for the Samoa event, amplitude maxima predicted by the reference and forecast models are consistent with one another. The maximum amplitude at the tide gauge is approximately 0.8 m in both predicted and observed time series. Modeling results for the 2010 Chile event are presented in **Figure 18**. The forecast model predicts wave heights of approximately 0.2 m along the open coast while the reference model predicts waves on order 0.3 m. Maximum wave heights predicted by the two models within Yaquina Bay are better matched. For both events, time series at the tide gauge show temporal offsets between predicted and observed. Predictions lead observations by approximately 12 min for 2010 Chile and by approximately 9 min for 2009 Samoa. These time shifts, as mentioned previously, hint at an inexact source location within a 50 × 100 km unit source block.

The last of the historical events modeled and presented here is the 2007 Solomon Islands event. Generated by a moderate, magnitude Mw 8.1 earthquake, the impact to Newport is shown in **Figure 19**. Along the Newport coastline, the reference model predicts significantly larger maximum waves than those predicted by the forecast model. Within Yaquina Bay, the reference model predicts a higher response than the forecast model, but at the time series, predictions by the two models are well correlated in both magnitude and time. Observations at the tide gauge for this event are not available for direct comparison.

4.2 Model robustness and stability

Historical tsunamis provide only a limited number of events, generated from a limited number of source locations. More comprehensive test cases of destructive tsunamis with full basin directionalities are needed to check the tsunami forecast model stability and robustness. Therefore, 19 synthetic Mw 9.3 mega-tsunami events, one Mw 7.5 synthetic scenario, and one synthetic Mw 6.6 micro-tsunami scenario, as listed in **Table 3**, were selected for further testing. These scenarios originate from unit source combinations around the Pacific Ocean basin and along the South American coast. The spatial coverage of the scenarios is shown in **Figure 20**, in which all scenarios are plotted relative to one another. The sources used as input to the computational grids for this phase of testing are the Pacific basin subset of sources from a worldwide propagation database developed by the NCTR (Gica *et al.*, 2008). Details of these Pacific basin unit sources are provided in Appendix B.

Predicted tsunami waves at the South Beach tide gauge and forecast model predicted wave maxima are shown in **Figures 21–41**. The forecast model remained stable during testing for all synthetic scenarios. Scenarios run using Alaska-Cascadia and Kuril-Kamchatka sources are projected to generate the largest waves impacting Newport, and as expected, the largest predicted waves result from a near-field mega-tsunami scenario along the Alaska-Cascadia Subduction Zone, specifically ACSZ 56–65 (**Figure 29**). This synthetic scenario exhibits extreme inundation south of the Yaquina Bay breakwaters and along Highway 101 to South Beach. Wave heights of 10 m are possible along the coast from this scenario. In the far field, the greatest impact at Newport is from a tsunami generated along the Kuril-Kamchatka Subduction Zone (**Figures 21–24.**) The impact to Newport from a tsunami generated by all remaining synthetic scenarios varies depending on magnitude and wave energy directionality from the source.

These and all specific results should be considered in the context of this report and should not be used as a proxy for a complete hazard assessment, which is more appropriately conducted using the reference model. Testing of the tsunami forecast model within the SIFT system was conducted to ensure that operational performance remained consistent with that observed on individual servers during development and testing. Differences in amplitude predictions between development model runs and operational system runs, noted in Appendix C, are due to MOST version updates made in the years after forecast model development. Predictions for Newport made during the 2011 Tohoku tsunami show closer agreement with tide gauge observations than would be expected of the model using the MOST version in use during development. Therefore, the results show that the forecast model developed for Newport provides an operational forecast that meets accuracy requirements.

Table 3: Synthetic tsunami events used in the forecast model testing for Newport, Oregon.

Scenario No.	Name	Source Zone	Tsunami Source	α [m]
Mega-tsunami Scenario				
1	KISZ 1–10	Kamchatka–Kuril–Japan–Izu–Mariana–Yap	A1–10, B1–10	25
2	KISZ 22–31	Kamchatka–Kuril–Japan–Izu–Mariana–Yap	A22–31, B22–31	25
3	KISZ 32–41	Kamchatka–Kuril–Japan–Izu–Mariana–Yap	A32–41, B32–41	25
4	KISZ 56–65	Kamchatka–Kuril–Japan–Izu–Mariana–Yap	A56–65, B56–65	25
5	ACSZ 6–15	Aleutian–Alaska–Cascadia	A6–15, B6–15	25
6	ACSZ 16–25	Aleutian–Alaska–Cascadia	A16–25, B16–25	25
7	ACSZ 22–31	Aleutian–Alaska–Cascadia	A22–31, B22–31	25
8	ACSZ 50–59	Aleutian–Alaska–Cascadia	A50–59, B50–59	25
9	ACSZ 56–65	Aleutian–Alaska–Cascadia	A56–65, B56–65	25
10	CSSZ 1–10	Central and South America	A1–10, B1–10	25
11	CSSZ 37–46	Central and South America	A37–46, B37–46	25
12	CSSZ 89–98	Central and South America	A89–98, B89–98	25
13	CSSZ 102–111	Central and South America	A102–111, B102–111	25
14	NTSZ 30–39	New Zealand–Kermadec–Tonga	A30–39, B30–39	25
15	NVSZ 28–37	New Britain–Solomons–Vanuatu	A28–37, B28–37	25
16	MOSZ 1–10	Manus–Oceanic Convergent Boundary	A1–10, B1–10	25
17	NGSZ 3–12	North New Guinea	A3–12, B3–12	25
18	EPSZ 6–15	East Philippines	A6–15, B6–15	25
19	RNSZ 12–21	Ryukyu–Kyushu–Nankai	A12–21, B12–21	25
Mw 7.5 Tsunami Scenario				
20	NTSZ B36	New Zealand–Kermadec–Tonga	B36	1
Micro-tsunami Scenario				
21	ACSZ B6	Aleutian–Alaska–Cascadia	B6	0.05

5. Summary and Conclusions

A digital elevation model, a high-resolution reference model, and a tsunami forecast model were each developed for Newport, Oregon. The tsunami forecast model was developed by reducing reference model grid resolution in order to provide forecasts of tsunami wave amplitude, arrival time, and inundation within time constraints dictated by operational forecast requirements. Forecast model C-grid resolution is 2.7 arc sec in longitude and 2.0 arc sec in latitude. The computational grids were derived from the best bathymetric and topographic source data available at the time of grid construction.

Eleven historical events were simulated and tsunami forecast model performance was evaluated by comparing predicted results with both reference model results and observations at the South Beach tide gauge, when available, to validate the forecast model predictions. The stability and sensitivity of the model were tested with 19 Mw 9.3 synthetic tsunami scenarios originating from unit source combinations around the Pacific Ocean basin and along the South American coast. The forecast model remained stable during testing for all synthetic scenarios. Scenarios run using Alaska-Cascadia and Kuril-Kamchatka sources are predicted to generate waves as high as 7 m. These and all specific results should be considered in the context of this report and should not be used as a proxy for a complete hazard assessment, which is more appropriately conducted using the reference model.

Testing of the tsunami forecast model within the operational SIFT system was conducted to ensure that operational performance remained consistent with that observed on individual servers during development and testing. Differences in amplitude predictions noted between development model runs and operational system runs, as presented in Appendix C, are due to MOST version updates made in the years after forecast model development. Predictions for Newport made during the 2011 Tohoku tsunami show closer agreement with tide gauge observations than would be expected of the model using the MOST version in use during development. Based on all test results presented in this report, the Newport tsunami forecast model can provide a 4 hr forecast of the first tsunami wave arrival time, wave amplitudes, and inundation of normally dry land within 10 min of wall-clock time, and meets operational accuracy requirements.

6. Acknowledgments

The authors wish to than Dylan Righi for grid development and testing, Yong Wei for his assistance with model setup and troubleshooting, the team of Lindsey Wright, Nicolas Arcos, Katherine Burgess, and Nazila Merati for providing much appreciated comments and editorial assistance, and Burak Uslu for providing propagation database unit source information as well as the unit source graphics in Appendix B. The authors especially thank Ryan Layne Whitney and Sandra Bigley for technical assistance and for their thorough editorial review of the report draft versions generated over the course of many months. Collaborative contributions of the National Weather Service, the National Geophysical Data Center, the National Ocean Survey, and the National Data Buoy Center were invaluable.

The National Oceanic and Atmospheric Administration provided funding for all work culminating in the development of the Newport, Oregon, tsunami forecast model and report. This publication was partially funded by the Joint Institute for the Study of the Atmosphere and Ocean (JISAO) under NOAA Cooperative Agreement No. NA17RJ1232, JISAO Contribution No. 1771, PMEL Contribution No. 3449, and NOAA ISI ID280.

7. References

Audubon Society of Portland (2014): "Yaquina Bay." The Audubon Society. http://audubonportland.org/local-birding/iba/iba-map/yaquina. Accessed 22 February 2014.

Carignan, K.S., L.A. Taylor, B.W. Eakins, R.R. Warnken, E. Lim, and P.R. Medley (2009): Digital elevation model of central Oregon Coast: Procedures, data sources and analysis. NOAA Tech. Memo. NESDIS NGDC-25, U.S. Dept. of Commerce, Boulder, CO, 38 pp.

Census (2010): factfinder2.census.gov/faces/nav/jsf/pages/community_facts.xhtml.

Gica, E., M.C. Spillane, V.V. Titov, C.D. Chamberlin, and J.C. Newman (2008): Development of the forecast propagation database for NOAA's Short-term Inundation Forecast for Tsunamis (SIFT). NOAA Tech. Memo. OAR PMEL-139, NTIS: PB2008-109391, NOAA/Pacific Marine Environmental Laboratory, Seattle, WA, 89 pp.

Kanamori, H., and J.J. Cipar (1974): Focal process of the great Chilean earthquake, May 22, 1960. *Phys. Earth Planet. In., 9*, 128–136.

López, A.M., and E.A. Okal (2006): A seismological reassessment of the source of the 1946 Aleutian "tsunami" earthquake. *Geophys. J. Int., 165*(3), 835–849, doi: 10.1111/j.1365-246x.2006.02899.x.

National Tsunami Hazard Mitigation Program (2012): Proceedings and results of the 2011 NTHMP model benchmarking workshop (NOAA Special Report). U.S. Department of Commerce/NOAA/NTHMP, Boulder, CO, 436 pp.

NGDC (2009): Global Tsunami Database (2000 BC to present). National Geophysical Data Center, http://www.ngdc.noaa.gov/hazard/tsu_db.shtml.

Oregon Coast Aquarium (2010) "Estuary Trail." Oregon Coast Aquarium Newport. The Oregon Coast Aquarium. http://aquarium.org/exhibits/estuary-trail. Accessed 19 February 2014.

Synolakis, C.E., E.N. Bernard, V.V. Titov, U. Kânoğlu, and F.I. González (2007): Standards, criteria, and procedures for NOAA evaluation of tsunami numerical models. NOAA Tech. Memo. OAR PMEL-135, NTIS: PB2007-109601, NOAA/Pacific Marine Environmental Laboratory, Seattle, WA, 55 pp.

Synolakis, C.E., E.N. Bernard, V.V. Titov, U. Kânoğlu, and F.I. González (2008): Validation and verification of tsunami numerical models. *Pure Appl. Geophys., 165*(11–12), 2197–2228.

Tang, L., V.V. Titov, and C.D. Chamberlin (2009): Development, testing, and applications of site-specific tsunami inundation models for real-time forecasting. *J. Geophys. Res., 114*, C12025, doi: 10.1029/2009JC005476.

Titov, V.V. (2009): Tsunami forecasting. In *The Sea*, Vol. 15, Chapter 12, Harvard University Press, Cambridge, MA, and London, England, 371–400.

Titov, V.V., and F.I. González (1997): Implementation and testing of the Method of Splitting Tsunami (MOST) model. NOAA Tech. Memo. ERL PMEL-112 (PB98-122773), NOAA/Pacific Marine Environmental Laboratory, Seattle, WA, 11 pp.

Titov, V.V., F.I. González, E.N. Bernard, M.C. Eble, H.O. Mofjeld, J.C. Newman, and A.J. Venturato (2005): Real-time tsunami forecasting: Challenges and solutions. *Nat. Hazards, 35*(1), Special Issue, U.S. National Tsunami Hazard Mitigation Program, 41–58.

Wei, Y., E. Bernard, L. Tang, R. Weiss, V. Titov, C. Moore, M. Spillane, M. Hopkins, and U. Kânoğlu (2008): Real-time experimental forecast of the Peruvian tsunami of August 2007 for U.S. coastlines. *Geophys. Res. Lett., 35*, L04609, doi: 10.1029/2007GL032250.

FIGURES

Figure 1: (a) Aerial view of Yaquina Bay showing the South Beach area in the foreground and historic Nye Beach along the opposite shore. The city of Newport in the background is situated between the Pacific Ocean and the Yaquina River. The historic Yaquina Bay Bridge serves as the single point of connection between the city of Newport and South Beach. (b) A detailed view of the NOAA Marine Operations Center – Pacific. (`http://www.moc.noaa.gov`).

Figure 2: Aerial view of Newport, Oregon. The arrow shows the approximate location of the South Beach tide gauge used for comparison with model results (from NCTR/Oregon Graduate Institute CCALMR archives).

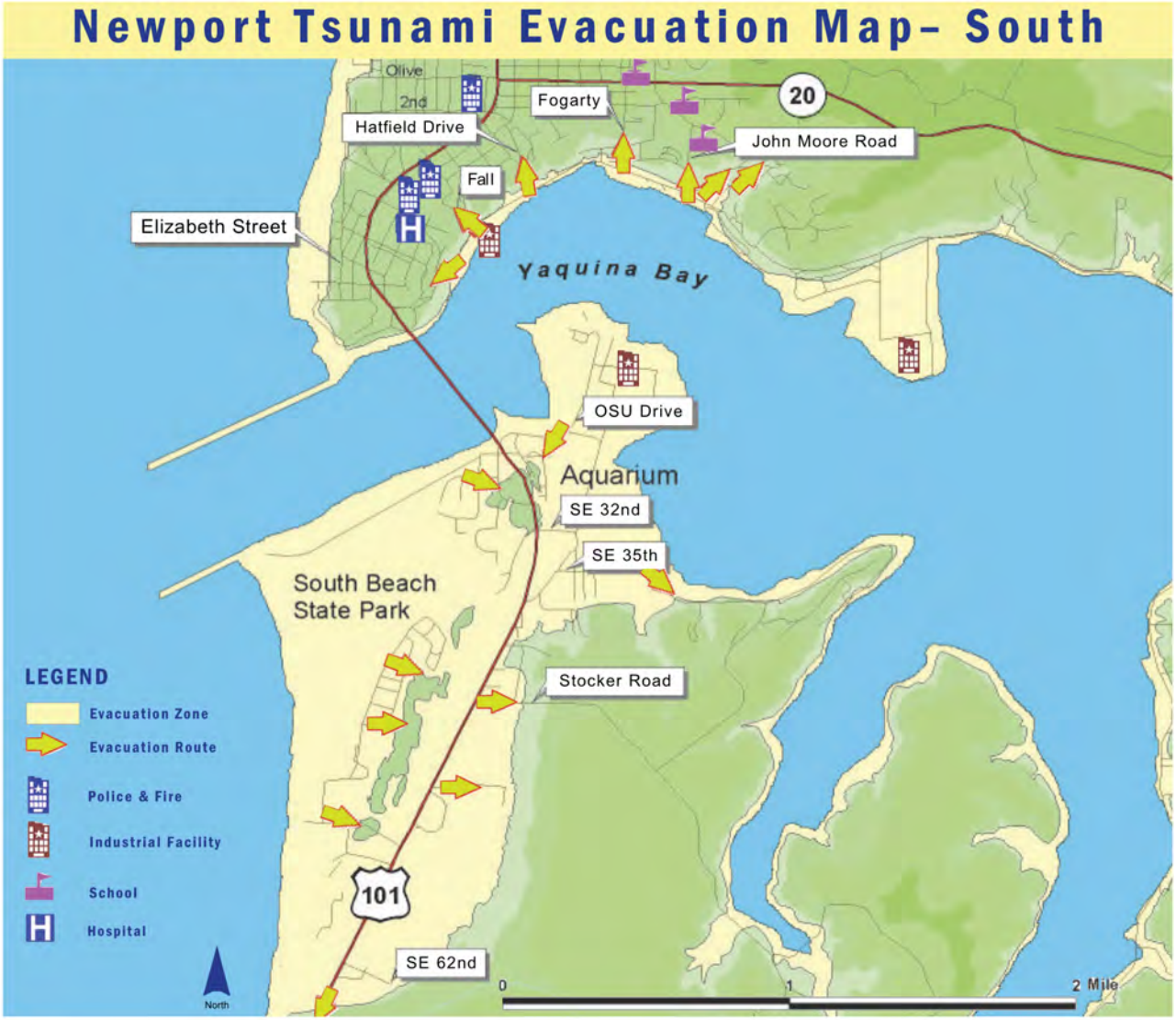

Figure 3: Evacuation map for Newport, Oregon, developed in the mid-1990s by the Oregon Department of Geology and Mineral Industries in consultation with local officials (`http://www.oregongeology.com/sub/earthquakes/coastal/tsubrochures/NewportEvac.pdf`). Evacuation routes were developed in response to a worst-case scenario for a tsunami caused by an undersea earthquake off the Oregon coast.

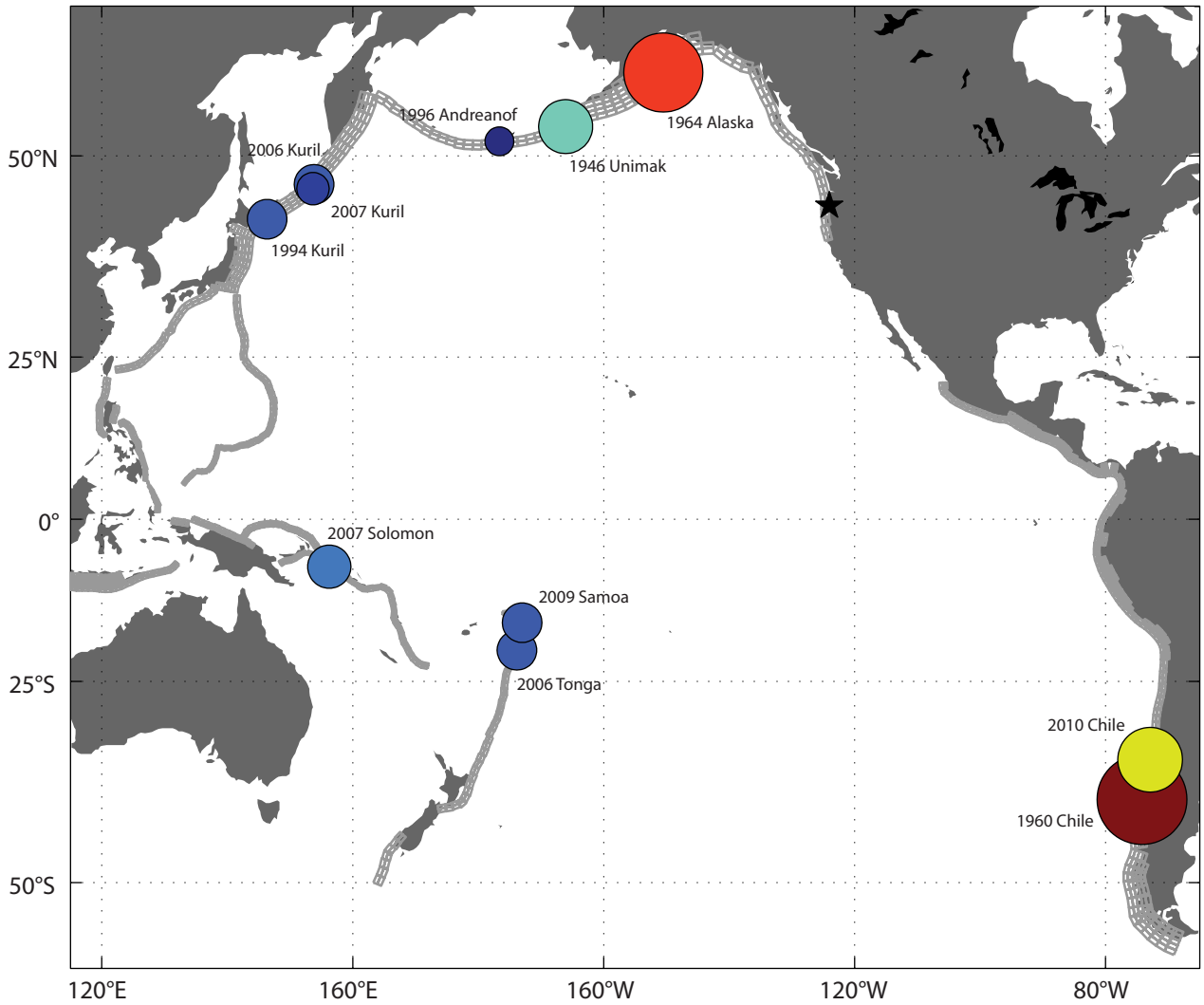

Figure 4: Map of the Pacific Ocean basin showing the location of the 11 historical events used to test and validate the Newport model. Relative earthquake magnitude is shown by the varying sizes and colors of the filled circles. The largest magnitude earthquake used in model validation was the 1960 Chile Mw 9.5 earthquake, denoted by the burnt umber circle.

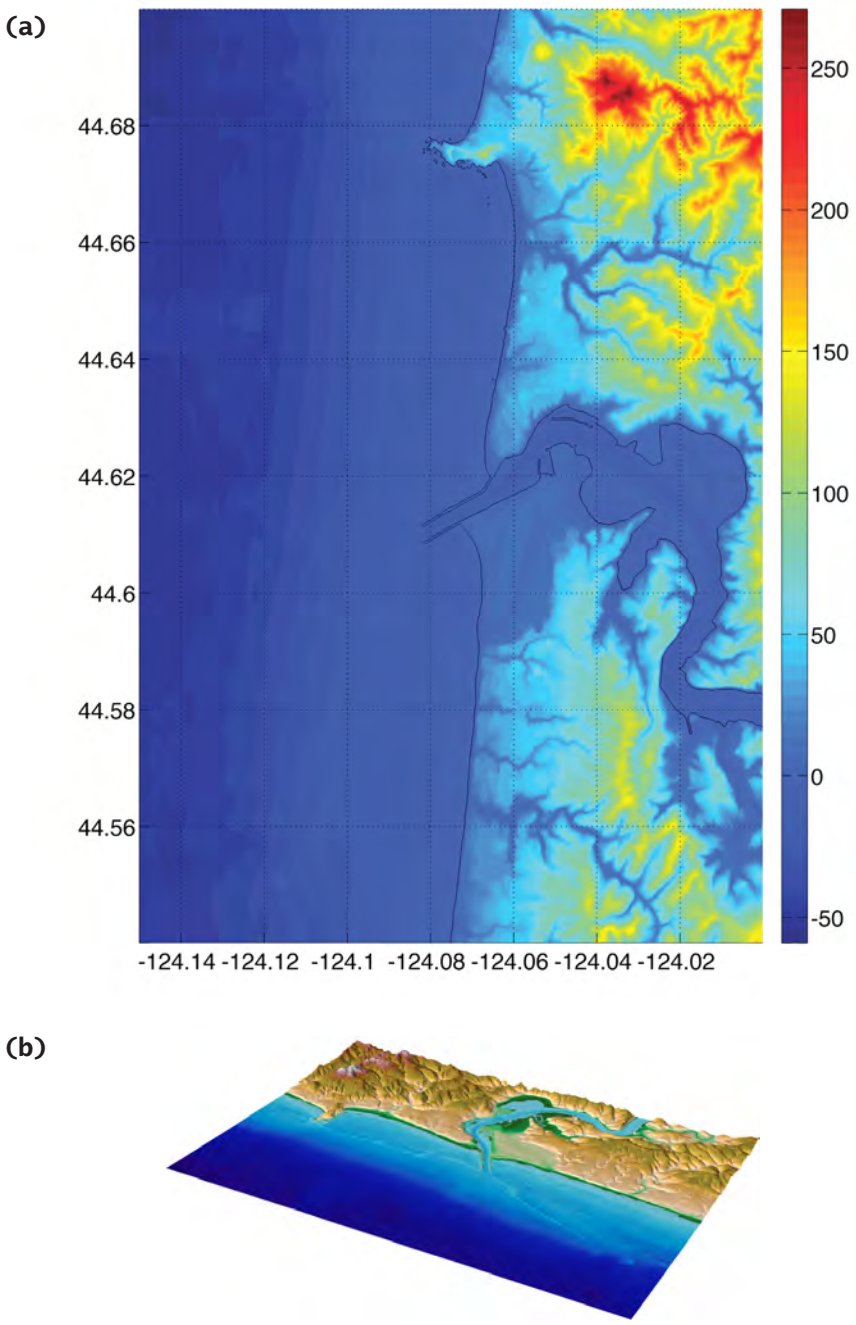

Figure 5: Digital elevation model constructed in 2004 by the NOAA Center for Tsunami Research for Newport, Oregon. (a) Shows the full extent of the grid and (b) provides an oblique view to aid in visualization. Bathymetry and topography elevations are plotted on a consistent scale represented by the color bar in (a).

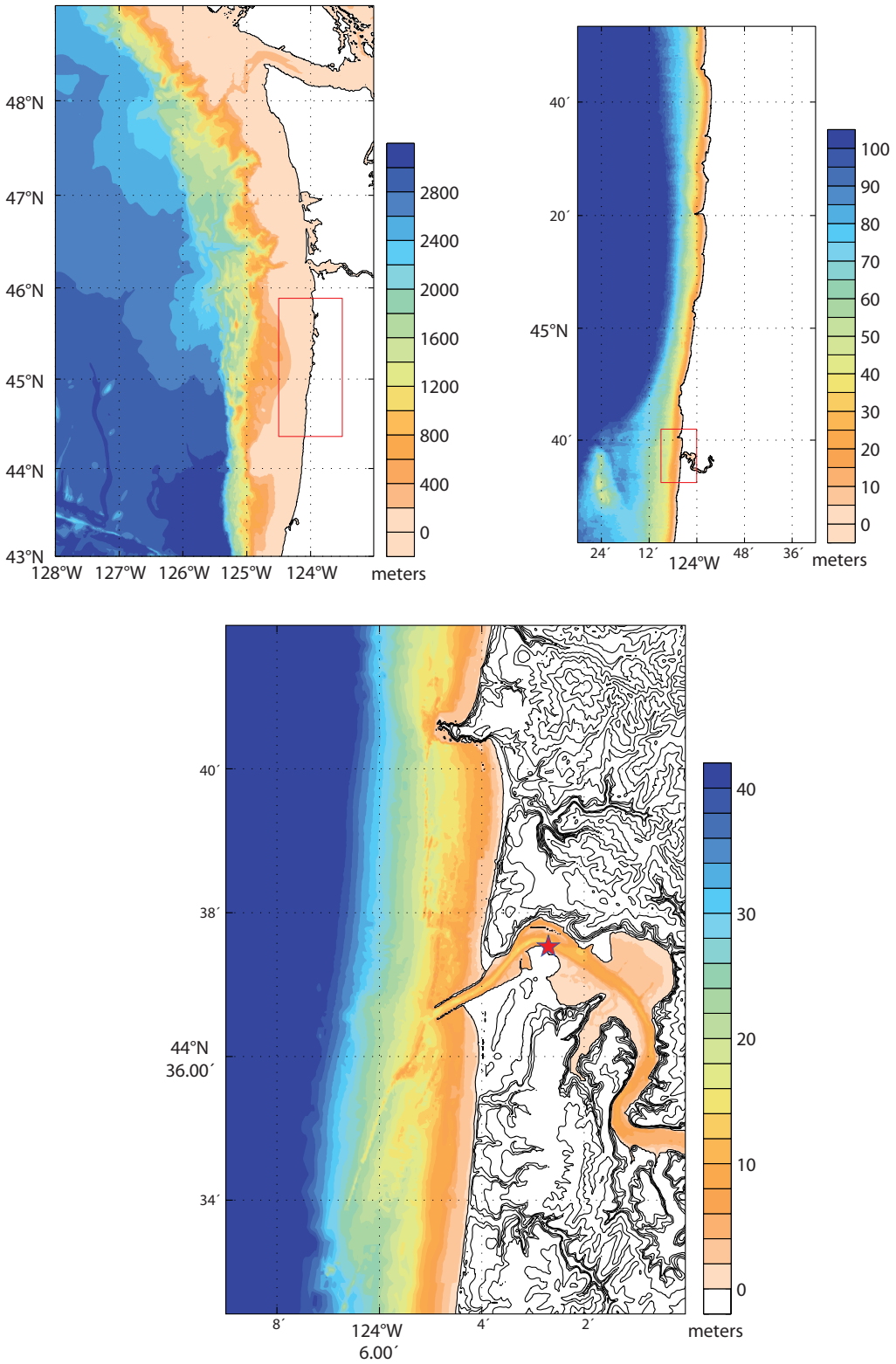

Figure 6: Bathymetry and topography for the reference inundation model grids A (top–left), B (top–right), and C (bottom). The topography of the C grid is shown using contours with 40 m intervals. The red boxes in the A and B plots show the position of the B and C grids, respectively.

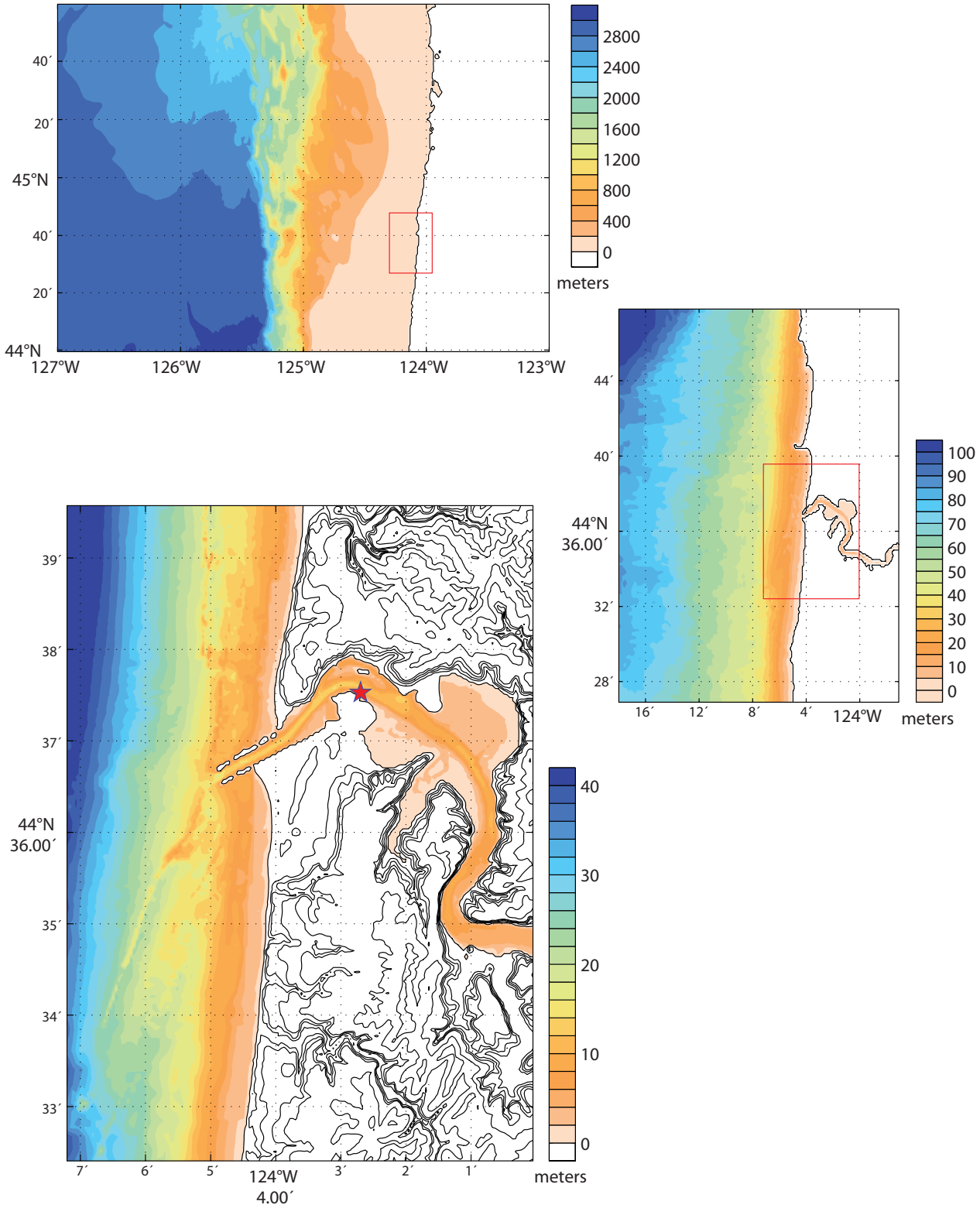

Figure 7: Bathymetry and topography for the tsunami forecast model grids A (top), B (middle–right), and C (bottom). The topography of the C grid is shown using contours with 40 m intervals. The red boxes in the A and B plots show the positions of the B and C grids, respectively.

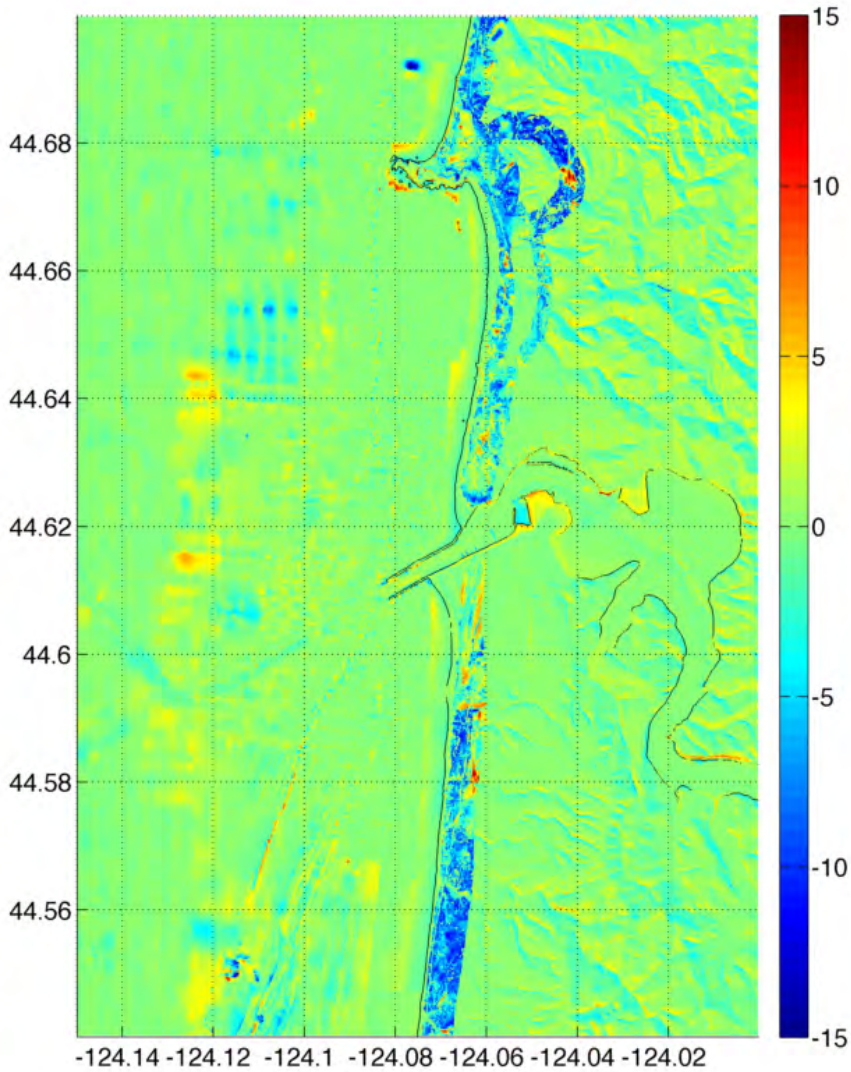

Figure 8: Difference plot showing the result of subtracting the digital elevation model constructed by the National Geophysical Data Center in 2008 from the digital elevation model constructed by the NOAA Center for Tsunami Research in 2004. The primary differences are evident along the coast from inclusion of LIDAR data in the 2008 model.

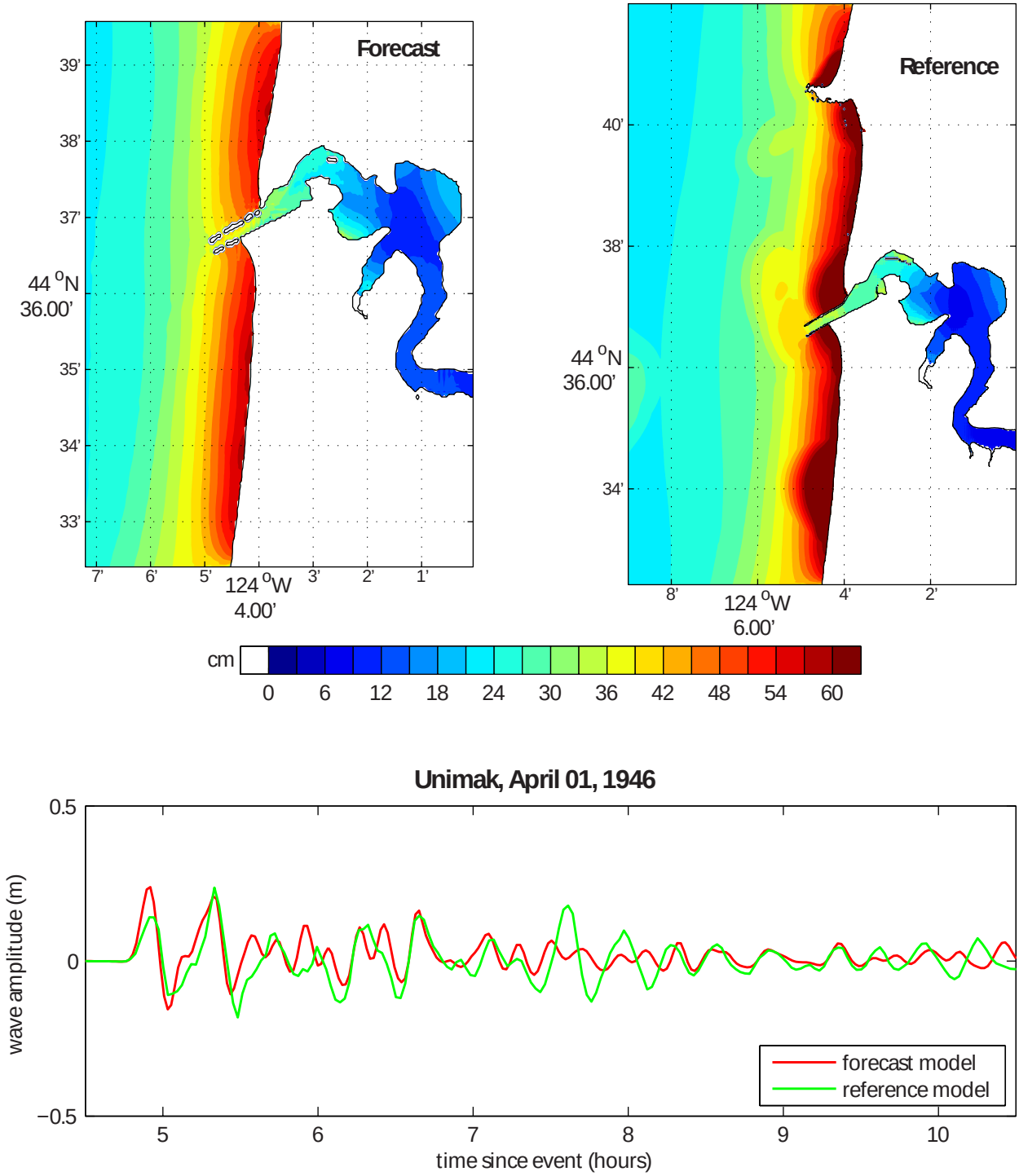

Figure 9: Model results for the 1946 Unimak Mw 8.5 event. From left to right, the upper two panels show, respectively, the forecast and reference model maximum wave height predictions. The lower panel shows the forecast model (red) and reference model (green) wave amplitudes at the Newport tide gauge.

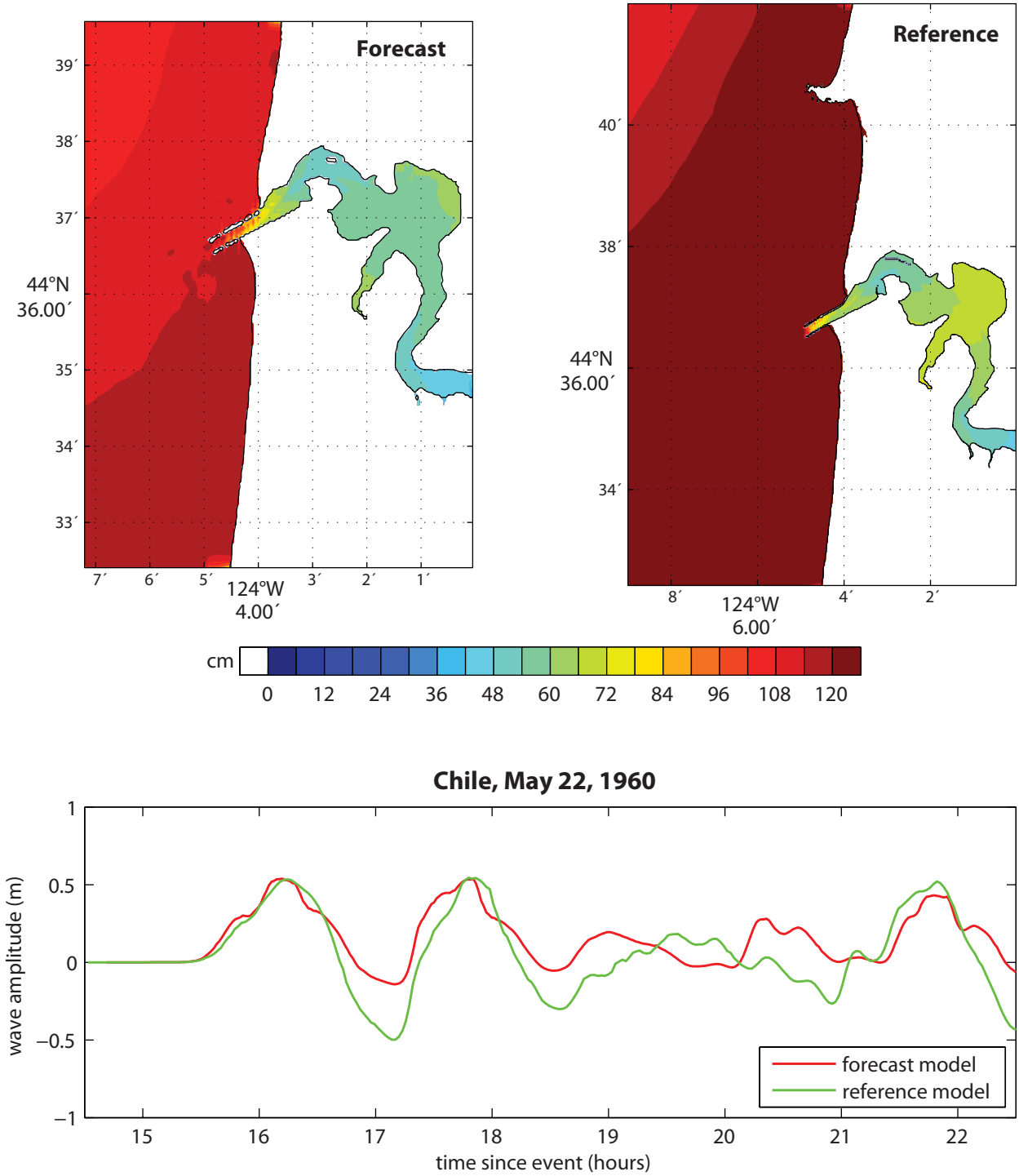

Figure 10: Model results for the 1960 Chile Mw 9.5 event. From left to right, the upper two panels show, respectively, the forecast and reference model maximum wave height predictions. The lower panel shows the forecast (red) and reference model (green) wave amplitudes at the Newport tide gauge.

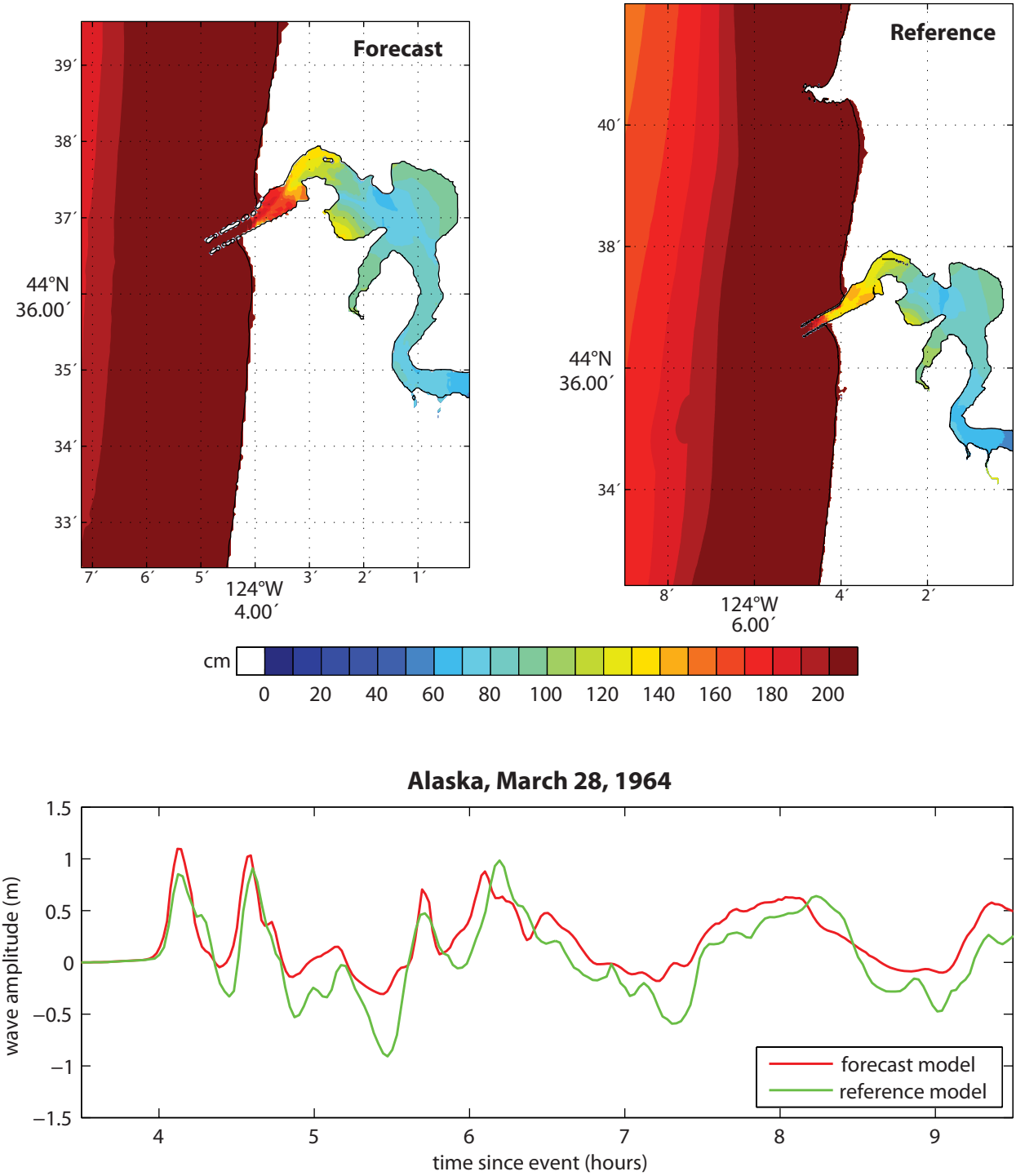

Figure 11: Model results for the 1964 Alaska Mw 9.2 event. From left to right, the upper two panels show, respectively, the forecast and reference model maximum wave height predictions. The lower panel shows the forecast model (red) and reference model (green) wave amplitudes at the Newport tide gauge.

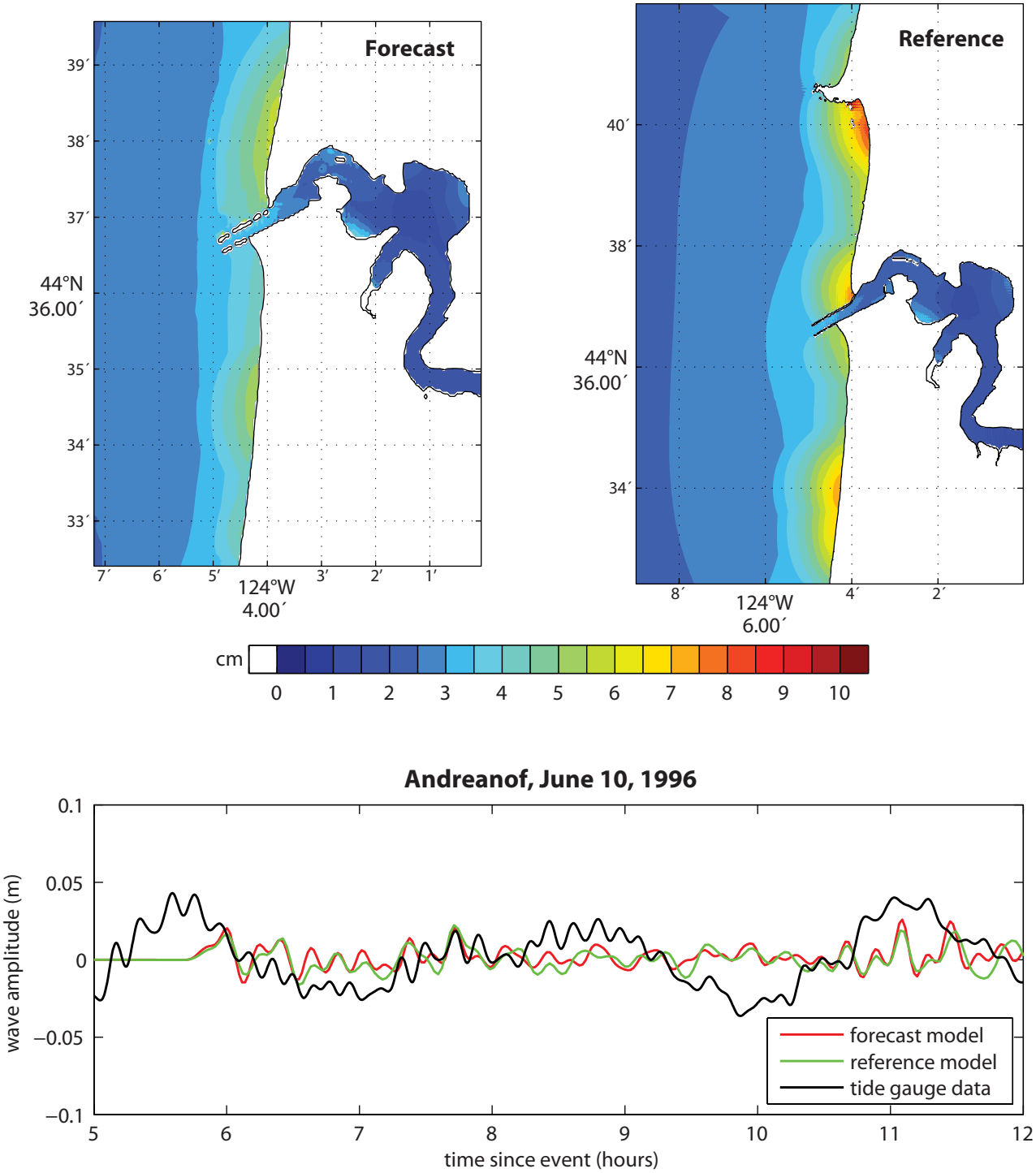

Figure 12: Model results for the 1996 Andreanof Mw 7.9 event. From left to right, the upper two panels show, respectively, the forecast and reference model maximum wave height predictions. The lower panel shows the forecast model (red), reference model (green), and observed (black) wave amplitudes at the Newport tide gauge.

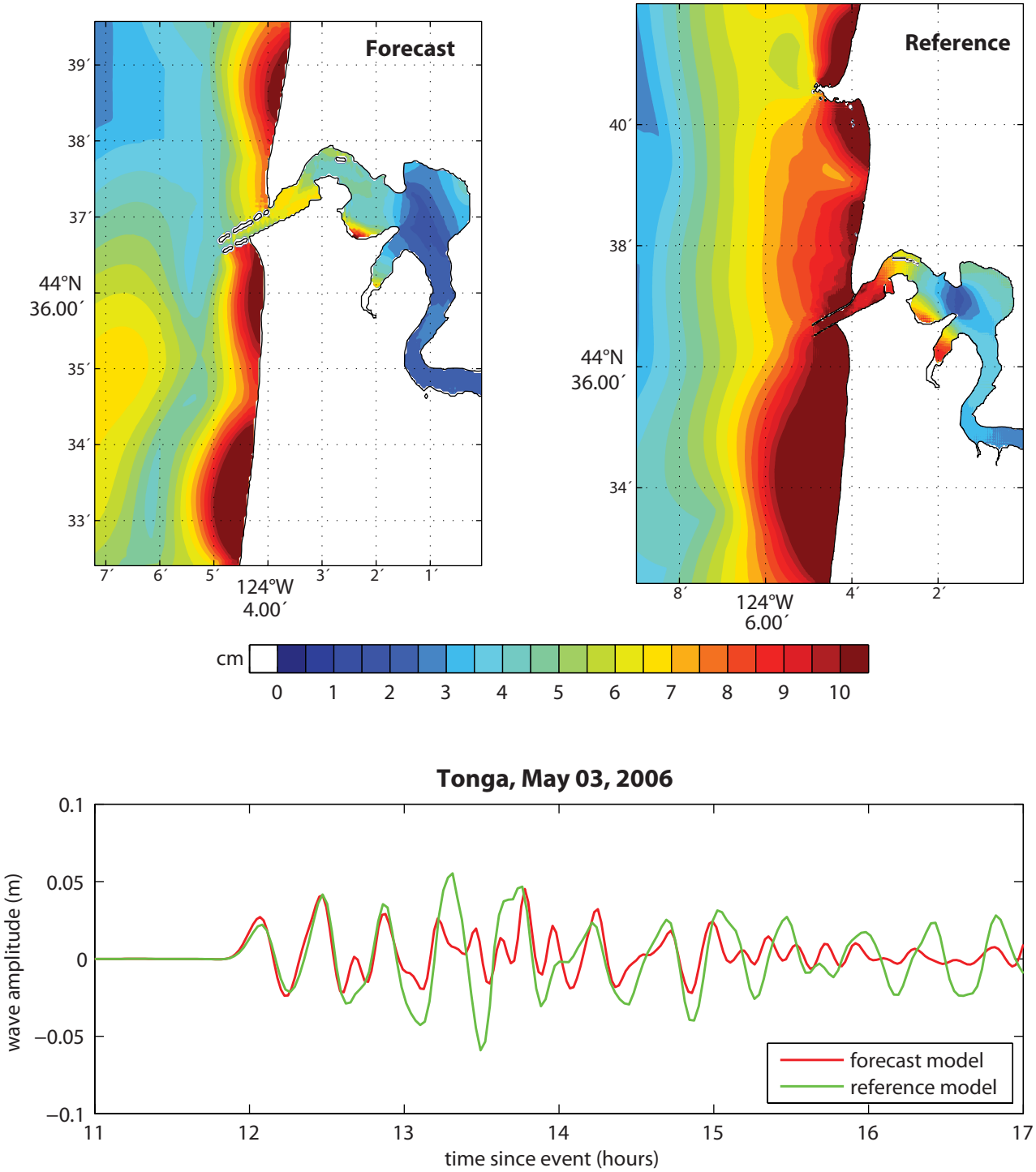

Figure 13: Model results for the 2006 Tonga Mw 8.0 event. From left to right, the upper two panels show, respectively, the forecast and reference model maximum wave height predictions. The lower panel shows the forecast model (red) and reference model (green) wave amplitudes at the Newport tide gauge.

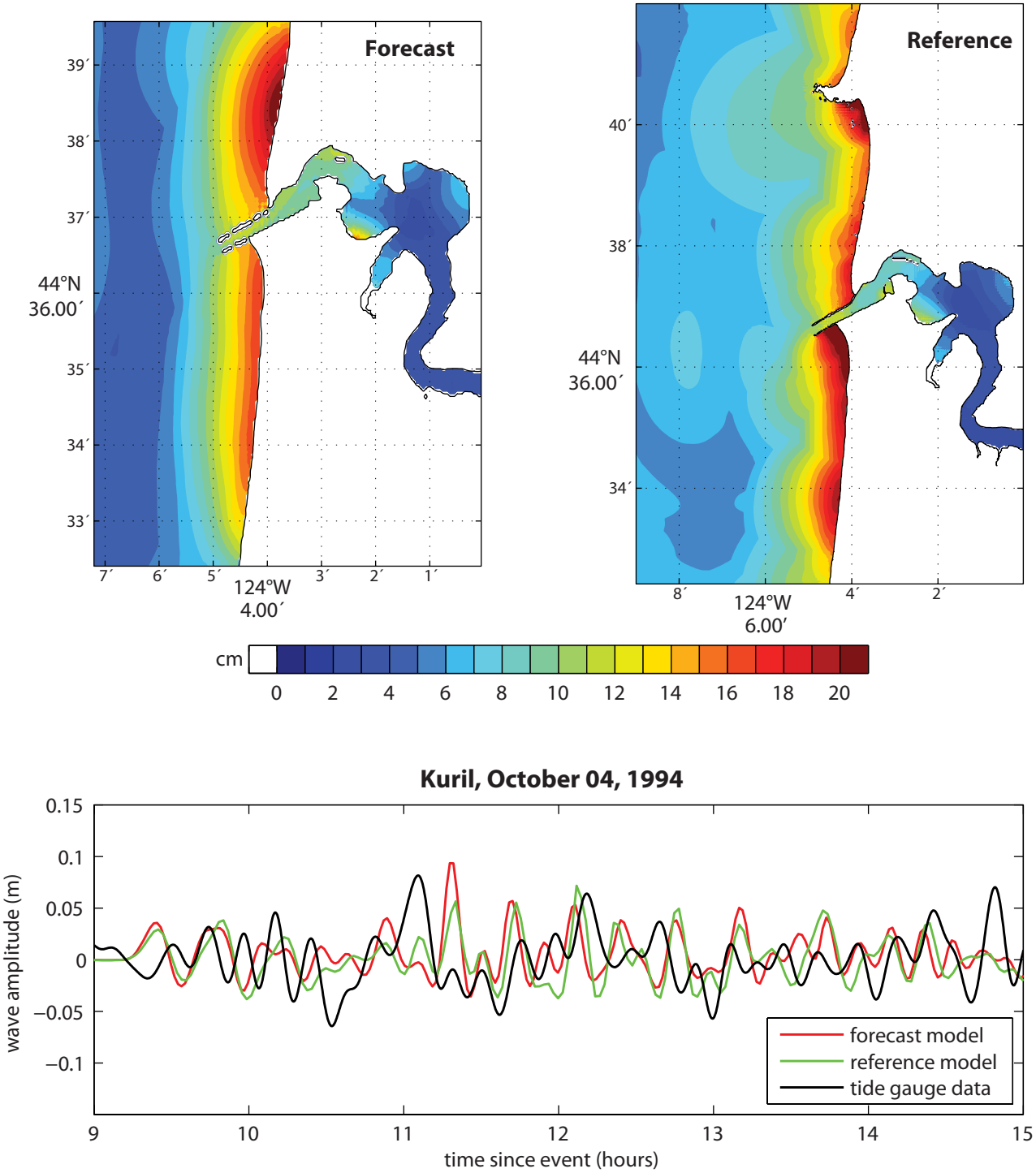

Figure 14: Model results for the 1994 Kuril Mw 8.3 event. From left to right, the upper two panels show, respectively, the forecast and reference model maximum wave height predictions. The lower panel shows the forecast model (red), reference model (green), and observed (black) wave amplitudes at the Newport tide gauge.

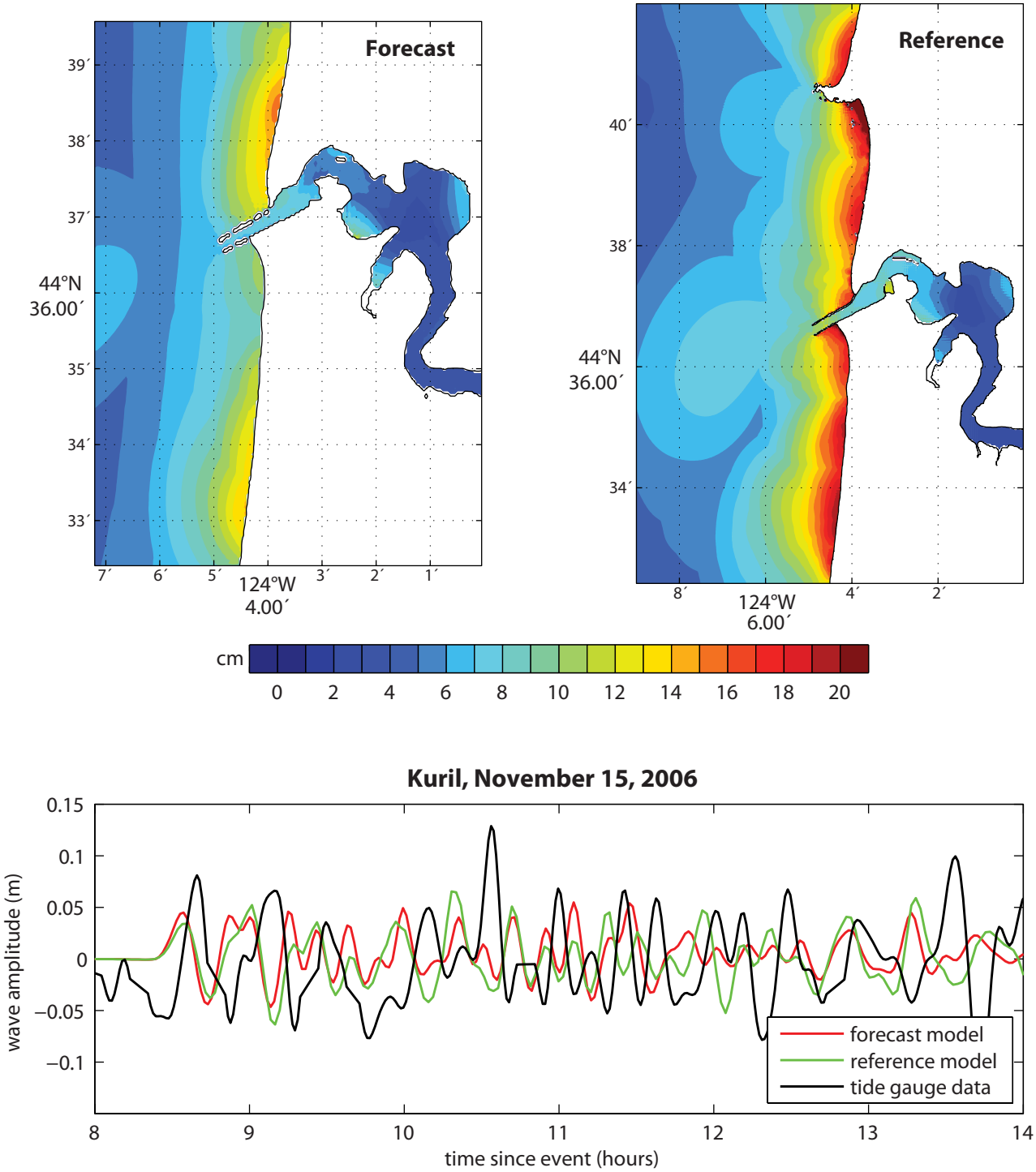

Figure 15: Model results for the 2006 Kuril Mw 8.3 event. From left to right, the upper two panels show, respectively, the forecast and reference model maximum wave height predictions. The lower panel shows the forecast model (red), reference model (green), and observed (black) wave amplitudes at the Newport tide gauge.

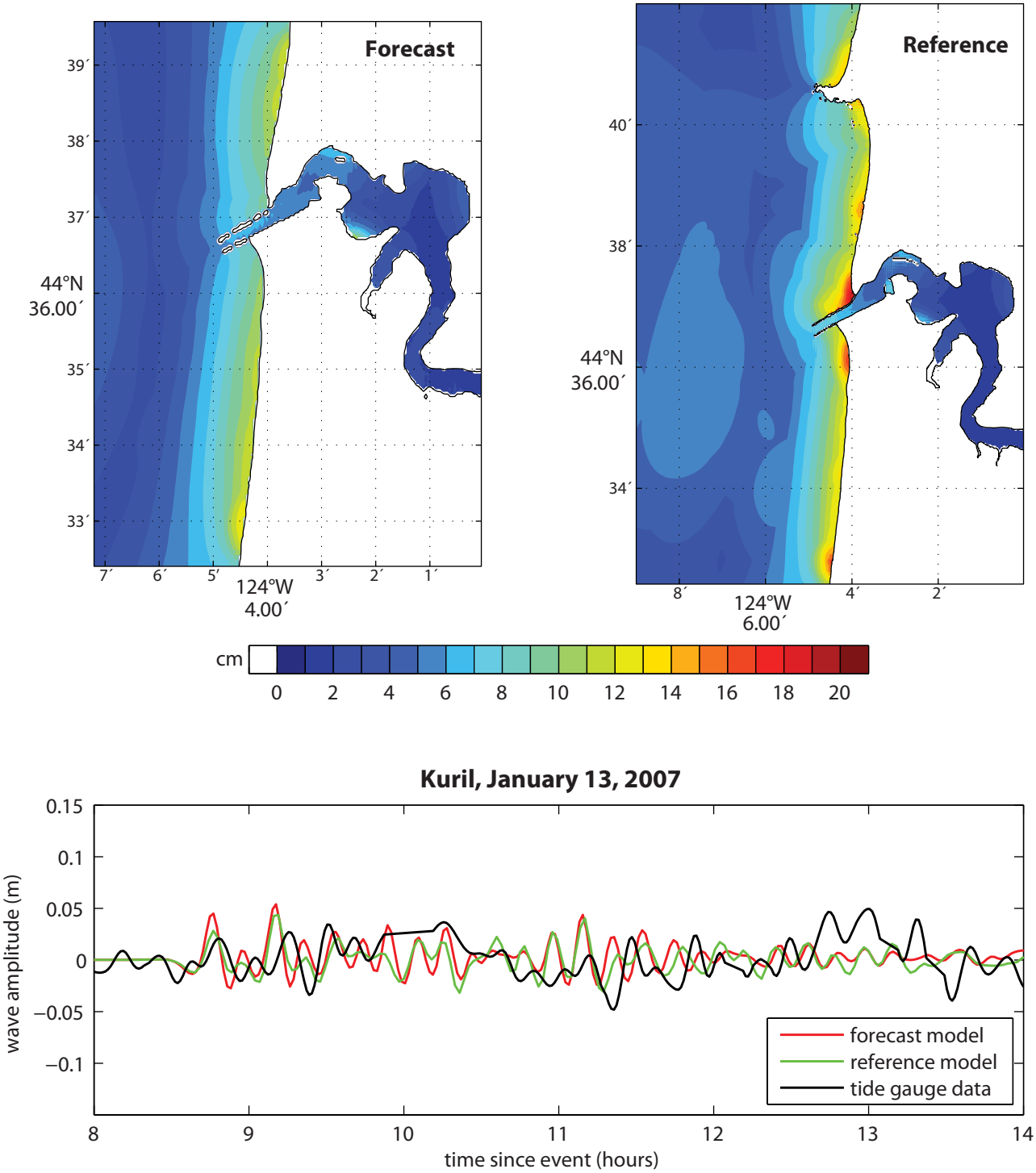

Figure 16: Model results for the 2007 Kuril Mw 8.1 event. From left to right, the upper two panels show, respectively, the forecast and reference model maximum wave height predictions. The lower panel shows the forecast model (red), reference model (green), and observed (black) wave amplitudes at the Newport tide gauge.

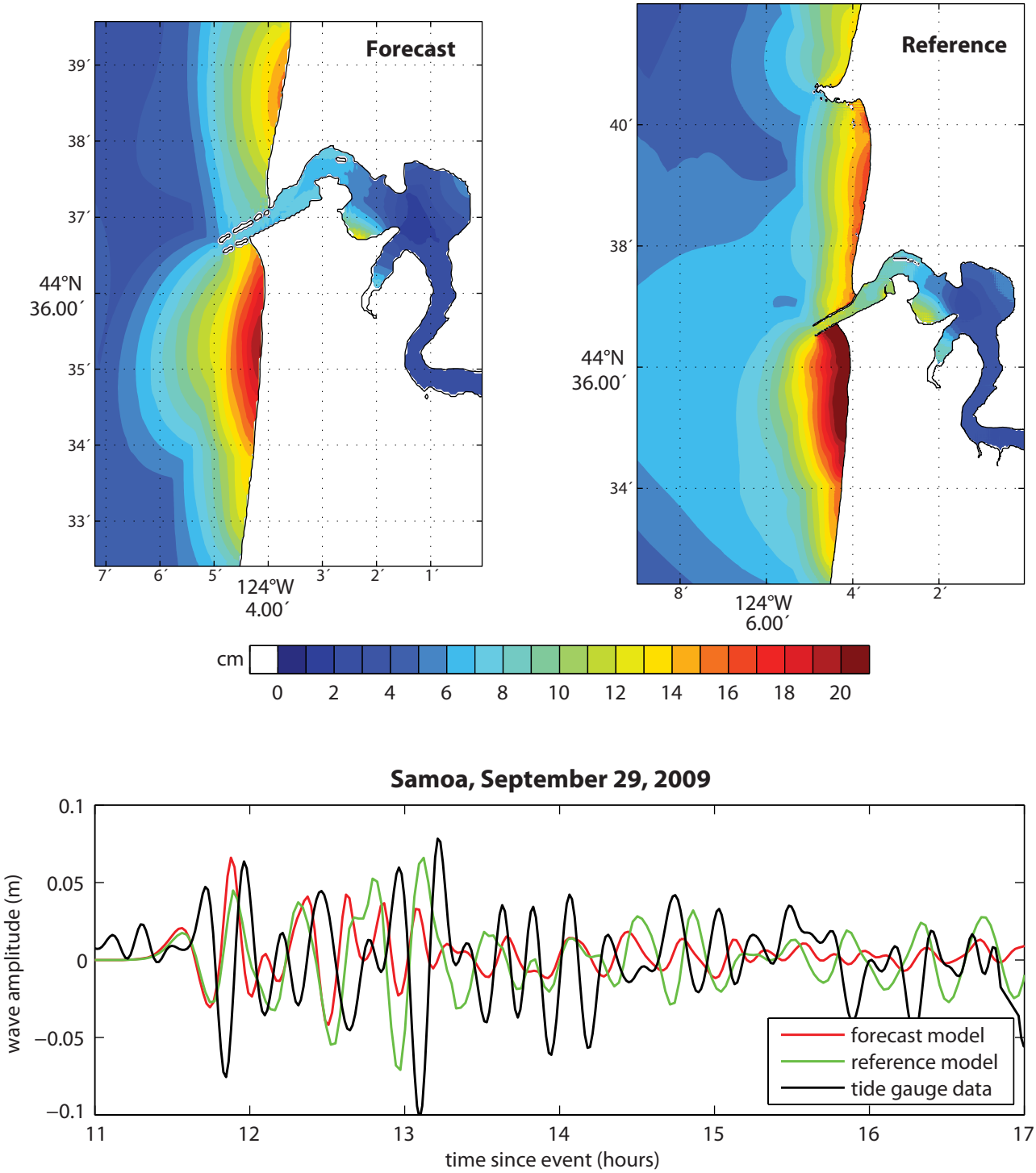

Figure 17: Model results for the 2009 Samoa Mw 8.1 event. From left to right, the upper two panels show, respectively, the forecast and reference model maximum wave height predictions. The lower panel shows the forecast model (red), reference model (green), and observed (black) wave amplitudes at the Newport tide gauge.

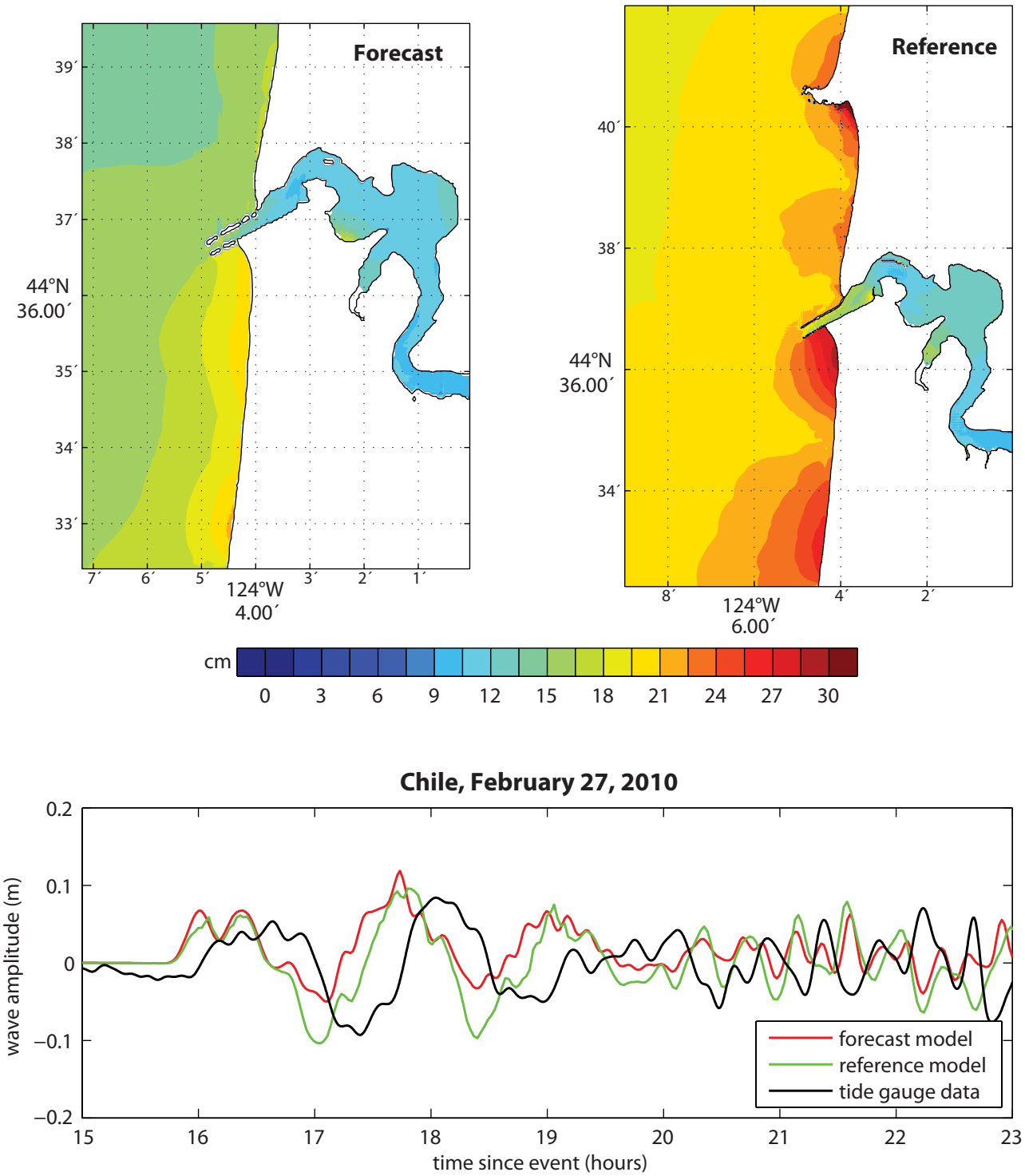

Figure 18: Model results for the 2010 Chile Mw 8.8 event. From left to right, the upper two panels show, respectively, the forecast and reference model maximum wave height predictions. The lower panel shows the forecast model (red), reference model (green), and observed (black) wave amplitudes at the Newport tide gauge.

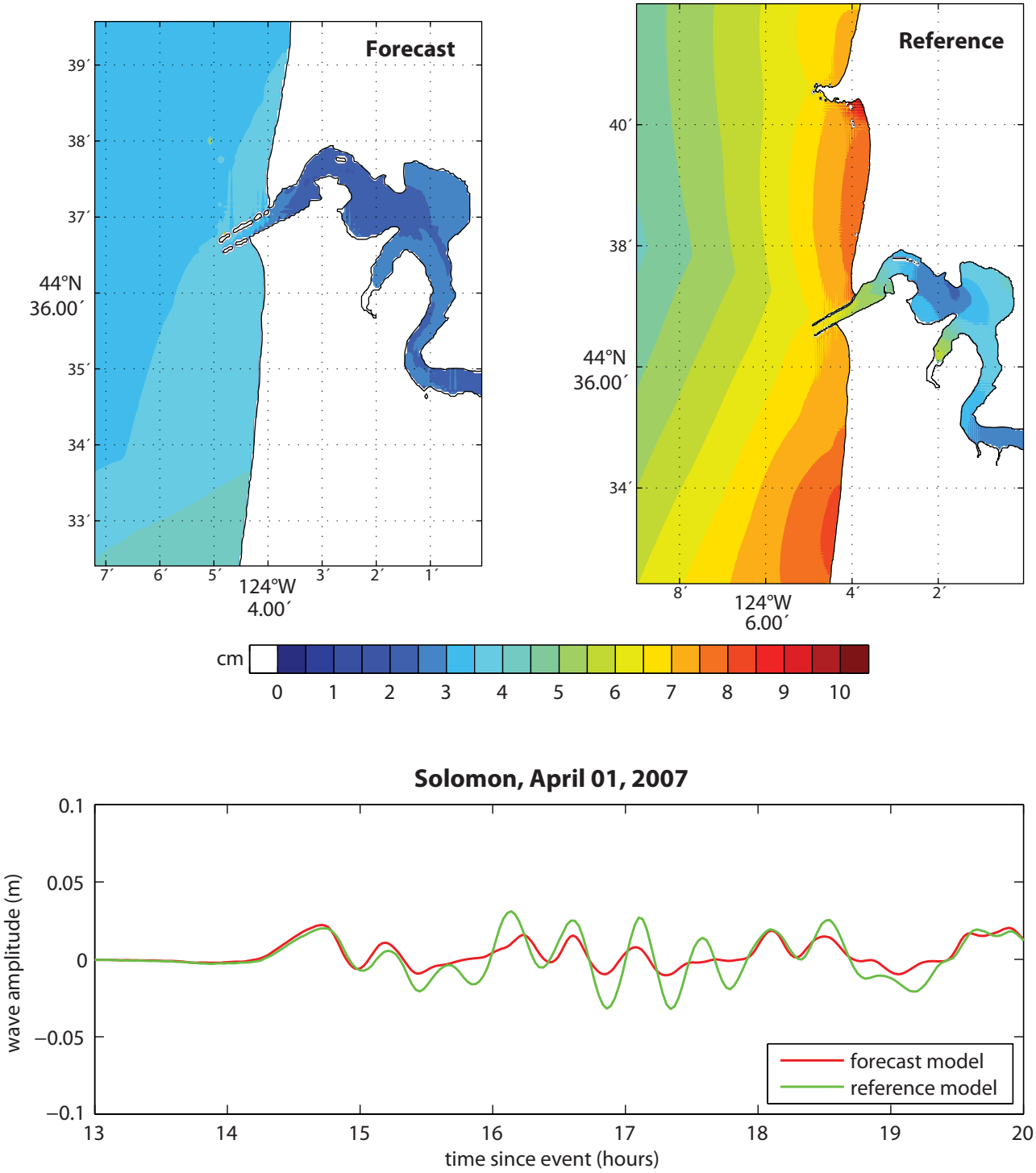

Figure 19: Model results for the 2007 Solomon Mw 8.1 event. From left to right, the upper two panels show, respectively, the forecast and reference model maximum wave height predictions. The lower panel shows the forecast model (red) and reference model (green) wave amplitudes at the Newport tide gauge.

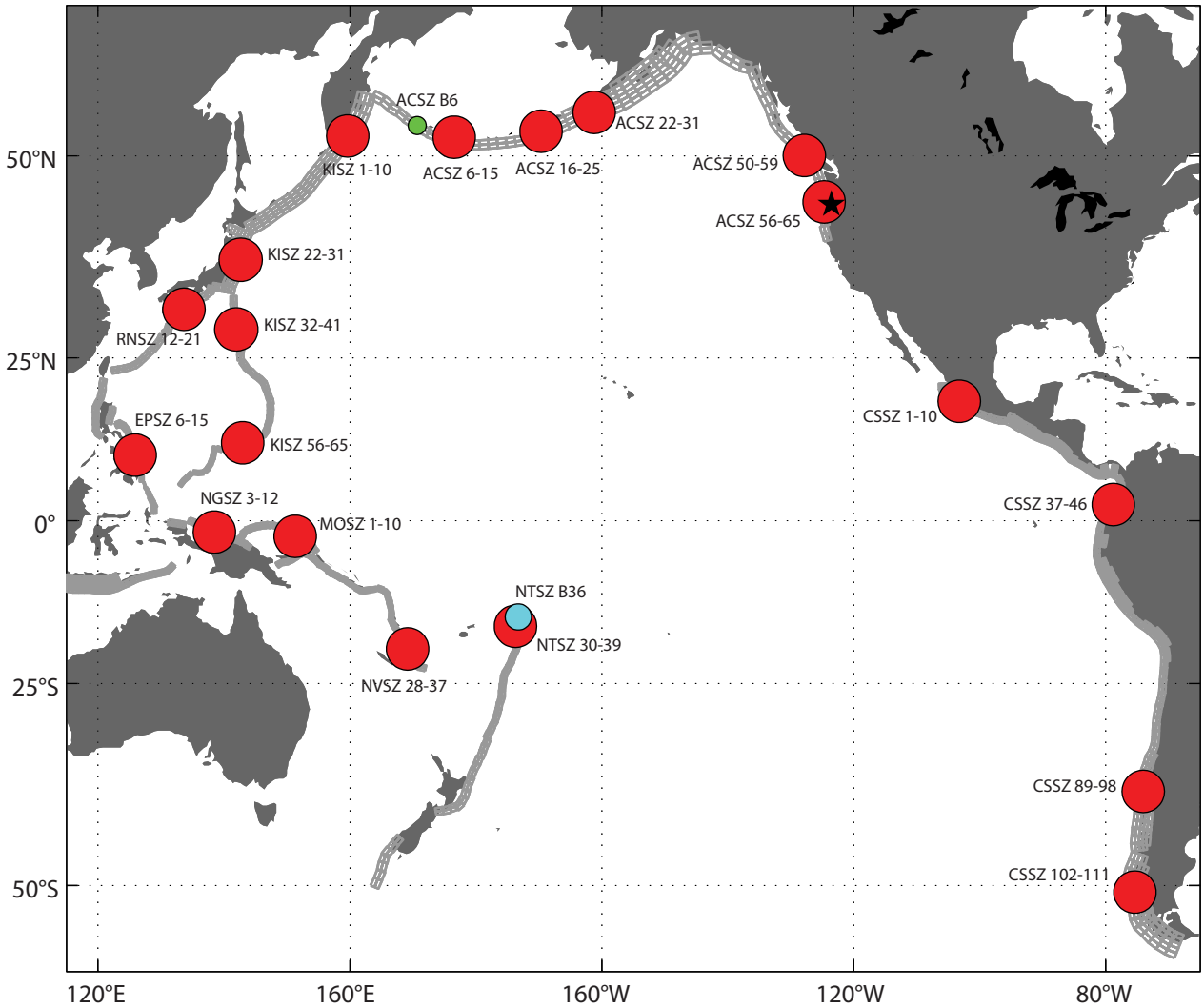

Figure 20: Map of the Pacific Ocean basin showing the locations of the 19 simulated Mw 9.3 events, the Mw 7.5 medium event, and the micro-tsunami event used to test and validate the Newport model. The solid star denotes the location of Newport.

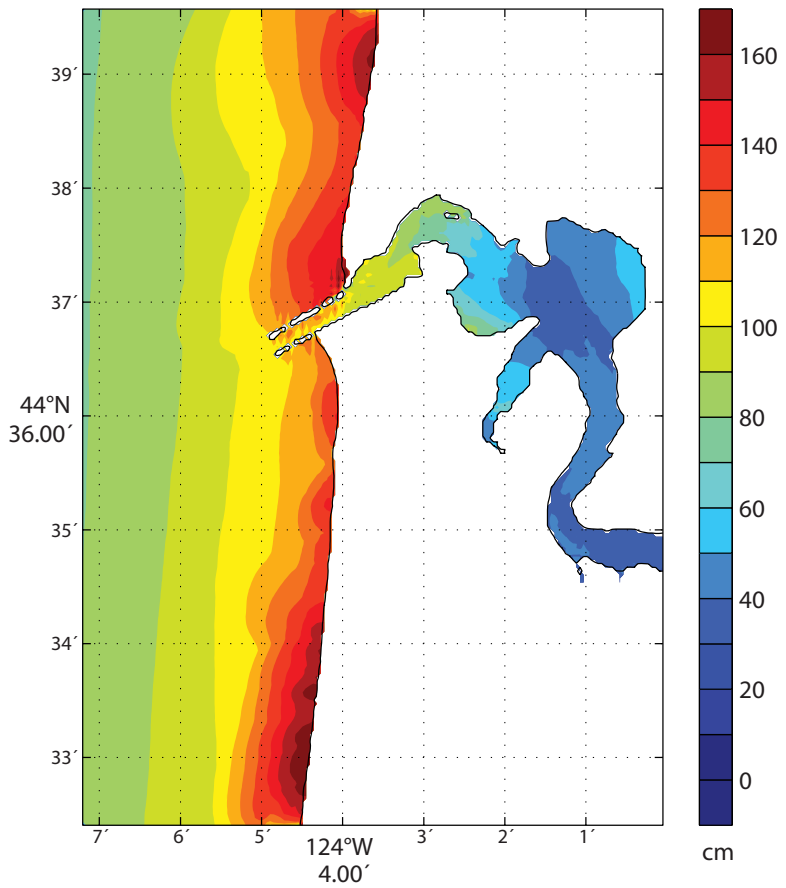

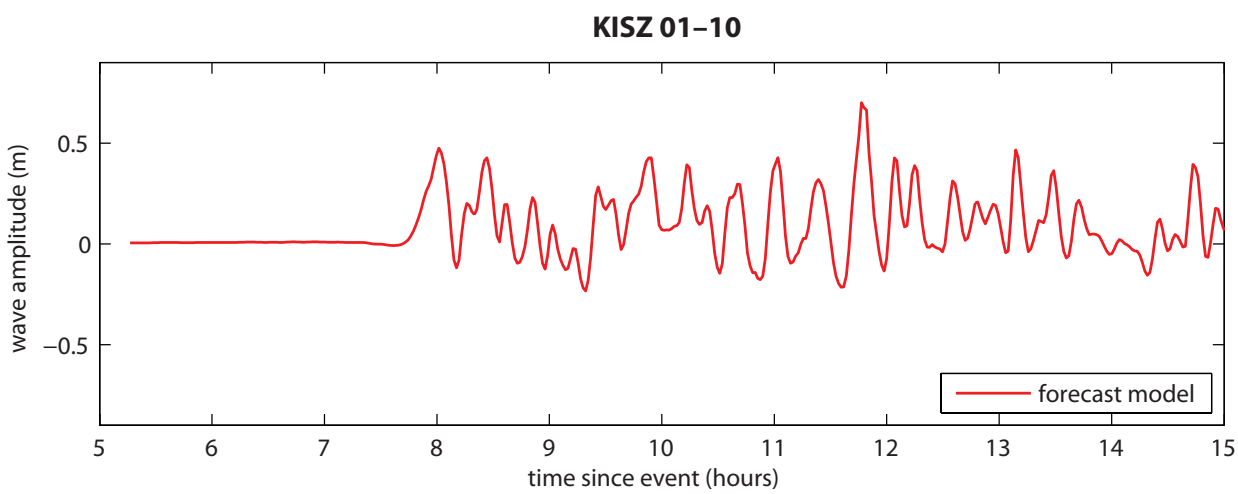

Figure 21: Results from the forecast model for the KISZ 1–10 synthetic event. The upper panel shows the map of predicted maximum wave height in the Newport C grid and the lower panel shows the time series of wave amplitude at the tide gauge location.

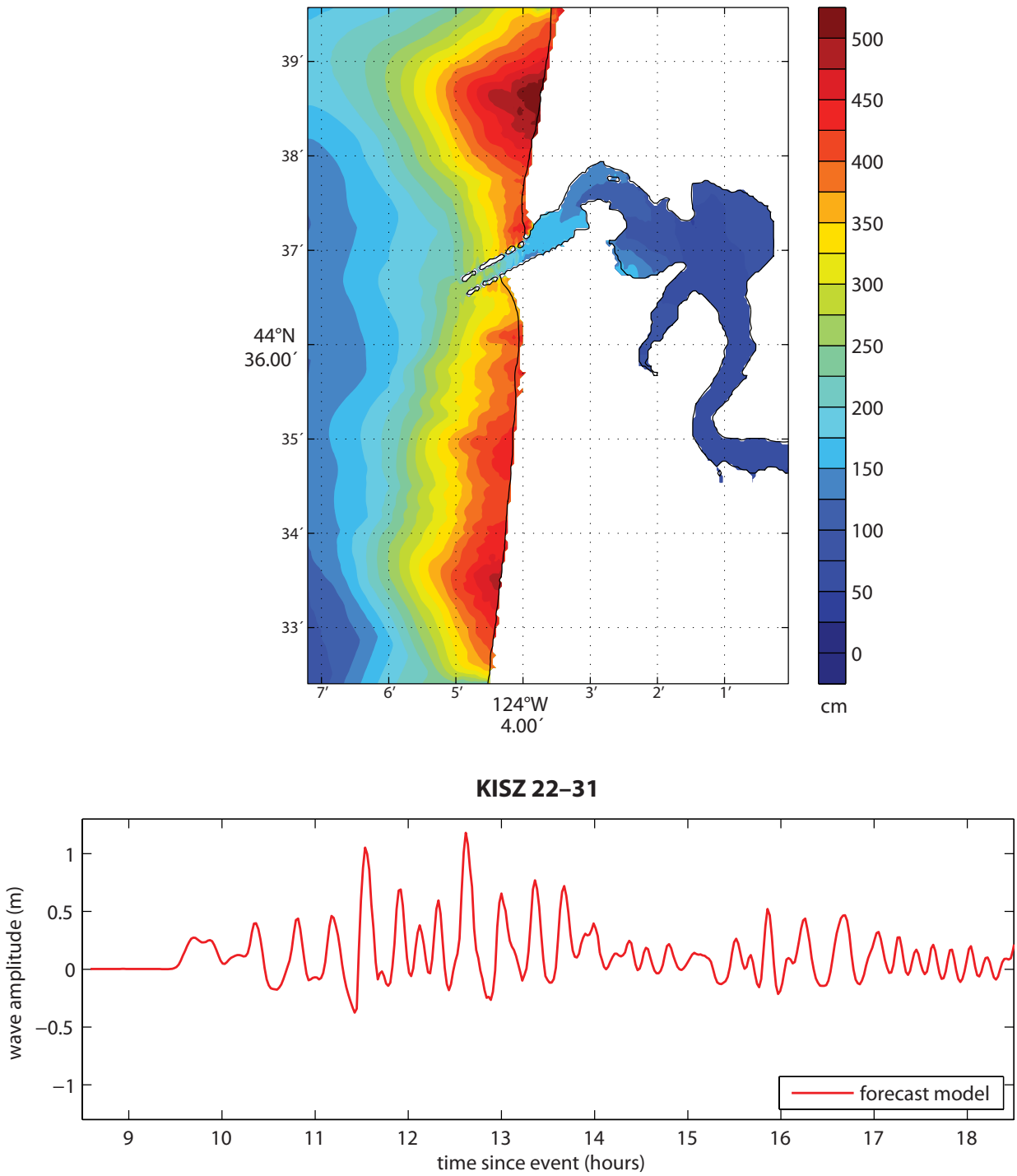

Figure 22: Results from the forecast model for the KISZ 22–31 synthetic event. The upper panel shows the map of predicted maximum wave height in the Newport C grid and the lower panel shows the time series of wave amplitude at the tide gauge location.

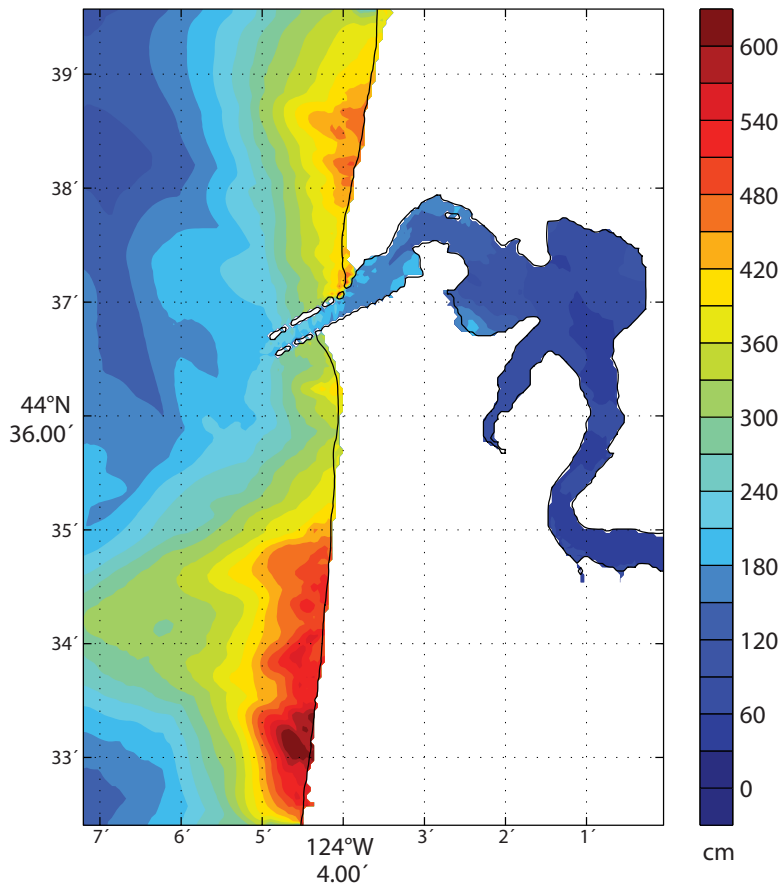

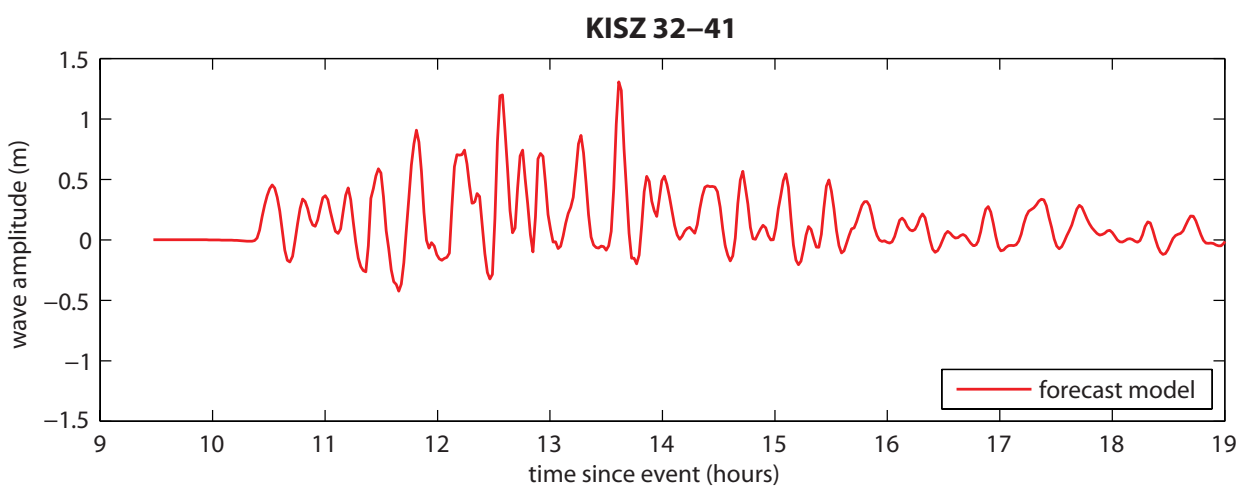

Figure 23: Results from the forecast model for the KISZ 32–41 synthetic event. The upper panel shows the map of predicted maximum wave height in the Newport C grid and the lower panel shows the time series of wave amplitude at the tide gauge location.

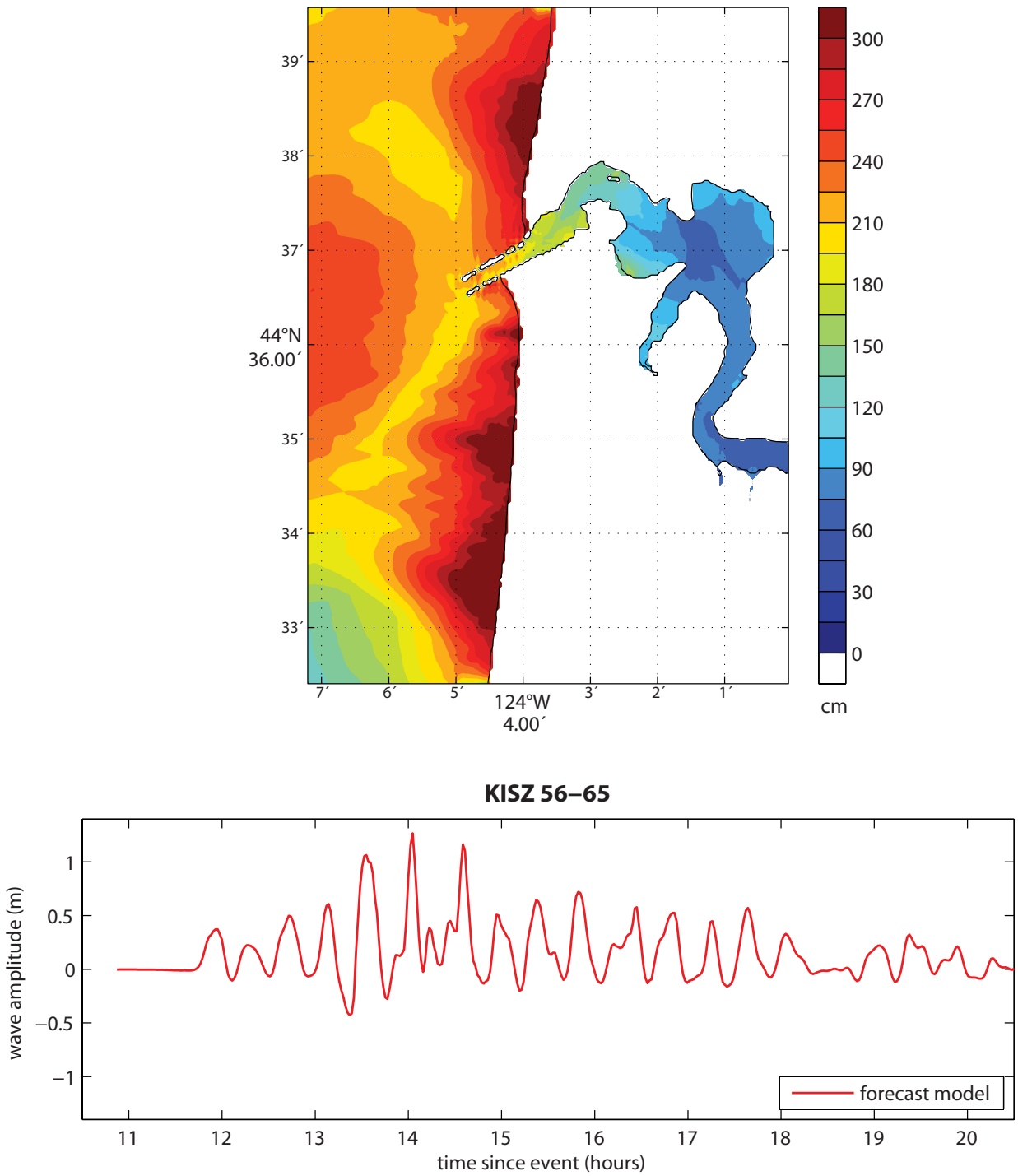

Figure 24: Results from the forecast model for the KISZ 56–65 synthetic event. The upper panel shows the map of predicted maximum wave height in the Newport C grid and the lower panel shows the time series of wave amplitude at the tide gauge location.

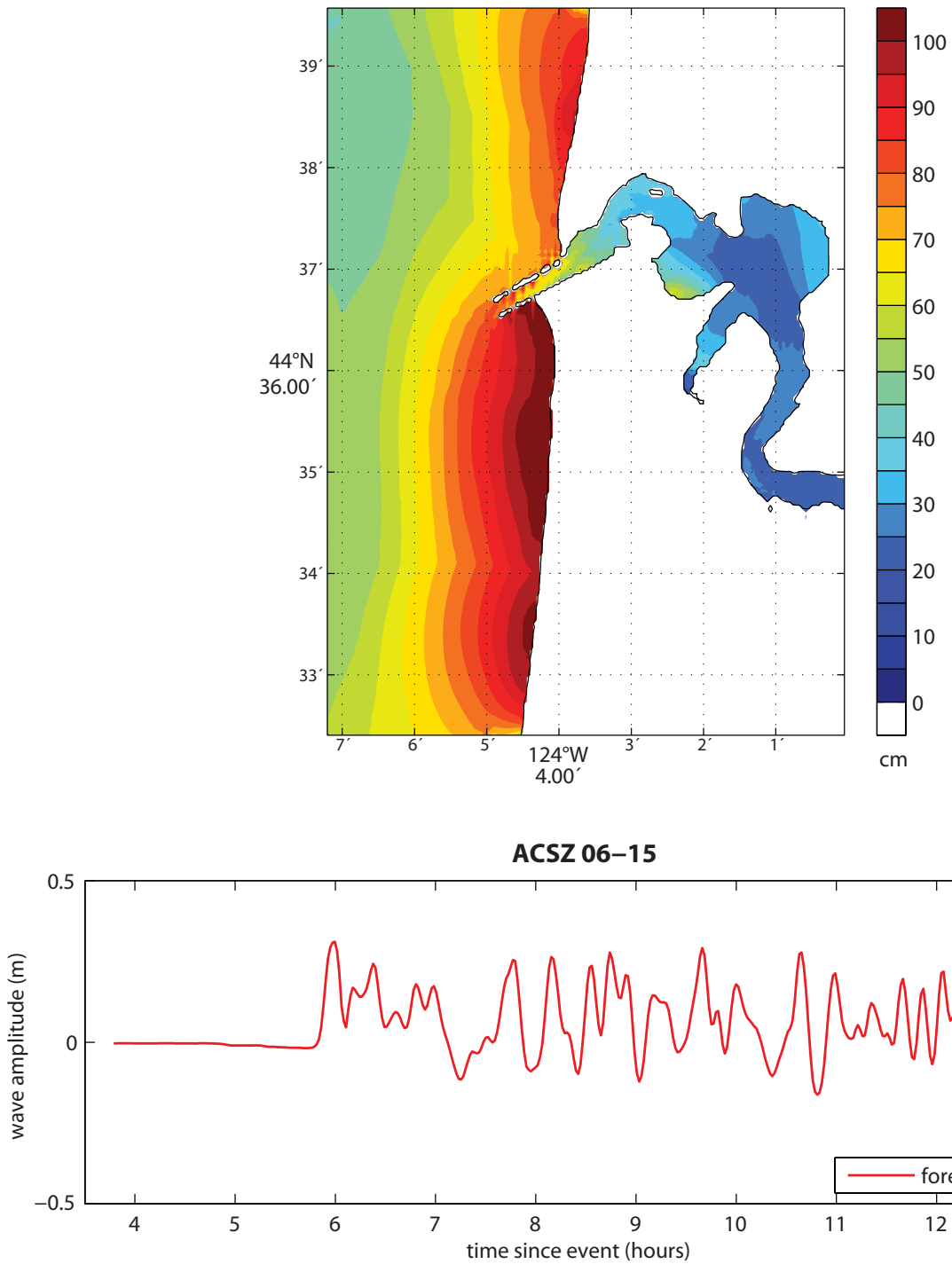

Figure 25: Results from the forecast model for the ACSZ 6–15 synthetic event. The upper panel shows the map of predicted maximum wave height in the Newport C grid and the lower panel shows the time series of wave amplitude at the tide gauge location.

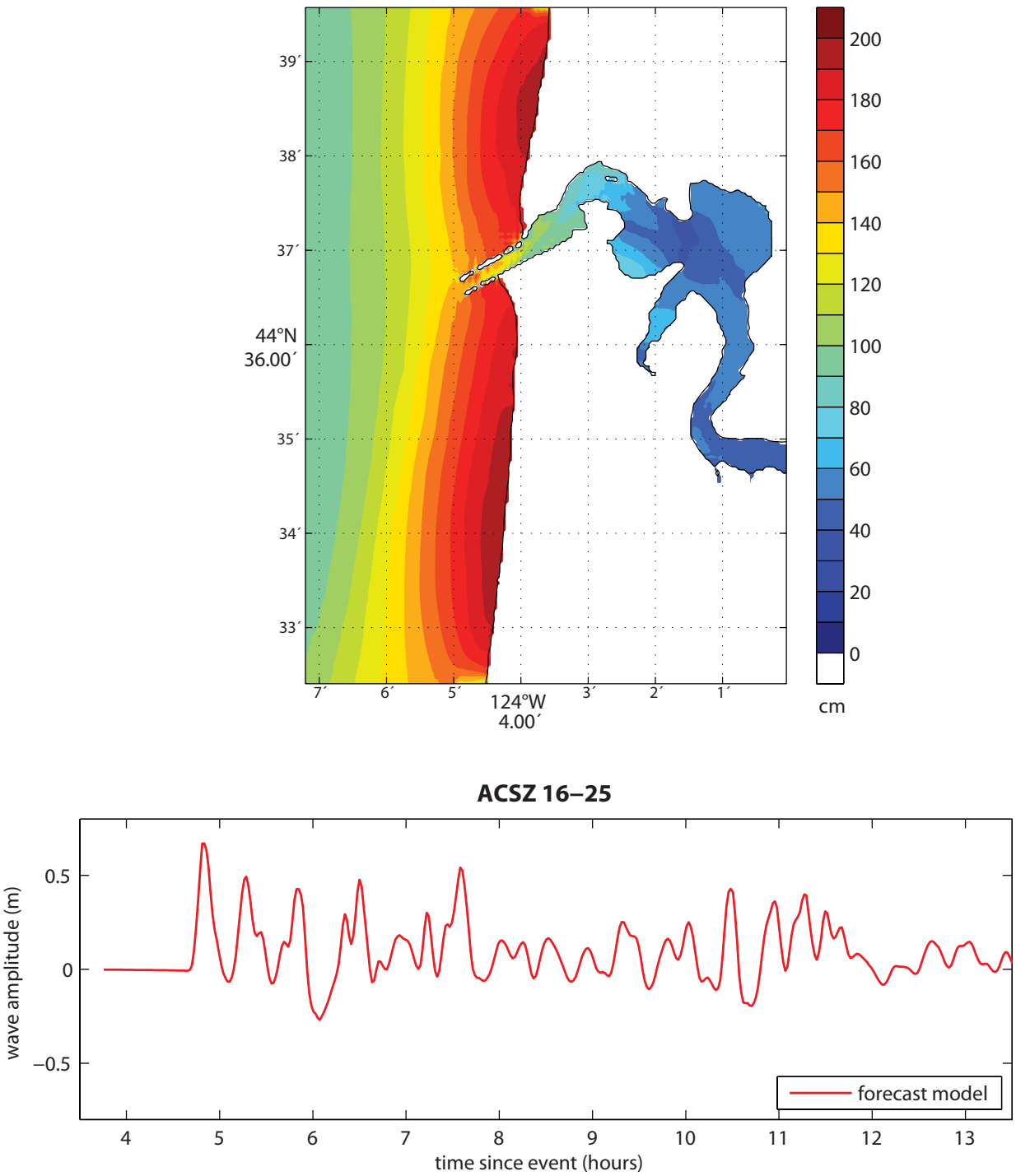

Figure 26: Results from the forecast model for the ACSZ 16–25 synthetic event. The upper panel shows the map of predicted maximum wave height in the Newport C grid and the lower panel shows the time series of wave amplitude at the tide gauge location.

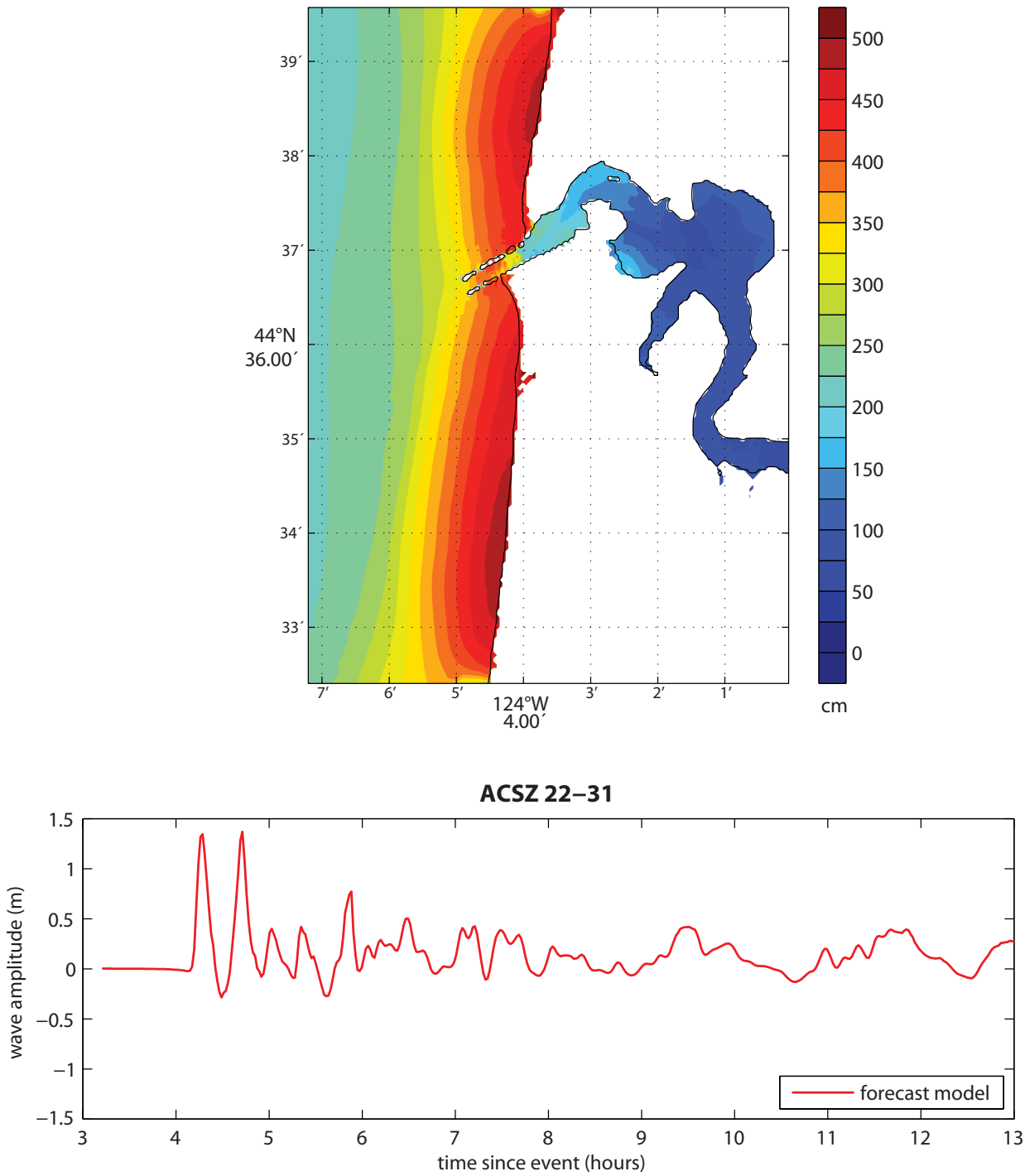

Figure 27: Results from the forecast model for the ACSZ 22–31 synthetic event. The upper panel shows the map of predicted maximum wave height in the Newport C grid and the lower panel shows the time series of wave amplitude at the tide gauge location.

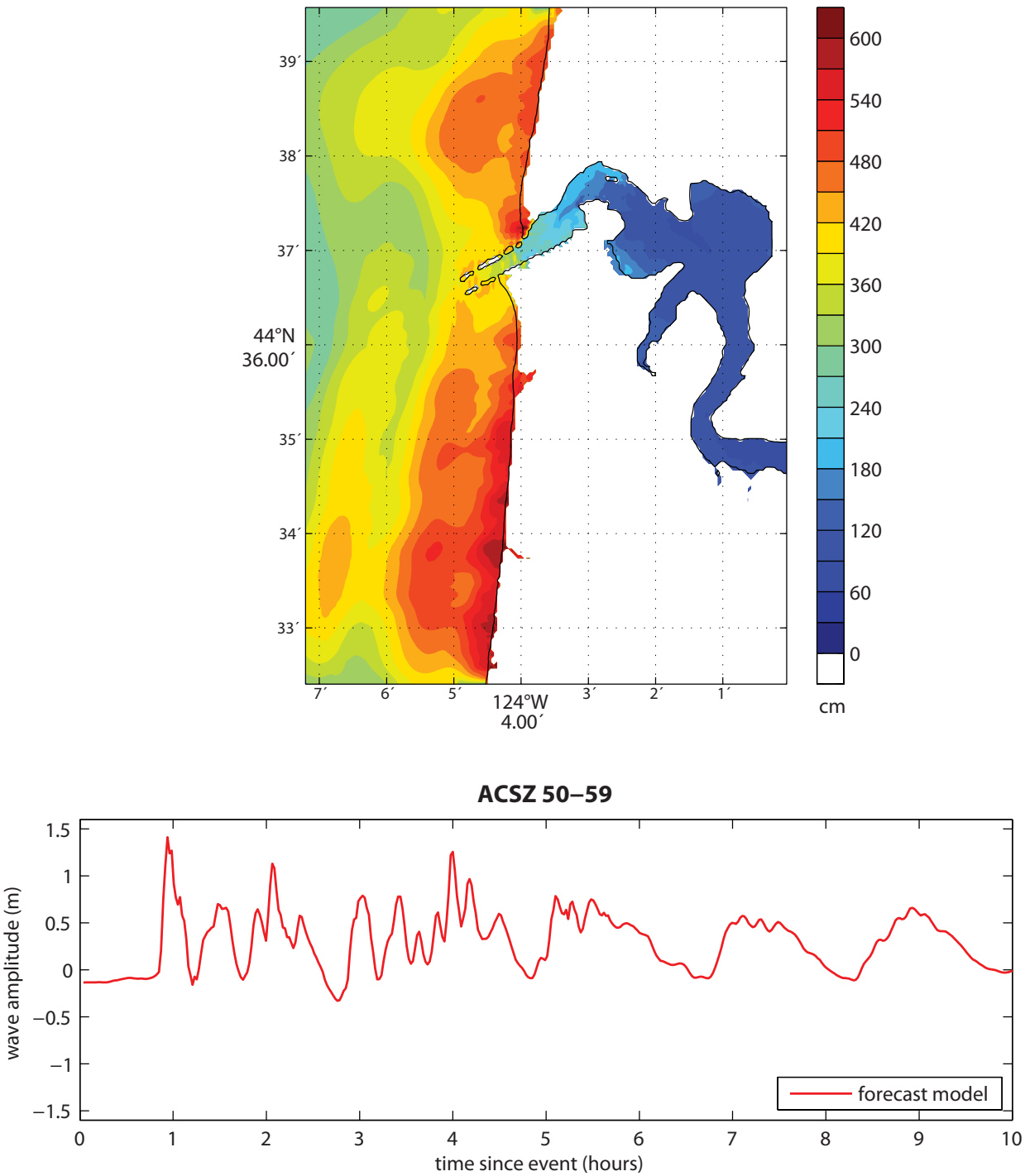

Figure 28: Results from the forecast model for the ACSZ 50–59 synthetic event. The upper panel shows the map of predicted maximum wave height in the Newport C grid and the lower panel shows the time series of wave amplitude at the tide gauge location.

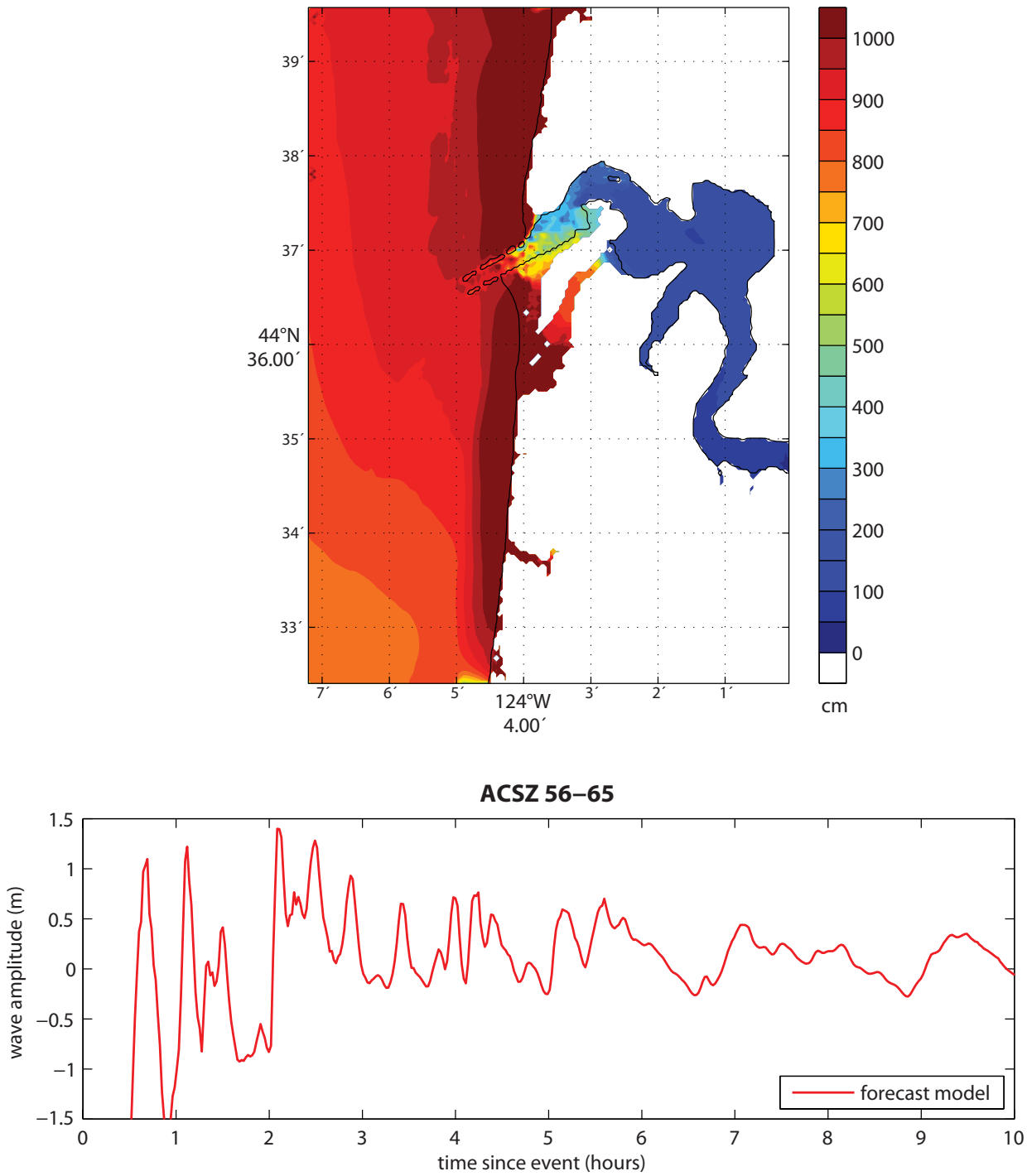

Figure 29: Results from the forecast model for the ACSZ 56–65 synthetic event. The upper panel shows the map of predicted maximum wave height in the Newport C grid and the lower panel shows the time series of wave amplitude at the tide gauge location.

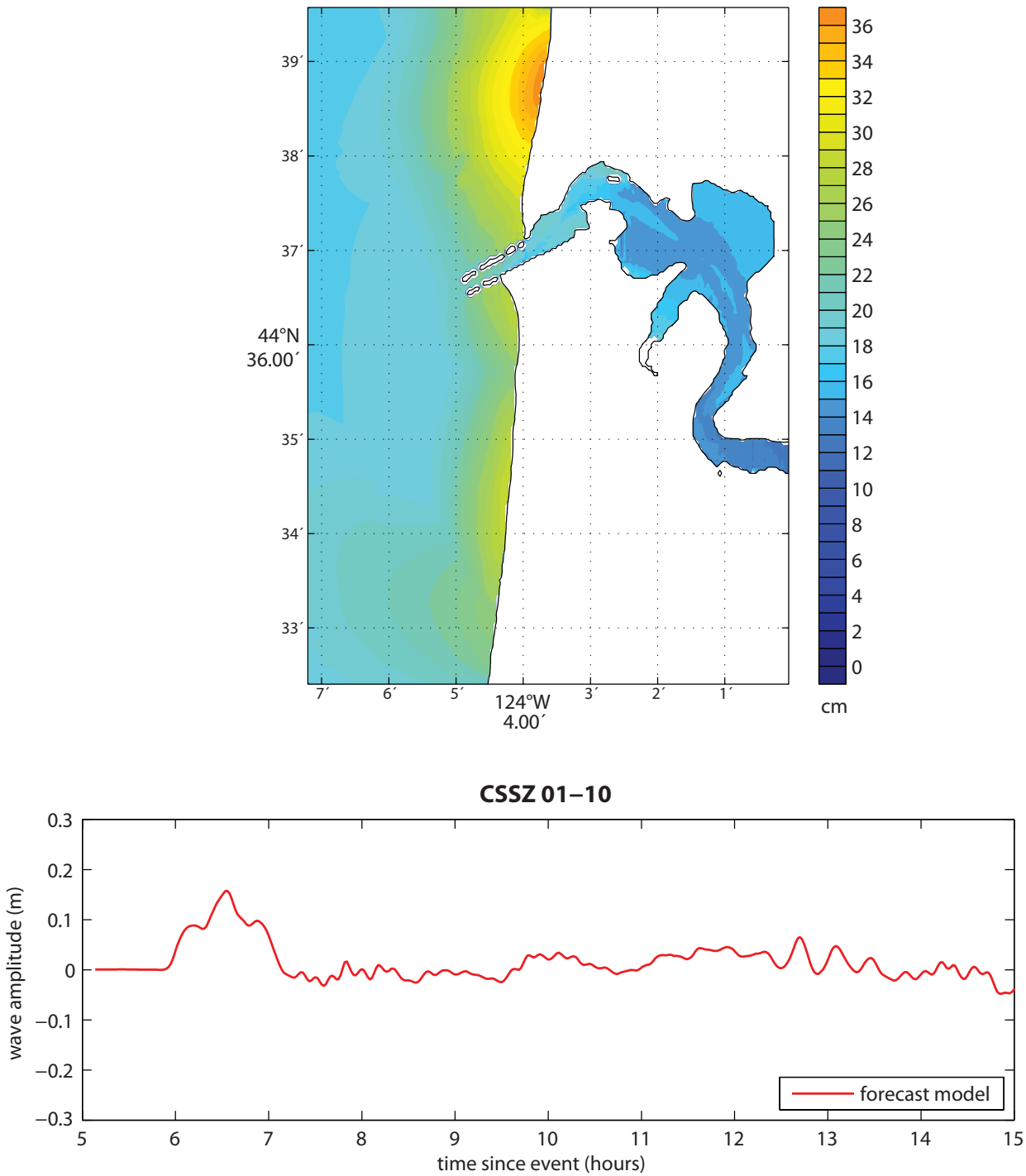

Figure 30: Results from the forecast model for the CSSZ 1–10 synthetic event. The upper panel shows the map of predicted maximum wave height in the Newport C grid and the lower panel shows the time series of wave amplitude at the tide gauge location.

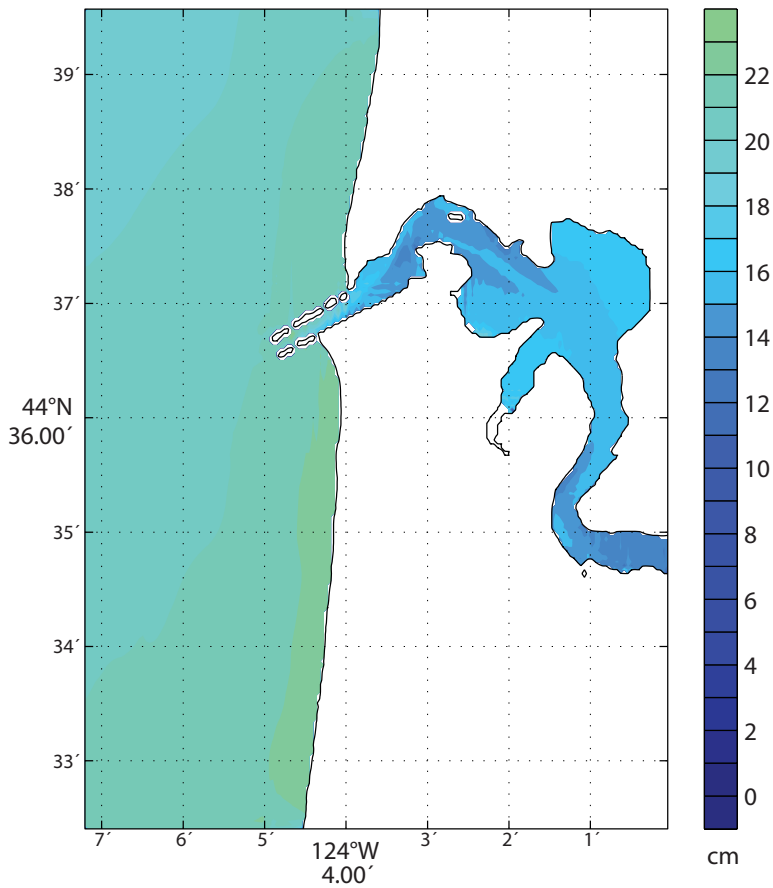

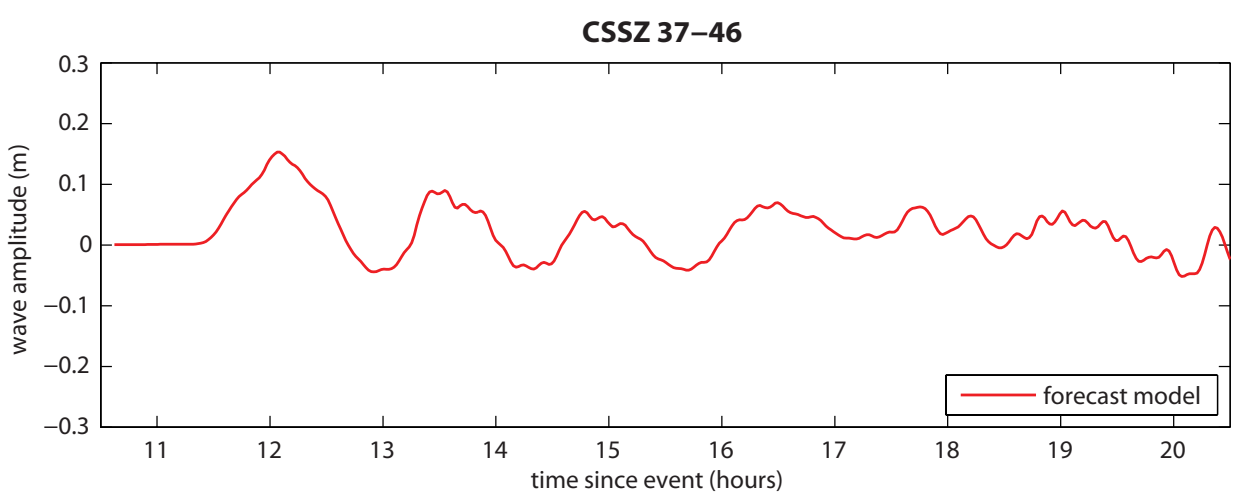

Figure 31: Results from the forecast model for the CSSZ 37–46 synthetic event. The upper panel shows the map of predicted maximum wave height in the Newport C grid and the lower panel shows the time series of wave amplitude at the tide gauge location.

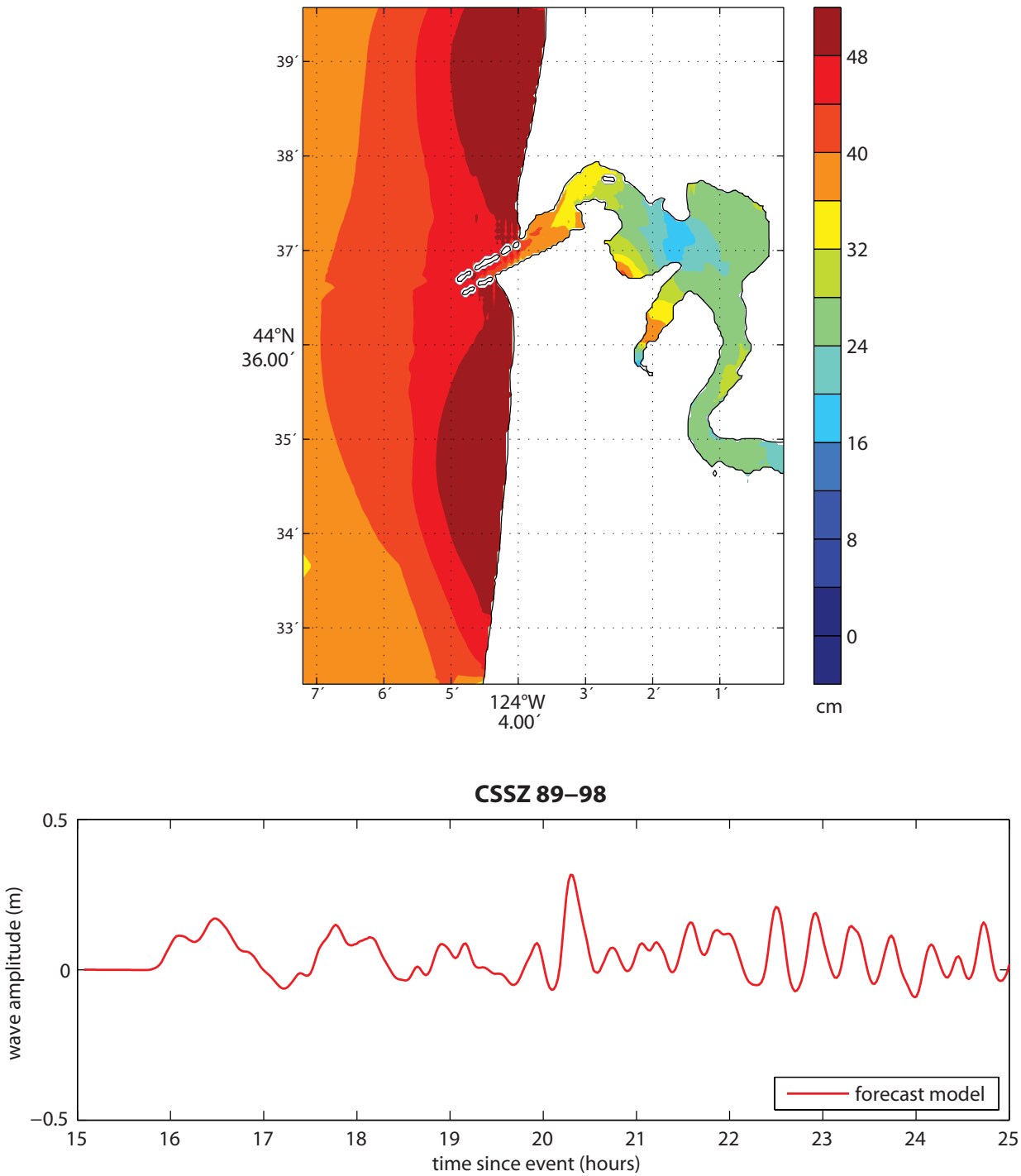

Figure 32: Results from the forecast model for the CSSZ 89–98 synthetic event. The upper panel shows the map of predicted maximum wave height in the Newport C grid and the lower panel shows the time series of wave amplitude at the tide gauge location.

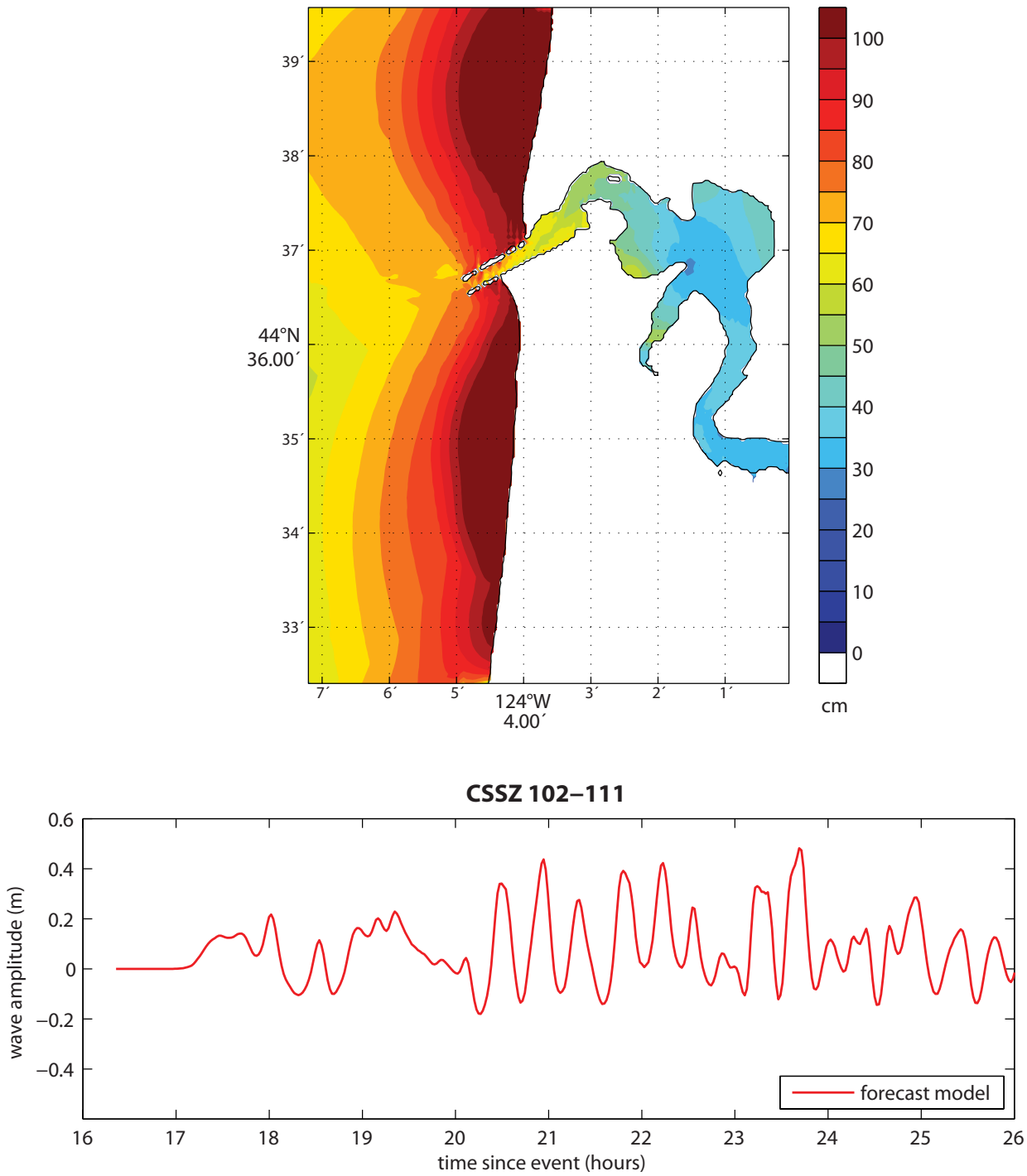

Figure 33: Results from the forecast model for the CSSZ 102–111 synthetic event. The upper panel shows the map of predicted maximum wave height in the Newport C grid and the lower panel shows the time series of wave amplitude at the tide gauge location.

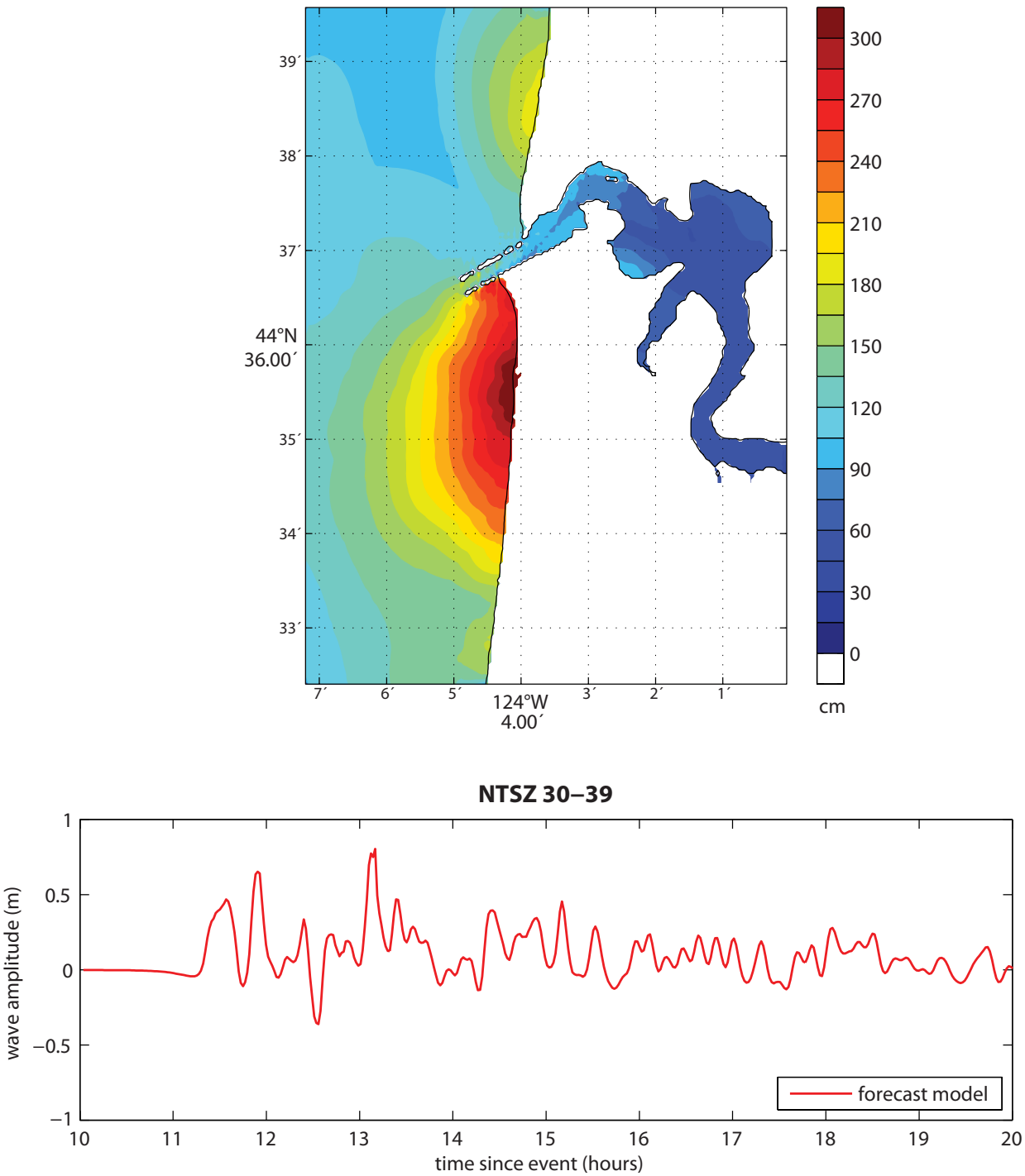

Figure 34: Results from the forecast model for the NTSZ 30–39 synthetic event. The upper panel shows the map of predicted maximum wave height in the Newport C grid and the lower panel shows the time series of wave amplitude at the tide gauge location.

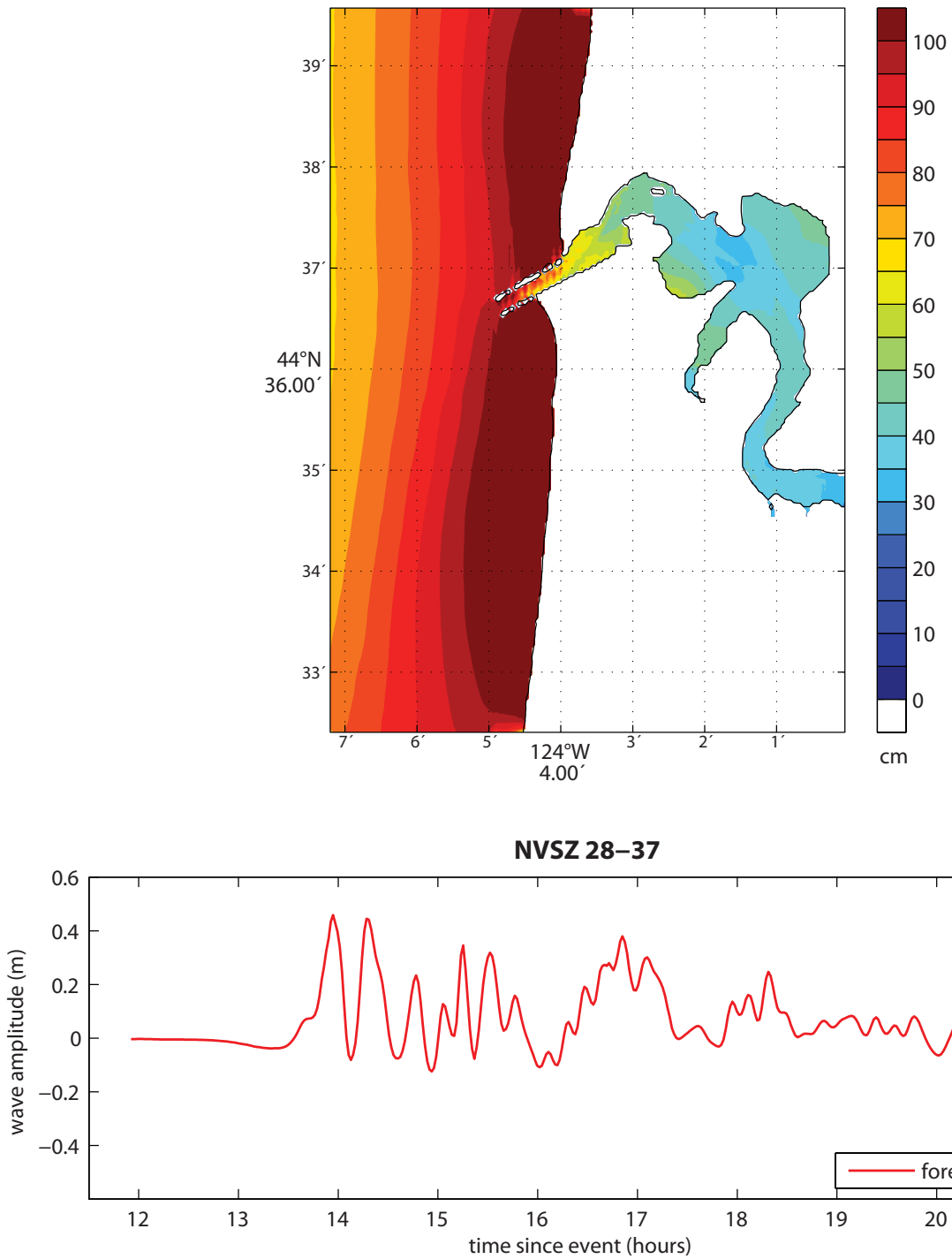

Figure 35: Results from the forecast model for the NVSZ 28–37 synthetic event. The upper panel shows the map of predicted maximum wave height in the Newport C grid and the lower panel shows the time series of wave amplitude at the tide gauge location.

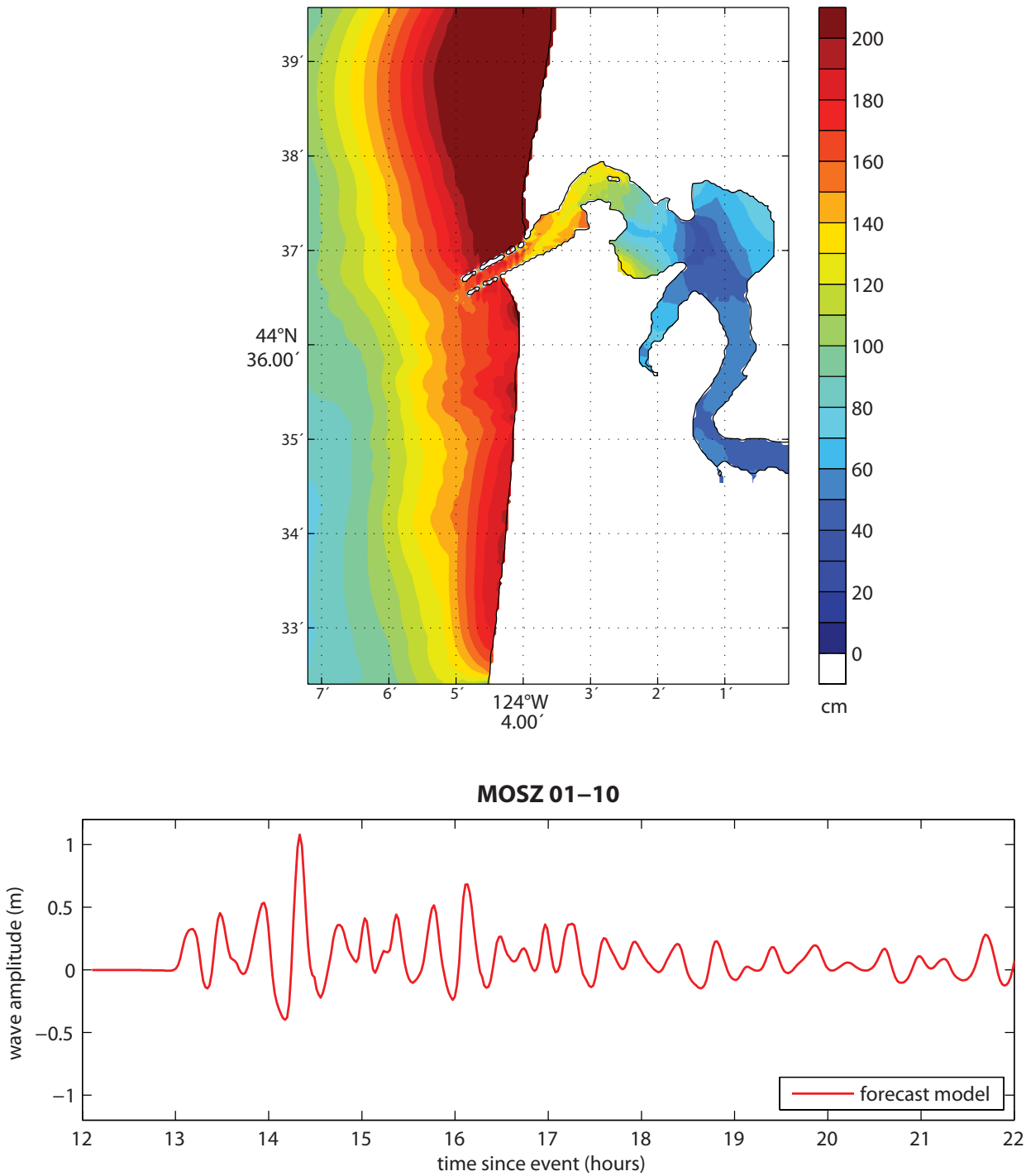

Figure 36: Results from the forecast model for the MOSZ 1–10 synthetic event. The upper panel shows the map of predicted maximum wave height in the Newport C grid and the lower panel shows the time series of wave amplitude at the tide gauge location.

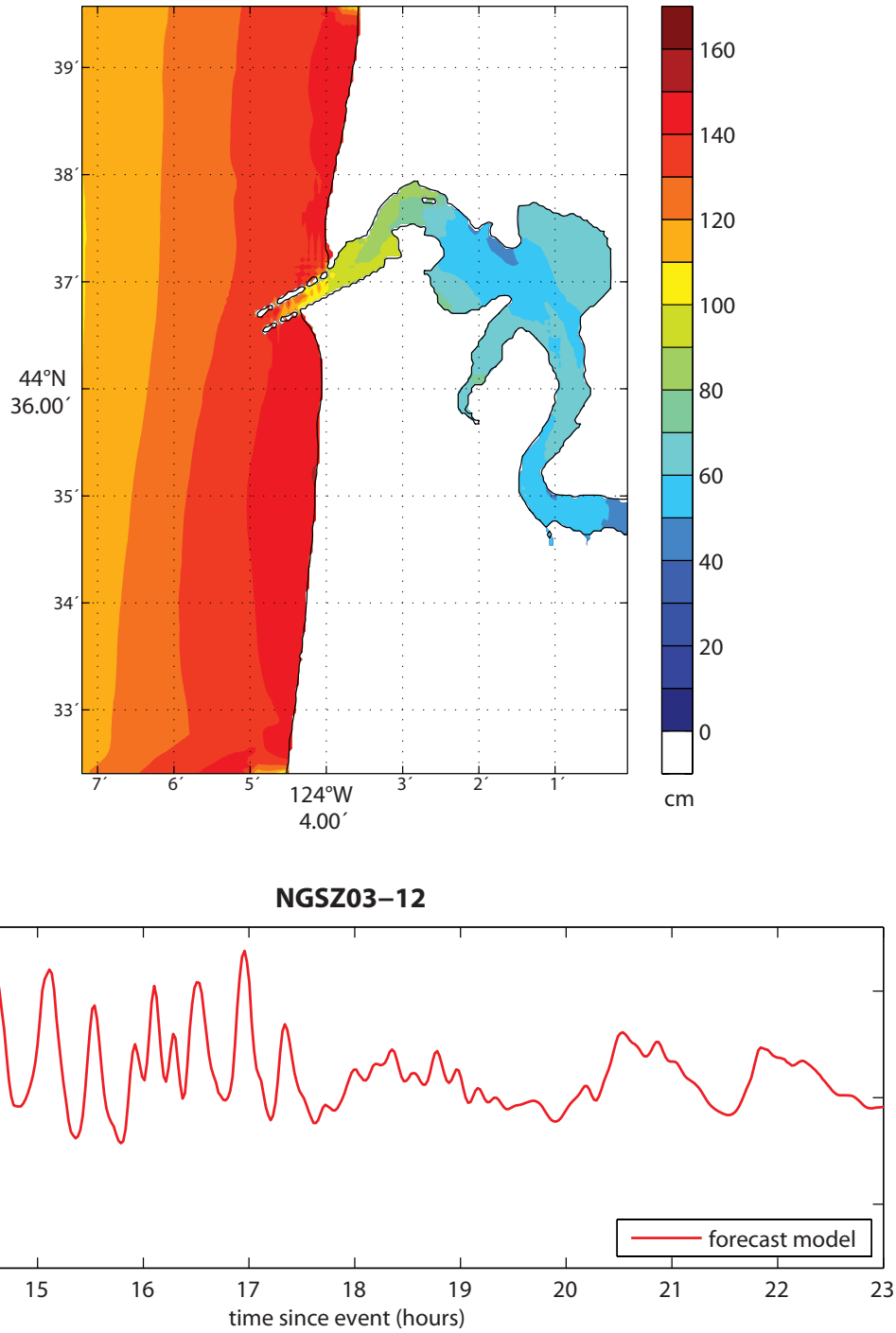

Figure 37: Results from the forecast model for the NGSZ 3–12 synthetic event. The upper panel shows the map of predicted maximum wave height in the Newport C grid and the lower panel shows the time series of wave amplitude at the tide gauge location.

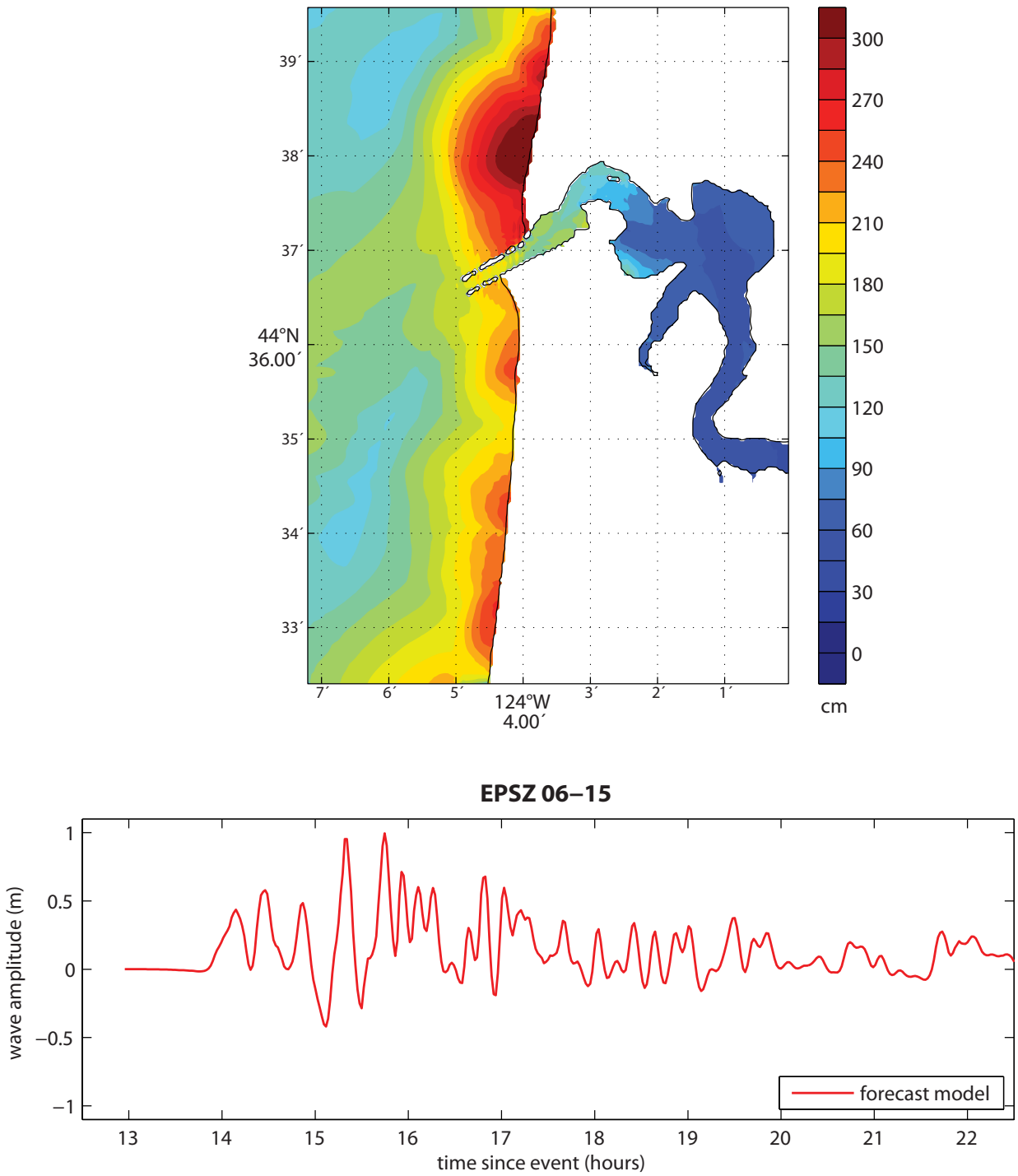

Figure 38: Results from the forecast model for the EPSZ 6–15 synthetic event. The upper panel shows the map of predicted maximum wave height in the Newport C grid and the lower panel shows the time series of wave amplitude at the tide gauge location.

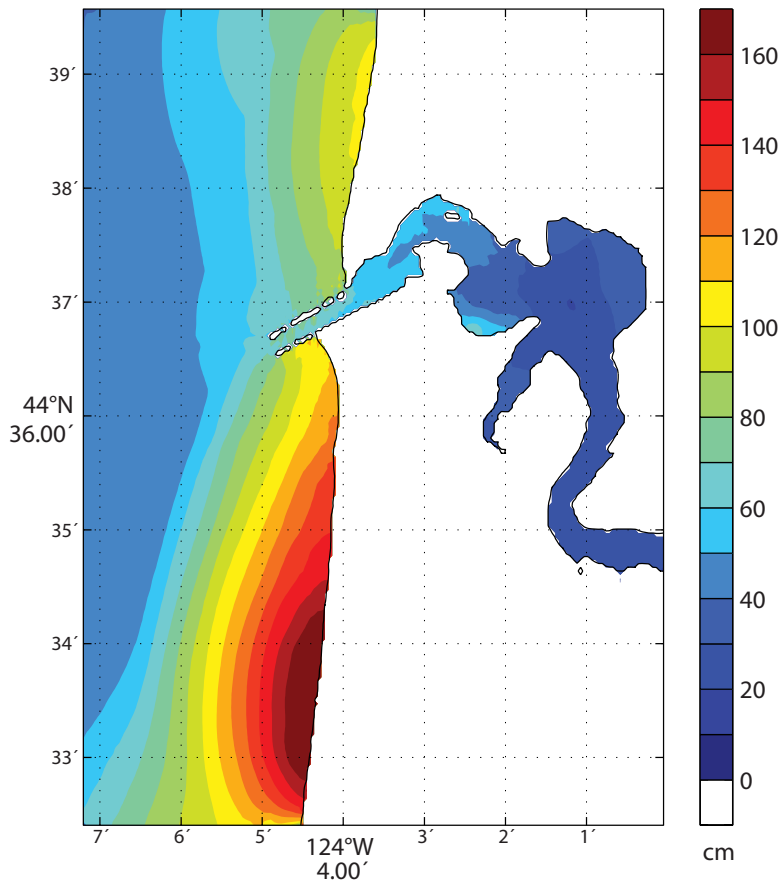

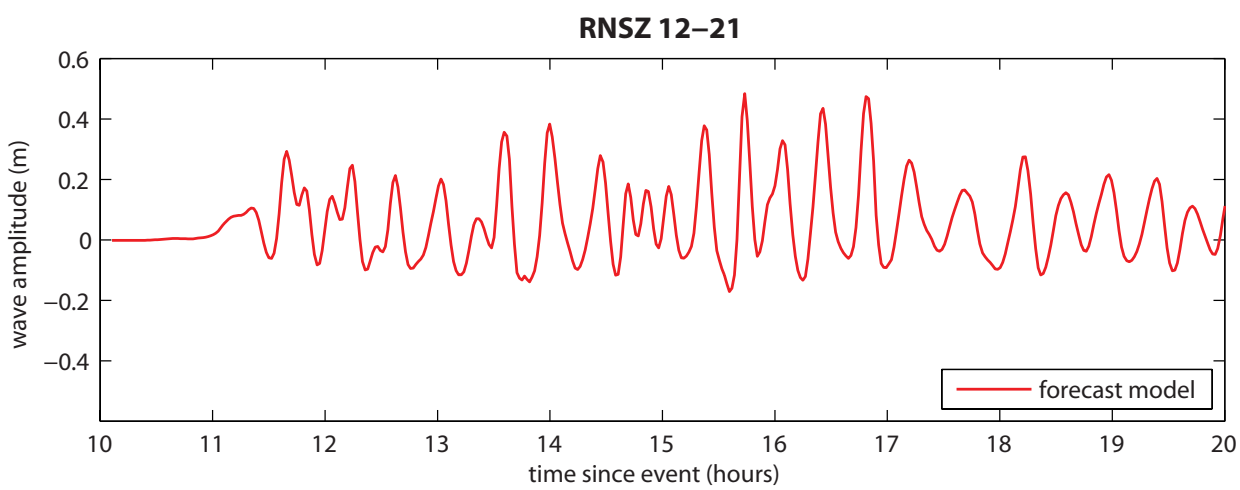

Figure 39: Results from the forecast model for the RNSZ 12–21 synthetic event. The upper panel shows the map of predicted maximum wave height in the Newport C grid and the lower panel shows the time series of wave amplitude at the tide gauge location.

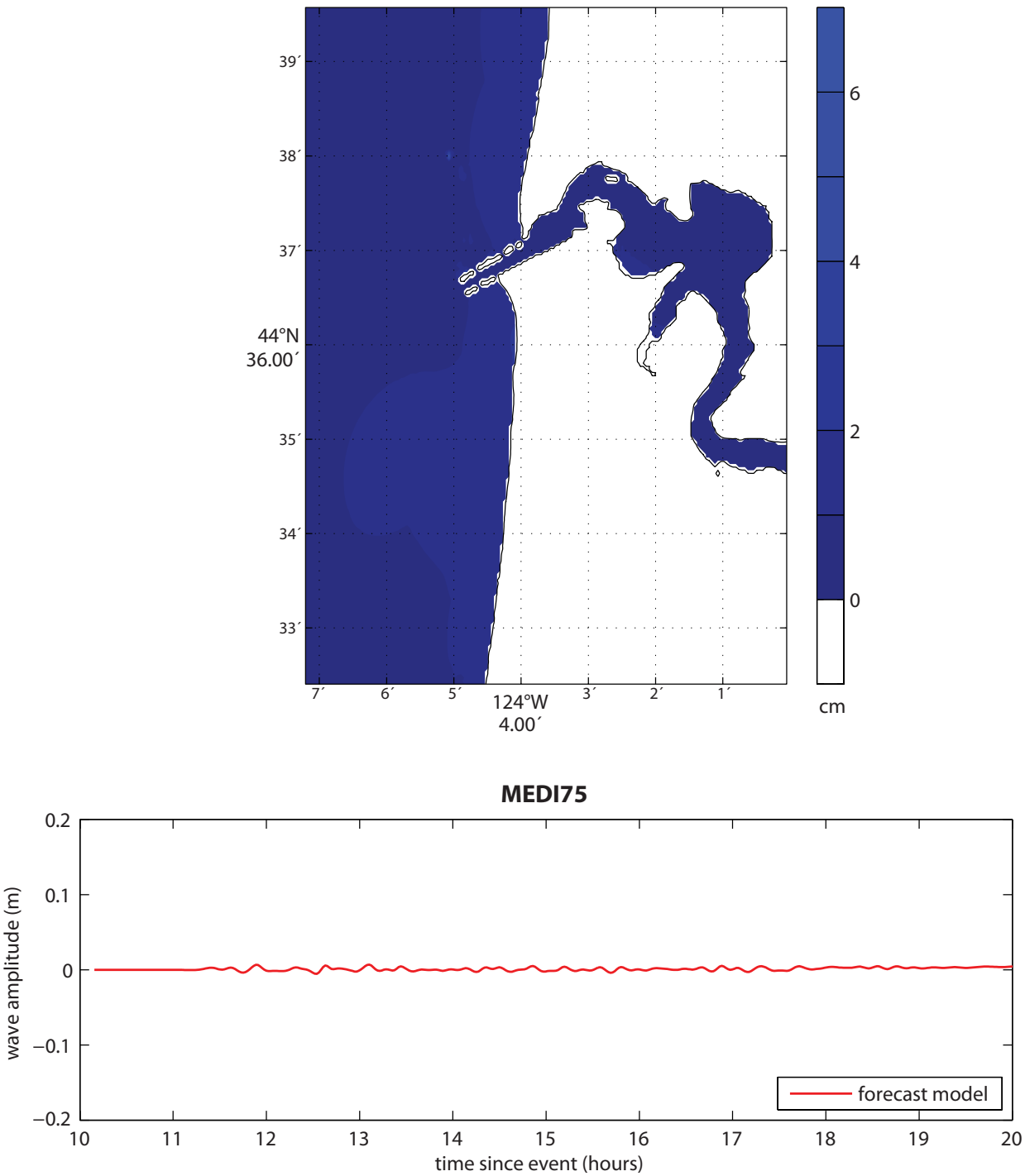

Figure 40: Results from the forecast model for the MEDI7.5 synthetic event forced by a small rupture of NTSZ B36. The upper panel shows the map of predicted maximum wave height in the Newport C grid and the lower panel shows the time series of wave amplitude at the tide gauge location.

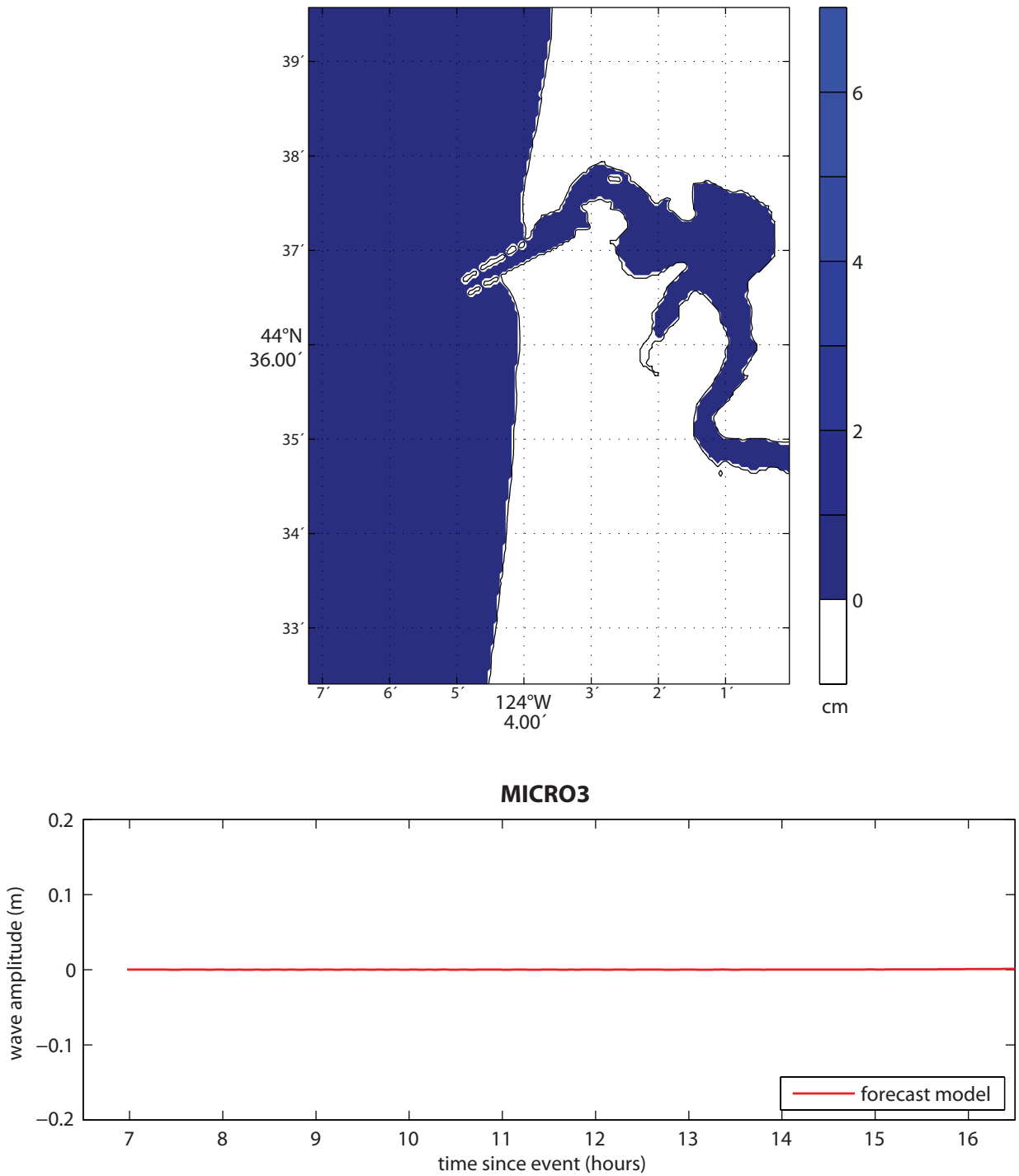

Figure 41: Results from the forecast model for the MICRO3 synthetic event forced by a Mw 7.5 rupture of ACSZ B6. The upper panel shows the map of predicted maximum wave height in the Newport C grid and the lower panel shows the time series of wave amplitude at the tide gauge location.

Appendix A.

Since the initial development of the Newport, Oregon, forecast model (SIM), the parameters for the input file for running the forecast model and reference model in MOST have been changed to reflect changes to the MOST model code. The following appendix lists the new input files for Newport, Oregon.

A1. Reference model *.in file for Newport, Oregon

```
0.0001xx    Minimum
0.001       Minimum amplitude of input offshore wave (m):
5           Input minimum depth for offshore (m)
0.1         Input “dry land” depth for inundation (m)
0.0009      Input friction coefficient (n**2)
1           let a and b run up
100.0       max eta before blow up (m)
0.6         Input time step (sec)
72000       Input amount of steps
6           Compute “A” arrays every n-th time step, n=
3           Compute “B” arrays every n-th time step, n=
180         Input number of steps between snapshots
0           ...Starting from
1           ...Saving grid every n-th node, n=
```

A2. Forecast model *.in file for Newport, Oregon

```
0.0001xx    Minimum
0.001       Minimum amplitude of input offshore wave (m):
5           Input minimum depth for offshore (m)
0.1         Input “dry land” depth for inundation (m)
0.0009      Input friction coefficient (n**2)
1           let a and b run up
100.0       max eta before blow up (m)
2.5         Input time step (sec)
14400       Input amount of steps
1           Compute “A” arrays every n-th time step, n=
1           Compute “B” arrays every n-th time step, n=
15          Input number of steps between snapshots
0           ...Starting from
1           ...Saving grid every n-th node, n=
```

Appendix B. Propagation Database

Pacific Ocean Unit Sources

The NOAA Propagation Database presented in this section is the representation of the database as of March 2013. This database may have been updated since March 2013.

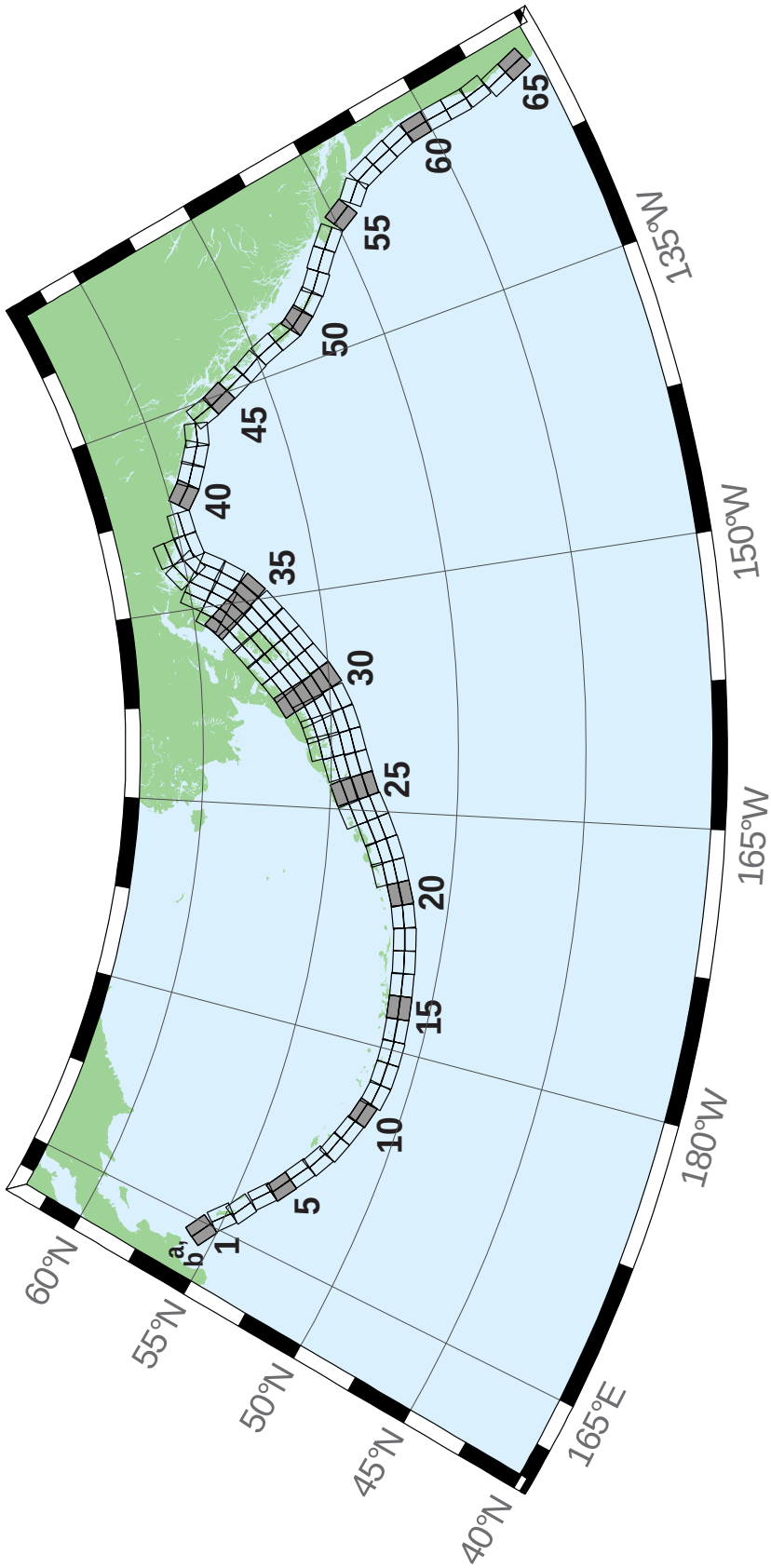

Figure B1: Aleutian–Alaska–Cascadia Subduction Zone unit sources.

Table B1: Earthquake parameters for Aleutian–Alaska–Cascadia Subduction Zone unit sources.

Segment	Description	Longitude (°E)	Latitude (°N)	Strike (°)	Dip (°)	Depth (km)
acsz-1a	Aleutian–Alaska–Cascadia	164.7994	55.9606	299	17	19.61
acsz-1b	Aleutian–Alaska–Cascadia	164.4310	55.5849	299	17	5
acsz-2a	Aleutian–Alaska–Cascadia	166.3418	55.4016	310.2	17	19.61
acsz-2b	Aleutian–Alaska–Cascadia	165.8578	55.0734	310.2	17	5
acsz-3a	Aleutian–Alaska–Cascadia	167.2939	54.8919	300.2	23.36	24.82
acsz-3b	Aleutian–Alaska–Cascadia	166.9362	54.5356	300.2	23.36	5
acsz-4a	Aleutian–Alaska–Cascadia	168.7131	54.2852	310.2	38.51	25.33
acsz-4b	Aleutian–Alaska–Cascadia	168.3269	54.0168	310.2	24	5
acsz-5a	Aleutian–Alaska–Cascadia	169.7447	53.7808	302.8	37.02	23.54
acsz-5b	Aleutian–Alaska–Cascadia	169.4185	53.4793	302.8	21.77	5
acsz-6a	Aleutian–Alaska–Cascadia	171.0144	53.3054	303.2	35.31	22.92
acsz-6b	Aleutian–Alaska–Cascadia	170.6813	52.9986	303.2	21	5
acsz-7a	Aleutian–Alaska–Cascadia	172.1500	52.8528	298.2	35.56	20.16
acsz-7b	Aleutian–Alaska–Cascadia	171.8665	52.5307	298.2	17.65	5
acsz-8a	Aleutian–Alaska–Cascadia	173.2726	52.4579	290.8	37.92	20.35
acsz-8b	Aleutian–Alaska–Cascadia	173.0681	52.1266	290.8	17.88	5
acsz-9a	Aleutian–Alaska–Cascadia	174.5866	52.1434	289	39.09	21.05
acsz-9b	Aleutian–Alaska–Cascadia	174.4027	51.8138	289	18.73	5
acsz-10a	Aleutian–Alaska–Cascadia	175.8784	51.8526	286.1	40.51	20.87
acsz-10b	Aleutian–Alaska–Cascadia	175.7265	51.5245	286.1	18.51	5
acsz-11a	Aleutian–Alaska–Cascadia	177.1140	51.6488	280	15	17.94
acsz-11b	Aleutian–Alaska–Cascadia	176.9937	51.2215	280	15	5
acsz-12a	Aleutian–Alaska–Cascadia	178.4500	51.5690	273	15	17.94
acsz-12b	Aleutian–Alaska–Cascadia	178.4130	51.1200	273	15	5
acsz-13a	Aleutian–Alaska–Cascadia	179.8550	51.5340	271	15	17.94
acsz-13b	Aleutian–Alaska–Cascadia	179.8420	51.0850	271	15	5
acsz-14a	Aleutian–Alaska–Cascadia	181.2340	51.5780	267	15	17.94
acsz-14b	Aleutian–Alaska–Cascadia	181.2720	51.1290	267	15	5
acsz-15a	Aleutian–Alaska–Cascadia	182.6380	51.6470	265	15	17.94
acsz-15b	Aleutian–Alaska–Cascadia	182.7000	51.2000	265	15	5
acsz-16a	Aleutian–Alaska–Cascadia	184.0550	51.7250	264	15	17.94
acsz-16b	Aleutian–Alaska–Cascadia	184.1280	51.2780	264	15	5
acsz-17a	Aleutian–Alaska–Cascadia	185.4560	51.8170	262	15	17.94
acsz-17b	Aleutian–Alaska–Cascadia	185.5560	51.3720	262	15	5
acsz-18a	Aleutian–Alaska–Cascadia	186.8680	51.9410	261	15	17.94
acsz-18b	Aleutian–Alaska–Cascadia	186.9810	51.4970	261	15	5
acsz-19a	Aleutian–Alaska–Cascadia	188.2430	52.1280	257	15	17.94
acsz-19b	Aleutian–Alaska–Cascadia	188.4060	51.6900	257	15	5

continued on next page

Table B1: (continued)

Segment	Description	Longitude (°E)	Latitude (°N)	Strike (°)	Dip (°)	Depth (km)
acsz-20a	Aleutian–Alaska–Cascadia	189.5810	52.3550	251	15	17.94
acsz-20b	Aleutian–Alaska–Cascadia	189.8180	51.9300	251	15	5
acsz-21a	Aleutian–Alaska–Cascadia	190.9570	52.6470	251	15	17.94
acsz-21b	Aleutian–Alaska–Cascadia	191.1960	52.2220	251	15	5
acsz-21z	Aleutian–Alaska–Cascadia	190.7399	53.0443	250.8	15	30.88
acsz-22a	Aleutian–Alaska–Cascadia	192.2940	52.9430	247	15	17.94
acsz-22b	Aleutian–Alaska–Cascadia	192.5820	52.5300	247	15	5
acsz-22z	Aleutian–Alaska–Cascadia	192.0074	53.3347	247.8	15	30.88
acsz-23a	Aleutian–Alaska–Cascadia	193.6270	53.3070	245	15	17.94
acsz-23b	Aleutian–Alaska–Cascadia	193.9410	52.9000	245	15	5
acsz-23z	Aleutian–Alaska–Cascadia	193.2991	53.6768	244.6	15	30.88
acsz-24a	Aleutian–Alaska–Cascadia	194.9740	53.6870	245	15	17.94
acsz-24b	Aleutian–Alaska–Cascadia	195.2910	53.2800	245	15	5
acsz-24y	Aleutian–Alaska–Cascadia	194.3645	54.4604	244.4	15	43.82
acsz-24z	Aleutian–Alaska–Cascadia	194.6793	54.0674	244.6	15	30.88
acsz-25a	Aleutian–Alaska–Cascadia	196.4340	54.0760	250	15	17.94
acsz-25b	Aleutian–Alaska–Cascadia	196.6930	53.6543	250	15	5
acsz-25y	Aleutian–Alaska–Cascadia	195.9009	54.8572	247.9	15	43.82
acsz-25z	Aleutian–Alaska–Cascadia	196.1761	54.4536	248.1	15	30.88
acsz-26a	Aleutian–Alaska–Cascadia	197.8970	54.3600	253	15	17.94
acsz-26b	Aleutian–Alaska–Cascadia	198.1200	53.9300	253	15	5
acsz-26y	Aleutian–Alaska–Cascadia	197.5498	55.1934	253.1	15	43.82
acsz-26z	Aleutian–Alaska–Cascadia	197.7620	54.7770	253.3	15	30.88
acsz-27a	Aleutian–Alaska–Cascadia	199.4340	54.5960	256	15	17.94
acsz-27b	Aleutian–Alaska–Cascadia	199.6200	54.1600	256	15	5
acsz-27x	Aleutian–Alaska–Cascadia	198.9736	55.8631	256.5	15	56.24
acsz-27y	Aleutian–Alaska–Cascadia	199.1454	55.4401	256.6	15	43.82
acsz-27z	Aleutian–Alaska–Cascadia	199.3135	55.0170	256.8	15	30.88
acsz-28a	Aleutian–Alaska–Cascadia	200.8820	54.8300	253	15	17.94
acsz-28b	Aleutian–Alaska–Cascadia	201.1080	54.4000	253	15	5
acsz-28x	Aleutian–Alaska–Cascadia	200.1929	56.0559	252.5	15	56.24
acsz-28y	Aleutian–Alaska–Cascadia	200.4167	55.6406	252.7	15	43.82
acsz-28z	Aleutian–Alaska–Cascadia	200.6360	55.2249	252.9	15	30.88
acsz-29a	Aleutian–Alaska–Cascadia	202.2610	55.1330	247	15	17.94
acsz-29b	Aleutian–Alaska–Cascadia	202.5650	54.7200	247	15	5
acsz-29x	Aleutian–Alaska–Cascadia	201.2606	56.2861	245.7	15	56.24
acsz-29y	Aleutian–Alaska–Cascadia	201.5733	55.8888	246	15	43.82
acsz-29z	Aleutian–Alaska–Cascadia	201.8797	55.4908	246.2	15	30.88

continued on next page

Table B1: (continued)

Segment	Description	Longitude (°E)	Latitude (°N)	Strike (°)	Dip (°)	Depth (km)
acsz-30a	Aleutian–Alaska–Cascadia	203.6040	55.5090	240	15	17.94
acsz-30b	Aleutian–Alaska–Cascadia	203.9970	55.1200	240	15	5
acsz-30w	Aleutian–Alaska–Cascadia	201.9901	56.9855	239.5	15	69.12
acsz-30x	Aleutian–Alaska–Cascadia	202.3851	56.6094	239.8	15	56.24
acsz-30y	Aleutian–Alaska–Cascadia	202.7724	56.2320	240.2	15	43.82
acsz-30z	Aleutian–Alaska–Cascadia	203.1521	55.8534	240.5	15	30.88
acsz-31a	Aleutian–Alaska–Cascadia	204.8950	55.9700	236	15	17.94
acsz-31b	Aleutian–Alaska–Cascadia	205.3400	55.5980	236	15	5
acsz-31w	Aleutian–Alaska–Cascadia	203.0825	57.3740	234.5	15	69.12
acsz-31x	Aleutian–Alaska–Cascadia	203.5408	57.0182	234.9	15	56.24
acsz-31y	Aleutian–Alaska–Cascadia	203.9904	56.6607	235.3	15	43.82
acsz-31z	Aleutian–Alaska–Cascadia	204.4315	56.3016	235.7	15	30.88
acsz-32a	Aleutian–Alaska–Cascadia	206.2080	56.4730	236	15	17.94
acsz-32b	Aleutian–Alaska–Cascadia	206.6580	56.1000	236	15	5
acsz-32w	Aleutian–Alaska–Cascadia	204.4129	57.8908	234.3	15	69.12
acsz-32x	Aleutian–Alaska–Cascadia	204.8802	57.5358	234.7	15	56.24
acsz-32y	Aleutian–Alaska–Cascadia	205.3385	57.1792	235.1	15	43.82
acsz-32z	Aleutian–Alaska–Cascadia	205.7880	56.8210	235.5	15	30.88
acsz-33a	Aleutian–Alaska–Cascadia	207.5370	56.9750	236	15	17.94
acsz-33b	Aleutian–Alaska–Cascadia	207.9930	56.6030	236	15	5
acsz-33w	Aleutian–Alaska–Cascadia	205.7126	58.3917	234.2	15	69.12
acsz-33x	Aleutian–Alaska–Cascadia	206.1873	58.0371	234.6	15	56.24
acsz-33y	Aleutian–Alaska–Cascadia	206.6527	57.6808	235	15	43.82
acsz-33z	Aleutian–Alaska–Cascadia	207.1091	57.3227	235.4	15	30.88
acsz-34a	Aleutian–Alaska–Cascadia	208.9371	57.5124	236	15	17.94
acsz-34b	Aleutian–Alaska–Cascadia	209.4000	57.1400	236	15	5
acsz-34w	Aleutian–Alaska–Cascadia	206.9772	58.8804	233.5	15	69.12
acsz-34x	Aleutian–Alaska–Cascadia	207.4677	58.5291	233.9	15	56.24
acsz-34y	Aleutian–Alaska–Cascadia	207.9485	58.1760	234.3	15	43.82
acsz-34z	Aleutian–Alaska–Cascadia	208.4198	57.8213	234.7	15	30.88
acsz-35a	Aleutian–Alaska–Cascadia	210.2597	58.0441	230	15	17.94
acsz-35b	Aleutian–Alaska–Cascadia	210.8000	57.7000	230	15	5
acsz-35w	Aleutian–Alaska–Cascadia	208.0204	59.3199	228.8	15	69.12
acsz-35x	Aleutian–Alaska–Cascadia	208.5715	58.9906	229.3	15	56.24
acsz-35y	Aleutian–Alaska–Cascadia	209.1122	58.6590	229.7	15	43.82
acsz-35z	Aleutian–Alaska–Cascadia	209.6425	58.3252	230.2	15	30.88
acsz-36a	Aleutian–Alaska–Cascadia	211.3249	58.6565	218	15	17.94
acsz-36b	Aleutian–Alaska–Cascadia	212.0000	58.3800	218	15	5

continued on next page

Table B1: (continued)

Segment	Description	Longitude (°E)	Latitude (°N)	Strike (°)	Dip (°)	Depth (km)
acsz-36w	Aleutian–Alaska–Cascadia	208.5003	59.5894	215.6	15	69.12
acsz-36x	Aleutian–Alaska–Cascadia	209.1909	59.3342	216.2	15	56.24
acsz-36y	Aleutian–Alaska–Cascadia	209.8711	59.0753	216.8	15	43.82
acsz-36z	Aleutian–Alaska–Cascadia	210.5412	58.8129	217.3	15	30.88
acsz-37a	Aleutian–Alaska–Cascadia	212.2505	59.2720	213.7	15	17.94
acsz-37b	Aleutian–Alaska–Cascadia	212.9519	59.0312	213.7	15	5
acsz-37x	Aleutian–Alaska–Cascadia	210.1726	60.0644	213	15	56.24
acsz-37y	Aleutian–Alaska–Cascadia	210.8955	59.8251	213.7	15	43.82
acsz-37z	Aleutian–Alaska–Cascadia	211.6079	59.5820	214.3	15	30.88
acsz-38a	Aleutian–Alaska–Cascadia	214.6555	60.1351	260.1	0	15
acsz-38b	Aleutian–Alaska–Cascadia	214.8088	59.6927	260.1	0	15
acsz-38y	Aleutian–Alaska–Cascadia	214.3737	60.9838	259	0	15
acsz-38z	Aleutian–Alaska–Cascadia	214.5362	60.5429	259	0	15
acsz-39a	Aleutian–Alaska–Cascadia	216.5607	60.2480	267	0	15
acsz-39b	Aleutian–Alaska–Cascadia	216.6068	59.7994	267	0	15
acsz-40a	Aleutian–Alaska–Cascadia	219.3069	59.7574	310.9	0	15
acsz-40b	Aleutian–Alaska–Cascadia	218.7288	59.4180	310.9	0	15
acsz-41a	Aleutian–Alaska–Cascadia	220.4832	59.3390	300.7	0	15
acsz-41b	Aleutian–Alaska–Cascadia	220.0382	58.9529	300.7	0	15
acsz-42a	Aleutian–Alaska–Cascadia	221.8835	58.9310	298.9	0	15
acsz-42b	Aleutian–Alaska–Cascadia	221.4671	58.5379	298.9	0	15
acsz-43a	Aleutian–Alaska–Cascadia	222.9711	58.6934	282.3	0	15
acsz-43b	Aleutian–Alaska–Cascadia	222.7887	58.2546	282.3	0	15
acsz-44a	Aleutian–Alaska–Cascadia	224.9379	57.9054	340.9	12	11.09
acsz-44b	Aleutian–Alaska–Cascadia	224.1596	57.7617	340.9	7	5
acsz-45a	Aleutian–Alaska–Cascadia	225.4994	57.1634	334.1	12	11.09
acsz-45b	Aleutian–Alaska–Cascadia	224.7740	56.9718	334.1	7	5
acsz-46a	Aleutian–Alaska–Cascadia	226.1459	56.3552	334.1	12	11.09
acsz-46b	Aleutian–Alaska–Cascadia	225.4358	56.1636	334.1	7	5
acsz-47a	Aleutian–Alaska–Cascadia	226.7731	55.5830	332.3	12	11.09
acsz-47b	Aleutian–Alaska–Cascadia	226.0887	55.3785	332.3	7	5
acsz-48a	Aleutian–Alaska–Cascadia	227.4799	54.6763	339.4	12	11.09
acsz-48b	Aleutian–Alaska–Cascadia	226.7713	54.5217	339.4	7	5
acsz-49a	Aleutian–Alaska–Cascadia	227.9482	53.8155	341.2	12	11.09
acsz-49b	Aleutian–Alaska–Cascadia	227.2462	53.6737	341.2	7	5
acsz-50a	Aleutian–Alaska–Cascadia	228.3970	53.2509	324.5	12	11.09
acsz-50b	Aleutian–Alaska–Cascadia	227.8027	52.9958	324.5	7	5
acsz-51a	Aleutian–Alaska–Cascadia	229.1844	52.6297	318.4	12	11.09

continued on next page

Table B1: (continued)

Segment	Description	Longitude (°E)	Latitude (°N)	Strike (°)	Dip (°)	Depth (km)
acsz-51b	Aleutian–Alaska–Cascadia	228.6470	52.3378	318.4	7	5
acsz-52a	Aleutian–Alaska–Cascadia	230.0306	52.0768	310.9	12	11.09
acsz-52b	Aleutian–Alaska–Cascadia	229.5665	51.7445	310.9	7	5
acsz-53a	Aleutian–Alaska–Cascadia	231.1735	51.5258	310.9	12	11.09
acsz-53b	Aleutian–Alaska–Cascadia	230.7150	51.1935	310.9	7	5
acsz-54a	Aleutian–Alaska–Cascadia	232.2453	50.8809	314.1	12	11.09
acsz-54b	Aleutian–Alaska–Cascadia	231.7639	50.5655	314.1	7	5
acsz-55a	Aleutian–Alaska–Cascadia	233.3066	49.9032	333.7	12	11.09
acsz-55b	Aleutian–Alaska–Cascadia	232.6975	49.7086	333.7	7	5
acsz-56a	Aleutian–Alaska–Cascadia	234.0588	49.1702	315	11	12.82
acsz-56b	Aleutian–Alaska–Cascadia	233.5849	48.8584	315	9	5
acsz-57a	Aleutian–Alaska–Cascadia	234.9041	48.2596	341	11	12.82
acsz-57b	Aleutian–Alaska–Cascadia	234.2797	48.1161	341	9	5
acsz-58a	Aleutian–Alaska–Cascadia	235.3021	47.3812	344	11	12.82
acsz-58b	Aleutian–Alaska–Cascadia	234.6776	47.2597	344	9	5
acsz-59a	Aleutian–Alaska–Cascadia	235.6432	46.5082	345	11	12.82
acsz-59b	Aleutian–Alaska–Cascadia	235.0257	46.3941	345	9	5
acsz-60a	Aleutian–Alaska–Cascadia	235.8640	45.5429	356	11	12.82
acsz-60b	Aleutian–Alaska–Cascadia	235.2363	45.5121	356	9	5
acsz-61a	Aleutian–Alaska–Cascadia	235.9106	44.6227	359	11	12.82
acsz-61b	Aleutian–Alaska–Cascadia	235.2913	44.6150	359	9	5
acsz-62a	Aleutian–Alaska–Cascadia	235.9229	43.7245	359	11	12.82
acsz-62b	Aleutian–Alaska–Cascadia	235.3130	43.7168	359	9	5
acsz-63a	Aleutian–Alaska–Cascadia	236.0220	42.9020	350	11	12.82
acsz-63b	Aleutian–Alaska–Cascadia	235.4300	42.8254	350	9	5
acsz-64a	Aleutian–Alaska–Cascadia	235.9638	41.9818	345	11	12.82
acsz-64b	Aleutian–Alaska–Cascadia	235.3919	41.8677	345	9	5
acsz-65a	Aleutian–Alaska–Cascadia	236.2643	41.1141	345	11	12.82
acsz-65b	Aleutian–Alaska–Cascadia	235.7000	41.0000	345	9	5
acsz-238a	Aleutian–Alaska–Cascadia	213.2878	59.8406	236.8	15	17.94
acsz-238y	Aleutian–Alaska–Cascadia	212.3424	60.5664	236.8	15	43.82
acsz-238z	Aleutian–Alaska–Cascadia	212.8119	60.2035	236.8	15	30.88

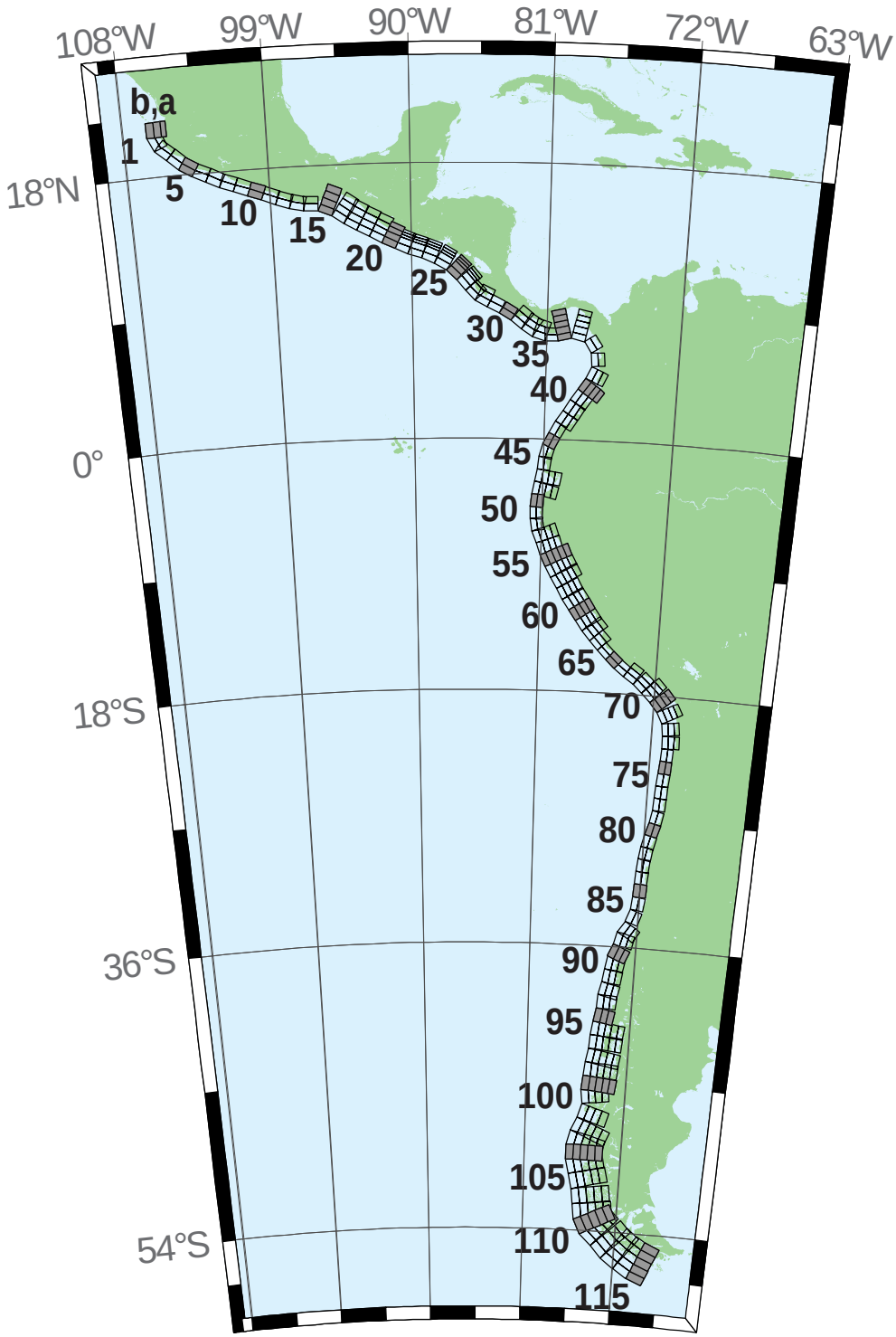

Figure B2: Central and South America Subduction Zone unit sources.

Table B2: Earthquake parameters for Central and South America Subduction Zone unit sources.

Segment	Description	Longitude (°E)	Latitude (°N)	Strike (°)	Dip (°)	Depth (km)
cssz-1a	Central and South America	254.4573	20.8170	359	19	15.4
cssz-1b	Central and South America	254.0035	20.8094	359	12	5
cssz-1z	Central and South America	254.7664	20.8222	359	50	31.67
cssz-2a	Central and South America	254.5765	20.2806	336.8	19	15.4
cssz-2b	Central and South America	254.1607	20.1130	336.8	12	5
cssz-3a	Central and South America	254.8789	19.8923	310.6	18.31	15.27
cssz-3b	Central and South America	254.5841	19.5685	310.6	11.85	5
cssz-4a	Central and South America	255.6167	19.2649	313.4	17.62	15.12
cssz-4b	Central and South America	255.3056	18.9537	313.4	11.68	5
cssz-5a	Central and South America	256.2240	18.8148	302.7	16.92	15
cssz-5b	Central and South America	255.9790	18.4532	302.7	11.54	5
cssz-6a	Central and South America	256.9425	18.4383	295.1	16.23	14.87
cssz-6b	Central and South America	256.7495	18.0479	295.1	11.38	5
cssz-7a	Central and South America	257.8137	18.0339	296.9	15.54	14.74
cssz-7b	Central and South America	257.6079	17.6480	296.9	11.23	5
cssz-8a	Central and South America	258.5779	17.7151	290.4	14.85	14.61
cssz-8b	Central and South America	258.4191	17.3082	290.4	11.08	5
cssz-9a	Central and South America	259.4578	17.4024	290.5	14.15	14.47
cssz-9b	Central and South America	259.2983	16.9944	290.5	10.92	5
cssz-10a	Central and South America	260.3385	17.0861	290.8	13.46	14.34
cssz-10b	Central and South America	260.1768	16.6776	290.8	10.77	5
cssz-11a	Central and South America	261.2255	16.7554	291.8	12.77	14.21
cssz-11b	Central and South America	261.0556	16.3487	291.8	10.62	5
cssz-12a	Central and South America	262.0561	16.4603	288.9	12.08	14.08
cssz-12b	Central and South America	261.9082	16.0447	288.9	10.46	5
cssz-13a	Central and South America	262.8638	16.2381	283.2	11.38	13.95
cssz-13b	Central and South America	262.7593	15.8094	283.2	10.31	5
cssz-14a	Central and South America	263.6066	16.1435	272.1	10.69	13.81
cssz-14b	Central and South America	263.5901	15.7024	272.1	10.15	5
cssz-15a	Central and South America	264.8259	15.8829	293	10	13.68
cssz-15b	Central and South America	264.6462	15.4758	293	10	5
cssz-15y	Central and South America	265.1865	16.6971	293	10	31.05
cssz-15z	Central and South America	265.0060	16.2900	293	10	22.36
cssz-16a	Central and South America	265.7928	15.3507	304.9	15	15.82
cssz-16b	Central and South America	265.5353	14.9951	304.9	12.5	5
cssz-16y	Central and South America	266.3092	16.0619	304.9	15	41.7
cssz-16z	Central and South America	266.0508	15.7063	304.9	15	28.76
cssz-17a	Central and South America	266.4947	14.9019	299.5	20	17.94
cssz-17b	Central and South America	266.2797	14.5346	299.5	15	5
cssz-17y	Central and South America	266.9259	15.6365	299.5	20	52.14

continued on next page

Table B2: (continued)

Segment	Description	Longitude (°E)	Latitude (°N)	Strike (°)	Dip (°)	Depth (km)
cssz-17z	Central and South America	266.7101	15.2692	299.5	20	35.04
cssz-18a	Central and South America	267.2827	14.4768	298	21.5	17.94
cssz-18b	Central and South America	267.0802	14.1078	298	15	5
cssz-18y	Central and South America	267.6888	15.2148	298	21.5	54.59
cssz-18z	Central and South America	267.4856	14.8458	298	21.5	36.27
cssz-19a	Central and South America	268.0919	14.0560	297.6	23	17.94
cssz-19b	Central and South America	267.8943	13.6897	297.6	15	5
cssz-19y	Central and South America	268.4880	14.7886	297.6	23	57.01
cssz-19z	Central and South America	268.2898	14.4223	297.6	23	37.48
cssz-20a	Central and South America	268.8929	13.6558	296.2	24	17.94
cssz-20b	Central and South America	268.7064	13.2877	296.2	15	5
cssz-20y	Central and South America	269.1796	14.2206	296.2	45.5	73.94
cssz-20z	Central and South America	269.0362	13.9382	296.2	45.5	38.28
cssz-21a	Central and South America	269.6797	13.3031	292.6	25	17.94
cssz-21b	Central and South America	269.5187	12.9274	292.6	15	5
cssz-21x	Central and South America	269.8797	13.7690	292.6	68	131.8
cssz-21y	Central and South America	269.8130	13.6137	292.6	68	85.43
cssz-21z	Central and South America	269.7463	13.4584	292.6	68	39.07
cssz-22a	Central and South America	270.4823	13.0079	288.6	25	17.94
cssz-22b	Central and South America	270.3492	12.6221	288.6	15	5
cssz-22x	Central and South America	270.6476	13.4864	288.6	68	131.8
cssz-22y	Central and South America	270.5925	13.3269	288.6	68	85.43
cssz-22z	Central and South America	270.5374	13.1674	288.6	68	39.07
cssz-23a	Central and South America	271.3961	12.6734	292.4	25	17.94
cssz-23b	Central and South America	271.2369	12.2972	292.4	15	5
cssz-23x	Central and South America	271.5938	13.1399	292.4	68	131.8
cssz-23y	Central and South America	271.5279	12.9844	292.4	68	85.43
cssz-23z	Central and South America	271.4620	12.8289	292.4	68	39.07
cssz-24a	Central and South America	272.3203	12.2251	300.2	25	17.94
cssz-24b	Central and South America	272.1107	11.8734	300.2	15	5
cssz-24x	Central and South America	272.5917	12.6799	300.2	67	131.1
cssz-24y	Central and South America	272.5012	12.5283	300.2	67	85.1
cssz-24z	Central and South America	272.4107	12.3767	300.2	67	39.07
cssz-25a	Central and South America	273.2075	11.5684	313.8	25	17.94
cssz-25b	Central and South America	272.9200	11.2746	313.8	15	5
cssz-25x	Central and South America	273.5950	11.9641	313.8	66	130.4
cssz-25y	Central and South America	273.4658	11.8322	313.8	66	84.75
cssz-25z	Central and South America	273.3366	11.7003	313.8	66	39.07
cssz-26a	Central and South America	273.8943	10.8402	320.4	25	17.94

continued on next page

Table B2: (continued)

Segment	Description	Longitude (°E)	Latitude (°N)	Strike (°)	Dip (°)	Depth (km)
cssz-26b	Central and South America	273.5750	10.5808	320.4	15	5
cssz-26x	Central and South America	274.3246	11.1894	320.4	66	130.4
cssz-26y	Central and South America	274.1811	11.0730	320.4	66	84.75
cssz-26z	Central and South America	274.0377	10.9566	320.4	66	39.07
cssz-27a	Central and South America	274.4569	10.2177	316.1	25	17.94
cssz-27b	Central and South America	274.1590	9.9354	316.1	15	5
cssz-27z	Central and South America	274.5907	10.3444	316.1	66	39.07
cssz-28a	Central and South America	274.9586	9.8695	297.1	22	14.54
cssz-28b	Central and South America	274.7661	9.4988	297.1	11	5
cssz-28z	Central and South America	275.1118	10.1643	297.1	42.5	33.27
cssz-29a	Central and South America	275.7686	9.4789	296.6	19	11.09
cssz-29b	Central and South America	275.5759	9.0992	296.6	7	5
cssz-30a	Central and South America	276.6346	8.9973	302.2	19	9.36
cssz-30b	Central and South America	276.4053	8.6381	302.2	5	5
cssz-31a	Central and South America	277.4554	8.4152	309.1	19	7.62
cssz-31b	Central and South America	277.1851	8.0854	309.1	3	5
cssz-31z	Central and South America	277.7260	8.7450	309.1	19	23.9
cssz-32a	Central and South America	278.1112	7.9425	303	18.67	8.49
cssz-32b	Central and South America	277.8775	7.5855	303	4	5
cssz-32z	Central and South America	278.3407	8.2927	303	21.67	24.49
cssz-33a	Central and South America	278.7082	7.6620	287.6	18.33	10.23
cssz-33b	Central and South America	278.5785	7.2555	287.6	6	5
cssz-33z	Central and South America	278.8328	8.0522	287.6	24.33	25.95
cssz-34a	Central and South America	279.3184	7.5592	269.5	18	17.94
cssz-34b	Central and South America	279.3223	7.1320	269.5	15	5
cssz-35a	Central and South America	280.0039	7.6543	255.9	17.67	14.54
cssz-35b	Central and South America	280.1090	7.2392	255.9	11	5
cssz-35x	Central and South America	279.7156	8.7898	255.9	29.67	79.22
cssz-35y	Central and South America	279.8118	8.4113	255.9	29.67	54.47
cssz-35z	Central and South America	279.9079	8.0328	255.9	29.67	29.72
cssz-36a	Central and South America	281.2882	7.6778	282.5	17.33	11.09
cssz-36b	Central and South America	281.1948	7.2592	282.5	7	5
cssz-36x	Central and South America	281.5368	8.7896	282.5	32.33	79.47
cssz-36y	Central and South America	281.4539	8.4190	282.5	32.33	52.73
cssz-36z	Central and South America	281.3710	8.0484	282.5	32.33	25.99
cssz-37a	Central and South America	282.5252	6.8289	326.9	17	10.23
cssz-37b	Central and South America	282.1629	6.5944	326.9	6	5
cssz-38a	Central and South America	282.9469	5.5973	355.4	17	10.23
cssz-38b	Central and South America	282.5167	5.5626	355.4	6	5

continued on next page

Table B2: (continued)

Segment	Description	Longitude (°E)	Latitude (°N)	Strike (°)	Dip (°)	Depth (km)
cssz-39a	Central and South America	282.7236	4.3108	24.13	17	10.23
cssz-39b	Central and South America	282.3305	4.4864	24.13	6	5
cssz-39z	Central and South America	283.0603	4.1604	24.13	35	24.85
cssz-40a	Central and South America	282.1940	3.3863	35.28	17	10.23
cssz-40b	Central and South America	281.8427	3.6344	35.28	6	5
cssz-40y	Central and South America	282.7956	2.9613	35.28	35	53.52
cssz-40z	Central and South America	282.4948	3.1738	35.28	35	24.85
cssz-41a	Central and South America	281.6890	2.6611	34.27	17	10.23
cssz-41b	Central and South America	281.3336	2.9030	34.27	6	5
cssz-41z	Central and South America	281.9933	2.4539	34.27	35	24.85
cssz-42a	Central and South America	281.2266	1.9444	31.29	17	10.23
cssz-42b	Central and South America	280.8593	2.1675	31.29	6	5
cssz-42z	Central and South America	281.5411	1.7533	31.29	35	24.85
cssz-43a	Central and South America	280.7297	1.1593	33.3	17	10.23
cssz-43b	Central and South America	280.3706	1.3951	33.3	6	5
cssz-43z	Central and South America	281.0373	0.9573	33.3	35	24.85
cssz-44a	Central and South America	280.3018	0.4491	28.8	17	10.23
cssz-44b	Central and South America	279.9254	0.6560	28.8	6	5
cssz-45a	Central and South America	279.9083	-0.3259	26.91	10	8.49
cssz-45b	Central and South America	279.5139	-0.1257	26.91	4	5
cssz-46a	Central and South America	279.6461	-0.9975	15.76	10	8.49
cssz-46b	Central and South America	279.2203	-0.8774	15.76	4	5
cssz-47a	Central and South America	279.4972	-1.7407	6.9	10	8.49
cssz-47b	Central and South America	279.0579	-1.6876	6.9	4	5
cssz-48a	Central and South America	279.3695	-2.6622	8.96	10	8.49
cssz-48b	Central and South America	278.9321	-2.5933	8.96	4	5
cssz-48y	Central and South America	280.2444	-2.8000	8.96	10	25.85
cssz-48z	Central and South America	279.8070	-2.7311	8.96	10	17.17
cssz-49a	Central and South America	279.1852	-3.6070	13.15	10	8.49
cssz-49b	Central and South America	278.7536	-3.5064	13.15	4	5
cssz-49y	Central and South America	280.0486	-3.8082	13.15	10	25.85
cssz-49z	Central and South America	279.6169	-3.7076	13.15	10	17.17
cssz-50a	Central and South America	279.0652	-4.3635	4.78	10.33	9.64
cssz-50b	Central and South America	278.6235	-4.3267	4.78	5.33	5
cssz-51a	Central and South America	279.0349	-5.1773	359.4	10.67	10.81
cssz-51b	Central and South America	278.5915	-5.1817	359.4	6.67	5
cssz-52a	Central and South America	279.1047	-5.9196	349.8	11	11.96
cssz-52b	Central and South America	278.6685	-5.9981	349.8	8	5
cssz-53a	Central and South America	279.3044	-6.6242	339.2	10.25	11.74

continued on next page

Table B2: (continued)

Segment	Description	Longitude (°E)	Latitude (°N)	Strike (°)	Dip (°)	Depth (km)
cssz-53b	Central and South America	278.8884	-6.7811	339.2	7.75	5
cssz-53y	Central and South America	280.1024	-6.3232	339.2	19.25	37.12
cssz-53z	Central and South America	279.7035	-6.4737	339.2	19.25	20.64
cssz-54a	Central and South America	279.6256	-7.4907	340.8	9.5	11.53
cssz-54b	Central and South America	279.2036	-7.6365	340.8	7.5	5
cssz-54y	Central and South America	280.4267	-7.2137	340.8	20.5	37.29
cssz-54z	Central and South America	280.0262	-7.3522	340.8	20.5	19.78
cssz-55a	Central and South America	279.9348	-8.2452	335.4	8.75	11.74
cssz-55b	Central and South America	279.5269	-8.4301	335.4	7.75	5
cssz-55x	Central and South America	281.0837	-7.7238	335.4	21.75	56.4
cssz-55y	Central and South America	280.7009	-7.8976	335.4	21.75	37.88
cssz-55z	Central and South America	280.3180	-8.0714	335.4	21.75	19.35
cssz-56a	Central and South America	280.3172	-8.9958	331.6	8	11.09
cssz-56b	Central and South America	279.9209	-9.2072	331.6	7	5
cssz-56x	Central and South America	281.4212	-8.4063	331.6	23	57.13
cssz-56y	Central and South America	281.0534	-8.6028	331.6	23	37.59
cssz-56z	Central and South America	280.6854	-8.7993	331.6	23	18.05
cssz-57a	Central and South America	280.7492	-9.7356	328.7	8.6	10.75
cssz-57b	Central and South America	280.3640	-9.9663	328.7	6.6	5
cssz-57x	Central and South America	281.8205	-9.0933	328.7	23.4	57.94
cssz-57y	Central and South America	281.4636	-9.3074	328.7	23.4	38.08
cssz-57z	Central and South America	281.1065	-9.5215	328.7	23.4	18.22
cssz-58a	Central and South America	281.2275	-10.5350	330.5	9.2	10.4
cssz-58b	Central and South America	280.8348	-10.7532	330.5	6.2	5
cssz-58y	Central and South America	281.9548	-10.1306	330.5	23.8	38.57
cssz-58z	Central and South America	281.5913	-10.3328	330.5	23.8	18.39
cssz-59a	Central and South America	281.6735	-11.2430	326.2	9.8	10.05
cssz-59b	Central and South America	281.2982	-11.4890	326.2	5.8	5
cssz-59y	Central and South America	282.3675	-10.7876	326.2	24.2	39.06
cssz-59z	Central and South America	282.0206	-11.0153	326.2	24.2	18.56
cssz-60a	Central and South America	282.1864	-11.9946	326.5	10.4	9.71
cssz-60b	Central and South America	281.8096	-12.2384	326.5	5.4	5
cssz-60y	Central and South America	282.8821	-11.5438	326.5	24.6	39.55
cssz-60z	Central and South America	282.5344	-11.7692	326.5	24.6	18.73
cssz-61a	Central and South America	282.6944	-12.7263	325.5	11	9.36
cssz-61b	Central and South America	282.3218	-12.9762	325.5	5	5
cssz-61y	Central and South America	283.3814	-12.2649	325.5	25	40.03
cssz-61z	Central and South America	283.0381	-12.4956	325.5	25	18.9
cssz-62a	Central and South America	283.1980	-13.3556	319	11	9.79

continued on next page

Table B2: (continued)

Segment	Description	Longitude (°E)	Latitude (°N)	Strike (°)	Dip (°)	Depth (km)
cssz-62b	Central and South America	282.8560	-13.6451	319	5.5	5
cssz-62y	Central and South America	283.8178	-12.8300	319	27	42.03
cssz-62z	Central and South America	283.5081	-13.0928	319	27	19.33
cssz-63a	Central and South America	283.8032	-14.0147	317.9	11	10.23
cssz-63b	Central and South America	283.4661	-14.3106	317.9	6	5
cssz-63z	Central and South America	284.1032	-13.7511	317.9	29	19.77
cssz-64a	Central and South America	284.4144	-14.6482	315.7	13	11.96
cssz-64b	Central and South America	284.0905	-14.9540	315.7	8	5
cssz-65a	Central and South America	285.0493	-15.2554	313.2	15	13.68
cssz-65b	Central and South America	284.7411	-15.5715	313.2	10	5
cssz-66a	Central and South America	285.6954	-15.7816	307.7	14.5	13.68
cssz-66b	Central and South America	285.4190	-16.1258	307.7	10	5
cssz-67a	Central and South America	286.4127	-16.2781	304.3	14	13.68
cssz-67b	Central and South America	286.1566	-16.6381	304.3	10	5
cssz-67z	Central and South America	286.6552	-15.9365	304.3	23	25.78
cssz-68a	Central and South America	287.2481	-16.9016	311.8	14	13.68
cssz-68b	Central and South America	286.9442	-17.2264	311.8	10	5
cssz-68z	Central and South America	287.5291	-16.6007	311.8	26	25.78
cssz-69a	Central and South America	287.9724	-17.5502	314.9	14	13.68
cssz-69b	Central and South America	287.6496	-17.8590	314.9	10	5
cssz-69y	Central and South America	288.5530	-16.9934	314.9	29	50.02
cssz-69z	Central and South America	288.2629	-17.2718	314.9	29	25.78
cssz-70a	Central and South America	288.6731	-18.2747	320.4	14	13.25
cssz-70b	Central and South America	288.3193	-18.5527	320.4	9.5	5
cssz-70y	Central and South America	289.3032	-17.7785	320.4	30	50.35
cssz-70z	Central and South America	288.9884	-18.0266	320.4	30	25.35
cssz-71a	Central and South America	289.3089	-19.1854	333.2	14	12.82
cssz-71b	Central and South America	288.8968	-19.3820	333.2	9	5
cssz-71y	Central and South America	290.0357	-18.8382	333.2	31	50.67
cssz-71z	Central and South America	289.6725	-19.0118	333.2	31	24.92
cssz-72a	Central and South America	289.6857	-20.3117	352.4	14	12.54
cssz-72b	Central and South America	289.2250	-20.3694	352.4	8.67	5
cssz-72z	Central and South America	290.0882	-20.2613	352.4	32	24.63
cssz-73a	Central and South America	289.7731	-21.3061	358.9	14	12.24
cssz-73b	Central and South America	289.3053	-21.3142	358.9	8.33	5
cssz-73z	Central and South America	290.1768	-21.2991	358.9	33	24.34
cssz-74a	Central and South America	289.7610	-22.2671	3.06	14	11.96
cssz-74b	Central and South America	289.2909	-22.2438	3.06	8	5

continued on next page

Table B2: (continued)

Segment	Description	Longitude (°E)	Latitude (°N)	Strike (°)	Dip (°)	Depth (km)
cssz-75a	Central and South America	289.6982	-23.1903	4.83	14.09	11.96
cssz-75b	Central and South America	289.2261	-23.1536	4.83	8	5
cssz-76a	Central and South America	289.6237	-24.0831	4.67	14.18	11.96
cssz-76b	Central and South America	289.1484	-24.0476	4.67	8	5
cssz-77a	Central and South America	289.5538	-24.9729	4.3	14.27	11.96
cssz-77b	Central and South America	289.0750	-24.9403	4.3	8	5
cssz-78a	Central and South America	289.4904	-25.8621	3.86	14.36	11.96
cssz-78b	Central and South America	289.0081	-25.8328	3.86	8	5
cssz-79a	Central and South America	289.3491	-26.8644	11.34	14.45	11.96
cssz-79b	Central and South America	288.8712	-26.7789	11.34	8	5
cssz-80a	Central and South America	289.1231	-27.7826	14.16	14.54	11.96
cssz-80b	Central and South America	288.6469	-27.6762	14.16	8	5
cssz-81a	Central and South America	288.8943	-28.6409	13.19	14.63	11.96
cssz-81b	Central and South America	288.4124	-28.5417	13.19	8	5
cssz-82a	Central and South America	288.7113	-29.4680	9.68	14.72	11.96
cssz-82b	Central and South America	288.2196	-29.3950	9.68	8	5
cssz-83a	Central and South America	288.5944	-30.2923	5.36	14.81	11.96
cssz-83b	Central and South America	288.0938	-30.2517	5.36	8	5
cssz-84a	Central and South America	288.5223	-31.1639	3.8	14.9	11.96
cssz-84b	Central and South America	288.0163	-31.1351	3.8	8	5
cssz-85a	Central and South America	288.4748	-32.0416	2.55	15	11.96
cssz-85b	Central and South America	287.9635	-32.0223	2.55	8	5
cssz-86a	Central and South America	288.3901	-33.0041	7.01	15	11.96
cssz-86b	Central and South America	287.8768	-32.9512	7.01	8	5
cssz-87a	Central and South America	288.1050	-34.0583	19.4	15	11.96
cssz-87b	Central and South America	287.6115	-33.9142	19.4	8	5
cssz-88a	Central and South America	287.5309	-35.0437	32.81	15	11.96
cssz-88b	Central and South America	287.0862	-34.8086	32.81	8	5
cssz-88z	Central and South America	287.9308	-35.2545	32.81	30	24.9
cssz-89a	Central and South America	287.2380	-35.5993	14.52	16.67	11.96
cssz-89b	Central and South America	286.7261	-35.4914	14.52	8	5
cssz-89z	Central and South America	287.7014	-35.6968	14.52	30	26.3
cssz-90a	Central and South America	286.8442	-36.5645	22.64	18.33	11.96
cssz-90b	Central and South America	286.3548	-36.4004	22.64	8	5
cssz-90z	Central and South America	287.2916	-36.7142	22.64	30	27.68
cssz-91a	Central and South America	286.5925	-37.2488	10.9	20	11.96
cssz-91b	Central and South America	286.0721	-37.1690	10.9	8	5
cssz-91z	Central and South America	287.0726	-37.3224	10.9	30	29.06

continued on next page

Table B2: (continued)

Segment	Description	Longitude (°E)	Latitude (°N)	Strike (°)	Dip (°)	Depth (km)
cssz-92a	Central and South America	286.4254	-38.0945	8.23	20	11.96
cssz-92b	Central and South America	285.8948	-38.0341	8.23	8	5
cssz-92z	Central and South America	286.9303	-38.1520	8.23	26.67	29.06
cssz-93a	Central and South America	286.2047	-39.0535	13.46	20	11.96
cssz-93b	Central and South America	285.6765	-38.9553	13.46	8	5
cssz-93z	Central and South America	286.7216	-39.1495	13.46	23.33	29.06
cssz-94a	Central and South America	286.0772	-39.7883	3.4	20	11.96
cssz-94b	Central and South America	285.5290	-39.7633	3.4	8	5
cssz-94z	Central and South America	286.6255	-39.8133	3.4	20	29.06
cssz-95a	Central and South America	285.9426	-40.7760	9.84	20	11.96
cssz-95b	Central and South America	285.3937	-40.7039	9.84	8	5
cssz-95z	Central and South America	286.4921	-40.8481	9.84	20	29.06
cssz-96a	Central and South America	285.7839	-41.6303	7.6	20	11.96
cssz-96b	Central and South America	285.2245	-41.5745	7.6	8	5
cssz-96x	Central and South America	287.4652	-41.7977	7.6	20	63.26
cssz-96y	Central and South America	286.9043	-41.7419	7.6	20	46.16
cssz-96z	Central and South America	286.3439	-41.6861	7.6	20	29.06
cssz-97a	Central and South America	285.6695	-42.4882	5.3	20	11.96
cssz-97b	Central and South America	285.0998	-42.4492	5.3	8	5
cssz-97x	Central and South America	287.3809	-42.6052	5.3	20	63.26
cssz-97y	Central and South America	286.8101	-42.5662	5.3	20	46.16
cssz-97z	Central and South America	286.2396	-42.5272	5.3	20	29.06
cssz-98a	Central and South America	285.5035	-43.4553	10.53	20	11.96
cssz-98b	Central and South America	284.9322	-43.3782	10.53	8	5
cssz-98x	Central and South America	287.2218	-43.6866	10.53	20	63.26
cssz-98y	Central and South America	286.6483	-43.6095	10.53	20	46.16
cssz-98z	Central and South America	286.0755	-43.5324	10.53	20	29.06
cssz-99a	Central and South America	285.3700	-44.2595	4.86	20	11.96
cssz-99b	Central and South America	284.7830	-44.2237	4.86	8	5
cssz-99x	Central and South America	287.1332	-44.3669	4.86	20	63.26
cssz-99y	Central and South America	286.5451	-44.3311	4.86	20	46.16
cssz-99z	Central and South America	285.9574	-44.2953	4.86	20	29.06
cssz-100a	Central and South America	285.2713	-45.1664	5.68	20	11.96
cssz-100b	Central and South America	284.6758	-45.1246	5.68	8	5
cssz-100x	Central and South America	287.0603	-45.2918	5.68	20	63.26
cssz-100y	Central and South America	286.4635	-45.2500	5.68	20	46.16
cssz-100z	Central and South America	285.8672	-45.2082	5.68	20	29.06
cssz-101a	Central and South America	285.3080	-45.8607	352.6	20	9.36

continued on next page

Table B2: (continued)

Segment	Description	Longitude (°E)	Latitude (°N)	Strike (°)	Dip (°)	Depth (km)
cssz-101b	Central and South America	284.7067	-45.9152	352.6	5	5
cssz-101y	Central and South America	286.5089	-45.7517	352.6	20	43.56
cssz-101z	Central and South America	285.9088	-45.8062	352.6	20	26.46
cssz-102a	Central and South America	285.2028	-47.1185	17.72	5	9.36
cssz-102b	Central and South America	284.5772	-46.9823	17.72	5	5
cssz-102y	Central and South America	286.4588	-47.3909	17.72	5	18.07
cssz-102z	Central and South America	285.8300	-47.2547	17.72	5	13.72
cssz-103a	Central and South America	284.7075	-48.0396	23.37	7.5	11.53
cssz-103b	Central and South America	284.0972	-47.8630	23.37	7.5	5
cssz-103x	Central and South America	286.5511	-48.5694	23.37	7.5	31.11
cssz-103y	Central and South America	285.9344	-48.3928	23.37	7.5	24.58
cssz-103z	Central and South America	285.3199	-48.2162	23.37	7.5	18.05
cssz-104a	Central and South America	284.3440	-48.7597	14.87	10	13.68
cssz-104b	Central and South America	283.6962	-48.6462	14.87	10	5
cssz-104x	Central and South America	286.2962	-49.1002	14.87	10	39.73
cssz-104y	Central and South America	285.6440	-48.9867	14.87	10	31.05
cssz-104z	Central and South America	284.9933	-48.8732	14.87	10	22.36
cssz-105a	Central and South America	284.2312	-49.4198	0.25	9.67	13.4
cssz-105b	Central and South America	283.5518	-49.4179	0.25	9.67	5
cssz-105x	Central and South America	286.2718	-49.4255	0.25	9.67	38.59
cssz-105y	Central and South America	285.5908	-49.4236	0.25	9.67	30.2
cssz-105z	Central and South America	284.9114	-49.4217	0.25	9.67	21.8
cssz-106a	Central and South America	284.3730	-50.1117	347.5	9.25	13.04
cssz-106b	Central and South America	283.6974	-50.2077	347.5	9.25	5
cssz-106x	Central and South America	286.3916	-49.8238	347.5	9.25	37.15
cssz-106y	Central and South America	285.7201	-49.9198	347.5	9.25	29.11
cssz-106z	Central and South America	285.0472	-50.0157	347.5	9.25	21.07
cssz-107a	Central and South America	284.7130	-50.9714	346.5	9	12.82
cssz-107b	Central and South America	284.0273	-51.0751	346.5	9	5
cssz-107x	Central and South America	286.7611	-50.6603	346.5	9	36.29
cssz-107y	Central and South America	286.0799	-50.7640	346.5	9	28.47
cssz-107z	Central and South America	285.3972	-50.8677	346.5	9	20.64
cssz-108a	Central and South America	285.0378	-51.9370	352	8.67	12.54
cssz-108b	Central and South America	284.3241	-51.9987	352	8.67	5
cssz-108x	Central and South America	287.1729	-51.7519	352	8.67	35.15
cssz-108y	Central and South America	286.4622	-51.8136	352	8.67	27.61
cssz-108z	Central and South America	285.7505	-51.8753	352	8.67	20.07
cssz-109a	Central and South America	285.2635	-52.8439	353.1	8.33	12.24
cssz-109b	Central and South America	284.5326	-52.8974	353.1	8.33	5

continued on next page

Table B2: (continued)

Segment	Description	Longitude (°E)	Latitude (°N)	Strike (°)	Dip (°)	Depth (km)
cssz-109x	Central and South America	287.4508	-52.6834	353.1	8.33	33.97
cssz-109y	Central and South America	286.7226	-52.7369	353.1	8.33	26.73
cssz-109z	Central and South America	285.9935	-52.7904	353.1	8.33	19.49
cssz-110a	Central and South America	285.5705	-53.4139	334.2	8	11.96
cssz-110b	Central and South America	284.8972	-53.6076	334.2	8	5
cssz-110x	Central and South America	287.5724	-52.8328	334.2	8	32.83
cssz-110y	Central and South America	286.9081	-53.0265	334.2	8	25.88
cssz-110z	Central and South America	286.2408	-53.2202	334.2	8	18.92
cssz-111a	Central and South America	286.1627	-53.8749	313.8	8	11.96
cssz-111b	Central and South America	285.6382	-54.1958	313.8	8	5
cssz-111x	Central and South America	287.7124	-52.9122	313.8	8	32.83
cssz-111y	Central and South America	287.1997	-53.2331	313.8	8	25.88
cssz-111z	Central and South America	286.6832	-53.5540	313.8	8	18.92
cssz-112a	Central and South America	287.3287	-54.5394	316.4	8	11.96
cssz-112b	Central and South America	286.7715	-54.8462	316.4	8	5
cssz-112x	Central and South America	288.9756	-53.6190	316.4	8	32.83
cssz-112y	Central and South America	288.4307	-53.9258	316.4	8	25.88
cssz-112z	Central and South America	287.8817	-54.2326	316.4	8	18.92
cssz-113a	Central and South America	288.3409	-55.0480	307.6	8	11.96
cssz-113b	Central and South America	287.8647	-55.4002	307.6	8	5
cssz-113x	Central and South America	289.7450	-53.9914	307.6	8	32.83
cssz-113y	Central and South America	289.2810	-54.3436	307.6	8	25.88
cssz-113z	Central and South America	288.8130	-54.6958	307.6	8	18.92
cssz-114a	Central and South America	289.5342	-55.5026	301.5	8	11.96
cssz-114b	Central and South America	289.1221	-55.8819	301.5	8	5
cssz-114x	Central and South America	290.7472	-54.3647	301.5	8	32.83
cssz-114y	Central and South America	290.3467	-54.7440	301.5	8	25.88
cssz-114z	Central and South America	289.9424	-55.1233	301.5	8	18.92
cssz-115a	Central and South America	290.7682	-55.8485	292.7	8	11.96
cssz-115b	Central and South America	290.4608	-56.2588	292.7	8	5
cssz-115x	Central and South America	291.6714	-54.6176	292.7	8	32.83
cssz-115y	Central and South America	291.3734	-55.0279	292.7	8	25.88
cssz-115z	Central and South America	291.0724	-55.4382	292.7	8	18.92

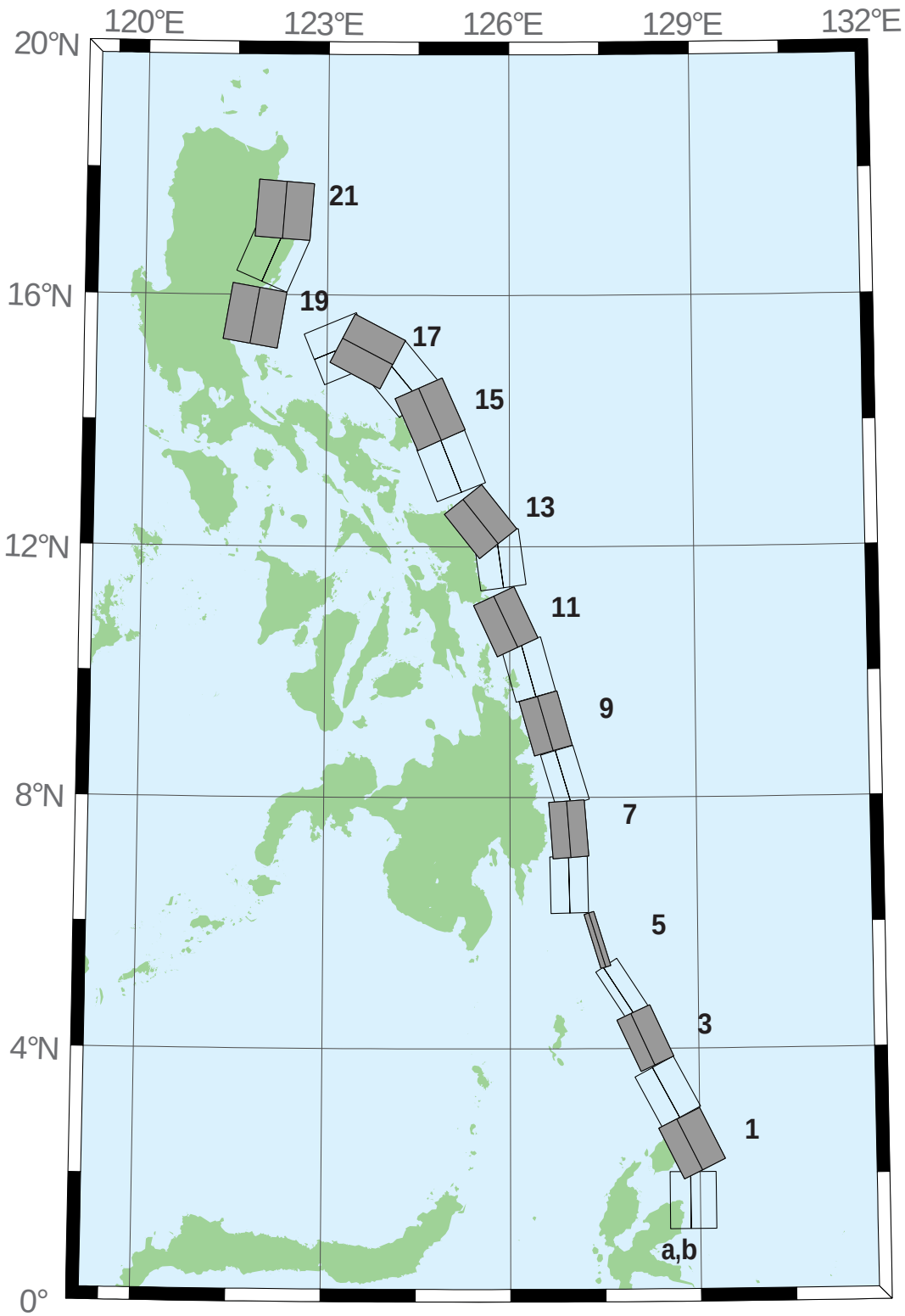

Figure B3: Eastern Philippines Subduction Zone unit sources.

Table B3: Earthquake parameters for Eastern Philippines Subduction Zone unit sources.

Segment	Description	Longitude (°E)	Latitude (°N)	Strike (°)	Dip (°)	Depth (km)
epsz-0a	Eastern Philippines	128.5264	1.5930	180	44	26.92
epsz-0b	Eastern Philippines	128.8496	1.5930	180	26	5
epsz-1a	Eastern Philippines	128.5521	2.3289	153.6	44.2	27.62
epsz-1b	Eastern Philippines	128.8408	2.4720	153.6	26.9	5
epsz-2a	Eastern Philippines	128.1943	3.1508	151.9	45.9	32.44
epsz-2b	Eastern Philippines	128.4706	3.2979	151.9	32.8	5.35
epsz-3a	Eastern Philippines	127.8899	4.0428	155.2	57.3	40.22
epsz-3b	Eastern Philippines	128.1108	4.1445	155.2	42.7	6.31
epsz-4a	Eastern Philippines	127.6120	4.8371	146.8	71.4	48.25
epsz-4b	Eastern Philippines	127.7324	4.9155	146.8	54.8	7.39
epsz-5a	Eastern Philippines	127.3173	5.7040	162.9	79.9	57.4
epsz-5b	Eastern Philippines	127.3930	5.7272	162.9	79.4	8.25
epsz-6a	Eastern Philippines	126.6488	6.6027	178.9	48.6	45.09
epsz-6b	Eastern Philippines	126.9478	6.6085	178.9	48.6	7.58
epsz-7a	Eastern Philippines	126.6578	7.4711	175.8	50.7	45.52
epsz-7b	Eastern Philippines	126.9439	7.4921	175.8	50.7	6.83
epsz-8a	Eastern Philippines	126.6227	8.2456	163.3	56.7	45.6
epsz-8b	Eastern Philippines	126.8614	8.3164	163.3	48.9	7.92
epsz-9a	Eastern Philippines	126.2751	9.0961	164.1	47	43.59
epsz-9b	Eastern Philippines	126.5735	9.1801	164.1	44.9	8.3
epsz-10a	Eastern Philippines	125.9798	9.9559	164.5	43.1	42.25
epsz-10b	Eastern Philippines	126.3007	10.0438	164.5	43.1	8.09
epsz-11a	Eastern Philippines	125.6079	10.6557	155	37.8	38.29
epsz-11b	Eastern Philippines	125.9353	10.8059	155	37.8	7.64
epsz-12a	Eastern Philippines	125.4697	11.7452	172.1	36	37.01
epsz-12b	Eastern Philippines	125.8374	11.7949	172.1	36	7.62
epsz-13a	Eastern Philippines	125.2238	12.1670	141.5	32.4	33.87
epsz-13b	Eastern Philippines	125.5278	12.4029	141.5	32.4	7.08
epsz-14a	Eastern Philippines	124.6476	13.1365	158.2	23	25.92
epsz-14b	Eastern Philippines	125.0421	13.2898	158.2	23	6.38
epsz-15a	Eastern Philippines	124.3107	13.9453	156.1	24.1	26.51
epsz-15b	Eastern Philippines	124.6973	14.1113	156.1	24.1	6.09
epsz-16a	Eastern Philippines	123.8998	14.4025	140.3	19.5	21.69
epsz-16b	Eastern Philippines	124.2366	14.6728	140.3	19.5	5
epsz-17a	Eastern Philippines	123.4604	14.7222	117.6	15.3	18.19
epsz-17b	Eastern Philippines	123.6682	15.1062	117.6	15.3	5
epsz-18a	Eastern Philippines	123.3946	14.7462	67.4	15	17.94
epsz-18b	Eastern Philippines	123.2219	15.1467	67.4	15	5
epsz-19a	Eastern Philippines	121.3638	15.7400	189.6	15	17.94
epsz-19b	Eastern Philippines	121.8082	15.6674	189.6	15	5
epsz-20a	Eastern Philippines	121.6833	16.7930	203.3	15	17.94
epsz-20b	Eastern Philippines	122.0994	16.6216	203.3	15	5
epsz-21a	Eastern Philippines	121.8279	17.3742	184.2	15	17.94
epsz-21b	Eastern Philippines	122.2814	17.3425	184.2	15	5

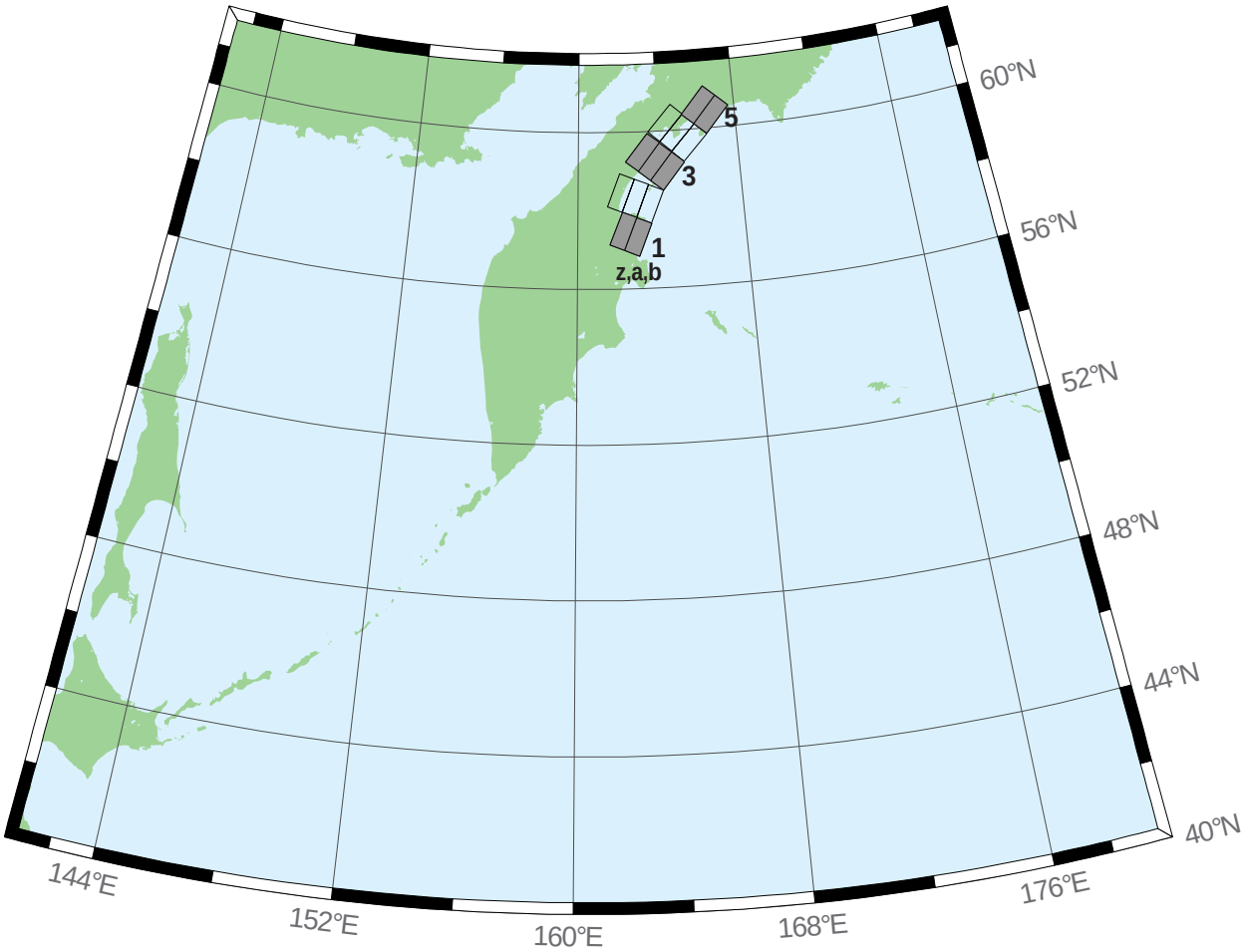

Figure B4: Kamchatka–Bering Subduction Zone unit sources.

Table B4: Earthquake parameters for Kamchatka–Bering Subduction Zone unit sources.

Segment	Description	Longitude (°E)	Latitude (°N)	Strike (°)	Dip (°)	Depth (km)
kbsz-1a	Kamchatka-Bering	161.8374	57.5485	201.5	29	26.13
kbsz-1b	Kamchatka-Bering	162.5162	57.4030	202.1	25	5
kbsz-2a	Kamchatka-Bering	162.4410	58.3816	201.7	29	26.13
kbsz-2b	Kamchatka-Bering	163.1344	58.2343	202.3	25	5
kbsz-2z	Kamchatka-Bering	161.7418	58.5249	201.1	29	50.37
kbsz-3a	Kamchatka-Bering	163.5174	59.3493	218.9	29	26.13
kbsz-3b	Kamchatka-Bering	164.1109	59.1001	219.4	25	5
kbsz-3z	Kamchatka-Bering	162.9150	59.5958	218.4	29	50.37
kbsz-4a	Kamchatka-Bering	164.7070	60.0632	222.2	29	26.13
kbsz-4b	Kamchatka-Bering	165.2833	59.7968	222.7	25	5
kbsz-4z	Kamchatka-Bering	164.1212	60.3270	221.7	29	50.37
kbsz-5a	Kamchatka-Bering	165.8652	60.7261	220.5	29	26.13
kbsz-5b	Kamchatka-Bering	166.4692	60.4683	221	25	5

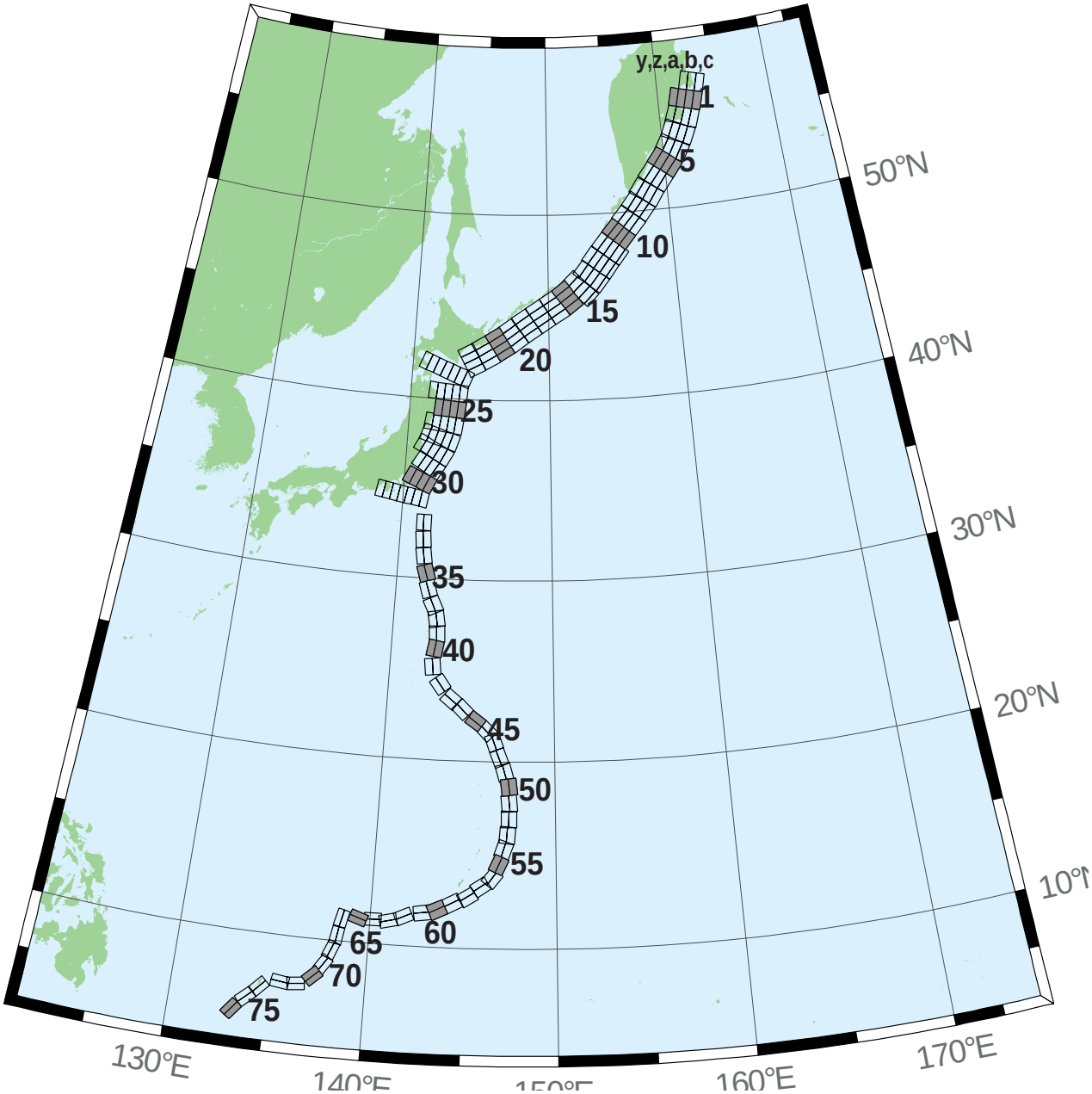

Figure B5: Kamchatka–Kuril–Japan–Izu–Mariana–Yap Subduction Zone unit sources.

Table B5: Earthquake parameters for Kamchatka-Kuril-Japan-Izu-Mariana-Yap Subduction Zone unit sources.

Segment	Description	Longitude (°E)	Latitude (°N)	Strike (°)	Dip (°)	Depth (km)
kisz-0a	Kamchatka-Kuril-Japan-Izu-Mariana-Yap	162.8200	56.3667	194.4	29	26.13
kisz-0b	Kamchatka-Kuril-Japan-Izu-Mariana-Yap	163.5057	56.2677	195	25	5
kisz-0z	Kamchatka-Kuril-Japan-Izu-Mariana-Yap	162.1309	56.4618	193.8	29	50.37
kisz-1a	Kamchatka-Kuril-Japan-Izu-Mariana-Yap	162.4318	55.5017	195	29	26.13
kisz-1b	Kamchatka-Kuril-Japan-Izu-Mariana-Yap	163.1000	55.4000	195	25	5
kisz-1y	Kamchatka-Kuril-Japan-Izu-Mariana-Yap	161.0884	55.7050	195	29	74.61
kisz-1z	Kamchatka-Kuril-Japan-Izu-Mariana-Yap	161.7610	55.6033	195	29	50.37
kisz-2a	Kamchatka-Kuril-Japan-Izu-Mariana-Yap	161.9883	54.6784	200	29	26.13
kisz-2b	Kamchatka-Kuril-Japan-Izu-Mariana-Yap	162.6247	54.5440	200	25	5
kisz-2y	Kamchatka-Kuril-Japan-Izu-Mariana-Yap	160.7072	54.9471	200	29	74.61
kisz-2z	Kamchatka-Kuril-Japan-Izu-Mariana-Yap	161.3488	54.8127	200	29	50.37
kisz-3a	Kamchatka-Kuril-Japan-Izu-Mariana-Yap	161.4385	53.8714	204	29	26.13
kisz-3b	Kamchatka-Kuril-Japan-Izu-Mariana-Yap	162.0449	53.7116	204	25	5
kisz-3y	Kamchatka-Kuril-Japan-Izu-Mariana-Yap	160.2164	54.1910	204	29	74.61
kisz-3z	Kamchatka-Kuril-Japan-Izu-Mariana-Yap	160.8286	54.0312	204	29	50.37
kisz-4a	Kamchatka-Kuril-Japan-Izu-Mariana-Yap	160.7926	53.1087	210	29	26.13
kisz-4b	Kamchatka-Kuril-Japan-Izu-Mariana-Yap	161.3568	52.9123	210	25	5
kisz-4y	Kamchatka-Kuril-Japan-Izu-Mariana-Yap	159.6539	53.5015	210	29	74.61
kisz-4z	Kamchatka-Kuril-Japan-Izu-Mariana-Yap	160.2246	53.3051	210	29	50.37
kisz-5a	Kamchatka-Kuril-Japan-Izu-Mariana-Yap	160.0211	52.4113	218	29	26.13
kisz-5b	Kamchatka-Kuril-Japan-Izu-Mariana-Yap	160.5258	52.1694	218	25	5
kisz-5y	Kamchatka-Kuril-Japan-Izu-Mariana-Yap	159.0005	52.8950	218	29	74.61
kisz-5z	Kamchatka-Kuril-Japan-Izu-Mariana-Yap	159.5122	52.6531	218	29	50.37
kisz-6a	Kamchatka-Kuril-Japan-Izu-Mariana-Yap	159.1272	51.7034	218	29	26.13
kisz-6b	Kamchatka-Kuril-Japan-Izu-Mariana-Yap	159.6241	51.4615	218	25	5
kisz-6y	Kamchatka-Kuril-Japan-Izu-Mariana-Yap	158.1228	52.1871	218	29	74.61
kisz-6z	Kamchatka-Kuril-Japan-Izu-Mariana-Yap	158.6263	51.9452	218	29	50.37
kisz-7a	Kamchatka-Kuril-Japan-Izu-Mariana-Yap	158.2625	50.9549	214	29	26.13
kisz-7b	Kamchatka-Kuril-Japan-Izu-Mariana-Yap	158.7771	50.7352	214	25	5
kisz-7y	Kamchatka-Kuril-Japan-Izu-Mariana-Yap	157.2236	51.3942	214	29	74.61
kisz-7z	Kamchatka-Kuril-Japan-Izu-Mariana-Yap	157.7443	51.1745	214	29	50.37
kisz-8a	Kamchatka-Kuril-Japan-Izu-Mariana-Yap	157.4712	50.2459	218	31	27.7
kisz-8b	Kamchatka-Kuril-Japan-Izu-Mariana-Yap	157.9433	50.0089	218	27	5
kisz-8y	Kamchatka-Kuril-Japan-Izu-Mariana-Yap	156.5176	50.7199	218	31	79.2
kisz-8z	Kamchatka-Kuril-Japan-Izu-Mariana-Yap	156.9956	50.4829	218	31	53.45
kisz-9a	Kamchatka-Kuril-Japan-Izu-Mariana-Yap	156.6114	49.5583	220	31	27.7
kisz-9b	Kamchatka-Kuril-Japan-Izu-Mariana-Yap	157.0638	49.3109	220	27	5
kisz-9y	Kamchatka-Kuril-Japan-Izu-Mariana-Yap	155.6974	50.0533	220	31	79.2
kisz-9z	Kamchatka-Kuril-Japan-Izu-Mariana-Yap	156.1556	49.8058	220	31	53.45

continued on next page

Table B5: (continued)

Segment	Description	Longitude (°E)	Latitude (°N)	Strike (°)	Dip (°)	Depth (km)
kisz-10a	Kamchatka-Kuril-Japan-Izu-Mariana-Yap	155.7294	48.8804	221	31	27.7
kisz-10b	Kamchatka-Kuril-Japan-Izu-Mariana-Yap	156.1690	48.6278	221	27	5
kisz-10y	Kamchatka-Kuril-Japan-Izu-Mariana-Yap	154.8413	49.3856	221	31	79.2
kisz-10z	Kamchatka-Kuril-Japan-Izu-Mariana-Yap	155.2865	49.1330	221	31	53.45
kisz-11a	Kamchatka-Kuril-Japan-Izu-Mariana-Yap	154.8489	48.1821	219	31	27.7
kisz-11b	Kamchatka-Kuril-Japan-Izu-Mariana-Yap	155.2955	47.9398	219	27	5
kisz-11y	Kamchatka-Kuril-Japan-Izu-Mariana-Yap	153.9472	48.6667	219	31	79.2
kisz-11z	Kamchatka-Kuril-Japan-Izu-Mariana-Yap	154.3991	48.4244	219	31	53.45
kisz-11c	Kamchatka-Kuril-Japan-Izu-Mariana-Yap	156.0358	47.5374	39	57.89	4.602
kisz-12a	Kamchatka-Kuril-Japan-Izu-Mariana-Yap	153.9994	47.4729	217	31	27.7
kisz-12b	Kamchatka-Kuril-Japan-Izu-Mariana-Yap	154.4701	47.2320	217	27	5
kisz-12y	Kamchatka-Kuril-Japan-Izu-Mariana-Yap	153.0856	47.9363	217	31	79.2
kisz-12z	Kamchatka-Kuril-Japan-Izu-Mariana-Yap	153.5435	47.7046	217	31	53.45
kisz-12c	Kamchatka-Kuril-Japan-Izu-Mariana-Yap	155.2208	46.8473	37	57.89	4.602
kisz-13a	Kamchatka-Kuril-Japan-Izu-Mariana-Yap	153.2239	46.7564	218	31	27.7
kisz-13b	Kamchatka-Kuril-Japan-Izu-Mariana-Yap	153.6648	46.5194	218	27	5
kisz-13y	Kamchatka-Kuril-Japan-Izu-Mariana-Yap	152.3343	47.2304	218	31	79.2
kisz-13z	Kamchatka-Kuril-Japan-Izu-Mariana-Yap	152.7801	46.9934	218	31	53.45
kisz-13c	Kamchatka-Kuril-Japan-Izu-Mariana-Yap	154.3957	46.1257	38	57.89	4.602
kisz-14a	Kamchatka-Kuril-Japan-Izu-Mariana-Yap	152.3657	46.1514	225	23	24.54
kisz-14b	Kamchatka-Kuril-Japan-Izu-Mariana-Yap	152.7855	45.8591	225	23	5
kisz-14y	Kamchatka-Kuril-Japan-Izu-Mariana-Yap	151.5172	46.7362	225	23	63.62
kisz-14z	Kamchatka-Kuril-Japan-Izu-Mariana-Yap	151.9426	46.4438	225	23	44.08
kisz-14c	Kamchatka-Kuril-Japan-Izu-Mariana-Yap	153.4468	45.3976	45	57.89	4.602
kisz-15a	Kamchatka-Kuril-Japan-Izu-Mariana-Yap	151.4663	45.5963	233	25	23.73
kisz-15b	Kamchatka-Kuril-Japan-Izu-Mariana-Yap	151.8144	45.2712	233	22	5
kisz-15y	Kamchatka-Kuril-Japan-Izu-Mariana-Yap	150.7619	46.2465	233	25	65.99
kisz-15z	Kamchatka-Kuril-Japan-Izu-Mariana-Yap	151.1151	45.9214	233	25	44.86
kisz-16a	Kamchatka-Kuril-Japan-Izu-Mariana-Yap	150.4572	45.0977	237	25	23.73
kisz-16b	Kamchatka-Kuril-Japan-Izu-Mariana-Yap	150.7694	44.7563	237	22	5
kisz-16y	Kamchatka-Kuril-Japan-Izu-Mariana-Yap	149.8253	45.7804	237	25	65.99
kisz-16z	Kamchatka-Kuril-Japan-Izu-Mariana-Yap	150.1422	45.4390	237	25	44.86
kisz-17a	Kamchatka-Kuril-Japan-Izu-Mariana-Yap	149.3989	44.6084	237	25	23.73
kisz-17b	Kamchatka-Kuril-Japan-Izu-Mariana-Yap	149.7085	44.2670	237	22	5
kisz-17y	Kamchatka-Kuril-Japan-Izu-Mariana-Yap	148.7723	45.2912	237	25	65.99
kisz-17z	Kamchatka-Kuril-Japan-Izu-Mariana-Yap	149.0865	44.9498	237	25	44.86
kisz-18a	Kamchatka-Kuril-Japan-Izu-Mariana-Yap	148.3454	44.0982	235	25	23.73
kisz-18b	Kamchatka-Kuril-Japan-Izu-Mariana-Yap	148.6687	43.7647	235	22	5
kisz-18y	Kamchatka-Kuril-Japan-Izu-Mariana-Yap	147.6915	44.7651	235	25	65.99

continued on next page

Table B5: (continued)

Segment	Description	Longitude (°E)	Latitude (°N)	Strike (°)	Dip (°)	Depth (km)
kisz-18z	Kamchatka-Kuril-Japan-Izu-Mariana-Yap	148.0194	44.4316	235	25	44.86
kisz-19a	Kamchatka-Kuril-Japan-Izu-Mariana-Yap	147.3262	43.5619	233	25	23.73
kisz-19b	Kamchatka-Kuril-Japan-Izu-Mariana-Yap	147.6625	43.2368	233	22	5
kisz-19y	Kamchatka-Kuril-Japan-Izu-Mariana-Yap	146.6463	44.2121	233	25	65.99
kisz-19z	Kamchatka-Kuril-Japan-Izu-Mariana-Yap	146.9872	43.8870	233	25	44.86
kisz-20a	Kamchatka-Kuril-Japan-Izu-Mariana-Yap	146.3513	43.0633	237	25	23.73
kisz-20b	Kamchatka-Kuril-Japan-Izu-Mariana-Yap	146.6531	42.7219	237	22	5
kisz-20y	Kamchatka-Kuril-Japan-Izu-Mariana-Yap	145.7410	43.7461	237	25	65.99
kisz-20z	Kamchatka-Kuril-Japan-Izu-Mariana-Yap	146.0470	43.4047	237	25	44.86
kisz-21a	Kamchatka-Kuril-Japan-Izu-Mariana-Yap	145.3331	42.5948	239	25	23.73
kisz-21b	Kamchatka-Kuril-Japan-Izu-Mariana-Yap	145.6163	42.2459	239	22	5
kisz-21y	Kamchatka-Kuril-Japan-Izu-Mariana-Yap	144.7603	43.2927	239	25	65.99
kisz-21z	Kamchatka-Kuril-Japan-Izu-Mariana-Yap	145.0475	42.9438	239	25	44.86
kisz-22a	Kamchatka-Kuril-Japan-Izu-Mariana-Yap	144.3041	42.1631	242	25	23.73
kisz-22b	Kamchatka-Kuril-Japan-Izu-Mariana-Yap	144.5605	41.8037	242	22	5
kisz-22y	Kamchatka-Kuril-Japan-Izu-Mariana-Yap	143.7854	42.8819	242	25	65.99
kisz-22z	Kamchatka-Kuril-Japan-Izu-Mariana-Yap	144.0455	42.5225	242	25	44.86
kisz-23a	Kamchatka-Kuril-Japan-Izu-Mariana-Yap	143.2863	41.3335	202	21	21.28
kisz-23b	Kamchatka-Kuril-Japan-Izu-Mariana-Yap	143.8028	41.1764	202	19	5
kisz-23v	Kamchatka-Kuril-Japan-Izu-Mariana-Yap	140.6816	42.1189	202	21	110.9
kisz-23w	Kamchatka-Kuril-Japan-Izu-Mariana-Yap	141.2050	41.9618	202	21	92.95
kisz-23x	Kamchatka-Kuril-Japan-Izu-Mariana-Yap	141.7273	41.8047	202	21	75.04
kisz-23y	Kamchatka-Kuril-Japan-Izu-Mariana-Yap	142.2482	41.6476	202	21	57.12
kisz-23z	Kamchatka-Kuril-Japan-Izu-Mariana-Yap	142.7679	41.4905	202	21	39.2
kisz-24a	Kamchatka-Kuril-Japan-Izu-Mariana-Yap	142.9795	40.3490	185	21	21.28
kisz-24b	Kamchatka-Kuril-Japan-Izu-Mariana-Yap	143.5273	40.3125	185	19	5
kisz-24x	Kamchatka-Kuril-Japan-Izu-Mariana-Yap	141.3339	40.4587	185	21	75.04
kisz-24y	Kamchatka-Kuril-Japan-Izu-Mariana-Yap	141.8827	40.4221	185	21	57.12
kisz-24z	Kamchatka-Kuril-Japan-Izu-Mariana-Yap	142.4312	40.3856	185	21	39.2
kisz-25a	Kamchatka-Kuril-Japan-Izu-Mariana-Yap	142.8839	39.4541	185	21	21.28
kisz-25b	Kamchatka-Kuril-Japan-Izu-Mariana-Yap	143.4246	39.4176	185	19	5
kisz-25y	Kamchatka-Kuril-Japan-Izu-Mariana-Yap	141.8012	39.5272	185	21	57.12
kisz-25z	Kamchatka-Kuril-Japan-Izu-Mariana-Yap	142.3426	39.4907	185	21	39.2
kisz-26a	Kamchatka-Kuril-Japan-Izu-Mariana-Yap	142.7622	38.5837	188	21	21.28
kisz-26b	Kamchatka-Kuril-Japan-Izu-Mariana-Yap	143.2930	38.5254	188	19	5
kisz-26x	Kamchatka-Kuril-Japan-Izu-Mariana-Yap	141.1667	38.7588	188	21	75.04
kisz-26y	Kamchatka-Kuril-Japan-Izu-Mariana-Yap	141.6990	38.7004	188	21	57.12
kisz-26z	Kamchatka-Kuril-Japan-Izu-Mariana-Yap	142.2308	38.6421	188	21	39.2
kisz-27a	Kamchatka-Kuril-Japan-Izu-Mariana-Yap	142.5320	37.7830	198	21	21.28

continued on next page

Table B5: (continued)

Segment	Description	Longitude (°E)	Latitude (°N)	Strike (°)	Dip (°)	Depth (km)
kisz-27b	Kamchatka-Kuril-Japan-Izu-Mariana-Yap	143.0357	37.6534	198	19	5
kisz-27x	Kamchatka-Kuril-Japan-Izu-Mariana-Yap	141.0142	38.1717	198	21	75.04
kisz-27y	Kamchatka-Kuril-Japan-Izu-Mariana-Yap	141.5210	38.0421	198	21	57.12
kisz-27z	Kamchatka-Kuril-Japan-Izu-Mariana-Yap	142.0269	37.9126	198	21	39.2
kisz-28a	Kamchatka-Kuril-Japan-Izu-Mariana-Yap	142.1315	37.0265	208	21	21.28
kisz-28b	Kamchatka-Kuril-Japan-Izu-Mariana-Yap	142.5941	36.8297	208	19	5
kisz-28x	Kamchatka-Kuril-Japan-Izu-Mariana-Yap	140.7348	37.6171	208	21	75.04
kisz-28y	Kamchatka-Kuril-Japan-Izu-Mariana-Yap	141.2016	37.4202	208	21	57.12
kisz-28z	Kamchatka-Kuril-Japan-Izu-Mariana-Yap	141.6671	37.2234	208	21	39.2
kisz-29a	Kamchatka-Kuril-Japan-Izu-Mariana-Yap	141.5970	36.2640	211	21	21.28
kisz-29b	Kamchatka-Kuril-Japan-Izu-Mariana-Yap	142.0416	36.0481	211	19	5
kisz-29y	Kamchatka-Kuril-Japan-Izu-Mariana-Yap	140.7029	36.6960	211	21	57.12
kisz-29z	Kamchatka-Kuril-Japan-Izu-Mariana-Yap	141.1506	36.4800	211	21	39.2
kisz-30a	Kamchatka-Kuril-Japan-Izu-Mariana-Yap	141.0553	35.4332	205	21	21.28
kisz-30b	Kamchatka-Kuril-Japan-Izu-Mariana-Yap	141.5207	35.2560	205	19	5
kisz-30y	Kamchatka-Kuril-Japan-Izu-Mariana-Yap	140.1204	35.7876	205	21	57.12
kisz-30z	Kamchatka-Kuril-Japan-Izu-Mariana-Yap	140.5883	35.6104	205	21	39.2
kisz-31a	Kamchatka-Kuril-Japan-Izu-Mariana-Yap	140.6956	34.4789	190	22	22.1
kisz-31b	Kamchatka-Kuril-Japan-Izu-Mariana-Yap	141.1927	34.4066	190	20	5
kisz-31v	Kamchatka-Kuril-Japan-Izu-Mariana-Yap	138.2025	34.8405	190	22	115.8
kisz-31w	Kamchatka-Kuril-Japan-Izu-Mariana-Yap	138.7021	34.7682	190	22	97.02
kisz-31x	Kamchatka-Kuril-Japan-Izu-Mariana-Yap	139.2012	34.6958	190	22	78.29
kisz-31y	Kamchatka-Kuril-Japan-Izu-Mariana-Yap	139.6997	34.6235	190	22	59.56
kisz-31z	Kamchatka-Kuril-Japan-Izu-Mariana-Yap	140.1979	34.5512	190	22	40.83
kisz-32a	Kamchatka-Kuril-Japan-Izu-Mariana-Yap	141.0551	33.0921	180	32	23.48
kisz-32b	Kamchatka-Kuril-Japan-Izu-Mariana-Yap	141.5098	33.0921	180	21.69	5
kisz-33a	Kamchatka-Kuril-Japan-Izu-Mariana-Yap	141.0924	32.1047	173.8	27.65	20.67
kisz-33b	Kamchatka-Kuril-Japan-Izu-Mariana-Yap	141.5596	32.1473	173.8	18.27	5
kisz-34a	Kamchatka-Kuril-Japan-Izu-Mariana-Yap	141.1869	31.1851	172.1	25	18.26
kisz-34b	Kamchatka-Kuril-Japan-Izu-Mariana-Yap	141.6585	31.2408	172.1	15.38	5
kisz-35a	Kamchatka-Kuril-Japan-Izu-Mariana-Yap	141.4154	30.1707	163	25	17.12
kisz-35b	Kamchatka-Kuril-Japan-Izu-Mariana-Yap	141.8662	30.2899	163	14.03	5
kisz-36a	Kamchatka-Kuril-Japan-Izu-Mariana-Yap	141.6261	29.2740	161.7	25.73	18.71
kisz-36b	Kamchatka-Kuril-Japan-Izu-Mariana-Yap	142.0670	29.4012	161.7	15.91	5
kisz-37a	Kamchatka-Kuril-Japan-Izu-Mariana-Yap	142.0120	28.3322	154.7	20	14.54
kisz-37b	Kamchatka-Kuril-Japan-Izu-Mariana-Yap	142.4463	28.5124	154.7	11	5
kisz-38a	Kamchatka-Kuril-Japan-Izu-Mariana-Yap	142.2254	27.6946	170.3	20	14.54
kisz-38b	Kamchatka-Kuril-Japan-Izu-Mariana-Yap	142.6955	27.7659	170.3	11	5
kisz-39a	Kamchatka-Kuril-Japan-Izu-Mariana-Yap	142.3085	26.9127	177.2	24.23	17.42

continued on next page

Table B5: (continued)

Segment	Description	Longitude (°E)	Latitude (°N)	Strike (°)	Dip (°)	Depth (km)
kisz-39b	Kamchatka-Kuril-Japan-Izu-Mariana-Yap	142.7674	26.9325	177.2	14.38	5
kisz-40a	Kamchatka-Kuril-Japan-Izu-Mariana-Yap	142.2673	26.1923	189.4	26.49	22.26
kisz-40b	Kamchatka-Kuril-Japan-Izu-Mariana-Yap	142.7090	26.1264	189.4	20.2	5
kisz-41a	Kamchatka-Kuril-Japan-Izu-Mariana-Yap	142.1595	25.0729	173.7	22.07	19.08
kisz-41b	Kamchatka-Kuril-Japan-Izu-Mariana-Yap	142.6165	25.1184	173.7	16.36	5
kisz-42a	Kamchatka-Kuril-Japan-Izu-Mariana-Yap	142.7641	23.8947	143.5	21.54	18.4
kisz-42b	Kamchatka-Kuril-Japan-Izu-Mariana-Yap	143.1321	24.1432	143.5	15.54	5
kisz-43a	Kamchatka-Kuril-Japan-Izu-Mariana-Yap	143.5281	23.0423	129.2	23.02	18.77
kisz-43b	Kamchatka-Kuril-Japan-Izu-Mariana-Yap	143.8128	23.3626	129.2	15.99	5
kisz-44a	Kamchatka-Kuril-Japan-Izu-Mariana-Yap	144.2230	22.5240	134.6	28.24	18.56
kisz-44b	Kamchatka-Kuril-Japan-Izu-Mariana-Yap	144.5246	22.8056	134.6	15.74	5
kisz-45a	Kamchatka-Kuril-Japan-Izu-Mariana-Yap	145.0895	21.8866	125.8	36.73	22.79
kisz-45b	Kamchatka-Kuril-Japan-Izu-Mariana-Yap	145.3171	22.1785	125.8	20.84	5
kisz-46a	Kamchatka-Kuril-Japan-Izu-Mariana-Yap	145.6972	21.3783	135.9	30.75	20.63
kisz-46b	Kamchatka-Kuril-Japan-Izu-Mariana-Yap	145.9954	21.6469	135.9	18.22	5
kisz-47a	Kamchatka-Kuril-Japan-Izu-Mariana-Yap	146.0406	20.9341	160.1	29.87	19.62
kisz-47b	Kamchatka-Kuril-Japan-Izu-Mariana-Yap	146.4330	21.0669	160.1	17	5
kisz-48a	Kamchatka-Kuril-Japan-Izu-Mariana-Yap	146.3836	20.0690	158	32.75	19.68
kisz-48b	Kamchatka-Kuril-Japan-Izu-Mariana-Yap	146.7567	20.2108	158	17.07	5
kisz-49a	Kamchatka-Kuril-Japan-Izu-Mariana-Yap	146.6689	19.3123	164.5	25.07	21.41
kisz-49b	Kamchatka-Kuril-Japan-Izu-Mariana-Yap	147.0846	19.4212	164.5	19.16	5
kisz-50a	Kamchatka-Kuril-Japan-Izu-Mariana-Yap	146.9297	18.5663	172.1	22	22.1
kisz-50b	Kamchatka-Kuril-Japan-Izu-Mariana-Yap	147.3650	18.6238	172.1	20	5
kisz-51a	Kamchatka-Kuril-Japan-Izu-Mariana-Yap	146.9495	17.7148	175.1	22.06	22.04
kisz-51b	Kamchatka-Kuril-Japan-Izu-Mariana-Yap	147.3850	17.7503	175.1	19.93	5
kisz-52a	Kamchatka-Kuril-Japan-Izu-Mariana-Yap	146.9447	16.8869	180	25.51	18.61
kisz-52b	Kamchatka-Kuril-Japan-Izu-Mariana-Yap	147.3683	16.8869	180	15.79	5
kisz-53a	Kamchatka-Kuril-Japan-Izu-Mariana-Yap	146.8626	16.0669	185.2	27.39	18.41
kisz-53b	Kamchatka-Kuril-Japan-Izu-Mariana-Yap	147.2758	16.0309	185.2	15.56	5
kisz-54a	Kamchatka-Kuril-Japan-Izu-Mariana-Yap	146.7068	15.3883	199.1	28.12	20.91
kisz-54b	Kamchatka-Kuril-Japan-Izu-Mariana-Yap	147.0949	15.2590	199.1	18.56	5
kisz-55a	Kamchatka-Kuril-Japan-Izu-Mariana-Yap	146.4717	14.6025	204.3	29.6	26.27
kisz-55b	Kamchatka-Kuril-Japan-Izu-Mariana-Yap	146.8391	14.4415	204.3	25.18	5
kisz-56a	Kamchatka-Kuril-Japan-Izu-Mariana-Yap	146.1678	13.9485	217.4	32.04	26.79
kisz-56b	Kamchatka-Kuril-Japan-Izu-Mariana-Yap	146.4789	13.7170	217.4	25.84	5
kisz-57a	Kamchatka-Kuril-Japan-Izu-Mariana-Yap	145.6515	13.5576	235.8	37	24.54
kisz-57b	Kamchatka-Kuril-Japan-Izu-Mariana-Yap	145.8586	13.2609	235.8	23	5
kisz-58a	Kamchatka-Kuril-Japan-Izu-Mariana-Yap	144.9648	12.9990	237.8	37.72	24.54
kisz-58b	Kamchatka-Kuril-Japan-Izu-Mariana-Yap	145.1589	12.6984	237.8	23	5

continued on next page

Table B5: (continued)

Segment	Description	Longitude (°E)	Latitude (°N)	Strike (°)	Dip (°)	Depth (km)
kisz-59a	Kamchatka-Kuril-Japan-Izu-Mariana-Yap	144.1799	12.6914	242.9	34.33	22.31
kisz-59b	Kamchatka-Kuril-Japan-Izu-Mariana-Yap	144.3531	12.3613	242.9	20.25	5
kisz-60a	Kamchatka-Kuril-Japan-Izu-Mariana-Yap	143.3687	12.3280	244.9	30.9	20.62
kisz-60b	Kamchatka-Kuril-Japan-Izu-Mariana-Yap	143.5355	11.9788	244.9	18.2	5
kisz-61a	Kamchatka-Kuril-Japan-Izu-Mariana-Yap	142.7051	12.1507	261.8	35.41	25.51
kisz-61b	Kamchatka-Kuril-Japan-Izu-Mariana-Yap	142.7582	11.7883	261.8	24.22	5
kisz-62a	Kamchatka-Kuril-Japan-Izu-Mariana-Yap	141.6301	11.8447	245.7	39.86	34.35
kisz-62b	Kamchatka-Kuril-Japan-Izu-Mariana-Yap	141.7750	11.5305	245.7	35.94	5
kisz-63a	Kamchatka-Kuril-Japan-Izu-Mariana-Yap	140.8923	11.5740	256.2	42	38.46
kisz-63b	Kamchatka-Kuril-Japan-Izu-Mariana-Yap	140.9735	11.2498	256.2	42	5
kisz-64a	Kamchatka-Kuril-Japan-Izu-Mariana-Yap	140.1387	11.6028	269.6	42.48	38.77
kisz-64b	Kamchatka-Kuril-Japan-Izu-Mariana-Yap	140.1410	11.2716	269.6	42.48	5
kisz-65a	Kamchatka-Kuril-Japan-Izu-Mariana-Yap	139.4595	11.5883	288.7	44.16	39.83
kisz-65b	Kamchatka-Kuril-Japan-Izu-Mariana-Yap	139.3541	11.2831	288.7	44.16	5
kisz-66a	Kamchatka-Kuril-Japan-Izu-Mariana-Yap	138.1823	11.2648	193.1	45	40.36
kisz-66b	Kamchatka-Kuril-Japan-Izu-Mariana-Yap	138.4977	11.1929	193.1	45	5
kisz-67a	Kamchatka-Kuril-Japan-Izu-Mariana-Yap	137.9923	10.3398	189.8	45	40.36
kisz-67b	Kamchatka-Kuril-Japan-Izu-Mariana-Yap	138.3104	10.2856	189.8	45	5
kisz-68a	Kamchatka-Kuril-Japan-Izu-Mariana-Yap	137.7607	9.6136	201.7	45	40.36
kisz-68b	Kamchatka-Kuril-Japan-Izu-Mariana-Yap	138.0599	9.4963	201.7	45	5
kisz-69a	Kamchatka-Kuril-Japan-Izu-Mariana-Yap	137.4537	8.8996	213.5	45	40.36
kisz-69b	Kamchatka-Kuril-Japan-Izu-Mariana-Yap	137.7215	8.7241	213.5	45	5
kisz-70a	Kamchatka-Kuril-Japan-Izu-Mariana-Yap	137.0191	8.2872	226.5	45	40.36
kisz-70b	Kamchatka-Kuril-Japan-Izu-Mariana-Yap	137.2400	8.0569	226.5	45	5
kisz-71a	Kamchatka-Kuril-Japan-Izu-Mariana-Yap	136.3863	7.9078	263.9	45	40.36
kisz-71b	Kamchatka-Kuril-Japan-Izu-Mariana-Yap	136.4202	7.5920	263.9	45	5
kisz-72a	Kamchatka-Kuril-Japan-Izu-Mariana-Yap	135.6310	7.9130	276.9	45	40.36
kisz-72b	Kamchatka-Kuril-Japan-Izu-Mariana-Yap	135.5926	7.5977	276.9	45	5
kisz-73a	Kamchatka-Kuril-Japan-Izu-Mariana-Yap	134.3296	7.4541	224	45	40.36
kisz-73b	Kamchatka-Kuril-Japan-Izu-Mariana-Yap	134.5600	7.2335	224	45	5
kisz-74a	Kamchatka-Kuril-Japan-Izu-Mariana-Yap	133.7125	6.8621	228.1	45	40.36
kisz-74b	Kamchatka-Kuril-Japan-Izu-Mariana-Yap	133.9263	6.6258	228.1	45	5
kisz-75a	Kamchatka-Kuril-Japan-Izu-Mariana-Yap	133.0224	6.1221	217.7	45	40.36
kisz-75b	Kamchatka-Kuril-Japan-Izu-Mariana-Yap	133.2751	5.9280	217.7	45	5

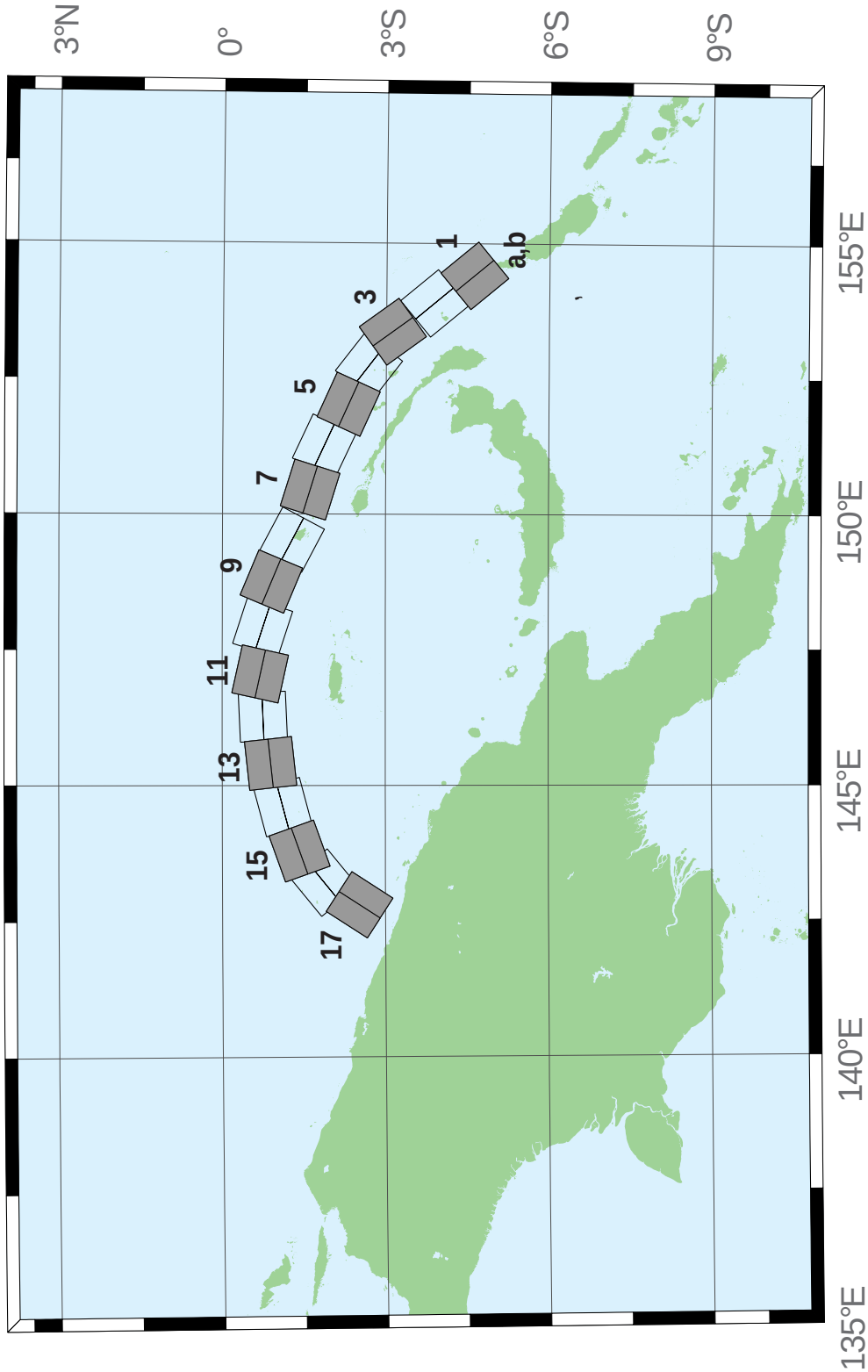

Figure B6: Manus–Oceanic Convergent Boundary Subduction Zone unit sources.

Table B6: Earthquake parameters for Manus–Oceanic Convergent Boundary Subduction Zone unit sources.

Segment	Description	Longitude (°E)	Latitude (°N)	Strike (°)	Dip (°)	Depth (km)
mosz-1a	Manus-Oceanic Convergent Boundary	154.0737	-4.8960	140.2	15	15.88
mosz-1b	Manus-Oceanic Convergent Boundary	154.4082	-4.6185	140.2	15	2.94
mosz-2a	Manus-Oceanic Convergent Boundary	153.5589	-4.1575	140.2	15	15.91
mosz-2b	Manus-Oceanic Convergent Boundary	153.8931	-3.8800	140.2	15	2.97
mosz-3a	Manus-Oceanic Convergent Boundary	153.0151	-3.3716	143.9	15	16.64
mosz-3b	Manus-Oceanic Convergent Boundary	153.3662	-3.1160	143.9	15	3.7
mosz-4a	Manus-Oceanic Convergent Boundary	152.4667	-3.0241	127.7	15	17.32
mosz-4b	Manus-Oceanic Convergent Boundary	152.7321	-2.6806	127.7	15	4.38
mosz-5a	Manus-Oceanic Convergent Boundary	151.8447	-2.7066	114.3	15	17.57
mosz-5b	Manus-Oceanic Convergent Boundary	152.0235	-2.3112	114.3	15	4.63
mosz-6a	Manus-Oceanic Convergent Boundary	151.0679	-2.2550	115	15	17.66
mosz-6b	Manus-Oceanic Convergent Boundary	151.2513	-1.8618	115	15	4.72
mosz-7a	Manus-Oceanic Convergent Boundary	150.3210	-2.0236	107.2	15	17.73
mosz-7b	Manus-Oceanic Convergent Boundary	150.4493	-1.6092	107.2	15	4.79
mosz-8a	Manus-Oceanic Convergent Boundary	149.3226	-1.6666	117.8	15	17.83
mosz-8b	Manus-Oceanic Convergent Boundary	149.5251	-1.2829	117.8	15	4.89
mosz-9a	Manus-Oceanic Convergent Boundary	148.5865	-1.3017	112.7	15	17.84
mosz-9b	Manus-Oceanic Convergent Boundary	148.7540	-0.9015	112.7	15	4.9
mosz-10a	Manus-Oceanic Convergent Boundary	147.7760	-1.1560	108	15	17.78
mosz-10b	Manus-Oceanic Convergent Boundary	147.9102	-0.7434	108	15	4.84
mosz-11a	Manus-Oceanic Convergent Boundary	146.9596	-1.1226	102.5	15	17.54
mosz-11b	Manus-Oceanic Convergent Boundary	147.0531	-0.6990	102.5	15	4.6
mosz-12a	Manus-Oceanic Convergent Boundary	146.2858	-1.1820	87.48	15	17.29
mosz-12b	Manus-Oceanic Convergent Boundary	146.2667	-0.7486	87.48	15	4.35
mosz-13a	Manus-Oceanic Convergent Boundary	145.4540	-1.3214	83.75	15	17.34
mosz-13b	Manus-Oceanic Convergent Boundary	145.4068	-0.8901	83.75	15	4.4
mosz-14a	Manus-Oceanic Convergent Boundary	144.7151	-1.5346	75.09	15	17.21
mosz-14b	Manus-Oceanic Convergent Boundary	144.6035	-1.1154	75.09	15	4.27
mosz-15a	Manus-Oceanic Convergent Boundary	143.9394	-1.8278	70.43	15	16.52
mosz-15b	Manus-Oceanic Convergent Boundary	143.7940	-1.4190	70.43	15	3.58
mosz-16a	Manus-Oceanic Convergent Boundary	143.4850	-2.2118	50.79	15	15.86
mosz-16b	Manus-Oceanic Convergent Boundary	143.2106	-1.8756	50.79	15	2.92
mosz-17a	Manus-Oceanic Convergent Boundary	143.1655	-2.7580	33	15	16.64
mosz-17b	Manus-Oceanic Convergent Boundary	142.8013	-2.5217	33	15	3.7

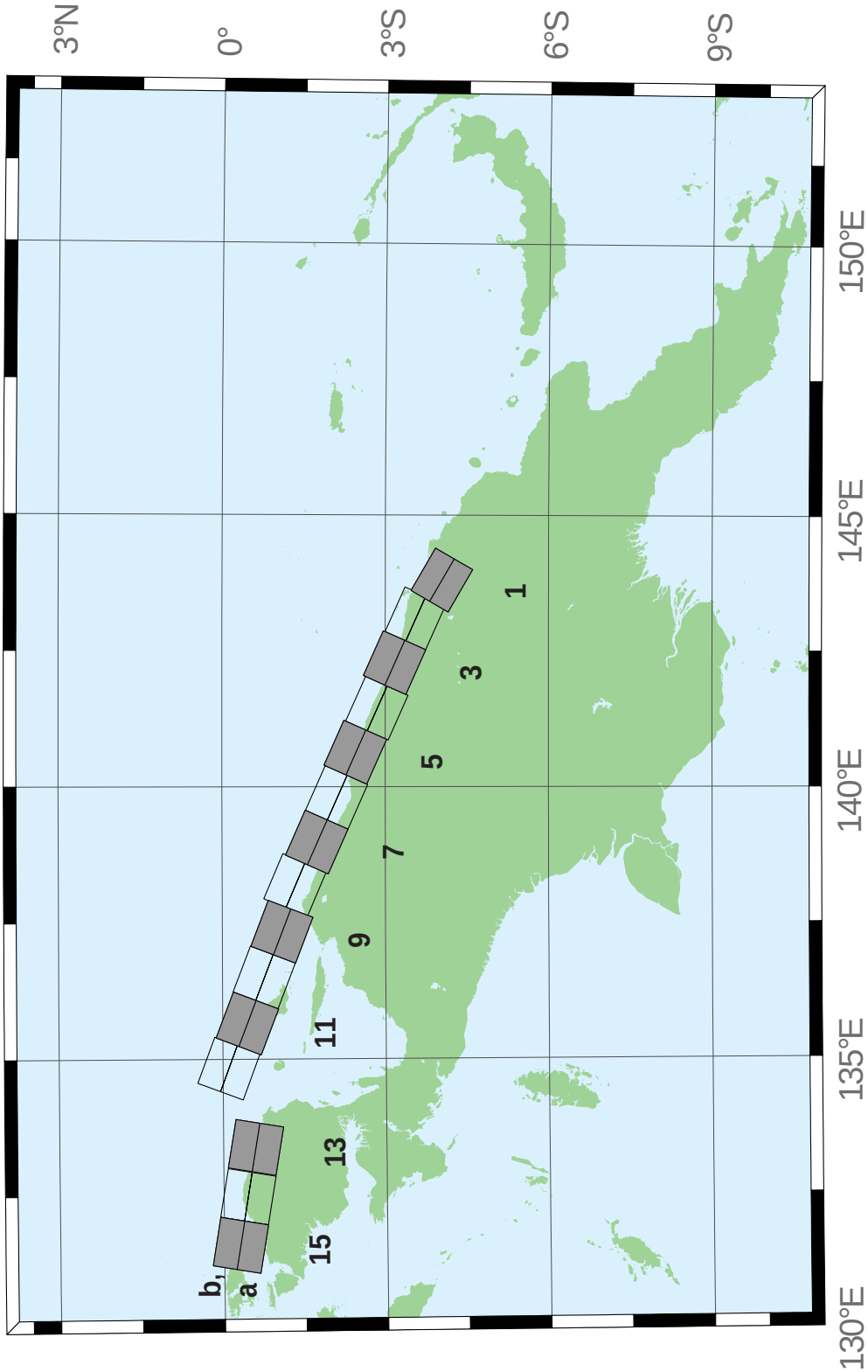

Figure B7: New Guinea Subduction Zone unit sources.

Table B7: Earthquake parameters for New Guinea Subduction Zone unit sources.

Segment	Description	Longitude (°E)	Latitude (°N)	Strike (°)	Dip (°)	Depth (km)
ngsz-1a	New Guinea	143.6063	-4.3804	120	29	25.64
ngsz-1b	New Guinea	143.8032	-4.0402	120	29	1.4
ngsz-2a	New Guinea	142.9310	-3.9263	114	27.63	20.1
ngsz-2b	New Guinea	143.0932	-3.5628	114	21.72	1.6
ngsz-3a	New Guinea	142.1076	-3.5632	114	20.06	18.73
ngsz-3b	New Guinea	142.2795	-3.1778	114	15.94	5
ngsz-4a	New Guinea	141.2681	-3.2376	114	21	17.76
ngsz-4b	New Guinea	141.4389	-2.8545	114	14.79	5
ngsz-5a	New Guinea	140.4592	-2.8429	114	21.26	16.14
ngsz-5b	New Guinea	140.6296	-2.4605	114	12.87	5
ngsz-6a	New Guinea	139.6288	-2.4960	114	22.72	15.4
ngsz-6b	New Guinea	139.7974	-2.1175	114	12	5
ngsz-7a	New Guinea	138.8074	-2.1312	114	21.39	15.4
ngsz-7b	New Guinea	138.9776	-1.7491	114	12	5
ngsz-8a	New Guinea	138.0185	-1.7353	113.1	18.79	15.14
ngsz-8b	New Guinea	138.1853	-1.3441	113.1	11.7	5
ngsz-9a	New Guinea	137.1805	-1.5037	111	15.24	13.23
ngsz-9b	New Guinea	137.3358	-1.0991	111	9.47	5
ngsz-10a	New Guinea	136.3418	-1.1774	111	13.51	11.09
ngsz-10b	New Guinea	136.4983	-0.7697	111	7	5
ngsz-11a	New Guinea	135.4984	-0.8641	111	11.38	12.49
ngsz-11b	New Guinea	135.6562	-0.4530	111	8.62	5
ngsz-12a	New Guinea	134.6759	-0.5216	110.5	10	13.68
ngsz-12b	New Guinea	134.8307	-0.1072	110.5	10	5
ngsz-13a	New Guinea	133.3065	-1.0298	99.5	10	13.68
ngsz-13b	New Guinea	133.3795	-0.5935	99.5	10	5
ngsz-14a	New Guinea	132.4048	-0.8816	99.5	10	13.68
ngsz-14b	New Guinea	132.4778	-0.4453	99.5	10	5
ngsz-15a	New Guinea	131.5141	-0.7353	99.5	10	13.68
ngsz-15b	New Guinea	131.5871	-0.2990	99.5	10	5

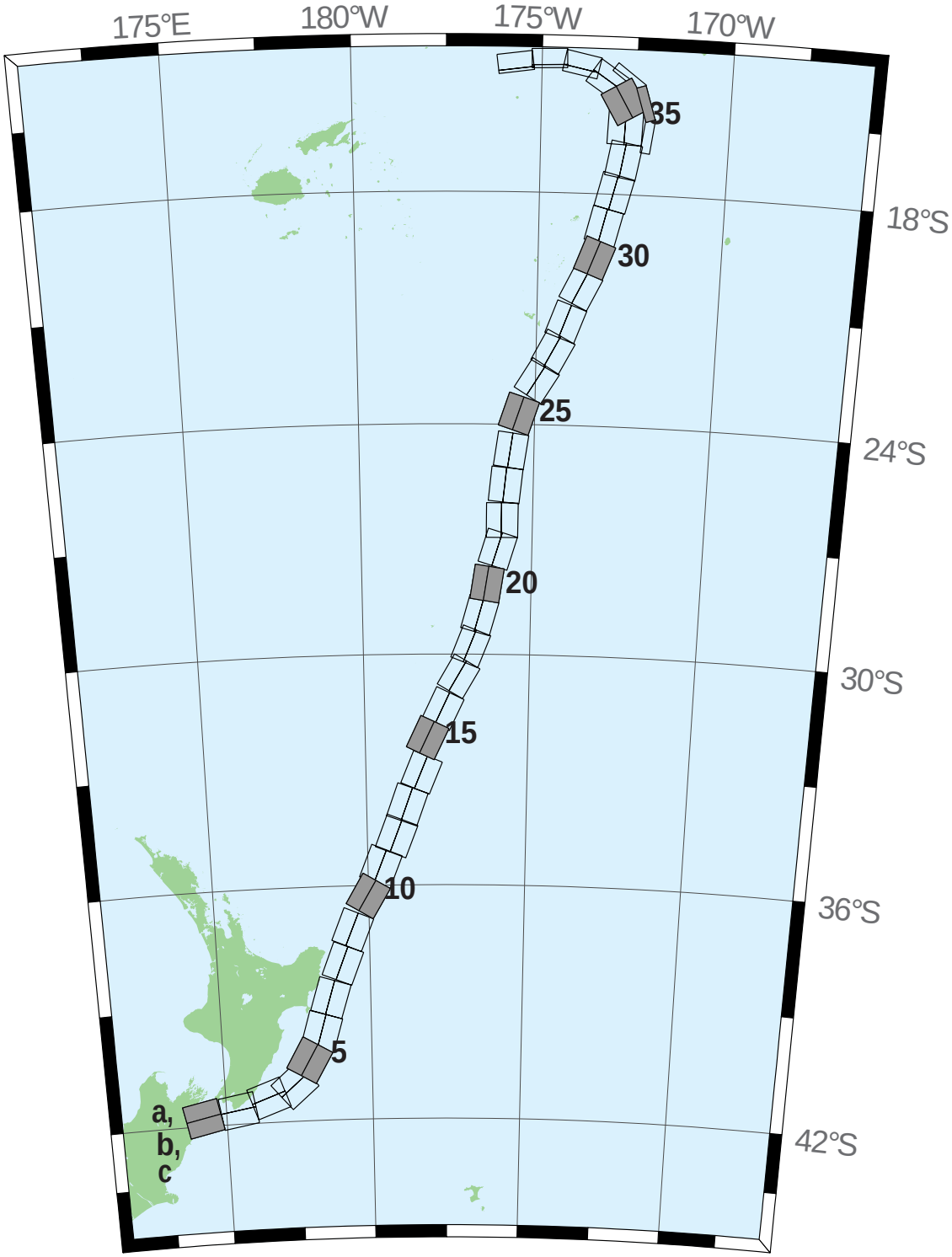

Figure B8: New Zealand–Kermadec–Tonga Subduction Zone unit sources.

Table B8: Earthquake parameters for New Zealand–Kermadec–Tonga Subduction Zone unit sources.

Segment	Description	Longitude (°E)	Latitude (°N)	Strike (°)	Dip (°)	Depth (km)
ntsz-1a	New Zealand–Kermadec–Tonga	174.0985	-41.3951	258.6	24	25.34
ntsz-1b	New Zealand–Kermadec–Tonga	174.2076	-41.7973	258.6	24	5
ntsz-2a	New Zealand–Kermadec–Tonga	175.3289	-41.2592	260.6	29.38	23.17
ntsz-2b	New Zealand–Kermadec–Tonga	175.4142	-41.6454	260.6	21.31	5
ntsz-3a	New Zealand–Kermadec–Tonga	176.2855	-40.9950	250.7	29.54	21.74
ntsz-3b	New Zealand–Kermadec–Tonga	176.4580	-41.3637	250.7	19.56	5
ntsz-4a	New Zealand–Kermadec–Tonga	177.0023	-40.7679	229.4	24.43	18.87
ntsz-4b	New Zealand–Kermadec–Tonga	177.3552	-41.0785	229.4	16.1	5
ntsz-5a	New Zealand–Kermadec–Tonga	177.4114	-40.2396	210	18.8	19.29
ntsz-5b	New Zealand–Kermadec–Tonga	177.8951	-40.4525	210	16.61	5
ntsz-6a	New Zealand–Kermadec–Tonga	177.8036	-39.6085	196.7	18.17	15.8
ntsz-6b	New Zealand–Kermadec–Tonga	178.3352	-39.7310	196.7	12.48	5
ntsz-7a	New Zealand–Kermadec–Tonga	178.1676	-38.7480	197	28.1	17.85
ntsz-7b	New Zealand–Kermadec–Tonga	178.6541	-38.8640	197	14.89	5
ntsz-8a	New Zealand–Kermadec–Tonga	178.6263	-37.8501	201.4	31.47	18.78
ntsz-8b	New Zealand–Kermadec–Tonga	179.0788	-37.9899	201.4	16	5
ntsz-9a	New Zealand–Kermadec–Tonga	178.9833	-36.9770	202.2	29.58	20.02
ntsz-9b	New Zealand–Kermadec–Tonga	179.4369	-37.1245	202.2	17.48	5
ntsz-10a	New Zealand–Kermadec–Tonga	179.5534	-36.0655	210.6	32.1	20.72
ntsz-10b	New Zealand–Kermadec–Tonga	179.9595	-36.2593	210.6	18.32	5
ntsz-11a	New Zealand–Kermadec–Tonga	179.9267	-35.3538	201.7	25	16.09
ntsz-11b	New Zealand–Kermadec–Tonga	180.3915	-35.5040	201.7	12.81	5
ntsz-12a	New Zealand–Kermadec–Tonga	180.4433	-34.5759	201.2	25	15.46
ntsz-12b	New Zealand–Kermadec–Tonga	180.9051	-34.7230	201.2	12.08	5
ntsz-13a	New Zealand–Kermadec–Tonga	180.7990	-33.7707	199.8	25.87	19.06
ntsz-13b	New Zealand–Kermadec–Tonga	181.2573	-33.9073	199.8	16.33	5
ntsz-14a	New Zealand–Kermadec–Tonga	181.2828	-32.9288	202.4	31.28	22.73
ntsz-14b	New Zealand–Kermadec–Tonga	181.7063	-33.0751	202.4	20.77	5
ntsz-15a	New Zealand–Kermadec–Tonga	181.4918	-32.0035	205.4	32.33	22.64
ntsz-15b	New Zealand–Kermadec–Tonga	181.8967	-32.1665	205.4	20.66	5
ntsz-16a	New Zealand–Kermadec–Tonga	181.9781	-31.2535	205.5	34.29	23.59
ntsz-16b	New Zealand–Kermadec–Tonga	182.3706	-31.4131	205.5	21.83	5
ntsz-17a	New Zealand–Kermadec–Tonga	182.4819	-30.3859	210.3	37.6	25.58
ntsz-17b	New Zealand–Kermadec–Tonga	182.8387	-30.5655	210.3	24.3	5
ntsz-18a	New Zealand–Kermadec–Tonga	182.8176	-29.6545	201.6	37.65	26.13
ntsz-18b	New Zealand–Kermadec–Tonga	183.1985	-29.7856	201.6	25	5
ntsz-19a	New Zealand–Kermadec–Tonga	183.0622	-28.8739	195.7	34.41	26.13
ntsz-19b	New Zealand–Kermadec–Tonga	183.4700	-28.9742	195.7	25	5
ntsz-20a	New Zealand–Kermadec–Tonga	183.2724	-28.0967	188.8	38	26.13
ntsz-20b	New Zealand–Kermadec–Tonga	183.6691	-28.1508	188.8	25	5

continued on next page

Table B8: (continued)

Segment	Description	Longitude (°E)	Latitude (°N)	Strike (°)	Dip (°)	Depth (km)
ntsz-21a	New Zealand–Kermadec–Tonga	183.5747	-27.1402	197.1	32.29	24.83
ntsz-21b	New Zealand–Kermadec–Tonga	183.9829	-27.2518	197.1	23.37	5
ntsz-22a	New Zealand–Kermadec–Tonga	183.6608	-26.4975	180	29.56	18.63
ntsz-22b	New Zealand–Kermadec–Tonga	184.0974	-26.4975	180	15.82	5
ntsz-23a	New Zealand–Kermadec–Tonga	183.7599	-25.5371	185.8	32.42	20.56
ntsz-23b	New Zealand–Kermadec–Tonga	184.1781	-25.5752	185.8	18.13	5
ntsz-24a	New Zealand–Kermadec–Tonga	183.9139	-24.6201	188.2	33.31	23.73
ntsz-24b	New Zealand–Kermadec–Tonga	184.3228	-24.6734	188.2	22	5
ntsz-25a	New Zealand–Kermadec–Tonga	184.1266	-23.5922	198.5	29.34	19.64
ntsz-25b	New Zealand–Kermadec–Tonga	184.5322	-23.7163	198.5	17.03	5
ntsz-26a	New Zealand–Kermadec–Tonga	184.6613	-22.6460	211.7	30.26	19.43
ntsz-26b	New Zealand–Kermadec–Tonga	185.0196	-22.8497	211.7	16.78	5
ntsz-27a	New Zealand–Kermadec–Tonga	185.0879	-21.9139	207.9	31.73	20.67
ntsz-27b	New Zealand–Kermadec–Tonga	185.4522	-22.0928	207.9	18.27	5
ntsz-28a	New Zealand–Kermadec–Tonga	185.4037	-21.1758	200.5	32.44	21.76
ntsz-28b	New Zealand–Kermadec–Tonga	185.7849	-21.3084	200.5	19.58	5
ntsz-29a	New Zealand–Kermadec–Tonga	185.8087	-20.2629	206.4	32.47	20.4
ntsz-29b	New Zealand–Kermadec–Tonga	186.1710	-20.4312	206.4	17.94	5
ntsz-30a	New Zealand–Kermadec–Tonga	186.1499	-19.5087	200.9	32.98	22.46
ntsz-30b	New Zealand–Kermadec–Tonga	186.5236	-19.6432	200.9	20.44	5
ntsz-31a	New Zealand–Kermadec–Tonga	186.3538	-18.7332	193.9	34.41	21.19
ntsz-31b	New Zealand–Kermadec–Tonga	186.7339	-18.8221	193.9	18.89	5
ntsz-32a	New Zealand–Kermadec–Tonga	186.5949	-17.8587	194.1	30	19.12
ntsz-32b	New Zealand–Kermadec–Tonga	186.9914	-17.9536	194.1	16.4	5
ntsz-33a	New Zealand–Kermadec–Tonga	186.8172	-17.0581	190	33.15	23.34
ntsz-33b	New Zealand–Kermadec–Tonga	187.2047	-17.1237	190	21.52	5
ntsz-34a	New Zealand–Kermadec–Tonga	186.7814	-16.2598	182.1	15	13.41
ntsz-34b	New Zealand–Kermadec–Tonga	187.2330	-16.2759	182.1	9.68	5
ntsz-34c	New Zealand–Kermadec–Tonga	187.9697	-16.4956	7.62	57.06	6.571
ntsz-35a	New Zealand–Kermadec–Tonga	186.8000	-15.8563	149.8	15	12.17
ntsz-35b	New Zealand–Kermadec–Tonga	187.1896	-15.6384	149.8	8.24	5
ntsz-35c	New Zealand–Kermadec–Tonga	187.8776	-15.6325	342.4	57.06	6.571
ntsz-36a	New Zealand–Kermadec–Tonga	186.5406	-15.3862	123.9	40.44	36.72
ntsz-36b	New Zealand–Kermadec–Tonga	186.7381	-15.1025	123.9	39.38	5
ntsz-36c	New Zealand–Kermadec–Tonga	187.3791	-14.9234	307	57.06	6.571
ntsz-37a	New Zealand–Kermadec–Tonga	185.9883	-14.9861	102	68.94	30.99
ntsz-37b	New Zealand–Kermadec–Tonga	186.0229	-14.8282	102	31.32	5
ntsz-38a	New Zealand–Kermadec–Tonga	185.2067	-14.8259	88.4	80	26.13
ntsz-38b	New Zealand–Kermadec–Tonga	185.2044	-14.7479	88.4	25	5
ntsz-39a	New Zealand–Kermadec–Tonga	184.3412	-14.9409	82.55	80	26.13
ntsz-39b	New Zealand–Kermadec–Tonga	184.3307	-14.8636	82.55	25	5

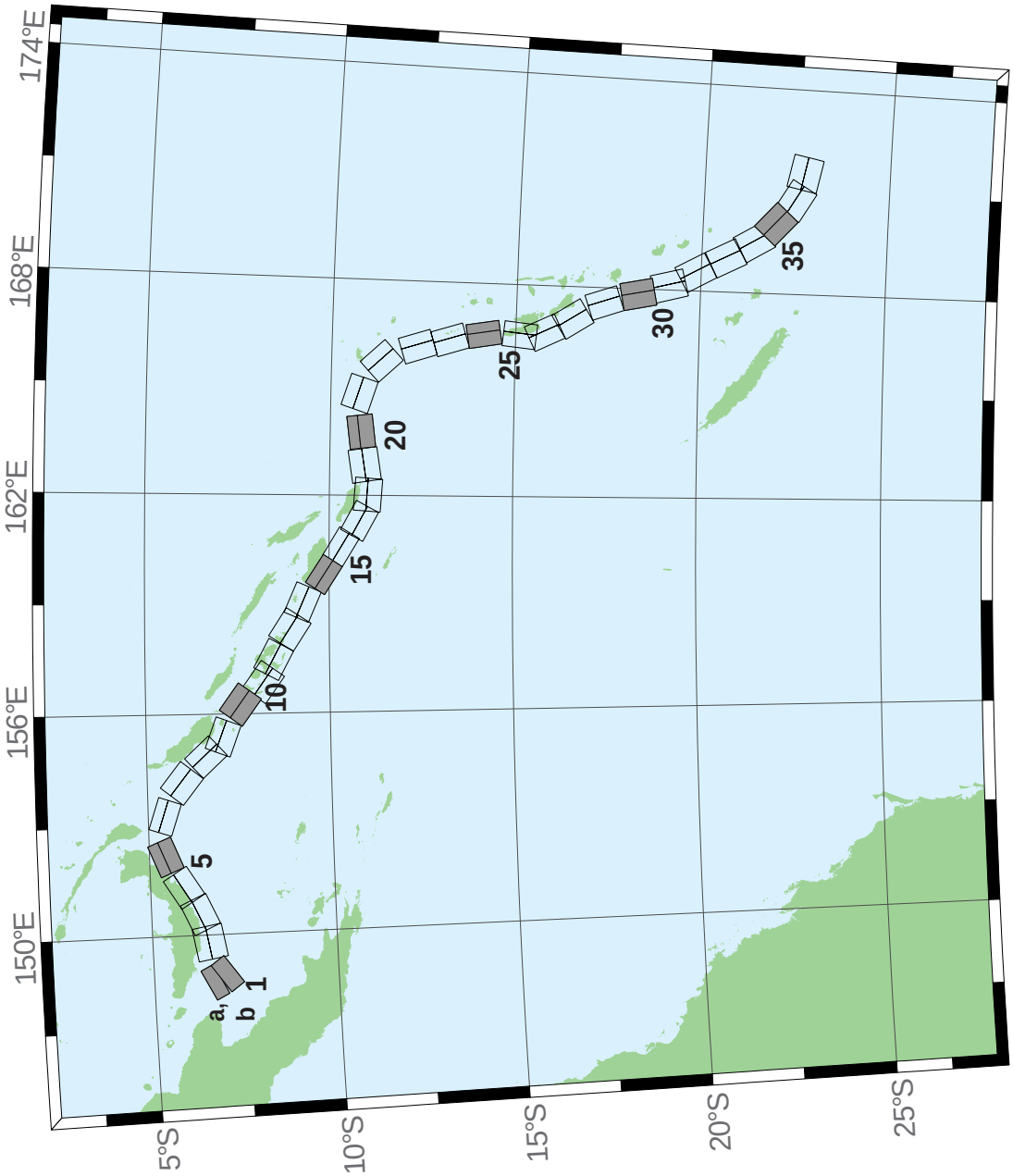

Figure B9: New Britain–Solomons–Vanuatu Subduction Zone unit sources.

Table B9: Earthquake parameters for New Britain–Solomons–Vanuatu Subduction Zone unit sources.

Segment	Description	Longitude (°E)	Latitude (°N)	Strike (°)	Dip (°)	Depth (km)
nvsz-1a	New Britain–Solomons–Vanuatu	148.6217	-6.4616	243.2	32.34	15.69
nvsz-1b	New Britain–Solomons–Vanuatu	148.7943	-6.8002	234.2	12.34	5
nvsz-2a	New Britain–Solomons–Vanuatu	149.7218	-6.1459	260.1	35.1	16.36
nvsz-2b	New Britain–Solomons–Vanuatu	149.7856	-6.5079	260.1	13.13	5
nvsz-3a	New Britain–Solomons–Vanuatu	150.4075	-5.9659	245.7	42.35	18.59
nvsz-3b	New Britain–Solomons–Vanuatu	150.5450	-6.2684	245.7	15.77	5
nvsz-4a	New Britain–Solomons–Vanuatu	151.1095	-5.5820	238.2	42.41	23.63
nvsz-4b	New Britain–Solomons–Vanuatu	151.2851	-5.8639	238.2	21.88	5
nvsz-5a	New Britain–Solomons–Vanuatu	152.0205	-5.1305	247.7	49.22	32.39
nvsz-5b	New Britain–Solomons–Vanuatu	152.1322	-5.4020	247.7	33.22	5
nvsz-6a	New Britain–Solomons–Vanuatu	153.3450	-5.1558	288.6	53.53	33.59
nvsz-6b	New Britain–Solomons–Vanuatu	153.2595	-5.4089	288.6	34.87	5
nvsz-7a	New Britain–Solomons–Vanuatu	154.3814	-5.6308	308.3	39.72	19.18
nvsz-7b	New Britain–Solomons–Vanuatu	154.1658	-5.9017	308.3	16.48	5
nvsz-8a	New Britain–Solomons–Vanuatu	155.1097	-6.3511	317.2	45.33	22.92
nvsz-8b	New Britain–Solomons–Vanuatu	154.8764	-6.5656	317.2	21	5
nvsz-9a	New Britain–Solomons–Vanuatu	155.5027	-6.7430	290.5	48.75	22.92
nvsz-9b	New Britain–Solomons–Vanuatu	155.3981	-7.0204	290.5	21	5
nvsz-10a	New Britain–Solomons–Vanuatu	156.4742	-7.2515	305.9	36.88	27.62
nvsz-10b	New Britain–Solomons–Vanuatu	156.2619	-7.5427	305.9	26.9	5
nvsz-11a	New Britain–Solomons–Vanuatu	157.0830	-7.8830	305.4	32.97	29.72
nvsz-11b	New Britain–Solomons–Vanuatu	156.8627	-8.1903	305.4	29.63	5
nvsz-12a	New Britain–Solomons–Vanuatu	157.6537	-8.1483	297.9	37.53	28.57
nvsz-12b	New Britain–Solomons–Vanuatu	157.4850	-8.4630	297.9	28.13	5
nvsz-13a	New Britain–Solomons–Vanuatu	158.5089	-8.5953	302.7	33.62	23.02
nvsz-13b	New Britain–Solomons–Vanuatu	158.3042	-8.9099	302.7	21.12	5
nvsz-14a	New Britain–Solomons–Vanuatu	159.1872	-8.9516	293.3	38.44	34.06
nvsz-14b	New Britain–Solomons–Vanuatu	159.0461	-9.2747	293.3	35.54	5
nvsz-15a	New Britain–Solomons–Vanuatu	159.9736	-9.5993	302.8	46.69	41.38
nvsz-15b	New Britain–Solomons–Vanuatu	159.8044	-9.8584	302.8	46.69	5
nvsz-16a	New Britain–Solomons–Vanuatu	160.7343	-10.0574	301	46.05	41
nvsz-16b	New Britain–Solomons–Vanuatu	160.5712	-10.3246	301	46.05	5
nvsz-17a	New Britain–Solomons–Vanuatu	161.4562	-10.5241	298.4	40.12	37.22
nvsz-17b	New Britain–Solomons–Vanuatu	161.2900	-10.8263	298.4	40.12	5
nvsz-18a	New Britain–Solomons–Vanuatu	162.0467	-10.6823	274.1	40.33	29.03
nvsz-18b	New Britain–Solomons–Vanuatu	162.0219	-11.0238	274.1	28.72	5
nvsz-19a	New Britain–Solomons–Vanuatu	162.7818	-10.5645	261.3	34.25	24.14
nvsz-19b	New Britain–Solomons–Vanuatu	162.8392	-10.9315	261.3	22.51	5
nvsz-20a	New Britain–Solomons–Vanuatu	163.7222	-10.5014	262.9	50.35	26.3

continued on next page

Table B9: (continued)

Segment	Description	Longitude (°E)	Latitude (°N)	Strike (°)	Dip (°)	Depth (km)
nvsz-20b	New Britain–Solomons–Vanuatu	163.7581	-10.7858	262.9	25.22	5
nvsz-21a	New Britain–Solomons–Vanuatu	164.9445	-10.4183	287.9	40.31	23.3
nvsz-21b	New Britain–Solomons–Vanuatu	164.8374	-10.7442	287.9	21.47	5
nvsz-22a	New Britain–Solomons–Vanuatu	166.0261	-11.1069	317.1	42.39	20.78
nvsz-22b	New Britain–Solomons–Vanuatu	165.7783	-11.3328	317.1	18.4	5
nvsz-23a	New Britain–Solomons–Vanuatu	166.5179	-12.2260	342.4	47.95	22.43
nvsz-23b	New Britain–Solomons–Vanuatu	166.2244	-12.3171	342.4	20.4	5
nvsz-24a	New Britain–Solomons–Vanuatu	166.7236	-13.1065	342.6	47.13	28.52
nvsz-24b	New Britain–Solomons–Vanuatu	166.4241	-13.1979	342.6	28.06	5
nvsz-25a	New Britain–Solomons–Vanuatu	166.8914	-14.0785	350.3	54.1	31.16
nvsz-25b	New Britain–Solomons–Vanuatu	166.6237	-14.1230	350.3	31.55	5
nvsz-26a	New Britain–Solomons–Vanuatu	166.9200	-15.1450	365.6	50.46	29.05
nvsz-26b	New Britain–Solomons–Vanuatu	166.6252	-15.1170	365.6	28.75	5
nvsz-27a	New Britain–Solomons–Vanuatu	167.0053	-15.6308	334.2	44.74	25.46
nvsz-27b	New Britain–Solomons–Vanuatu	166.7068	-15.7695	334.2	24.15	5
nvsz-28a	New Britain–Solomons–Vanuatu	167.4074	-16.3455	327.5	41.53	22.44
nvsz-28b	New Britain–Solomons–Vanuatu	167.1117	-16.5264	327.5	20.42	5
nvsz-29a	New Britain–Solomons–Vanuatu	167.9145	-17.2807	341.2	49.1	24.12
nvsz-29b	New Britain–Solomons–Vanuatu	167.6229	-17.3757	341.2	22.48	5
nvsz-30a	New Britain–Solomons–Vanuatu	168.2220	-18.2353	348.6	44.19	23.99
nvsz-30b	New Britain–Solomons–Vanuatu	167.8895	-18.2991	348.6	22.32	5
nvsz-31a	New Britain–Solomons–Vanuatu	168.5022	-19.0510	345.6	42.2	22.26
nvsz-31b	New Britain–Solomons–Vanuatu	168.1611	-19.1338	345.6	20.2	5
nvsz-32a	New Britain–Solomons–Vanuatu	168.8775	-19.6724	331.1	42.03	21.68
nvsz-32b	New Britain–Solomons–Vanuatu	168.5671	-19.8338	331.1	19.49	5
nvsz-33a	New Britain–Solomons–Vanuatu	169.3422	-20.4892	332.9	40.25	22.4
nvsz-33b	New Britain–Solomons–Vanuatu	169.0161	-20.6453	332.9	20.37	5
nvsz-34a	New Britain–Solomons–Vanuatu	169.8304	-21.2121	329.1	39	22.73
nvsz-34b	New Britain–Solomons–Vanuatu	169.5086	-21.3911	329.1	20.77	5
nvsz-35a	New Britain–Solomons–Vanuatu	170.3119	-21.6945	311.9	39	22.13
nvsz-35b	New Britain–Solomons–Vanuatu	170.0606	-21.9543	311.9	20.03	5
nvsz-36a	New Britain–Solomons–Vanuatu	170.9487	-22.1585	300.4	39.42	23.5
nvsz-36b	New Britain–Solomons–Vanuatu	170.7585	-22.4577	300.4	21.71	5
nvsz-37a	New Britain–Solomons–Vanuatu	171.6335	-22.3087	281.3	30	22.1
nvsz-37b	New Britain–Solomons–Vanuatu	171.5512	-22.6902	281.3	20	5

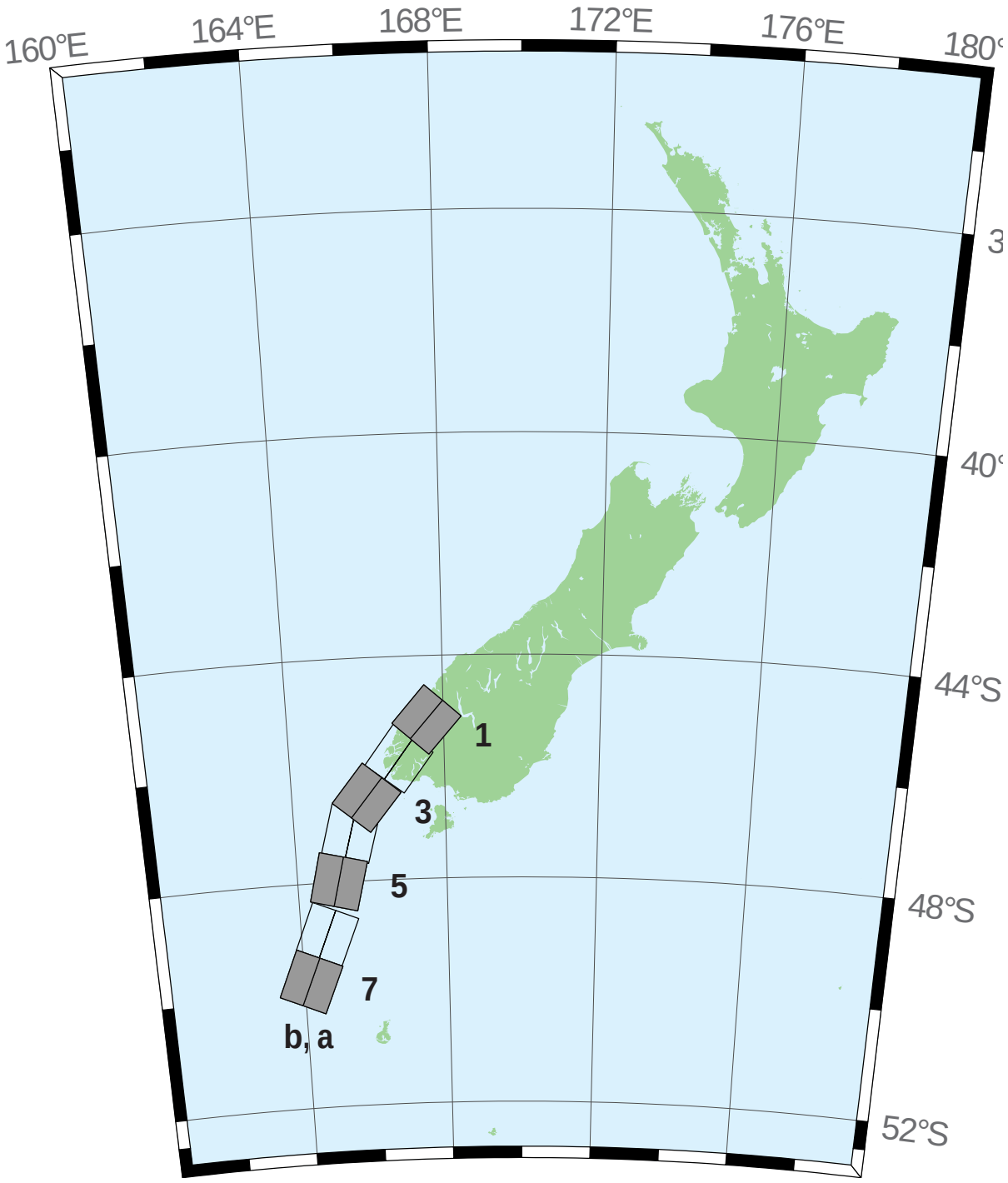

Figure B10: New Zealand–Puysegur Subduction Zone unit sources.

Table B10: Earthquake parameters for New Zealand–Puysegur Subduction Zone unit sources.

Segment	Description	Longitude (°E)	Latitude (°N)	Strike (°)	Dip (°)	Depth (km)
nzsz-1a	New Zealand–Puysegur	168.0294	-45.4368	41.5	15	17.94
nzsz-1b	New Zealand–Puysegur	167.5675	-45.1493	41.5	15	5
nzsz-2a	New Zealand–Puysegur	167.3256	-46.0984	37.14	15	17.94
nzsz-2b	New Zealand–Puysegur	166.8280	-45.8365	37.14	15	5
nzsz-3a	New Zealand–Puysegur	166.4351	-46.7897	39.53	15	17.94
nzsz-3b	New Zealand–Puysegur	165.9476	-46.5136	39.53	15	5
nzsz-4a	New Zealand–Puysegur	166.0968	-47.2583	15.38	15	17.94
nzsz-4b	New Zealand–Puysegur	165.4810	-47.1432	15.38	15	5
nzsz-5a	New Zealand–Puysegur	165.7270	-48.0951	13.94	15	17.94
nzsz-5b	New Zealand–Puysegur	165.0971	-47.9906	13.94	15	5
nzsz-6a	New Zealand–Puysegur	165.3168	-49.0829	22.71	15	17.94
nzsz-6b	New Zealand–Puysegur	164.7067	-48.9154	22.71	15	5
nzsz-7a	New Zealand–Puysegur	164.8017	-49.9193	23.25	15	17.94
nzsz-7b	New Zealand–Puysegur	164.1836	-49.7480	23.25	15	5

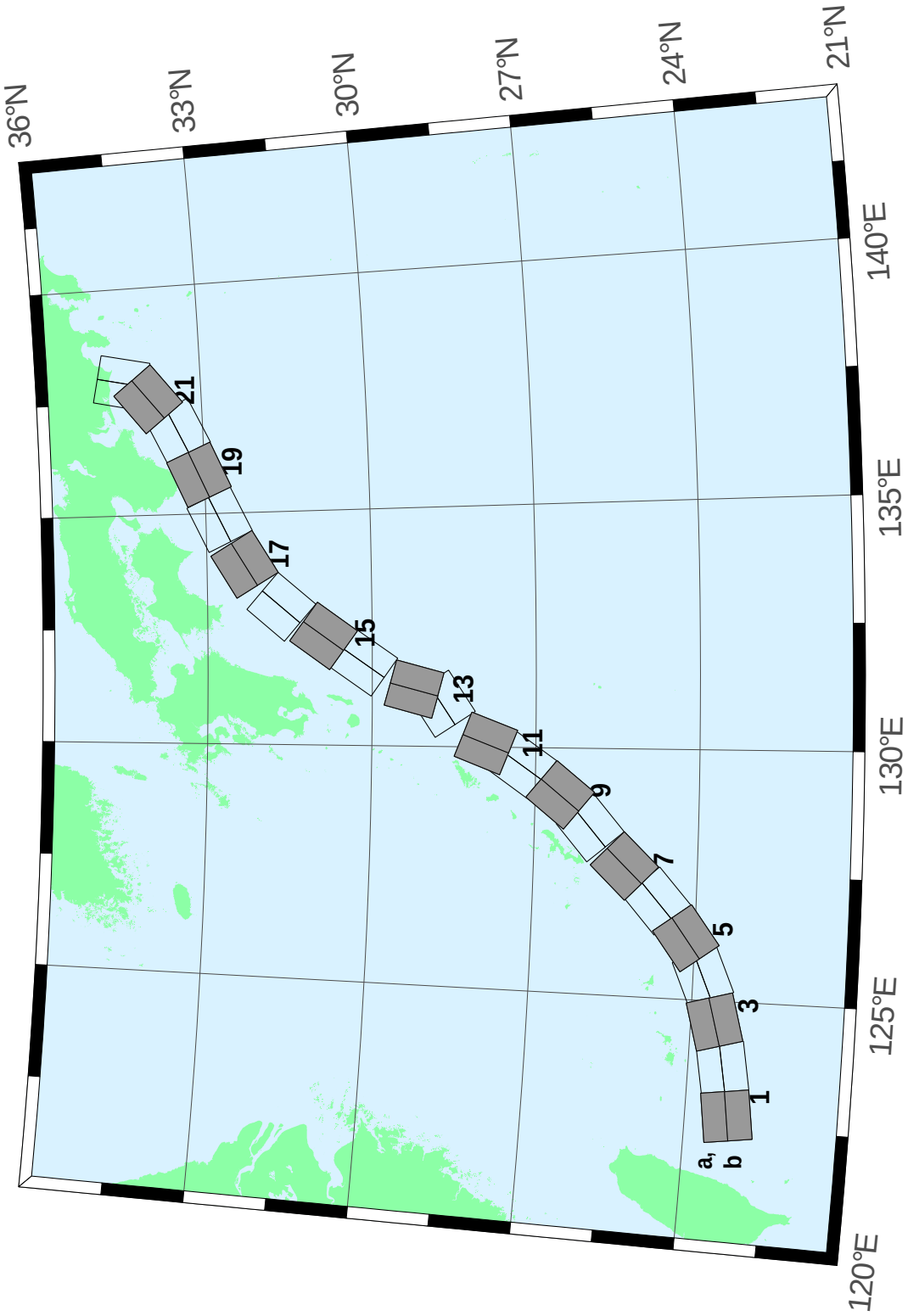

Figure B11: Ryukyu–Kyushu–Nankai Subduction Zone unit sources.

Table B11: Earthquake parameters for Ryukyu–Kyushu–Nankai Subduction Zone unit sources.

Segment	Description	Longitude (°E)	Latitude (°N)	Strike (°)	Dip (°)	Depth (km)
rnsz-1a	Ryukyu–Kyushu–Nankai	122.6672	23.6696	262	14	11.88
rnsz-1b	Ryukyu–Kyushu–Nankai	122.7332	23.2380	262	10	3.2
rnsz-2a	Ryukyu–Kyushu–Nankai	123.5939	23.7929	259.9	18.11	12.28
rnsz-2b	Ryukyu–Kyushu–Nankai	123.6751	23.3725	259.9	10	3.6
rnsz-3a	Ryukyu–Kyushu–Nankai	124.4604	23.9777	254.6	19.27	14.65
rnsz-3b	Ryukyu–Kyushu–Nankai	124.5830	23.5689	254.6	12.18	4.1
rnsz-4a	Ryukyu–Kyushu–Nankai	125.2720	24.2102	246.8	18	20.38
rnsz-4b	Ryukyu–Kyushu–Nankai	125.4563	23.8177	246.8	16	6.6
rnsz-5a	Ryukyu–Kyushu–Nankai	125.9465	24.5085	233.6	18	20.21
rnsz-5b	Ryukyu–Kyushu–Nankai	126.2241	24.1645	233.6	16	6.43
rnsz-6a	Ryukyu–Kyushu–Nankai	126.6349	25.0402	228.7	17.16	19.55
rnsz-6b	Ryukyu–Kyushu–Nankai	126.9465	24.7176	228.7	15.16	6.47
rnsz-7a	Ryukyu–Kyushu–Nankai	127.2867	25.6343	224	15.85	17.98
rnsz-7b	Ryukyu–Kyushu–Nankai	127.6303	25.3339	224	13.56	6.26
rnsz-8a	Ryukyu–Kyushu–Nankai	128.0725	26.3146	229.7	14.55	14.31
rnsz-8b	Ryukyu–Kyushu–Nankai	128.3854	25.9831	229.7	9.64	5.94
rnsz-9a	Ryukyu–Kyushu–Nankai	128.6642	26.8177	219.2	15.4	12.62
rnsz-9b	Ryukyu–Kyushu–Nankai	129.0391	26.5438	219.2	8	5.66
rnsz-10a	Ryukyu–Kyushu–Nankai	129.2286	27.4879	215.2	17	12.55
rnsz-10b	Ryukyu–Kyushu–Nankai	129.6233	27.2402	215.2	8.16	5.45
rnsz-11a	Ryukyu–Kyushu–Nankai	129.6169	28.0741	201.3	17	12.91
rnsz-11b	Ryukyu–Kyushu–Nankai	130.0698	27.9181	201.3	8.8	5.26
rnsz-12a	Ryukyu–Kyushu–Nankai	130.6175	29.0900	236.7	16.42	13.05
rnsz-12b	Ryukyu–Kyushu–Nankai	130.8873	28.7299	236.7	9.57	4.74
rnsz-13a	Ryukyu–Kyushu–Nankai	130.7223	29.3465	195.2	20.25	15.89
rnsz-13b	Ryukyu–Kyushu–Nankai	131.1884	29.2362	195.2	12.98	4.66
rnsz-14a	Ryukyu–Kyushu–Nankai	131.3467	30.3899	215.1	22.16	19.73
rnsz-14b	Ryukyu–Kyushu–Nankai	131.7402	30.1507	215.1	17.48	4.71
rnsz-15a	Ryukyu–Kyushu–Nankai	131.9149	31.1450	216	15.11	16.12
rnsz-15b	Ryukyu–Kyushu–Nankai	132.3235	30.8899	216	13.46	4.48
rnsz-16a	Ryukyu–Kyushu–Nankai	132.5628	31.9468	220.9	10.81	10.88
rnsz-16b	Ryukyu–Kyushu–Nankai	132.9546	31.6579	220.9	7.19	4.62
rnsz-17a	Ryukyu–Kyushu–Nankai	133.6125	32.6956	239	10.14	12.01
rnsz-17b	Ryukyu–Kyushu–Nankai	133.8823	32.3168	239	8.41	4.7
rnsz-18a	Ryukyu–Kyushu–Nankai	134.6416	33.1488	244.7	10.99	14.21
rnsz-18b	Ryukyu–Kyushu–Nankai	134.8656	32.7502	244.5	10.97	4.7
rnsz-19a	Ryukyu–Kyushu–Nankai	135.6450	33.5008	246.5	14.49	14.72
rnsz-19b	Ryukyu–Kyushu–Nankai	135.8523	33.1021	246.5	11.87	4.44
rnsz-20a	Ryukyu–Kyushu–Nankai	136.5962	33.8506	244.8	15	14.38
rnsz-20b	Ryukyu–Kyushu–Nankai	136.8179	33.4581	244.8	12	3.98
rnsz-21a	Ryukyu–Kyushu–Nankai	137.2252	34.3094	231.9	15	15.4
rnsz-21b	Ryukyu–Kyushu–Nankai	137.5480	33.9680	231.9	12	5
rnsz-22a	Ryukyu–Kyushu–Nankai	137.4161	34.5249	192.3	15	15.4
rnsz-22b	Ryukyu–Kyushu–Nankai	137.9301	34.4327	192.3	12	5

Appendix C.
Synthetic Testing Report: Newport, Oregon*

C1. Purpose

Forecast models are tested with synthetic tsunami events covering a range of tsunami source locations and magnitudes ranging from mega-events to micro-events. Testing is also done with selected historical tsunami events when available.

The purpose of forecast model testing is three-fold. The first objective is to assure that the results obtained with the NOAA tsunami forecast system, which has been released to the Tsunami Warning Centers for operational use, are consistent with those obtained by the researcher during the development of the forecast model. The second objective is to test the forecast model for consistency, accuracy, time efficiency, and quality of results over a range of possible tsunami locations and magnitudes. The third objective is to identify bugs and issues in need of resolution by the researcher who developed the forecast model or by the forecast software development team before the next version release to NOAA's two Tsunami Warning Centers.

Local hardware and software applications, and tools familiar to the researcher(s), are used to run the Method of Splitting Tsunami (MOST) model during the forecast model development. The test results presented in this report lend confidence that the model performs as developed and produces the same results when initiated within the forecast application in an operational setting as those produced by the researcher during the forecast model development. The test results assure those who rely on the Newport tsunami forecast model that consistent results are produced irrespective of system.

C2. Testing procedure

The general procedure for forecast model testing is to run a set of synthetic tsunami scenarios and a selected set of historical tsunami events through the forecast system application and compare the results with those obtained by the researcher during the forecast model development and presented in the Tsunami Forecast Model Report. Specific steps taken to test the model include:

1. Identification of testing scenarios, including the standard set of synthetic events, appropriate historical events, and customized synthetic scenarios that may have been used by the researcher(s) in developing the forecast model.
2. Creation of new events to represent customized synthetic scenarios used by the researcher(s) in developing the forecast model, if any.
3. Submission of test model runs with the forecast system, and export of the results from A, B, and C grids, along with time series.
4. Recording applicable metadata, including the specific forecast system used for testing.

---

* Author: Lindsey Wright

5. Examination of forecast model results for instabilities in both time series and plot results.
6. Comparison of forecast model results obtained through the forecast system with those obtained during the forecast model development.
7. Summarization of results with specific mention of quality, consistency, and time efficiency.
8. Reporting of issues identified to modeler and and forecast system software development team.
9. Retesting the forecast models in the forecast system when reported issues have been addressed or explained.

Synthetic model runs were tested on a DELL PowerEdge R510 computer equipped with two Xeon E5670 processors at 2.93 Ghz, each with 12 MBytes of cache and 32 GB memory. The processors are hex core and support hyperthreading, resulting in the computer performing as a 24 processor core machine. Additionally, the testing computer supports 10 Gigabit Ethernet for fast network connections. This computer configuration is similar or the same as the configurations of the computers installed at the Tsunami Warning Centers so the compute times should only vary slightly.

C3. Results

The Newport, Oregon, forecast model was tested with SIFT version 3.2.

The Newport forecast model was tested with four synthetic scenarios and two historical tsunami events. Test results from and comparisons with the results obtained during the forecast model development are shown numerically in **Table C1** and graphically in **Figures C1 to C6**. The results show that the minimum and maximum amplitudes and time series obtained from SIFT agree with those obtained during the forecast model development, and that the forecast model is stable and robust, with consistent and high quality results across geographically distributed tsunami sources and tsunami magnitudes from micro-events to mega-events. There are some small differences in magnitudes evident in the table, possibly due to differing output frequencies used to track extrema between the development and SIFT model runs. The authors feel that these differences are within acceptable ranges. The model run time (wall-clock time) was 12.05 min for 9.99 hr of simulation time, and 4.80 min for 4.0 hr. This run time is within the 10 min run time for 4 hr of simulation time and satisfies time efficiency requirements.

A suite of synthetic events was run on the Newport forecast model. The modeled scenarios were stable for all cases tested. Of the cases tested, the largest maximum amplitude of 146 cm originated in the Aleutian-Alaska Cascadia (ACSZ) 56–65 source zone and the smallest signal (approximately 32 cm) was seen from the Central and South America (CSSZ) 89–98 source. Comparisons between the development results and the forecast system output were identical in shape and amplitude for synthetic and historical cases tested, with very little variation in maximum and minimum values. The Newport reference point used for the forecast model development is the same as what is deployed in the forecast system, so the results can be considered valid for all cases studied.

Table C1: Maximum and minimum amplitudes (cm) at the Newport, Oregon warning point for synthetic and historical events tested using SIFT 3.2 and obtained during development.

Scenarios	Source Zone	Tsunami Source	α [m]	SIFT Max (cm)	Development Max (cm)	SIFT Min (cm)	Development Min (cm)
Mega-tsunami Scenarios							
KISZ 22–31	Kamchatka-Kuril-Japan-Izu-Mariana-Yap	A22–31, B22–31	30	100.6	118.1	–33.8	–37.5
ACSZ 56–65	Aleutian-Alaska-Cascadia	A56–65, B56–65	30	146.4	139.8	–485.7	–484.0
CSSZ 89–98	Central and South America	A89–98, B89–98	30	31.9	31.6	–9.2	–9.1
NTSZ 30–39	New Zealand-Kermadec-Tonga	A30–39, B30–39	30	78.6	80.4	–36.4	–36.2
Historical Events							
2006 Tonga	n/a	n/a	n/a	3.5	4.5	–2.0	–2.4
2006 Kuril	n/a	n/a	n/a	5.4	5.5	–4.6	–4.7

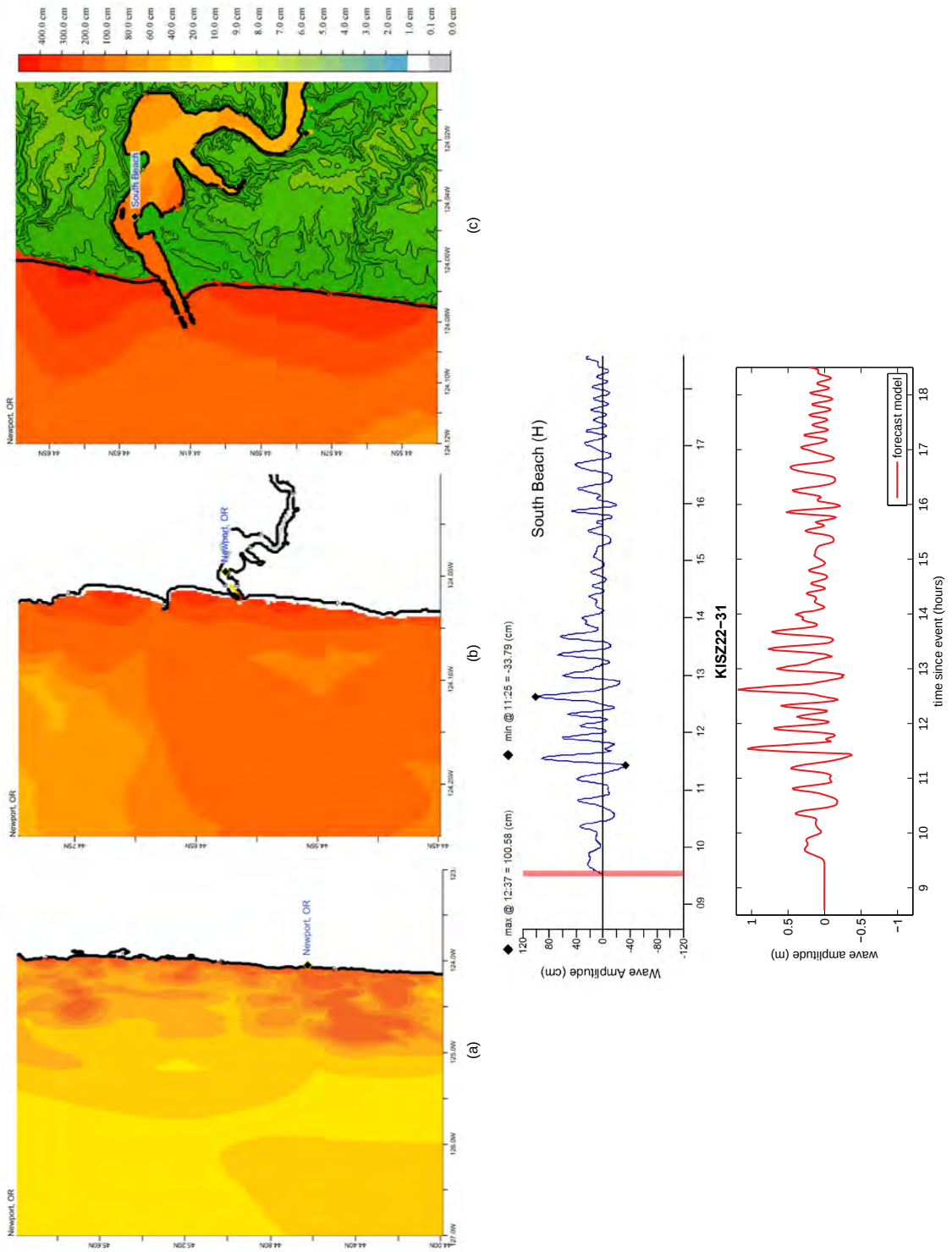

Figure C1: Response of the Newport forecast model to synthetic scenario KISZ 22−31 (α=25). Maximum sea surface elevation for (a) A grid, (b) B grid, and (c) C grid. Sea surface elevation time series at the C-grid warning point (d). The lower time series plot is the result obtained during model development and is shown for comparison with test results.

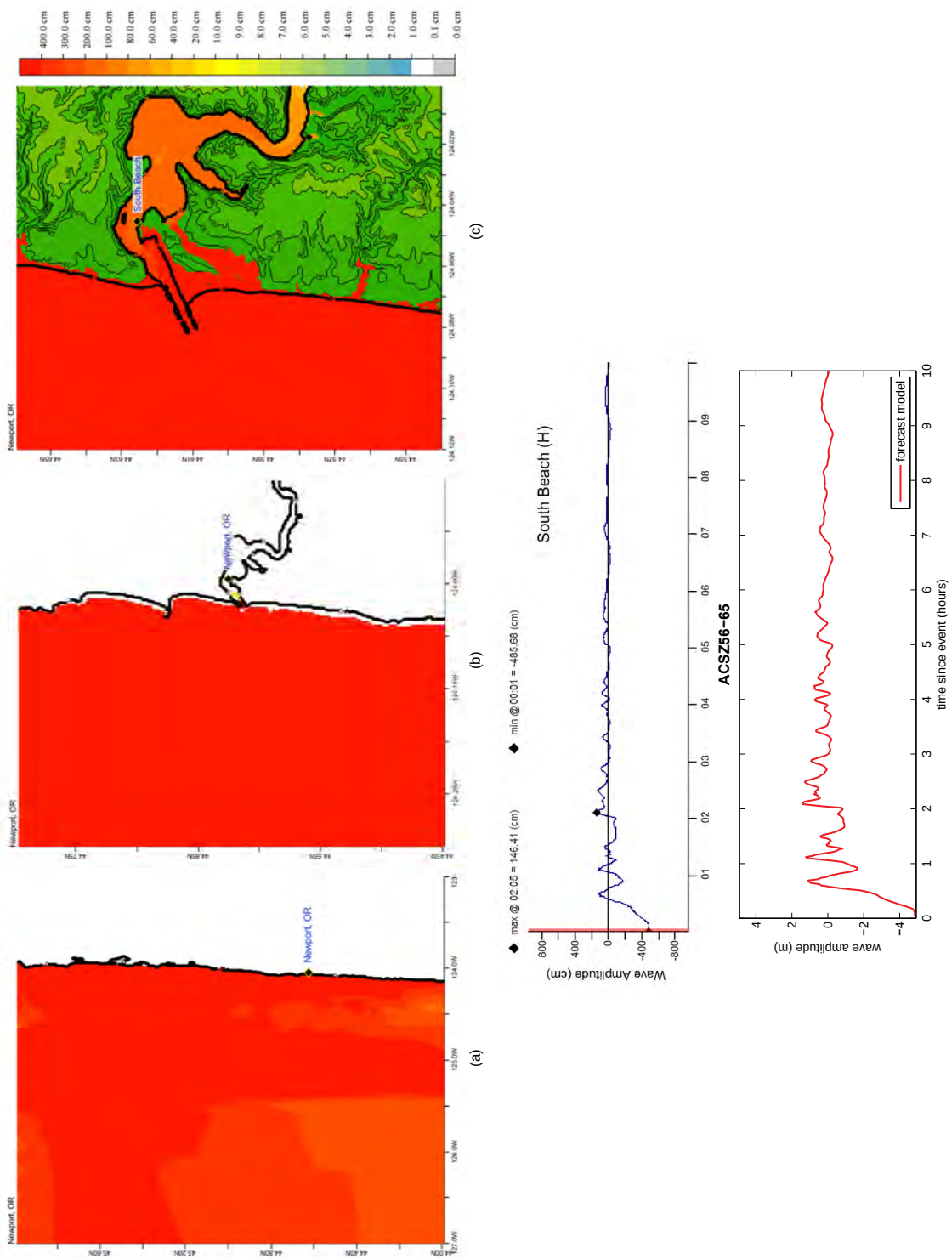

Figure C2: Response of the Newport forecast model to synthetic scenario ACSZ 56–65 (a=25). Maximum sea surface elevation for (a) A grid, (b) B grid, and (c) C grid. Sea surface elevation time series at the C-grid warning point (d). The lower time series plot is the result obtained during model development and is shown for comparison with test results.

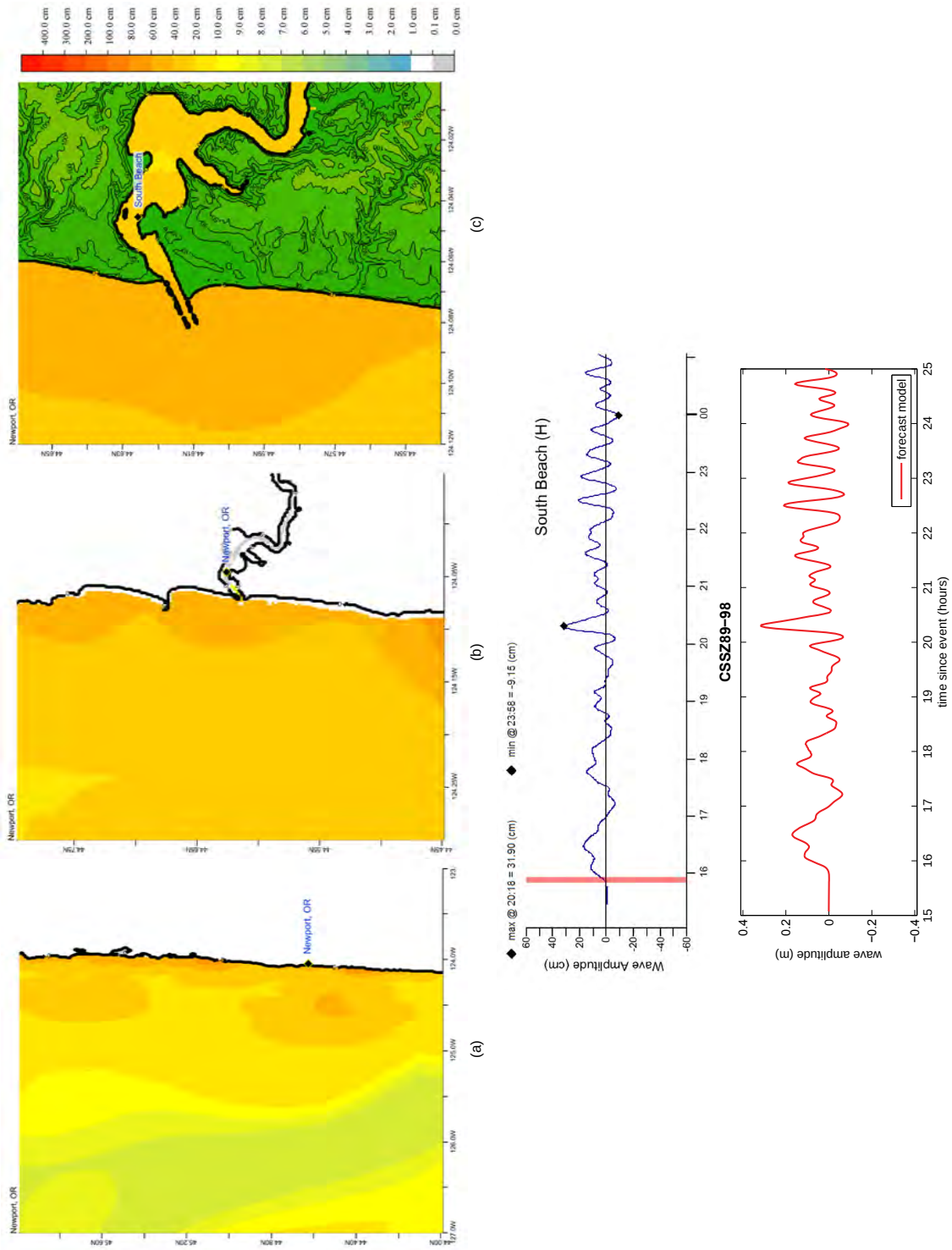

Figure C3: Response of the Newport forecast model to synthetic scenario CSSZ 89–98 (a=25). Maximum sea surface elevation for (a) A grid, (b) B grid, and (c) C grid. Sea surface elevation time series at the C-grid warning point (d). The lower time series plot is the result obtained during model development and is shown for comparison with test results.

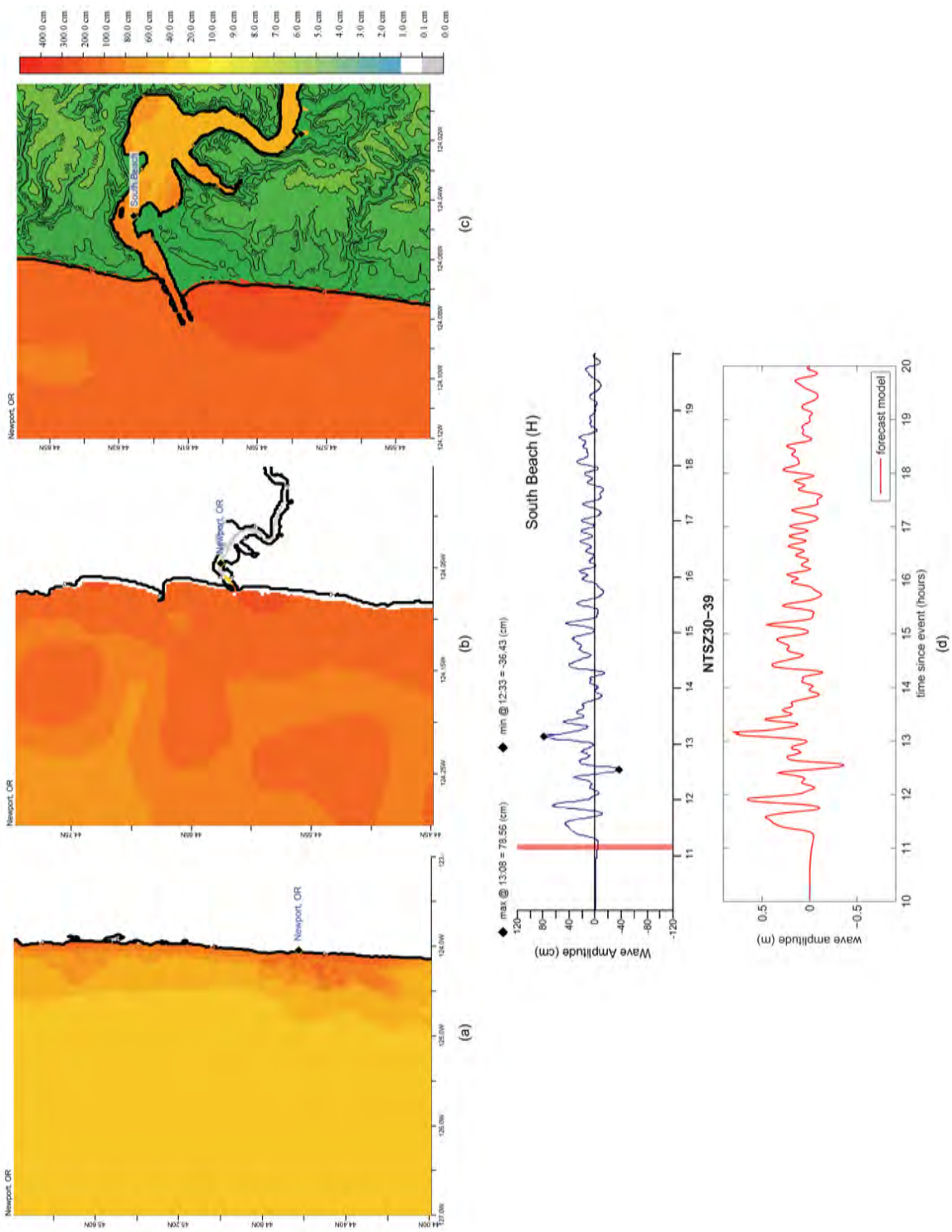

Figure C4: Response of the Newport forecast model to synthetic scenario NTSZ 30–39 (α=25). Maximum sea surface elevation for (a) A grid, (b) B grid, and (c) C grid. Sea surface elevation time series at the C-grid warning point (d). The lower time series plot is the result obtained during model development and is shown for comparison with test results.

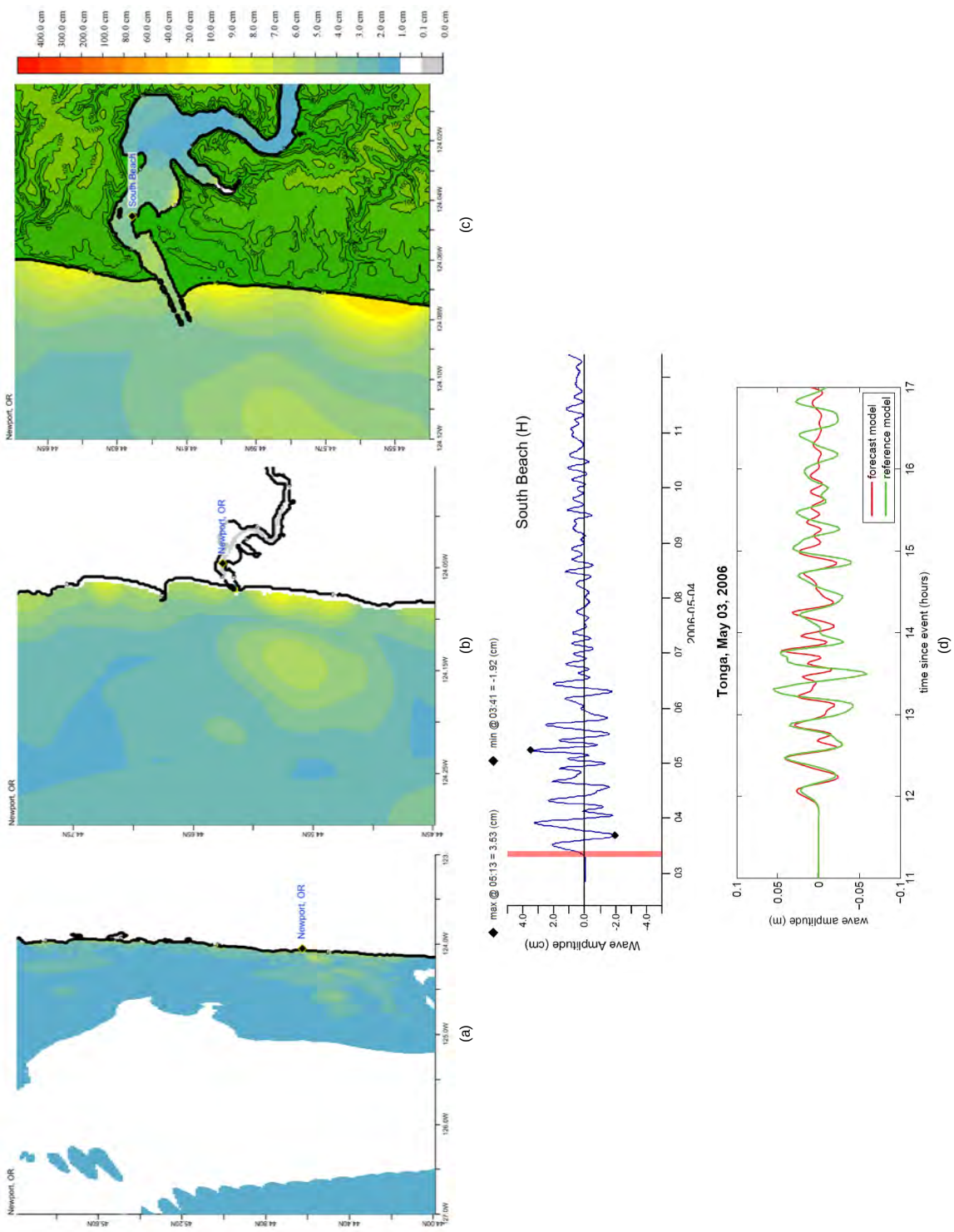

Figure C5: Response of the Newport forecast model to the 2006 Tonga tsunami. Maximum sea surface elevation for (a) A grid, (b) B grid, and (c) C grid. Sea surface elevation time series at the C-grid warning point (d). The lower time series plot is the result obtained during model development and is shown for comparison with test results.

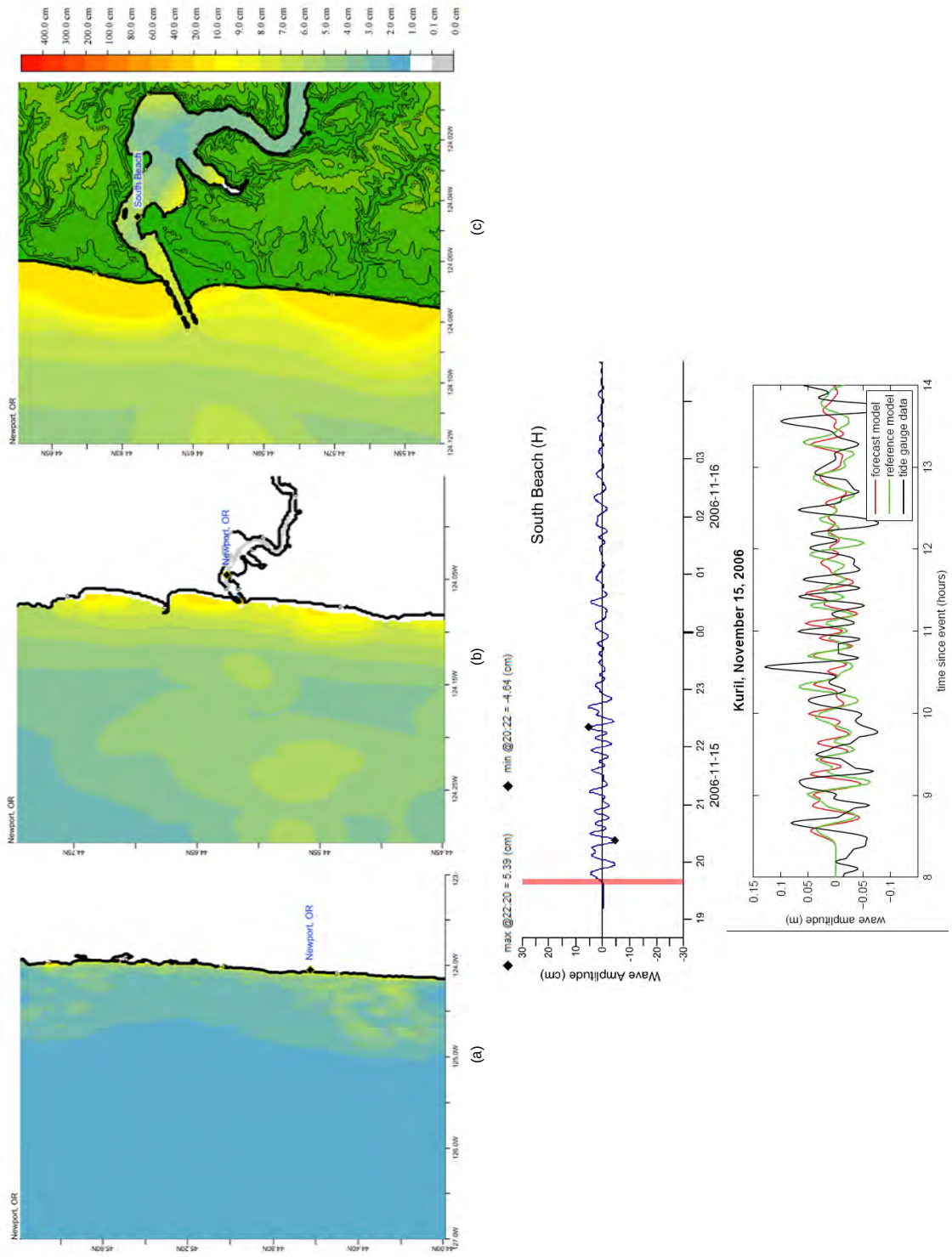

Figure C6: Response of the Newport forecast model to the 2006 Kuril tsunami. Maximum sea surface elevation for (a) A grid, (b) B grid, and (c) C grid. Sea surface elevation time series at the C-grid warning point (d). The lower time series plot is the result obtained during model development and is shown for comparison with test results.

Glossary

Arrival time The time when the first tsunami wave is observed at a particular location, typically given in local and/or universal time, but also commonly noted in minutes or hours relative to the time of the earthquake.

Bathymetry The measurement of water depth of an undisturbed body of water.

Cascadia Subduction Zone Fault that extends from Cape Mendocino in Northern California northward to mid-Vancouver Island, Canada. The fault marks the convergence boundary where the Juan de Fuca tectonic plate is being subducted under the margin of the North America plate.

Current speed The scalar rate of water motion measured as distance/time.

Current velocity Movement of water expressed as a vector quantity. Velocity is the distance of movement per time coupled with direction of motion.

Deep-ocean Assessment and Reporting of Tsunamis (DART®) Tsunami detection and transmission system that measures the pressure of an overlying column of water and detects the passage of a tsunami.

Digital Elevation Model (DEM) A digital representation of bathymetry or topography based on regional survey data or satellite imagery. Data are arrays of regularly spaced elevations referenced to a map projection of the geographic coordinate system.

Epicenter The point on the surface of the earth that is directly above the focus of an earthquake.

Far-field Region outside of the source of a tsunami where no direct observations of the tsunami-generating event are evident, except for the tsunami waves themselves.

Focus The point beneath the surface of the earth where a rupture or energy release occurs due to a buildup of stress or the movement of earth's tectonic plates relative to one another.

Inundation The horizontal inland extent of land that a tsunami penetrates, generally measured perpendicularly to a shoreline.

Marigram Tide gauge recording of wave level as a function of time at a particular location. The instrument used for recording is termed a marigraph.

Method of Splitting Tsunami (MOST) A suite of numerical simulation codes used to provide estimates of the three processes of tsunami evolution: tsunami generation, propagation, and inundation.

Moment magnitude (M_w) The magnitude of an earthquake on a logarithmic scale in terms of the energy released. Moment magnitude is based on the size and characteristics of a fault rupture as determined from long-period seismic waves.

Near–field Region of primary tsunami impact near the source of the tsunami. The near-field is defined as the region where non-tsunami effects of the tsunami-generating event have been observed, such as earth shaking from the earthquake, visible or measured ground deformation, or other direct (non-tsunami) evidences of the source of the tsunami wave.

Propagation database A basin-wide database of pre-computed water elevations and flow velocities at uniformly spaced grid points throughout the world oceans. Values are computed from tsunamis generated by earthquakes with a fault rupture at any one of discrete 100 × 50 km unit sources along worldwide subduction zones.

Runup Vertical difference between the elevation of tsunami inundation and the sea level at the time of a tsunami. Runup is the elevation of the highest point of land inundated by a tsunami as measured relative to a stated datum, such as mean sea level.

Short-term Inundation Forecasting for Tsunamis (SIFT) A tsunami forecast system that integrates tsunami observations in the deep ocean with numerical models to provide an estimate of tsunami wave arrival and amplitude at specific coastal locations while a tsunami propagates across an ocean basin.

Subduction zone A submarine region of the earth's crust at which two or more tectonic plates converge to cause one plate to sink under another, overriding plate. Subduction zones are regions of high seismic activity.

Synthetic event Hypothetical events based on computer simulations or theory of possible or even likely future scenarios.

Tele–tsunami or **distant tsunami** or **far–field tsunami** Most commonly, a tsunami originating from a source greater than 1000 km away from a particular location. In some contexts, a tele-tsunami is one that propagates through deep ocean before reaching a particular location without regard to distance separation.

Tidal wave Term frequently used incorrectly as a synonym for tsunami. A tsunami is unrelated to the predictable periodic rise and fall of sea level due to the gravitational attractions of the moon and sun (see **Tide**, below).

Tide The predictable rise and fall of a body of water (ocean, sea, bay, etc.) due to the gravitational attractions of the moon and sun.

Tide gauge An instrument for measuring the rise and fall of a column of water over time at a particular location.

Travel time The time it takes for a tsunami to travel from the generating source to a particular location.

Tsunameter An oceanographic instrument used to detect and measure tsunamis in the deep ocean. Tsunami measurements are typically transmitted acoustically to a surface buoy that in turn relays them in real time to ground stations via satellite.

Tsunami A Japanese term that literally translates to "harbor wave." Tsunamis are a series of long-period shallow water waves that are generated by the sudden displacement of water due to subsea disturbances such as earthquakes, submarine landslides, or volcanic eruptions. Less commonly, meteoric impact to the ocean or meteorological forcing can generate a tsunami.

Tsunami hazard assessment A systematic investigation of seismically active regions of the world oceans to determine their potential tsunami impact at a particular location. Numerical models are typically used to characterize tsunami generation, propagation, and inundation, and to quantify the risk posed to a particular community from tsunamis generated in each source region investigated.

Tsunami magnitude A number that characterizes the strength of a tsunami based on the tsunami wave amplitudes. Several different tsunami magnitude determination methods have been proposed.

Tsunami propagation The directional movement of a tsunami wave outward from the source of generation. The speed at which a tsunami propagates depends on the depth of the water column in which the wave is traveling. Tsunamis travel at a speed of 700 km/hr (450 mi/hr) over the average depth of 4000 m in the open deep Pacific Ocean.

Tsunami source Location of tsunami origin, most typically an underwater earthquake epicenter. Tsunamis are also generated by submarine landslides, underwater volcanic eruptions, or, less commonly, by meteoric impact of the ocean.

Wall-clock time The time that passes on a common clock or watch between the start and end of a model run, as distinguished from the time needed by a CPU or computer processor to complete the run, typically less than wall-clock time.

Wave amplitude The maximum vertical rise or drop of a column of water as measured from wave crest (peak) or trough to a defined mean water level state.

Wave crest or peak The highest part of a wave or maximum rise above a defined mean water level state, such as mean lower low water.

Wave height The vertical difference between the highest part of a specific wave (crest) and its corresponding lowest point (trough).

Wavelength The horizontal distance between two successive wave crests or troughs.

Wave period The length of time between the passage of two successive wave crests or troughs as measured at a fixed location.

Wave trough The lowest part of a wave or the maximum drop below a defined mean water level state, such as mean lower low water.

PMEL Tsunami Forecast Series Locations

Adak, AK
Apra Harbor, Guam
Arecibo, Puerto Rico
Arena Cove, CA
Atka, AK
Atlantic City, NJ
Bar Harbor, ME
Cape Hatteras, NC
Charlotte Amalie, U.S. Virgin Islands
Chignik, AK
Christiansted, U.S. Virgin Islands
Cordova, AK
Craig, AK
Crescent City, CA — **Vol. 2**
Daytona Beach, FL
Elfin Cove, AK
Eureka, CA
Fajardo, PR
Florence, OR
Garibaldi, OR
Haleiwa, HI
Hilo, HI — **Vol. 1**
Homer, AK
Honolulu, HI
Kahului, HI
Kailua-Kona, HI
Kawaihae, HI
Keauhou, HI
Key West, FL
Kihei, HI
King Cove, AK
Kodiak, AK — **Vol. 4**
Lahaina, HI
La Push, WA
Los Angeles, CA
Mayaguez, PR
Midway Atoll
Montauk, NY
Monterey, CA
Morehead City, NC
Myrtle Beach, SC
Nantucket, MA
Nawiliwili, HI
Neah Bay, WA
Newport, OR — **Vol. 5**
Nikolski, AK
Ocean City, MD
Pago Pago, American Samoa
Palm Beach, FL
Pearl Harbor, HI
Point Reyes, CA
Ponce, PR
Port Alexander, AK
Port Angeles, WA
Port Orford, OR
Port San Luis, CA
Port Townsend, WA
Portland, ME
San Diego, CA
San Francisco, CA — **Vol. 3**
San Juan, Puerto Rico
Sand Point, AK
Santa Barbara, CA
Santa Monica, CA
Savannah, GA
Seaside, OR
Seward, AK
Shemya, AK
Sitka, AK
Toke Point, WA
Unalaska, AK
Virginia Beach, VA
Wake Island, U.S. Territory
Westport, WA
Yakutat, AK

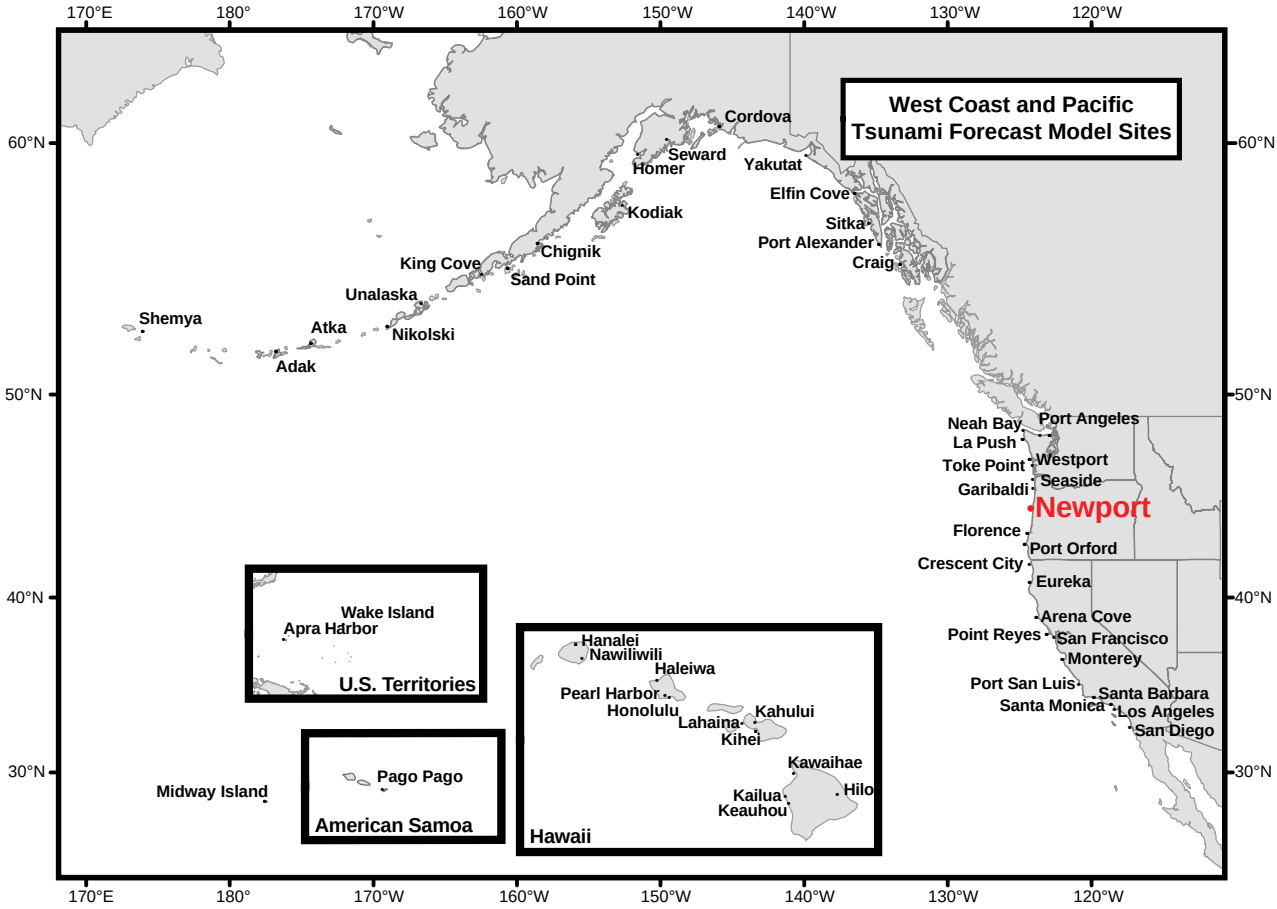
West Coast and Pacific Tsunami Forecast Model Sites
170°E
180°
170°W
160°W
150°W
140°W
130°W
120°W
60°N
50°N
40°N
30°N
Cordova
Seward
Homer
Yakutat
Elfin Cove
Kodiak
Sitka
Port Alexander
Craig
Chignik
King Cove
Sand Point
Unalaska
Shemya
Atka
Nikolski
Adak
Neah Bay
Port Angeles
La Push
Toke Point
Westport
Seaside
Garibaldi
Newport
Florence
Port Orford
Crescent City
Eureka
Arena Cove
Point Reyes
San Francisco
Monterey
Port San Luis
Santa Barbara
Santa Monica
Los Angeles
San Diego
Wake Island
Apra Harbor
U.S. Territories
Hanalei
Nawiliwili
Haleiwa
Pearl Harbor
Honolulu
Kahului
Lahaina
Kihei
Kawaihae
Hilo
Kailua
Keauhou
Hawaii
Pago Pago
American Samoa
Midway Island

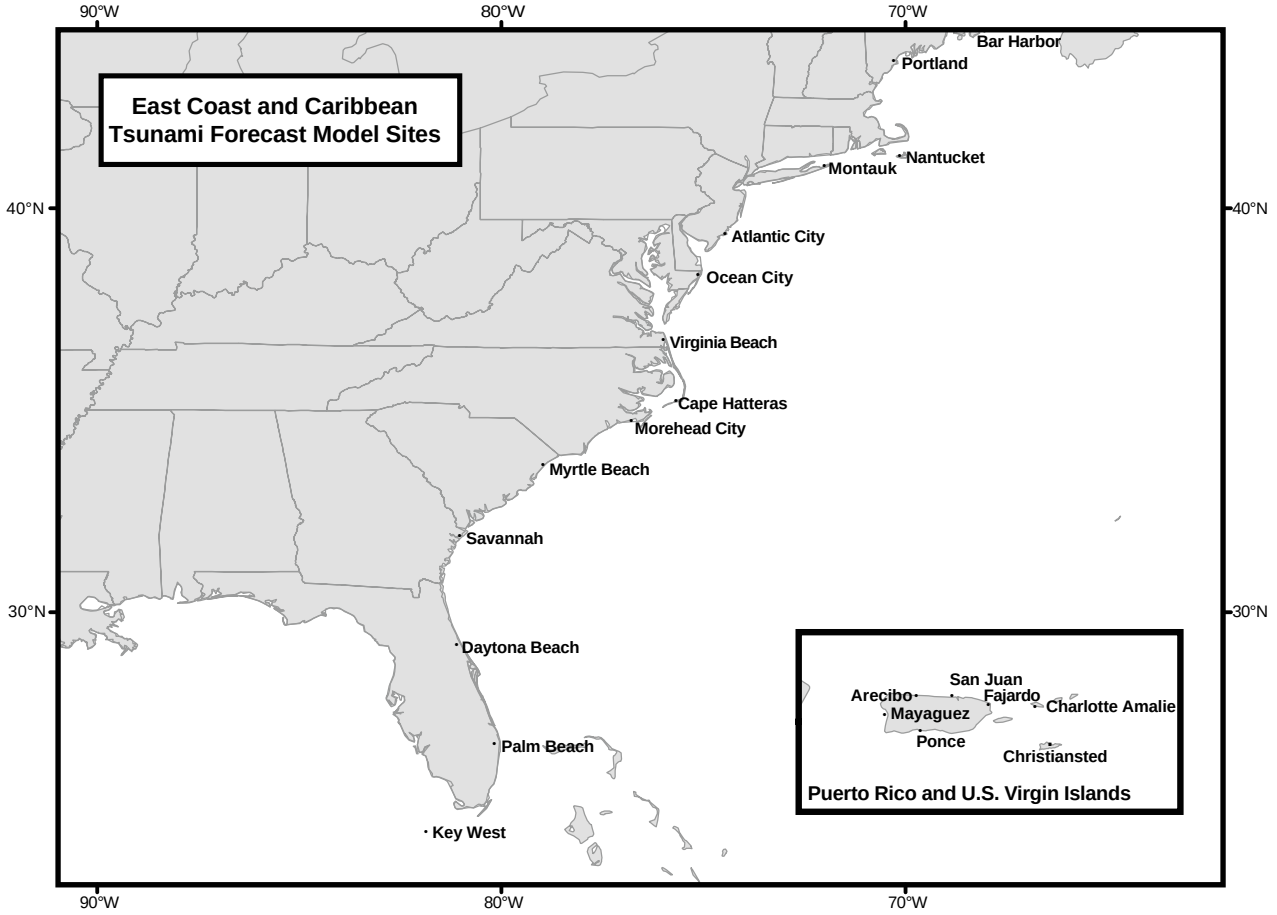
East Coast and Caribbean Tsunami Forecast Model Sites
90°W
80°W
70°W
40°N
30°N
Bar Harbor
Portland
Nantucket
Montauk
Atlantic City
Ocean City
Virginia Beach
Cape Hatteras
Morehead City
Myrtle Beach
Savannah
Daytona Beach
Palm Beach
Key West
San Juan
Arecibo
Fajardo
Mayaguez
Charlotte Amalie
Ponce
Christiansted
Puerto Rico and U.S. Virgin Islands